

Traffic Steering in Radio Level Integration of LTE and Wi-Fi Networks

Thomas Valerrian Pasca Santhappan

A Dissertation Submitted to
Indian Institute of Technology Hyderabad
In Partial Fulfillment of the Requirements for
The Degree of Doctor of Philosophy



भारतीय प्रौद्योगिकी संस्थान हैदराबाद
Indian Institute of Technology Hyderabad

Department of Computer Science and Engineering
Indian Institute of Technology Hyderabad

January 2019

Declaration

I declare that this written submission represents my ideas in my own words, and where ideas or words of others have been included, I have adequately cited and referenced the original sources. I also declare that I have adhered to all principles of academic honesty and integrity and have not misrepresented or fabricated or falsified any idea/data/fact/source in my submission. I understand that any violation of the above will be a cause for disciplinary action by the Institute and can also evoke penal action from the sources that have thus not been properly cited, or from whom proper permission has not been taken when needed.



(Signature)

(Thomas Valerrian Pasca Santhappan)

CS13P1002

(Roll No.)

Approval Sheet

This thesis entitled **Traffic Steering in Radio Level Integration of LTE and Wi-Fi Networks** by Thomas Valerrian Pasca Santhappan is approved for the degree of Doctor of Philosophy from IIT Hyderabad



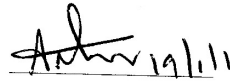
19/01/19

(Prof. Sukumar Nandi) Examiner 1
Dept. of Computer Science and Engineering
IIT Guwahati



19/1/19

(Prof. Swades De) Examiner 2
Dept. of Electrical Engineering
IIT Delhi



19/1/19

(Dr. Antony Franklin A) Internal Examiner
Dept. of Computer Science and Engineering
IIT Hyderabad



Reddy

(Dr. Bheemarjuna Reddy Tamma) Adviser
Dept. of Computer Science and Engineering
IIT Hyderabad



19/1/19

(Dr. Rajalakshmi P) Chairman
Dept. of Electrical Engineering
IIT Hyderabad

Acknowledgements

I thank everyone who supported my research career at IIT Hyderabad. I heartily thank people who extended me both moral and technical support.

I thank my advisor Dr. Bheemarjuna Reddy Tamma who trusted in me that I am capable of pursuing research career. I thank him for all the support which he has extended to me from the day I joined this campus till today. He is one of the most hardworking persons I have encountered in my life. I did learn many things from him in terms of technical writing, understanding problem in-sights, and developing interesting solutions. I thank him for all the things which he taught me. I am very blessed to work with him.

I thank Dr. Antony franklin for his support and guidance in my thesis works. I thank him for his special guidance in writing patents and presenting the works in standards forum. I also thank him for extending moral support during tough times of my research career.

I would like to thank my lab seniors Vanlin Sathya, Mukesh Giluka, Anil Kumar Rangiseti, and Mallikarjuna for the environment that they have set for me to work-in. Also, my supportive juniors Anand Baswade, Himank Gupta, Shashwat Kumar, Venkatarami Reddy, Nabhasmita Sen, Veerendra Kumar, Debashisha Mishra, Amogh PC, and Sumanta Patro. I thank all the students of NeWS Lab for being supportive to me in all the works.

I thank my colleagues Anand Baswade, Mukesh Giluka, and Himank Gupta for the best memories which they gave me. I thank Vanlin Sathya for his wonderful guidance throughout my research career. He supported me during ups and downs of my career. I thank Mukesh Giluka for providing me moral support throughout my stay at IIT Hyderabad.

I thank Chaganti Ramaraju who initiated the ambitious project of deploying an open source LTE using OpenAirInterface (OAI), which eventually become core of my Ph.D. work. I thank Dr. Raymon Knoop, Dr. Florain kaltenberger, Dr. Navid Nikaein, Lionel Gauthier, and Cedric Roux for mentoring during internship work at EURECOM, France.

I specially thank Himank Gupta, Siva sairam prasad Kodali, Mukesh Giluka, Sumanta Patro, Sreekanth Dama, Debashisha Mishra, Amogh PC, Nagamani Dheeravath, Vanlin Sathya, Anil Kumar Rangiseti, Adharsh Srivats, Dr. Kotaro Kataoka, Dr. Kiran kumar kuchi, Badrinaaraayanan Akilesh, Arjun V Anand, Prasanth Sharma, Ajay Brahmakshatriya, Naveen Kamath, Nabhasmita Sen, Venkatarami Reddy, and Tathagat Priyadarshi for their generous research contributions and supportive work in due course of solving my research problems.

I thank all my Doctoral Committee members, Dr. Kiran Kumar Kuchi, Dr. Kotaro Kataoka, Dr. Rajalakshmi P, and Dr. Sathya Peri. Special thanks to Dr. Antony Franklin for his guidance on every doctoral committee meeting.

I would heartily thank Goutham, Ramanjaneyulu Narayana, and Dileep Reddy towards their service as project staff in setting up and maintaining the precious NeWS LAB.

I extend my thanks to Yoghita, Aravind anna, Murugan, Karthick anna and all my friends at IIT Hyderabad for they have encouraged me throughout my Ph.D tenure. The

memories of the time which I spent on tamil new year is ever green, I thank all my friends for making it memorable. I would like to thank all the Ph.D. and M.Tech students of CSE department, for the unforgettable memories which they gave me each year on my birthdays, and moral support which they extended to me during different phases of my Ph.D program.

I thank Rakesh Lingam, Swarnalatha Mailaram, Veerla Swarnalatha, Angel Nivia, Dhanalakshmi, Suresh Reddy, Yanthan, Pravin J, Deep Khandavalli, Manjela Toppo, Murali, Nisha James, Pradeep Parchuri, Sathya Vanlin, Rajesh Nimmagadda, Sunil Reddy Mallireddy, Vidya Sagar, Anand Kakarla, Jedidiah, Joel Prakash, Keerthi Katam, Kimi, Koteswar Rao, Koteswara Rao Kandukuri, Krupa Teja, Kukkamudi Sreenivas, Mhatsomo W Yanthan, Jessy, Shekar, and Anu George for being part of the fellowship. I also thank them for the wonderful extended support and prayers.

I thank Roji Mol, Edin Michael, Jayashree, Martin, and Joseph for being part of the choir and extending their support. I specially thank Roji Mol and Edin Michael for their parental care. I also thank Saranya M S for supporting me both in my research works and in my personal life.

I would like to thank staff members in the Administrative block, Cyber Physical Systems lab (CPS) and Network Operations Center (ISAC-NOC), Jaya (CPS), Mr. Baswaraj (CPS), Mr. Raguram (ISAC), Lalitha, Pushapa, Madhu, and Mr. Vijay Chakri (ISAC) for their cheerful assistance.

I want to thank all my family members, and in particular, my parents A. Santhappan and M. Elizabeth, my brother S. Xavier ArockiaRaj, and my sister-in-law Ronica BIS. This entire journey, from research interests to my extra curricular activities, would not have been meaningful without their constant support and companionship.

I would like to thank staff members at the Hostel office and Mess, Mr. Vel Murugan (Hostel office), Mr. Prabhu (SGR Mess), and Mr. Logu (Shakthi Mess) for their true service and their compassion.

I like to conclude with the saying, “Unless the grain of wheat falls into the ground and dies, it remains what it was—a single grain; but that if it dies, it yields a rich harvest”. It says that unless someone is prepared and committed to take up a challenge inspite of how much bigger the challenge is, one cannot see a victory.

Thomas Valerrian Pasca Santhappan

Dedication

To
Almighty God,
My Parents & Friends.

Abstract

A smartphone generates approximately 1,614 MB of data per month which is 48 times of the data generated by a typical basic-feature cell phone. Cisco forecasts that the mobile data traffic growth will remain to increase and reach 49 Exabytes per month by 2021. However, the telecommunication service providers/operators face many challenges in order to improve cellular network capacity to match these ever-increasing data demands due to low, almost flat Average Revenue Per User (ARPU) and low Return on Investment (RoI). Spectrum resource crunch and licensing requirement for operation in cellular bands further complicate the procedure to support and manage the network.

In order to deal with the aforementioned challenges, one of the most vital solutions is to leverage the integration benefits of cellular networks with unlicensed operation of Wi-Fi networks. A closer level of cellular and Wi-Fi coupling/interworking improves Quality of Service (QoS) by unified connection management to user devices (UEs). It also offloads a significant portion of user traffic from cellular Base Station (BS) to Wi-Fi Access Point (AP). In this thesis, we have considered the cellular network to be Long Term Evolution (LTE) popularly known as 4G-LTE for interworking with Wi-Fi.

Third Generation Partnership Project (3GPP) defined various LTE and Wi-Fi interworking architectures from Rel-8 to Rel-11. Because of the limitations in these legacy LTE Wi-Fi interworking solutions, 3GPP proposed Radio Level Integration (RLI) architectures to enhance flow mobility and to react fast to channel dynamics. RLI node encompasses link level connection between Small cell evolved Node B (SeNB) and Wi-Fi AP. LTE WLAN Aggregation (LWA) and LTE Wi-Fi Integration with IPsec tunnel (LWIP) are the RLI architectures which are introduced in 3GPP Rel-12 and Rel-13.

The fundamental challenges for RLI architectures include: (1) Dynamic traffic steering across time-varying channel conditions on LTE and Wi-Fi links, (2) Out-of-order packet delivery problem when traffic steering is done at fine granularity (packet level steering), (3) Co-tier interference management in dense deployment scenarios, (4) Efficient placement of the RLI nodes and effective radio resource management in indoor deployments, and (5) High energy consumption at UEs and RLI nodes due to use of multiple radios simultaneously. This thesis addresses some of the fundamental challenges which prevent RLI architectures from achieving interworking benefits.

To address the problem of co-tier interference in dense deployment scenario and to enable efficient downlink traffic steering, this thesis proposes a novel Power aware dynamic traffic Steering (PRECISE) algorithm. The proposed algorithm targets to meet the following objectives in LWIP system: (i) Mitigation of co-tier interference in dense LWIP

deployments, (ii) Meeting Guaranteed Bit Rate (GBR) requirements of the users including those experiencing poor Signal to Interference plus Noise Ratio (SINR), and (iii) Dynamic steering of the flows across LTE and Wi-Fi links to maximize the system throughput.

The second important problem addressed is the uplink traffic steering. To enable efficient uplink traffic steering in LWIP system, in this thesis, Network Coordination Function (NCF) is proposed. NCF is realized at the LWIP node by implementing various uplink traffic steering algorithms. NCF encompasses four different uplink traffic steering algorithms for efficient utilization of Wi-Fi resources in LWIP system. NCF facilitates the network to take intelligent decisions rather than individual UEs deciding to steer the uplink traffic onto LTE link or Wi-Fi link. The NCF algorithms work by leveraging the availability of LTE as the anchor to improve the channel utilization of Wi-Fi.

The third most important problem is to enable packet level steering in LWIP. When data rates of LTE and Wi-Fi links are incomparable, steering packets across the links create problems for TCP traffic. When the packets are received Out-of-Order (OOO) at the TCP receiver due to variation in delay experienced on each link, it leads to the generation of DUPLICATE ACKNOWLEDGEMENTS (DUP-ACK). These unnecessary DUP-ACKs adversely affect the TCP congestion window growth and thereby lead to poor TCP performance. This thesis addresses this problem by proposing a virtual congestion control mechanism (VIRTUAL CONGESTION CONTROL WITH BOOST ACKNOWLEDGEMENT -VISIBLE). The proposed mechanism not only improves the throughput of a flow by reducing the number of unnecessary DUP-ACKs delivered to the TCP sender but also sends Boost ACKs in order to rapidly grow the congestion window to reap in aggregation benefits of heterogeneous links.

The fourth problem considered is the placement of LWIP nodes. In this thesis, we have addressed problems pertaining to the dense deployment of LWIP nodes. LWIP deployment can be realized in colocated and non-colocated fashion. The placement of LWIP nodes is done with the following objectives: (i) Minimizing the number of LWIP nodes deployed without any coverage holes, (ii) Maximizing SINR in every sub-region of a building, and (iii) Minimizing the energy spent by UEs and LWIP nodes.

Finally, prototypes of RLI architectures are presented (*i.e.*, LWIP and LWA testbeds). The prototypes are developed using open source LTE platform OpenAirInterface (OAI) and commercial-off-the-shelf hardware components. The developed LWIP prototype is made to work with commercial UE (Nexus 5). The LWA prototype requires modification at the UE protocol stack, hence it is realized using OAI-UE. The developed prototypes are coupled with the legacy multipath protocol such as MPTCP to investigate the coupling benefits.

Contents

Declaration	ii
Acknowledgements	iv
Abstract	vii
Nomenclature	xii
Abbreviations	7
1 Introduction	13
1.1 Components of Cellular Wi-Fi interworking	15
1.1.1 Overview of LTE networks	15
1.1.2 Overview of Wi-Fi networks	23
1.2 Interworking of different wireless access technologies	25
1.3 Evolution of Cellular Wi-Fi Interworking	27
1.4 Objectives and scope of the thesis	29
1.5 Organization of the thesis	30
2 Radio level integration architectures	32
2.1 Introduction to RLI architectures	32
2.1.1 Advantages of RLI architectures	33
2.2 Existing and proposed RLI architectures	35
2.2.1 3GPP architectures on radio level integration	35
2.2.2 Proposed RLI architectures	39
2.3 Link aggregation strategies for RLI architectures	43
2.4 Simulation setup	45
2.5 Performance results	48
2.5.1 Analysis of Expt #1 results	48
2.5.2 Analysis of Expt #2 results	48
2.5.3 Analysis of Expts #3 and #4 results	49
2.5.4 Analysis of Expt #5 results	51
2.6 Challenges associated with LWIP architecture	52
2.6.1 Does packet split (split bearer) has merits?	52

2.6.2	Is TCP a stumbling block for packet split?	52
2.7	Summary	53
3	Downlink traffic steering in LWIP architecture	54
3.1	Motivation	54
3.2	Related work	55
3.3	Proposed work: PRECISE	57
3.3.1	System model	58
3.3.2	IM Phase of PRECISE: Interference mitigation using orthogonal RATs	61
3.3.3	GI Phase of PRECISE: GBR improvement using dynamic power control	62
3.3.4	Flow steering across LTE and Wi-Fi links	63
3.3.5	Obtaining decision making parameters for TOPSIS	63
3.4	Simulation setup	65
3.5	Performance results	66
3.5.1	SINR distribution in the indoor scenario	66
3.5.2	Ensure GBR in the network	68
3.5.3	Different phases of PRECISE algorithm	68
3.5.4	Throughput analysis	68
3.6	Summary	70
4	Uplink traffic steering in LWIP architecture	71
4.1	Motivation	71
4.1.1	Design requirements for Uplink traffic steering	72
4.2	Related work	73
4.3	Proposed NCF algorithms for uplink traffic steering	74
4.3.1	Dynamic Optimal Uplink Traffic steering Algorithm (DOUTA)	77
4.3.2	Fast UpliNk through Direct medium access (FUND)	82
4.3.3	FUND with fair channel access (FUND++)	84
4.3.4	Enhanced UpliNk With viRtuAl Polling (E-UNWRAP)	86
4.3.5	Realization of NCF algorithms in LWIP System	89
4.3.6	Benefits of NCF algorithms	90
4.4	Simulation setup	91
4.5	Performance results	92
4.5.1	Performance results of DOUTA algorithm	93
4.5.2	Performance results of FUND algorithm	94
4.5.3	Performance results of FUND++ algorithm	96
4.5.4	Performance results of E-UNWRAP algorithm	96
4.6	Summary	100

5	Optimizing LWIP to efficiently support transport layer protocols	101
5.1	Motivation	101
5.2	Related work	102
5.3	Proposed VISIBLE mechanism for downlink traffic steering	104
5.3.1	LWIP packet steering	104
5.3.2	Analysis of packet steering techniques	105
5.3.3	Virtual congestion control with Boost acknowledgment: VISIBLE mechanism	107
5.4	Simulation setup	112
5.5	Performance results	112
5.5.1	Performance of different phases of VISIBLE mechanism	113
5.5.2	Performance of LWIP vs LWIP+VISIBLE	115
5.5.3	Performance of LWIP+VISIBLE vs MPTCP	115
5.5.4	Performance of different link aggregation architectures	116
5.6	Summary	117
6	Efficient placement of LWIP nodes	118
6.1	Related work	118
6.2	System model	119
6.2.1	Building model	119
6.2.2	Path Loss model for LTE network	120
6.2.3	Path Loss model for Wi-Fi network	120
6.3	Optimization models for placement of LWIP nodes	121
6.3.1	Models for determining minimal number of LWIP nodes required for deployment of LWIP system	122
6.3.2	Model for optimal placement of LWIP nodes	124
6.3.3	Models to obtain optimal power setting for operation of LWIP nodes and LWIP-UEs	125
6.4	Performance results	127
6.4.1	Result of Min-NC-LWIP and Min-C-LWIP models	127
6.4.2	Result of optimal LWIP placement model	128
6.4.3	Result for energy saving at LWIP nodes and LWIP-UEs	130
6.5	Summary	133
7	Prototyping of RLI architectures	135
7.1	Introduction to prototyping of RLI architectures	135
7.2	LWIP prototyping	135
7.2.1	LTE testbed using OAI platform	137
7.2.2	Realization of LWIP testbed using OAI platform	137
7.2.3	LWIP testbed: UDP results	141

7.2.4	LWIP testbed: TCP results	143
7.3	LWA prototyping	145
7.3.1	Traffic steering in LWA testbed	146
7.3.2	Realization of LWA testbed using OAI platform	147
7.4	Performance comparison of LWA and LWIP prototypes	147
7.5	Coupling LWA architecture with MPTCP	148
7.5.1	Multipath TCP	148
7.5.2	MPTCP over LWA	149
7.6	Performance results of MPTCP over LWA	149
7.6.1	Network congestion scenario	151
7.6.2	Channel contention scenario	153
7.6.3	Mixed: Network congestion and channel contention scenario	156
7.7	Summary	157
8	Conclusions and Future work	159
8.1	Conclusions	159
8.2	Future work	161
	List of Publications	163
	References	168

List of Figures

1.1	Enhancement of key capabilities from IMT-Advanced to IMT-2020 [1]. . . .	14
1.2	LTE architecture.	16
1.3	LTE protocol stack - Control plane.	19
1.4	LTE protocol stack - Data plane.	19
1.5	LTE frame structure.	21
1.6	Wi-Fi architecture.	24
1.7	Wi-Fi protocol stack.	25
1.8	Optimizations at different layers of protocol stack for interworking.	27
1.9	Evolution of cellular Wi-Fi interworking.	28
1.10	Organization of the thesis.	30
2.1	Colocated RLI Architecture.	33
2.2	Non-colocated RLI Architecture.	33
2.3	Diversification in the region of association with different RATs using RLI architectures.	34
2.4	3GPP colocated LTE Wi-Fi aggregation architecture [2].	36
2.5	3GPP non-colocated LTE Wi-Fi aggregation architecture [2].	36
2.6	3GPP LTE Wi-Fi Integration with IPsec tunnel (LWIP) architecture. . . .	38
2.7	Proposed LWIP, LWA, and LWIR architectures.	40
2.8	Link Aggregation Strategies for RLI architectures.	44
2.9	NS-3 class diagram for LWIP implementation.	45
2.10	Expt #1: Variation in UDP throughput vs ADR of UDP flows; One UE case. . . .	49
2.11	Expt #2: Variation in UDP throughput vs ADR of UDP flows; Four UEs case. . . .	49
2.12	Expt #3: Home Scenario with one LWIP node; variation in system throughput vs number of UEs; Mixed Traffic, UDP-Heavy.	50
2.13	Expt #4: Home Scenario with one LWIP node; variation in system throughput vs number of UEs; Mixed Traffic, TCP-Heavy.	50
2.14	Expt #5: REM Plot for Indoor Stadium layout with 10 LWIP Nodes. . . .	50
2.15	Expt #5; Indoor Stadium with 10 LWIP nodes; variation in system throughput vs number of UEs; Mixed Traffic.	50
2.16	Expt #5: Delay of Voice Traffic in Indoor Stadium with 10 LWIP nodes. . .	51

2.17	Expt #5: Jitter of Voice Traffic in Indoor Stadium with 10 LWIP nodes.	51
3.1	System Model.	59
3.2	Variation in coverage regions of LTE and Wi-Fi cells observed in different phases of PRECISE algorithm.	60
3.3	SINR distribution 3D-map of the building chosen for conducting experiment with four C-LWIP nodes. The x, y, and z values of C-LWIP nodes are also given in the map.	65
3.4	CDF of SINR of UEs.	67
3.5	Different events triggered over time in case of <i>load</i> = 100, 300, and 600 flows in the network.	67
3.6	Triggers for different network loads.	69
3.7	CDF of throughput of UEs.	69
3.8	Throughput observed with different loads.	70
3.9	Number of unmet GBR flows.	70
4.1	The optimization which is feasible in Wi-Fi domain.	73
4.2	Enhanced LWIP architecture which supports both downlink and uplink traffic steering.	74
4.3	Objectives of Network Coordination Function Algorithms.	75
4.4	Proposed NCF Algorithms.	76
4.5	Aggregate Wi-Fi throughput observed with five UEs in the network.	78
4.6	Aggregate Wi-Fi throughput observed with 10 UEs in the network.	78
4.7	Aggregate Wi-Fi throughput observed with 20 UEs in the network.	78
4.8	Traffic Steering at LWIP Node.	79
4.9	Traffic Steering at UE associated to LWIP Node.	79
4.10	Instantaneous network throughputs observed for different decision-making intervals (T).	83
4.11	Operation of FUND algorithm.	85
4.12	Operation of UNWRAP algorithm (Variable Operation Time).	88
4.13	Experimental scenario for evaluation of NCF algorithms.	92
4.14	Variation in Wi-Fi throughput with offered load - DCF:Wi-Fi Offloading vs DOUTA.	94
4.15	Variation in time elapsed in collisions with offered load - DCF:Wi-Fi Offloading vs DOUTA.	94
4.16	Variation in time elapsed in collisions with offered load - DCF vs NCF:FUND.	95
4.17	Variation in Wi-Fi throughput with offered load - DCF vs NCF:FUND.	95
4.18	Variation in system fairness with offered load - DCF vs NCF:FUND.	96
4.19	Variation in system fairness with offered load - NCF:FUND vs NCF:FUND++.	97
4.20	Variation in Wi-Fi throughput with offered load - NCF:FUND vs NCF:FUND++.	97

4.21	Variation in time elapsed in collisions with offered load - NCF:FUND vs NCF:FUND++.	97
4.22	Variation in Wi-Fi throughput with offered load - DCF vs NCF:UNWRAP - Variable operation.	98
4.23	Variation in time elapsed in collisions with offered load - DCF vs NCF:UNWRAP - Variable operation.	98
4.24	Variation in system fairness with offered load - DCF vs NCF:UNWRAP - Variable operation.	98
4.25	Variation in Wi-Fi Throughput with offered load - DCF vs NCF:E-UNWRAP - Full operation.	98
4.26	Variation in time elapsed in collisions with offered load - DCF vs NCF:E-UNWRAP - Full operation.	99
4.27	Variation in system fairness with offered load - DCF vs NCF:E-UNWRAP - Full operation.	99
5.1	Packet steering model at LWIP node.	105
5.2	Queue length of the system for L-RTT & Q-Depl steering techniques.	106
5.3	An example of virtual congestion control procedure in VISIBLE mechanism.	109
5.4	Experimental setup used for evaluation of VISIBLE mechanism.	113
5.5	Different phases of VISIBLE in VISIBLE+LWIP system.	114
5.6	Holding time of ACK packets in VISIBLE+LWIP system.	114
5.7	Number of DUP-ACKs held at VISIBLE+LWIP node.	114
5.8	Lengths of LTE and Wi-Fi queues.	114
5.9	Congestion window growth of LWIP and LWIP+VISIBLE architectures.	115
5.10	RTT of TCP flow in case of LWIP and LWIP+VISIBLE architectures.	115
5.11	Throughputs of MPTCP and LWIP+VISIBLE.	116
5.12	Throughputs of basic LWA, basic LWIP, and LWIP+VISIBLE.	116
6.1	Building model considered.	120
6.2	Non-colocated LWIP deployment with MIR placement.	128
6.3	Colocated LWIP deployment with MIR placement.	128
6.4	LTE SINR heatmap and subregion association in case of non-colocated LWIP deployment with optimal placement model.	129
6.5	Wi-Fi SINR heatmap and subregion association in case of non-colocated LWIP deployment with optimal placement model.	129
6.6	LTE SINR heatmap and subregion association in case of colocated LWIP deployment with optimal placement model.	130
6.7	Wi-Fi SINR heatmap and subregion association in case of colocated LWIP deployment with optimal placement model.	130

6.8	SINR CDF observed in all the sub-regions for a non-colocated deployment with optimal placement model.	131
6.9	SINR CDF observed in all the sub-regions for a colocated deployment with optimal placement model.	131
6.10	Sub-regions associativity : non-colocated placement.	131
6.11	Sub-regions associativity : colocated placement.	131
6.12	Energy consumed at LWIP node : non-colocated deployment.	132
6.13	Energy consumed at LWIP node : colocated deployment.	132
6.14	Average energy spent by a UE : non-colocated deployment.	132
6.15	Average energy spent by a UE : colocated deployment.	132
7.1	RLI architectures and their layer of integration.	136
7.2	OpenAirInterface LTE software stack [3].	137
7.3	Protocol implementation structure of LWIP prototype system.	138
7.4	LWIP testbed setup.	140
7.5	Instantaneous throughput in iPerf UDP test (in downlink \rightarrow 802.11b). . . .	142
7.6	Instantaneous throughput in iPerf UDP test (in downlink \rightarrow 802.11g). . . .	142
7.7	CDF of jitter for iPerf test (in downlink \rightarrow 802.11g).	143
7.8	Overall throughput observed for 16 MB and 32 MB file sizes in low contention scenario.	144
7.9	Throughput of Wi-Fi observed for 16 MB and 32 MB file sizes in low contention scenario.	144
7.10	Time to download a 32 MB file using different LASs in low contention scenario.	144
7.11	Overall throughput observed for 16 MB and 32 MB file sizes using different LASs in high contention scenario.	144
7.12	Throughput of Wi-Fi observed for 16 MB and 32 MB file sizes with high contention.	145
7.13	Time to download a 32 MB file with high contention for different LASs. . . .	145
7.14	LWA testbed setup.	147
7.15	Download time observed with different RLI prototypes.	148
7.16	Architecture of MPTCP over LWA (MLWA).	150
7.17	Experimental setup for evaluation of MPTCP, LWA and MLWA.	151
7.18	Throughput observed while downloading a file of 16 MB by varying congestion losses in the network.	152
7.19	Throughput observed while downloading a file of 32 MB by varying congestion losses in the network.	152
7.20	Throughput observed while downloading a file of 64 MB by varying congestion losses in the network.	153
7.21	Congestion window observed for LWA operation while downloading a file of 64 MB with 10^{-4} loss rate.	153

7.22	Congestion window observed for MPTCP operation while downloading a file of 64 MB with 10^{-4} loss rate.	153
7.23	Congestion window observed for MLWA operation while downloading a file of 64 MB with 10^{-4} loss rate.	154
7.24	Download time in case of LWA, MPTCP, and MLWA by varying file sizes under low Wi-Fi channel contention scenario.	155
7.25	Download time in case of LWA, MPTCP, and MLWA by varying file sizes under moderate Wi-Fi channel contention scenario.	155
7.26	Channel busy time observed in Wi-Fi channel when a 32 MB file was downloaded under low Wi-Fi channel contention scenario.	155
7.27	Channel busy time observed in Wi-Fi channel when a 32 MB file was downloaded under moderate Wi-Fi channel contention scenario.	155
7.28	Download time for a 32 MB file with network congestion and moderate channel contention scenario.	156
7.29	Download time for a 32 MB file with network congestion and moderate channel contention scenario.	156
7.30	Congestion window for LWA operation while a 32 MB file downloaded with 10^{-3} loss rate under moderate channel contention.	157
7.31	Congestion window for MPTCP operation while a 32 MB file is downloaded with 10^{-3} loss rate under moderate channel contention.	157
7.32	Congestion window for MLWA operation while a 32 MB file is downloaded with 10^{-3} loss rate under moderate channel contention.	157

List of Tables

1.1	Interfaces in LTE architecture and their purpose	16
1.2	Downlink OFDM modulation parameters of LTE	23
1.3	Comparison of various IEEE 802.11 standards	26
2.1	Comparison of proposed RLI architectures	43
2.2	Simulation parameters for evaluation of different LASs in LWIP architecture	46
2.3	Percentage distribution of user traffic	47
3.1	Notations used in PRECISE algorithm	58
3.2	Simulation parameters for evaluating PRECISE algorithm	66
4.1	Characteristics of proposed NCF algorithms	77
4.2	Simulation parameters for evaluation of NCF algorithms	93
4.3	Comparison of NCF algorithms	99
5.1	Notations used in VISIBLE mechanism	111
5.2	NS-3 parameters to evaluate VISIBLE mechanism	113
6.1	Notations used in optimization models for placement of LWIP nodes	121
7.1	Parameters to evaluate real-time performance of LWIP testbed	140
7.2	Hardware parameters of LWIP testbed	141

Abbreviation	Expanded
<i>ABS</i>	- Almost Blank Sub-frame
<i>ACK</i>	- Acknowledgement
<i>ADSN</i>	- ACK Duplication Sequence Number
<i>AM</i>	- Acknowledged Mode
<i>ANDSF</i>	- Access Network Discovery and Selection Function
<i>AP</i>	- Access Points
<i>ARPU</i>	- Average Revenue Per User
<i>ARQ</i>	- Automatic Repeat Request
<i>AS</i>	- Access Stratum
<i>BI</i>	- Bearer ID
<i>BS</i>	- Base Station
<i>BSR</i>	- Buffer Status Report
<i>BSSID</i>	- Basic Service Set Identifier
<i>BWA</i>	- Bandwidth Allocation
<i>C/DPlane</i>	- Control/Data Plane
<i>CA</i>	- Collision Avoidance
<i>CAPEX</i>	- Capital Expenditure
<i>CCA</i>	- Clear Channel Assessment
<i>CDF</i>	- Cumulative Distribution Function
<i>CSMA</i>	- Carrier Sense Multiple Access
<i>CWRP</i>	- Contention Window Regulation Procedure
<i>DCF</i>	- Distributed Coordination Function
<i>DC</i>	- Dual Connectivity
<i>DOUTA</i>	- Dynamic Optimal Uplink Traffic Steering Algorithm
<i>DRB</i>	- Data Radio Bearer
<i>DRX</i>	- Discontinuous Reception
<i>DSMIPv6</i>	- Dual Stack Mobile IPv6
<i>DUP – ACKs</i>	- DUPLICATE ACKnowledgements
<i>eMBB</i>	- Enhanced Mobile Broadband
<i>eNB</i>	- Evolved Node B
<i>eICIC</i>	- Enhanced Inter-Cell Interference Co-ordination

<i>E – UTRA</i>	- Evolved Universal Terrestrial Radio Access
<i>E – UNWRAP</i>	- Enhanced Uplink With virtual Polling
<i>EAP</i>	- Extensible Authentication Protocol
<i>EPC</i>	- Evolved Packet Core
<i>ePDG</i>	- Evolved Packet Gateway
<i>EPS</i>	- Evolved Packet System
<i>FDD</i>	- Frequency Division Duplex
<i>FFR</i>	- Fractional Frequency Reuse
<i>FI</i>	- Fairness Index
<i>FS – N – LAS</i>	- Flow Split Naive Link Aggregation Strategy
<i>FUND</i>	- Fast Uplink through Direct medium access
<i>FUND + +</i>	- FUND with fair Channel Access
<i>GBR</i>	- Guaranteed Bit Rate
<i>GRE</i>	- Generic Routing Encapsulation
<i>GTP</i>	- GPRS Tunneling Protocol
<i>HAF</i>	- Hybrid Access Femto
<i>HARQ</i>	- Hybrid Automatic Repeat Request
<i>HCF</i>	- Hybrid Coordination Function
<i>HetNet</i>	- Heterogeneous Network
<i>HeNB</i>	- Home evolved Node B
<i>HESSID</i>	- Homogeneous Extended Service Set Identifier
<i>HRW</i>	- Highest Received SN on WLAN
<i>HSS</i>	- Home Subscriber Server
<i>HTTP</i>	- Hyper Text Transfer Protocol
<i>IAT</i>	- Instantaneous Average Throughput
<i>ICIC</i>	- Inter-Cell Interference Coordination
<i>IFOM</i>	- IP flow mobility
<i>IKE</i>	- Internet Key Exchange
<i>IMS</i>	- IP Multimedia Subsystem
<i>ITU</i>	- International Telecommunications Union
<i>IP</i>	- Integer Programming

<i>ISI</i>	- Inter-Symbol Interference
<i>LAA</i>	- Licensed Assisted Access
<i>LAL</i>	- Link Aggregation Layer
<i>LIA</i>	- Link Increase Algorithm
<i>LP</i>	- Linear Programming
<i>LTE</i>	- Long Term Evolution
<i>LTE – U</i>	- LTE in Unlicensed
<i>LWA</i>	- LTE WLAN Aggregation
<i>LWAAP</i>	- LWA Adaptation Protocol
<i>LWIP</i>	- LTE WLAN Radio Level Integration with IPSec Tunnel
<i>LWIR</i>	- LTE WLAN Integration at RLC Layer
<i>MAC</i>	- Medium Access Control
<i>MADM</i>	- Multi Attribute Decision Making
<i>MAPCON</i>	- Multiple-Access PDN Connectivity
<i>MBR</i>	- Maximum Bit Rate
<i>MBS</i>	- Macro Base Station
<i>MCS</i>	- Modulation and Coding Scheme
<i>MIB</i>	- Master Information Block
<i>MINLP</i>	- Mixed Integer Non-Linear Programming
<i>MILP</i>	- Mixed Integer Linear Programming
<i>MIMO</i>	- Multiple Input Multiple Output
<i>MIR</i>	- Minimum Interference Region
<i>MME</i>	- Mobility Management Entity
<i>MPTCP</i>	- Multipath TCP
<i>MTC</i>	- Machine Type Communication
<i>NAT</i>	- Network Address Translation
<i>NAS</i>	- Non Access Stratum
<i>NIS</i>	- Negative Ideal Solution
<i>NMP</i>	- Number of Missing PDUs
<i>NCF</i>	- Network Coordination Function
<i>NSWO</i>	- Non-Seamless WLAN Offload
<i>OFDMA</i>	- Orthogonal Frequency Division Multiple Access

<i>OAI</i>	- OpenAirInterface
<i>OFDM</i>	- Orthogonal Frequency Division Multiplexing
<i>OOO</i>	- Out-of-Order
<i>OPEX</i>	- Operational Expenditure
<i>OPF</i>	- Optimal Placement of Femtocells
<i>P – GW</i>	- Packet Gateway
<i>PCF</i>	- Point Coordination Function
<i>PBR</i>	- Prioritised Bit Rate
<i>PC</i>	- Power Control
<i>PCEF</i>	- Policy and Charging Enforcement Function
<i>PCRF</i>	- Policy and Charging Rules Function
<i>PDCP</i>	- Packet Data Convergence Protocol
<i>PDF</i>	- Policy Decision Function
<i>PDN</i>	- Packet Data Network
<i>PDU</i>	- Protocol Data Unit
<i>PER</i>	- Packet Error Rate
<i>PF</i>	- Proportional Fair
<i>PIFS</i>	- PCF Inter Frame Spacing
<i>PIS</i>	- Positive Ideal Solution
<i>PL</i>	- Path Loss
<i>PMD</i>	- Physical Medium Dependent
<i>PMIP</i>	- Proxy Mobile IPv6
<i>PLCP</i>	- Physical Layer Convergence Procedure
<i>PRACH</i>	- Physical Random Access Channel
<i>PRB</i>	- Physical Resource Blocks
<i>PRECISE</i>	-Power awaRE dynamiC traffic StEering
<i>PMD</i>	- Physical Medium Dependent
<i>PSS</i>	- Primary synchronization Signals
<i>PS – N – LAS</i>	- Packet Split Naive Link Aggregation Strategy
<i>Q – Depl</i>	- Queue Depletion Rate
<i>QCI</i>	- QoS Class Indicator
<i>QoS</i>	- Quality of Service
<i>RAN</i>	- Radio Access Network

<i>RAT</i>	- Radio Access Technology
<i>RB</i>	- Resource Block
<i>RC</i>	- Relative Closeness
<i>REG – ORD</i>	- Regulated order
<i>REM</i>	- Radio Environmental Map
<i>RLC</i>	- Radio Link Control
<i>RLI</i>	- Radio Level Integration
<i>RNTI</i>	- Radio Network Temporary Identifier
<i>ROHC</i>	- Robust Header Compression
<i>RoI</i>	- Return on Investment
<i>RR Scheduler</i>	- Round Robin Scheduler
<i>RRC</i>	- Radio Resource Control
<i>RS</i>	- Remote Server
<i>RSSI</i>	- Received Signal Strength Indication
<i>RTT</i>	- Round Trip Time
<i>S – GW</i>	- Serving Gateway
<i>SAE</i>	- System Architecture Evolution
<i>SDF</i>	- Service Data Flow
<i>SDLC</i>	- Synchronous Data Link Control
<i>SDR</i>	- Software Defined Radio
<i>SDU</i>	- Service Data Unit
<i>SeNB</i>	- Small cell evolved NodeB
<i>SGSN</i>	- Serving GPRS Support Node
<i>SIBs</i>	- System Information Blocks
<i>SINR</i>	- Signal-to-Interference plus Noise Ratio
<i>SINR_{Th}</i>	- Threshold SINR
<i>S – LRTT</i>	- Smoothed Link Round Trip Time
<i>SON</i>	- Self Organizing Network
<i>SOPC</i>	- Sub-optimal Power Control
<i>SRB</i>	- Signalling Radio Bearer
<i>SPS</i>	- Semi-Persistent Scheduling
<i>STD – ORD</i>	- Standard order
<i>SSID</i>	- Service Set Identifier

<i>SSS</i>	- Secondary Synchronization Signals
<i>TB</i>	- Transport Block
<i>TCP</i>	- Transmission Control Protocol
<i>TDD</i>	- Time Division Duplex
<i>TEP</i>	- Tunnel End Point
<i>TM</i>	- Transparent Mode
<i>TOPSIS</i>	- Technique for Order Performance by Similarity to Ideal Solution
<i>TSM</i>	- Traffic Steering Master
<i>TSS</i>	- Traffic Steering Slave
<i>TTI</i>	- Transmission Time Interval
<i>UE</i>	- User Equipment
<i>UM</i>	- Unacknowledged Mode
<i>URLLC</i>	- Ultra-Reliable and Low-Latency Communications
<i>URI</i>	- User Location Information
<i>VCP</i>	- Virtual Contention Period
<i>VISIBLE</i>	- Virtual congestion control with Boost acknowledgment
<i>VWS</i>	- Virtual Wi-Fi Scheduler
<i>Wi-Fi</i>	- Wireless Fidelity
<i>WLAN</i>	- Wireless Local Area Network
<i>WT</i>	- Wireless Termination

Chapter 1

Introduction

The huge growth in the number of smartphones used and the traffic generated by them have become a major challenge to the telecommunication industry. International Telecommunications Union (ITU) envisions that by 2020 the requirements that a mobile network should cater will be humongous [1]. The penetration of multi-featured electronic gadgets such as smartphones, tablets, and laptops in the market and the popularity of mobile applications (native and web) developed for these devices are main reasons for this humongous data demand. It is observed that smartphones generate approximately 1,614 MB of data per month which is 48 times of the data generated by a typical basic-feature cell phone (which generates only 33 MB per month of mobile data traffic) [4]. Also, mobile data traffic growth will continue to increase and reach 49 Exabytes by per month by 2021, and annual traffic will exceed half a zettabyte.

Fig. 1.1 shows the key enhancements to International Mobile Telecommunication Advanced (IMT-Advanced) system with a target date set for 2020 (IMT-2020). ITU envisions the requirements for IMT-2020 a.k.a. 5G as follows, (1) Peak data rate of 20 Gbps, which is 20x higher, (2) Area traffic capacity of 10 Mbps/ m^2 , which is 100x higher, (3) Network energy efficiency of 100x, (4) Connection density of 10^6 , which is 10x higher, (5) latency of 1 ms, which is 10x lower, (6) Spectrum efficiency of 3x, (7) Support for mobility up to 500 Kmph, and (8) Per user experienced data rate of 100 Mbps, which is 10x high. Among these requirements, area traffic capacity, network energy efficiency, and peak data rate top the list. As densification of small cell deployment targets to serve the growth in area traffic capacity, the densification introduces challenges such as co-tier interference, improper

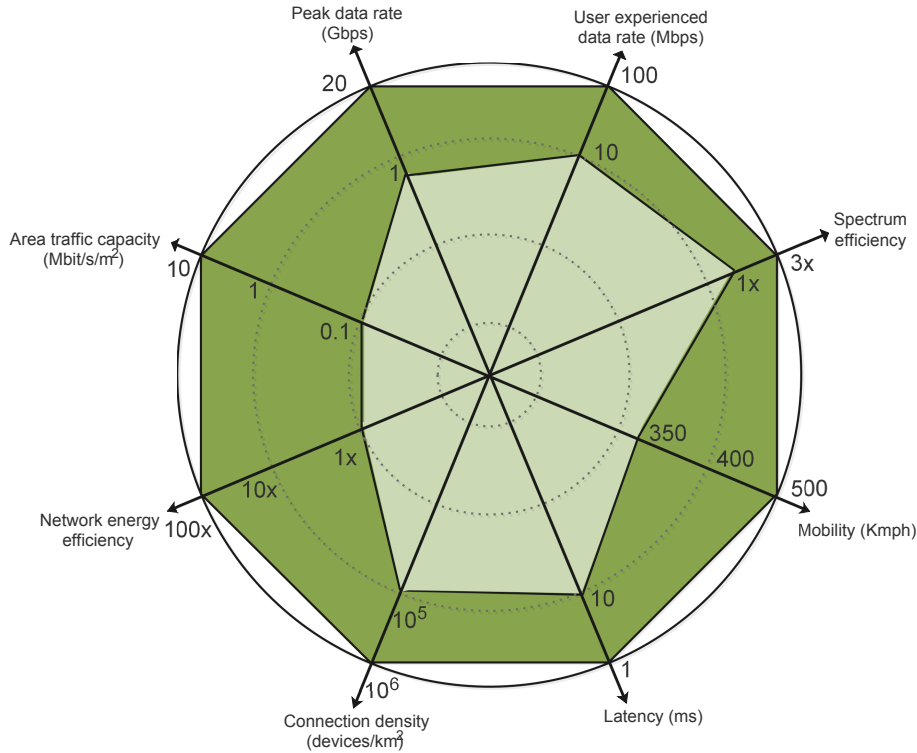


Figure 1.1: Enhancement of key capabilities from IMT-Advanced to IMT-2020 [1].

channel utilization, and inefficient placement of these small cells in indoor environments due to structural limitations of the buildings. The second highest requirement is on the energy efficiency of the networks, as the wireless services are contributing to larger volume of carbon foot-print [5]. Study from [6] reveals that the major energy component of the cellular network operation is from the Radio Access Network (RAN), of which cell site consumes 72% of the total energy spent. Redesigning cellular system architecture is the key to resolve the power consumption challenge at RAN of the next generation of cellular networks. The third major requirement which arises is the Quality of Service (QoS) provisioning. 5G is designed to be a service-oriented architecture with support for enhanced mobile broadband (eMBB), massive Machine-Type Communication (mMTC), and Ultra-Reliable and Low-Latency Communication (URLLC) [7]. The targeted QoS is viable when multiple RATs coexist and serve flexibly across in order to meet the demand. However, the telecommunication service providers/operators face many challenges in improving cellular network capacities to match these ever-increasing data demands due to low, almost flat Average Revenue Per User (ARPU) and low Return on Investment (RoI). Spectrum resource crunch and licensing requirement for operation in cellular bands further complicate

the procedure to support and manage the network.

In order to deal with the aforementioned challenges and to meet ITU's targeted 5G requirements, one of the most vital solutions is to leverage the integration benefits of multiple radio access technologies (Multi-RAT). For instance, cellular base stations (BSs) operating with a limited bandwidth on licensed band can be integrated with Wi-Fi Access Points (APs) which operate on unlicensed band with more bandwidth. A closer level of cellular and Wi-Fi coupling/interworking not only addresses the data demand but also improves QoS by unified connection management to user devices. In this thesis, we address some of the challenges associated with interworking of cellular and Wi-Fi networks.

1.1 Components of Cellular Wi-Fi interworking

In this section the overview of cellular networks, specifically LTE will be described, followed by the description of Wireless Local Area Network (WLAN).

1.1.1 Overview of LTE networks

LTE (Long Term Evolution) or E-UTRA (Evolved Universal Terrestrial Radio Access) is also referred to as "the gold standard of wireless technology" because of its speed and enhanced coverage compared to its predecessor technologies. Also, compared to 3G, LTE provides a higher data rate, low latency, improved network responsiveness, high spectrum efficiency, improved cost efficiency, enhanced security, and better QoS. The standards specifications for LTE system were developed by Third Generation Partnership Project (3GPP) [8].

The LTE architecture includes two major components: the radio access network and the core network. Evolved NodeB (eNB) or eNodeB is the radio access network component. Multiple eNBs are interconnected via X2-interface. The core network (called as Evolved Packet Core - EPC) components include Serving Gateway (S-GW), Packet Data Network Gateway (P-GW), Mobility Management Entity (MME), Policy and Charging Rules Function (PCRF) Server, and Home Subscriber Server (HSS). The access network is connected to the core network via S1-interface. A User Equipment (UE) refers to the device used by an end-user to communicate with eNodeB. Evolved Packet System (EPS) includes Evolved Universal Terrestrial Radio Access (E-UTRA) and EPC. Fig. 1.2 shows all the components

of LTE architecture and the interfaces across various components.

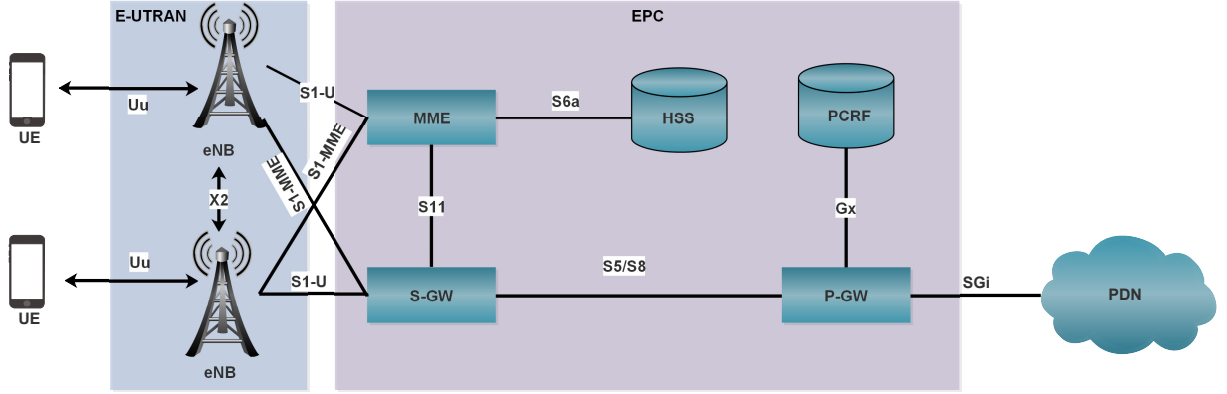


Figure 1.2: LTE architecture.

Table 1.1: Interfaces in LTE architecture and their purpose

Interface	Position and Function
S1-MME	Reference point for the control plane protocol between E-UTRAN and MME.
S1-U	Reference point between E-UTRAN and Serving GW for the per bearer user plane tunneling and inter eNodeB path switching during handover.
S5	It provides user plane tunneling and tunnel management between S-GW and P-GW. It is used for S-GW relocation due to UE mobility and if S-GW needs to connect to a non-located P-GW for the required PDN connectivity.
S6a	It enables transfer of subscription and authentication data for authenticating/authorizing user access to the evolved system (AAA interface) between MME and HSS.
Gx	It provides transfer of QoS policy and charging rules from PCRF to Policy and Charging Enforcement Function (PCEF) in the PDN GW.
S8	Inter-PLMN reference point providing user and control plane between S-GW in visiting PLMN and P-GW in the Home PLMN. S8 is the inter-PLMN variant of S5.
S9	It provides transfer of (QoS) policy and charging control information between Home PCRF and Visited PCRF in order to support local breakout function.
S11	Reference point between MME and S-GW.
SGi	It is the reference point between P-GW and PDN like Internet. PDN may be an operator external public or private packet data network or an intra operator PDN, <i>e.g.</i> , for the provision of IP Multimedia Subsystem (IMS) services. This reference point corresponds to Gi for 3GPP accesses.

Table 1.1 details the interfaces used in LTE architecture and their usage. The components of LTE architecture [9] and [10] are detailed as follows:

- 1. Evolved Node-B:** The eNB sends and receives radio transmissions to all the mobiles (UEs) using the analog and digital signal processing functions of the LTE air interface. It controls the low-level operation of UEs, by sending them signaling messages such as broadcast messages (MIB - Master Information Block), control messages (SIBs - System Information Blocks), synchronization signals (PSS, SSS *i.e.*, Primary and secondary synchronization signals), and handover commands. Each eNB connects with the EPC by means of S1 interface and it can also be connected to nearby base stations by X2 interface, which is mainly used for signaling and packet forwarding during handover. The eNB supports the following functions: (1) Inter-cell radio resource management, (2) Resource block control, (3) Radio admission control, (4) eNB measurement and configuration, and (5) Dynamic resource allocation.
- 2. Serving Gateway:** S-GW routes and forwards data packets to and from the UE. A UE can get associated utmost with one S-GW. It acts as a mobility anchor point. It plays a significant role during inter-eNodeB handovers. It acts as a local mobility anchor (LMA) point for inter-eNodeB handover and assists the eNodeB reordering function by sending one or more "end marker" packets to the source eNodeB immediately after switching the path. It also acts as a mobility anchor for inter-3GPP mobility (terminating the S4 interface from a Serving GPRS Support Node (SGSN) and relaying the traffic between 2G/3G system and a P-GW). It supports transport level packet marking and allows accounting and QoS class indicator (QCI) granularity for charging. Replicating of user traffic in the event of Lawful Interception is done at S-GW. It allows reporting of user location information (ULI).
- 3. Packet Data Network Gateway:** P-GW is the gateway which terminates SGi interface towards PDN. P-GW does the following functions: (1) Per-user based packet filtering (for *e.g.*, deep packet inspection), (2) Lawful Interception, (3) UE IP address allocation, (4) Transport level packet marking in the uplink and downlink, *e.g.*, setting the DiffServ Code Point, based on the QCI of the associated EPS bearer, (5) Uplink and downlink service level charging, gating control, and rate enforcement, and (6) Downlink rate enforcement based on the accumulated Maximum Bit Rate (MBRs) of the aggregate of Service Data Flows (SDFs) with the same Guaranteed Bit Rate (GBR) QCI (*e.g.*, by rate policing/shaping).

4. **Home Subscriber Server:** HSS is the master database for all UEs. It is the entity containing subscription-related information to support the network entities actually handling calls/sessions. The HSS is responsible for holding the following user related information: (1) User identification, numbering and addressing information, (2) User security information, network access control information for authentication and authorization, (3) User location information at the inter-system level, and (4) User profile information. The HSS generates user security information for mutual authentication, communication integrity check and ciphering.
5. **Mobility Management Entity:** MME is a control plane entity within EPC. It supports the following functions: (1) Mobility Management, (2) Non-Access Stratum (NAS) signalling and security, (3) Inter core network signalling for mobility between 3GPP access networks, (4) Tracking area list management, (5) P-GW and S-GW selection, (6) SGSN selection for handovers to 2G or 3G access networks, (7) Roaming, (8) Authentication, and (9) Bearer management functions including dedicated bearer establishment.
6. **Policy and Charging Rules Function:** PCRF also known as policy server or Policy Decision Function (PDF), is a component of EPC. It is responsible for enforcing charging decisions at P-GW. The policy charging can be based on, (1) Volume-based charging, (2) Time based charging, (3) Volume and time-based charging, or (4) Event-based charging.
7. **User Equipment:** UE refers to the mobile terminal. UE attaches to eNB of LTE network through a radio interface. UE sends Physical Random Access Channel (PRACH) preamble to eNB to latch onto eNB and gets completely attached on successful completion of Radio Resource Control (RRC) procedures. On successful attachment, UE gets an IP address, and a bearer is created from UE till P-GW. A bearer refers to a path that user traffic (IP flows) uses when passing through an LTE network (between UE and P-GW).

Protocol stack of LTE The protocol stacks of LTE networks are discussed here. LTE eNB includes the following layers: (1) Radio Resource Control (RRC), (2) Packet Data Convergence Protocol (PDCP), (3) Radio Link Control (RLC), (4) Medium Access Control

(MAC), and (5) Physical Layer (PHY). Figs. 1.3 and 1.4 show the control and data plane operations at LTE eNB, UE, MME and layers involved in each operation. The detailed functionalities of each layer are as follows:

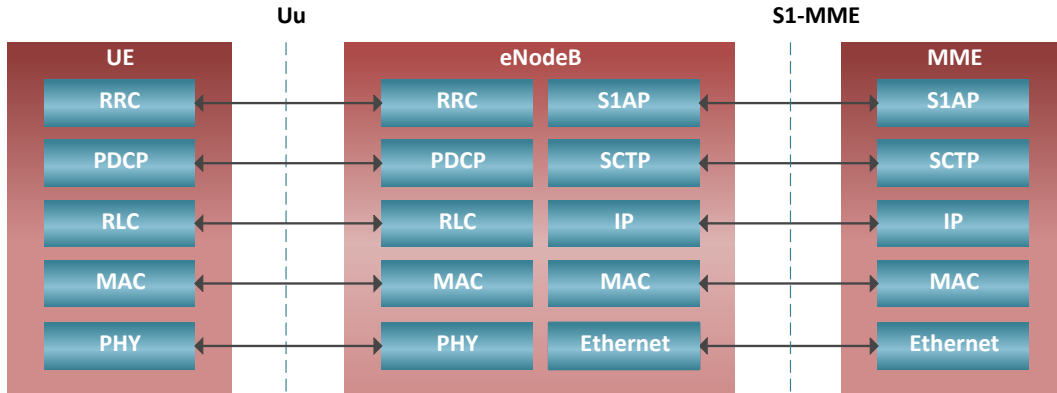


Figure 1.3: LTE protocol stack - Control plane.

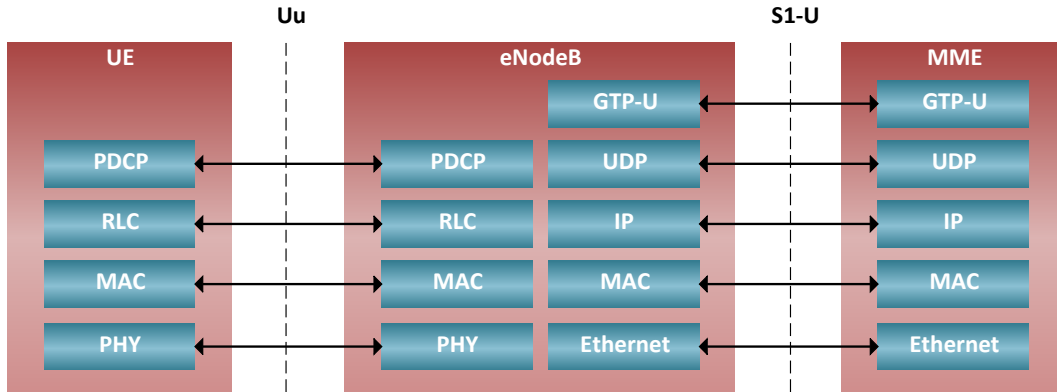


Figure 1.4: LTE protocol stack - Data plane.

1. **Radio Resource Control:** RRC [11] is the key component in LTE protocol stack which is responsible for allocating radio resources. The RRC protocol includes the following main functions: (1) Broadcast of system information, (2) Transmission of information applicable for UEs in RRC_IDLE, *e.g.*, cell (re-)selection parameters, neighbouring cell information and information applicable for UEs in RRC_CONNECTED *e.g.*, common channel configuration information, (3) Paging, (4) Establishment, modification, suspension, resumption, release of RRC connection, including *e.g.*, assignment, modification of UE identity (C-RNTI), establishment, modification, release of Signalling Radio Bearer (SRB) - SRB1, SRB2, and access class barring, (5) Initial security activation *i.e.*, initial configuration of AS integrity protection (SRBs) and AS

ciphering (SRBs, Data Radio Bearer - DRBs), (6) For RNs, configuration of Access Stratum (AS) integrity protection for DRBs, (7) RRC connection mobility including *e.g.*, intra-frequency and inter-frequency handovers, associated security handling *i.e.*, key, algorithm change, specification of RRC context information transferred between UE and eNB, (8) Establishment, modification, release of Radio Bearers (RBs) carrying user data (DRBs), (9) Radio configuration control including *e.g.*, assignment, modification of Automatic Repeat Request (ARQ) configuration, Hybrid ARQ (HARQ) configuration, Discontinuous Reception (DRX) [12] configuration, and (10) QoS control including assignment, modification of semi-persistent scheduling (SPS) configuration information for DL and UL, assignment, modification of parameters for UL rate control in the UE *i.e.*, allocation of a priority and a prioritised bit rate (PBR) for each RB.

2. **Packet Data Convergence Protocol:** PDCP [13] forwards packets to and from the RLC layer. PDCP does the following functions: (1) Header compression and decompression of IP packets using the Robust Header Compression (ROHC) mechanism, (2) Transfer of data (both user plane and control plane), (3) Tags PDCP sequence numbers, (4) In-sequence delivery of upper layer Protocol Data Units (PDUs) at re-establishment of lower layers, (5) Ciphering and deciphering of user plane data and control plane data, (6) Duplicate elimination of lower layer Service Data Units (SDUs) at re-establishment of lower layers for radio bearers mapped on RLC Acknowledged Mode (AM), (7) Integrity protection and integrity verification of control plane data and user plane data, (8) Timer based discard of packets, and (9) Discarding of duplicate packets.

3. **Radio Link Control:** RLC [14] is a layer embedded between MAC and PDCP layers of LTE eNB/UE stack. RLC sublayer sends and receives RLC SDUs to/from the upper layers, and it also sends and receives RLC PDUs to/from layers below. An RLC entity can be configured to perform data transfer in one of the following three modes: Transparent Mode (TM), Unacknowledged Mode (UM) or Acknowledged Mode (AM). RLC TM does not add any header to the PDU nor it does segmentation. It is used for control packet transmissions. RLC UM does not require any response from the receiver. Unlike RLC TM, it does reordering, segmentation, concatenation and adds

RLC header. RLC AM has all the features of RLC UM and it also does retransmission of unacknowledged packets.

The RLC supports the following functions: (1) Transfer of upper layer PDUs, (2) Error correction through ARQ (only for AM data transfer), (3) Concatenation, segmentation and reassembly of RLC SDUs (only for UM and AM modes of data transfer), (4) Re-segmentation of RLC data PDUs (only for AM mode data transfer), (5) Reordering of RLC data PDUs (only for UM and AM modes of data transfer), (6) Duplicate detection (only for UM and AM modes of data transfer), (7) RLC SDU discard (only for UM and AM modes of data transfer), and (8) Protocol error detection (only for AM mode data transfer).

4. **Medium Access Control:** MAC [15] layer lies in between RLC layer and physical layer of LTE stack. MAC in LTE is scheduling based and does the following functionalities: (1) Mapping between logical channels and transport channels, (2) Multiplexing of MAC SDUs from one or different logical channels onto transport blocks (TB) to be delivered to the physical layer on transport channels, (3) Demultiplexing of MAC SDUs from one or different logical channels from transport blocks (TB) delivered from the physical layer on transport channels, (4) Scheduling information reporting, (5) Error correction through HARQ, (6) Priority handling between UEs by means of dynamic scheduling, (7) Priority handling between logical channels of each MAC entity, and (8) Logical channel prioritisation.

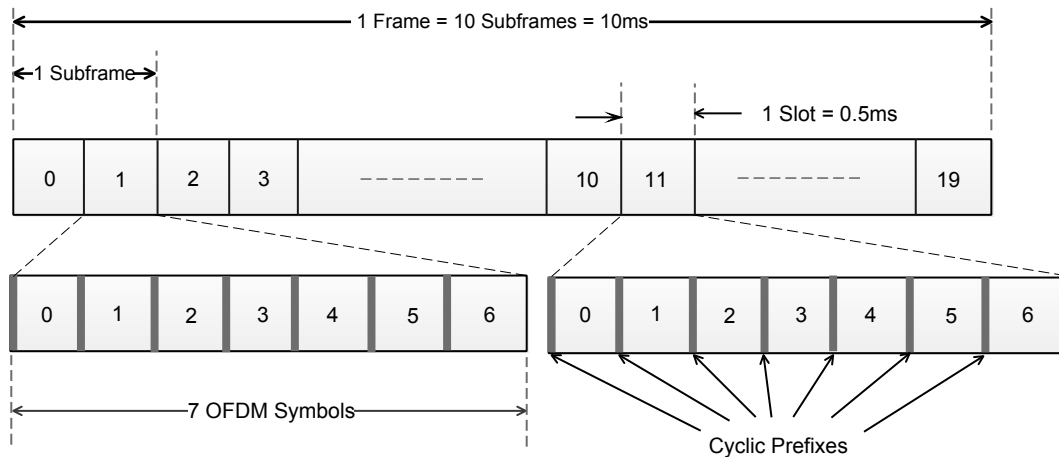


Figure 1.5: LTE frame structure.

5. **Physical Layer:** PHY [16] of LTE supports Time division duplex (TDD) and Fre-

quency division duplex (FDD) modes of operation. FDD is the widely used mode of operation. In FDD, LTE uplink and downlink are separated by a frequency offset specified by [17]. In this section, we discuss LTE multiplexing, frame structure, modulation, and channels. LTE delivers higher data rate compared to 3G due to the following features: (1) Orthogonal Frequency Division Multiplexing (OFDM), (2) Support for wider bandwidth (carrier aggregation), and (3) Multiple Input Multiple Output (MIMO).

Downlink Multiplexing: LTE uses Orthogonal Frequency Division Multiplexing (OFDM), which employs multiple subcarriers spaced orthogonal to each other in the frequency domain. Here, orthogonality means the cross-talks of the adjacent subcarrier is nil, and no guard band is required between subcarriers. The advantage of subcarrier transmission over single carrier transmission is that the symbol duration of each subcarrier is elongated which in turn reduces inter-symbol interference (ISI). Whereas, in case of single carrier transmission the symbol duration is very small hence ISI could be higher.

Frame Structure: Fig. 1.5 shows the LTE frame structure [18]. LTE transmission is segmented into frames, and each frame is of duration 10 ms. Each frame is further divided into 10 subframes. Each subframe prolongs for one millisecond duration. Each subframe comprises of a pair of resource blocks (RB) in frequency domain, and the number of such resource block pairs is determined by bandwidth. A resource block is the smallest unit in the LTE structure. RB has 12 subcarriers in the frequency domain and 7 symbols in the time domain, which corresponds to 0.5 ms. Each subcarrier is separated by 15 KHz, therefore in a RB there are 12 (subcarriers) \times 7 (symbols) = 84 (symbols) in normal cyclic prefix. The purpose of the cyclic prefix is to ensure that two symbols transmitted in the same subcarrier should not overlap in time domain due to multipath reception. Table 1.2 provides the OFDM modulation parameters in downlink for different bandwidths.

LTE supports higher order modulation (up to 64 QAM), large bandwidths (up to 20 MHz), and spatial multiplexing in the downlink (up to 4x4 MIMO). The theoretical peak data rate on the transport channel in uplink can reach up to 75 Mbps, and in the downlink, using spatial multiplexing, the rate can reach up to 300 Mbps.

Table 1.2: Downlink OFDM modulation parameters of LTE

Supported bandwidth	1.25 MHz	2.5 MHz	5 MHz	10 MHz	15 MHz	20 MHz
Sub-frame duration	0.5 ms	0.5 ms	0.5 ms	0.5 ms	0.5 ms	0.5 ms
Subcarrier spacing	15 KHz	15 KHz	15 KHz	15 KHz	15 KHz	15 KHz
Sampling frequency	192 MHz	3.84 MHz	7.68 MHz	15.36 MHz	23.04 MHz	30.72 MHz
FFT size	128	256	512	1024	1536	2048
OFDM symbol per slot (short/ long CP)	7/6	7/6	7/6	7/6	7/6	7/6
CP (usec/ Long samples)	(16.67/32)	(16.67/64)	(16.67/128)	(16.67/256)	(16.67/384)	(16.67/512)

1.1.2 Overview of Wi-Fi networks

IEEE 802.11 also known as Wireless Fidelity (Wi-Fi) is the most popular Wireless Local Area Network (WLAN) [19] technology for short-range communications. It appears to higher layers as a wired Ethernet (IEEE 802.3). The fundamental building block of 802.11 architecture is known as a Basic Service Set (BSS). A BSS typically contains one or more wireless stations and a base station also known as Access Point (AP). Multiple APs may be connected together to form a distributed system. Fig. 1.6 shows the BSS and Extended Service Set (ESS). IEEE 802.11 stations can also group themselves together to form an ad-hoc network. Fig. 1.7 shows different layers of Wi-Fi radio protocol stack, namely (1) Logical Link Control (LLC), (2) Medium Access Control (MAC), and (3) Physical Layer (PHY). A brief description of these layers is given below.

1. **Logical Link Control:** LLC layer is the upper sub-layer of the Data Link layer. It provides multiplexing mechanisms that make it possible for several network protocols (IP, IPX) to coexist within a multipoint network and to be transported over the same network media, and can also provide flow control mechanisms. The LLC sub-layer acts as an interface between the MAC sublayer and the network layer. The LLC multiplexing interface includes the following network protocol features: (1) Multipoint network operation, (2) Unified network media exchange, (3) Flow control, (4) Line protocol identification, like Synchronous Data Link Control (SDLC), (5) Frame

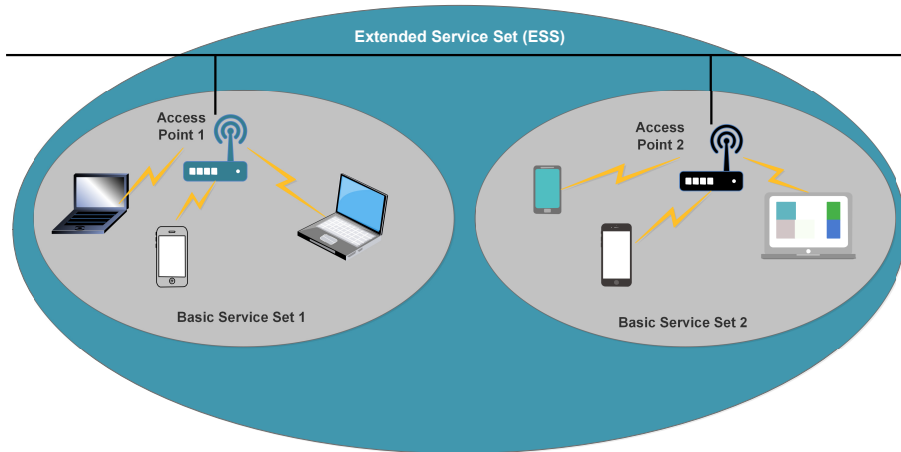


Figure 1.6: Wi-Fi architecture.

sequence number assignment, and (6) Acknowledgement tracking.

2. **Medium Access Control:** MAC in Wi-Fi follows carrier sense multiple access with collision avoidance (CSMA/CA) protocol. CSMA/CA enforces that AP or wireless station transmit after sensing the channel as idle *i.e.*, listen-before-talk. Unlike IEEE 802.3 standard where collisions can be detected by employing CSMA/CD, Wi-Fi cannot detect collisions on the channel. Hence, it tries to avoid collisions by employing one of the following methodologies for channel access: (1) Distributed Coordination Function (DCF) [20], (2) Point Coordination Function (PCF) [20], and (3) Hybrid Coordination Function (HCF) [21].

Distributed Coordination Function: In DCF, collisions are predominantly avoided by obeying to a backoff based transmission. Every station backs off for a random number of slots. A slot here refers to a fixed time unit. Each station observes the channel for the chosen backoff time. If the channel gets busy before the backoff time of the station expires, then the station freezes its backoff time and waits for the channel to become idle. A station/AP, on observing the channel to be idle for the chosen backoff time, goes for transmitting a frame. If the frame is delivered successfully to the intended receiver then the station/AP gets an acknowledgement. If the frame transmitted is lost (due to collision or channel error), then the station/AP doubles the contention window from which a random backoff is chosen.

Point Coordination Function: In PCF, the AP coordinates transmissions for all stations in the network. Thereby PCF mode ensures a contention free delivery of

frames and hence significantly reduces collisions. According to PCF, a station can transmit only when it receives CF-Poll frame from AP and the station is PCF capable. If AP polls a station and it does not have any frames to send, then it must transmit a null frame. Due to the priority of PCF over DCF, stations that only use DCF might not gain access to the medium. To prevent this, a repetition interval has been designed which includes both PCF (Contention free) & DCF (Contention Based) modes of operation.

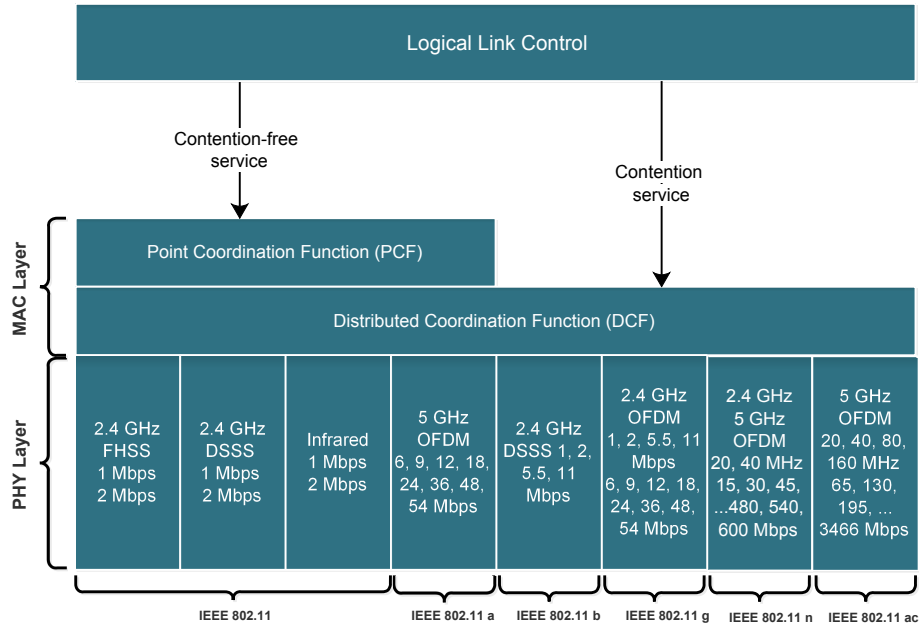


Figure 1.7: Wi-Fi protocol stack.

3. **Physical layer:** PHY of IEEE 802.11 is divided into two sub-layers [22]: (1) Physical Layer Convergence Procedure (PLCP) acts as an adaptation layer and it is responsible for Clear Channel Assessment (CCA) and building packets for different physical layer technologies, and (2) Physical Medium Dependent (PMD) layer which specifies modulation and coding techniques. Table 1.3 shows various PHY standards of IEEE 802.11.

1.2 Interworking of different wireless access technologies

Interworking of different radio access technologies corresponds to employing two or more radio access technologies in order to deliver data from a source to a destination in a coor-

Table 1.3: Comparison of various IEEE 802.11 standards

Rel. Date	Standard	Frequency Band (GHz)	Bandwidth (MHz)	Modulation	Advanced Antenna Technologies	Maximum Data Rate
1997	802.11	2.4 GHz	20 MHz	DSSS, FHSS	N/A	2 Mbits/s
1999	802.11b	2.4 GHz	20 MHz	DSSS	N/A	11 Mbits/s
1999	802.11a	5 GHz	20 MHz	OFDM	N/A	54 Mbits/s
2003	802.11g	2.4 GHz	20 MHz	DSSS, OFDM	N/A	54 Mbit-s/s
2009	802.11n	2.4 GHz, 5 GHz	20 MHz, 40 MHz	OFDM	MIMO, up to 4 spatial streams	600 Mbit-s/s
2013	802.11ac	5 GHz	40 MHz, 80 MHz, 160 MHz	OFDM	MIMO, MU-MIMO, up to 8 spatial streams	6.93 Gbit-s/s

minated fashion. Interworking of multiple radio access technologies can be done at different layers of protocol stack. Fig. 1.8 provides a snapshot of realizing interworking. Following are a few realizations which could be applied at different layers of the protocol stack.

1. **Application Layer :** Choosing the best link (LTE/Wi-Fi) for transmission among multiple links available at a device can be done at the application layer with limited information about each link. Samsung download booster [23] is one such application which creates multiple sockets and executes an Hyper Text Transfer Protocol (HTTP) range request for downloading a file which again gets reordered from application layer buffer. The available goodput information is used to decide number of HTTP queries that have to be made on a given interface. At the application layer, each HTTP request binds to a single TCP connection.
2. **Transport Layer :** The transport protocol at the sender creates multiple sub-flows for a single TCP connection as in Multipath-TCP (MPTCP) [24]. Each sub-flow can take different paths (*e.g.*, different interfaces in multi-homed devices) to reach the destination. MPTCP does scheduling of application layer data onto a sub-flow based on parameters like Round Trip Time (RTT), available bandwidth, and link delay. The packets received through multiple paths are reordered at MPTCP layer of the receiver

and delivered to the receiver's application layer.

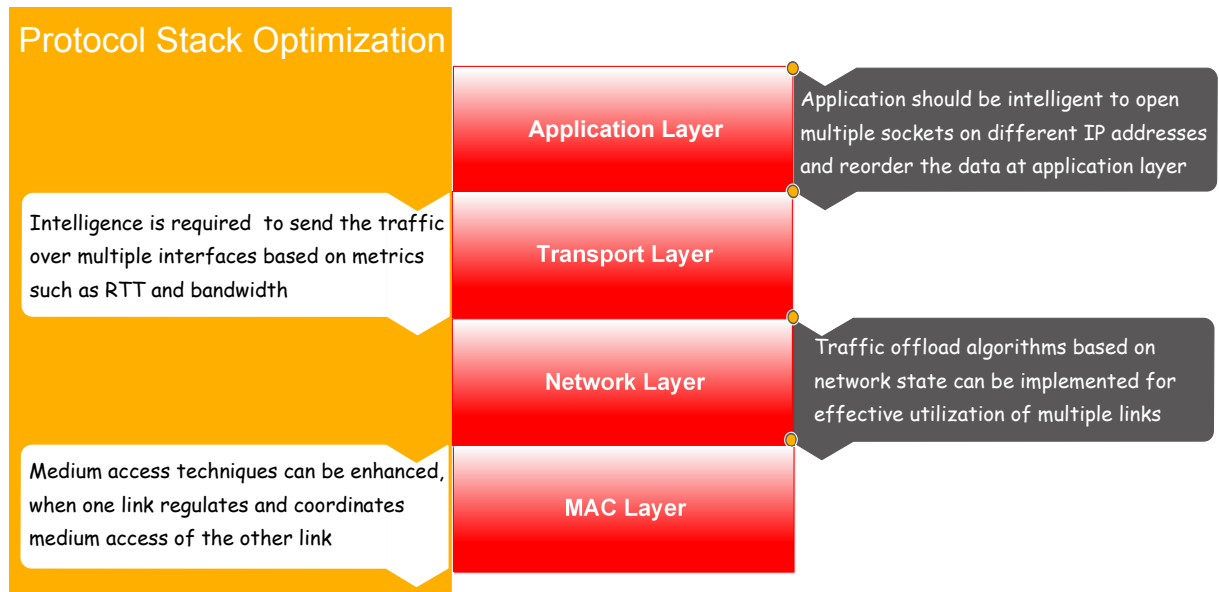


Figure 1.8: Optimizations at different layers of protocol stack for interworking.

- 3. Network Layer :** Interworking of multiple radio access technologies at IP layer can be realized by introducing a fine granularity of traffic offloading across different RATs. The decision is taken based on the collective information obtained from all the RATs. A quick decision is taken and the offloading is done, and the decision contrived is independent of the above layers. To yield a compelling performance, an intelligent traffic offloading algorithm is vital at this layer. IP Flow Mobility and Seamless Offload is an example which employs Dual Stack Mobile IPv6 (DSMIPv6) [25] to use two networks simultaneously.
- 4. MAC Layer :** MAC layer aggregates multiple RATs by employing fine co-ordination and enhanced regulation of traffic offloading across different RATs. Integration at MAC level has more control in taking a decision compared to realizing integration at higher layers.

1.3 Evolution of Cellular Wi-Fi Interworking

3GPP defined various LTE and Wi-Fi interworking architectures from Rel-8. The user mobility with IP address preservation for all the traffic from 3GPP access to non-3GPP

access (*e.g.*, Wi-Fi) got standardized in Rel-8. Enhancements of Rel-8 include WLAN accessible via legacy 3G-Core. S2-a and S2-b are standard interfaces which exist between cellular and Wi-Fi networks. S2-b interface is a Proxy Mobile IPv6 (PMIP) [26] based interface between P-GW and non-trusted non-3GPP access, which provides the user plane with related control and mobility support between evolved Packet Data Gateway (ePDG) and P-GW. For S2-b, an IPsec tunnel has to be established between UE and e-PDG, where the mobile operator need not trust the Wi-Fi network. S2-a corresponds to trusted access to cellular data through Wi-Fi. Wi-Fi APs connected through S2-a interface mostly include operator deployed Wi-Fi hotspots. In case of both S2-a and S2-b based interworking solutions, the offloading decision is taken at the core network in P-GW, and it involves high signaling overhead and incurs more latency. Also, a UE can be attached to either LTE or Wi-Fi, at any given time.

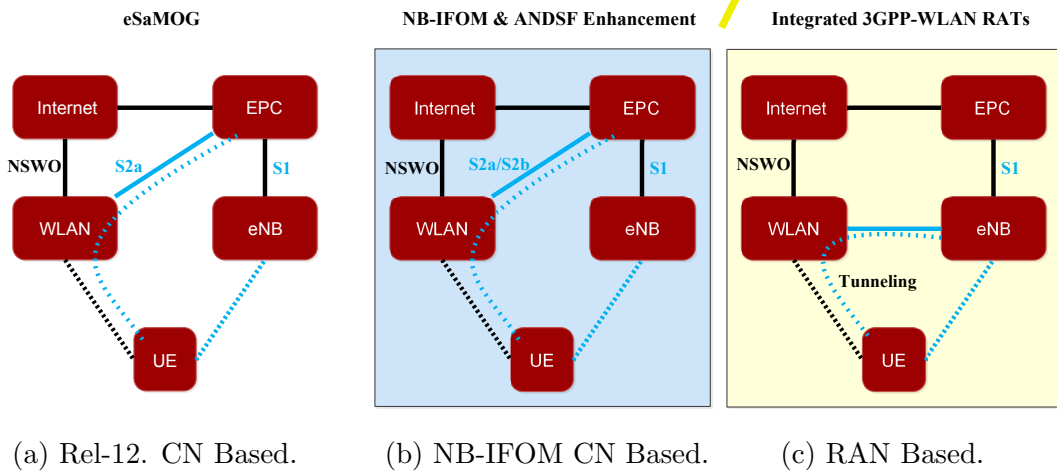


Figure 1.9: Evolution of cellular Wi-Fi interworking.

Access Network Discovery and Selection Function (ANDSF) [27] has also been introduced as part of Rel-8. It is an entity within EPC of the System Architecture Evolution (SAE) for 3GPP compliant mobile networks. The primary purpose of ANDSF is to assist UE to discover non-3GPP access networks, such as Wi-Fi, that can be used for data communications in addition to 3GPP access networks. It provides UEs with information about available non-3GPP networks and policies for selecting and using such networks. UE may then employ IP flow mobility (IFOM) [28], multiple-access PDN connectivity (MAPCON) or non-seamless Wi-Fi offload according to operator policy and user preferences. Numerous

works have been done on offloading LTE traffic to Wi-Fi and vice-versa [29], [30].

Access Network Discovery and Selection Function enhancements (eANDSF) has been proposed in Rel-9 which includes cellular network information, device mobility state, and further deals for intelligent network selection and traffic steering. The 3GPP Rel-10 specifies a variety of deployment scenarios and it allows a universal network connection irrespective of whether it is based on GPRS Tunnelling Protocol (GTP) [31] or PMIP with the help of UE support. In Rel-11, SaMOG-I [32] *i.e.*, S2-a mobility over GTP has been introduced which has an S2-a interface using GTP via trusted WLAN. Fig. 1.9(a) shows core network based enhanced SaMOG architecture. Location-based selection of gateways for WLAN has also been discussed in this release. In Rel-12, multiple IP connectivities via trusted WLAN using GTP, and IP flow mobility have been introduced. Fig. 1.9(b) shows the Rel-12 architecture with involves Network Based IP Flow Mobility (NB-IFOM) [33]. In Rel-12 and Rel-13, Radio Level Integration (RLI) of LTE and Wi-Fi is introduced, which enhances the interworking capability between LTE and Wi-Fi. Fig. 1.9(c) shows the evolved radio level integration architecture. All the architectures shown in Fig. 1.9 support Non-Seamless WLAN Offload (NSWO). 3GPP has defined NSWO as the ability for a device to send traffic directly to the Wi-Fi access network. In Rel-14, the RLI architectures are further enhanced to support uplink aggregation, mobility and enable Wi-Fi interworking for high frequency bands (60 GHz). RLI architectures introduced by 3GPP include:

1. LTE Wi-Fi Radio Level Integration with IPsec tunnel (LWIP)
2. LTE Wi-Fi Aggregation (LWA)

In RLI architecture, a node which logically comprises of LTE small cell and Wi-Fi AP is called as RLI node. Details of these architectures will be discussed in Chapter 2.

1.4 Objectives and scope of the thesis

In this thesis, LTE Wi-Fi Integration architectures are investigated in which LTE small cell eNodeB (SeNB) and Wi-Fi AP are tightly coupled at RAN level, as shown in Fig. 1.9(c). The scope of this thesis includes:

1. Addressing challenges which persist with radio level interworking architectures.

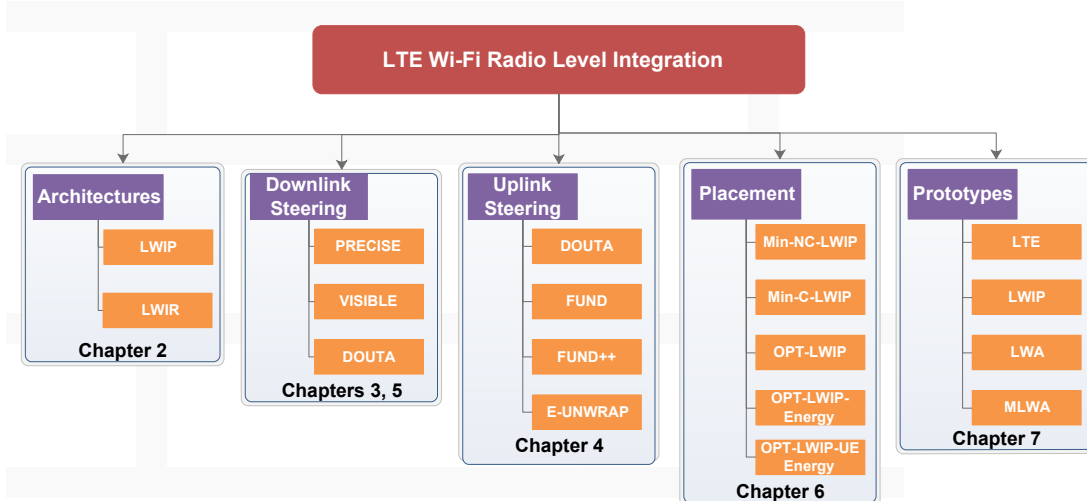


Figure 1.10: Organization of the thesis.

2. Efficient downlink steering solutions to enable faster steering of packets/flows across LTE and Wi-Fi networks in LWIP architecture.
3. Novel uplink steering solutions to enhance the performance of uplink traffic and also to improve the throughput of legacy users in the system.
4. Develop solution to address out-of-order packet delivery problem introduced by LWIP architecture in case of packet level steering. The solution targets to improve the performance of Transmission Control Protocol (TCP) by introducing intelligent operations at the link layer of RLI node.
5. Optimal placement of LWIP nodes in order to enhance capacity and coverage, and also to improve the energy savings at RLI nodes and UEs.
6. Design and develop prototype testbed for RLI architectures and study the aggregation benefits.

1.5 Organization of the thesis

In this chapter, introduction and background required to understand the work done in thesis were given and the contributions of the thesis were highlighted. Rest of the thesis is organized as follows, refer Fig. 1.10. In Chapter 2, various RLI architectures and their

features are presented. And the challenges associated with different RLI architectures are be enumerated. This chapter also introduces link aggregation strategies in RLI architectures. The proposed link aggregation strategies are evaluated through simulation experiments.

Chapter 3 explains the necessity for efficient downlink traffic steering in LWIP architecture. A downlink traffic steering solution has been proposed, Power-Aware Dynamic Traffic Steering (PRECISE). The performance of the proposed steering solution is examined from the perspective of Quality of Service (QoS) improvement and energy efficiency.

Chapter 4 presents the stringent requirements for uplink traffic steering solution in LWIP architecture. Network Coordination Function (NCF) is proposed to address the challenges in uplink traffic steering. NCF comprises of different uplink steering algorithm targeted to improve the network throughput by optimizing the uplink traffic steering ratio across LTE and Wi-Fi links. It also minimizes the number of collisions on the Wi-Fi channel. NCF is evaluated under different scenarios to observe its benefits.

Chapter 5 describes one of the problems with LWIP architecture, which is out-of-order (OOO) delivery of packets at the destination due to link diversity. The OOO delivery hinders Transmission Control Protocol (TCP) growth significantly. A solution is proposed to overcome this challenge, "Virtual Congestion Control with Boost ACKs for Packet Level Steering in LWIP Networks" (VISIBLE). Performance of the proposed solution is measured and compared with state-of-the-art solutions.

In Chapter 6, placement of LWIP nodes is discussed and problems such as (1) Minimum number of RLI nodes required in a region to ensure QoS guarantees, (2) Optimal transmit power settings at RLI nodes to enhance capacity and coverage, and (3) Energy efficient placement of these RLI nodes are addressed.

In Chapter 7, prototypes for RLI architectures were developed. The performance of different RLI architectures has been profiled. Also the co-operation between RLI architectures and multipath transport layer architecture is studied. Finally, Chapter 8 concludes the various works done on RLI architectures in this thesis and discusses some possible future extensions.

Chapter 2

Radio level integration architectures

In this chapter, Radio Level Integration (RLI) architectures and their advantages over traditional LTE Wi-Fi interworking architectures are discussed. Also, the challenges associated with RLI architectures and potential solutions to improve their benefits are also detailed.

2.1 Introduction to RLI architectures

Integrating different radio access technologies such as LTE and Wi-Fi at their radio protocol stacks is referred to as radio level integration. Such radio level integration [34], [35] can be realized at IP, PDCP, RLC, or MAC layers. 3GPP developed specifications for realizing the integration at IP layer and PDCP layer. 3GPP has coined the terms LTE Wi-Fi Aggregation (LWA) and LTE Wi-Fi interworking with IPsec tunnel (LWIP) for realizing integration at PDCP and IP, respectively. These architectures have enhanced capabilities compared to realizing interworking at the higher layers (Transport layer or Application layer). The radio level interworking architectures enable decision making functionality at layer 2 [36]. RLI architectures could be realized in two ways: (1) Colocated RLI and (2) Non-colocated RLI. In colocated RLI, SeNB and Wi-Fi AP are located in the same device and tightly integrated at RAN level in an RLI node, whereas in the latter case, Wi-Fi AP and SeNB are connected via a standardized interface referred to as X_w . Figs. 2.1 and 2.2 show the generic colocated and non-colocated RLI architectures, respectively.

RLI architectures have the following merits over traditional LTE Wi-Fi interworking

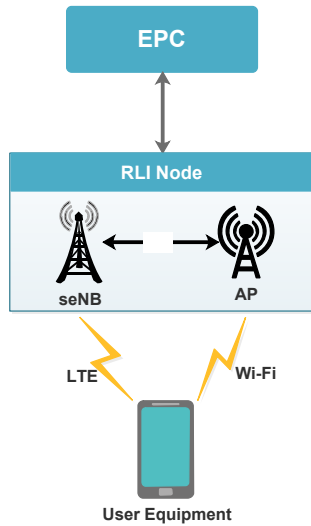


Figure 2.1: Colocated RLI Architecture.

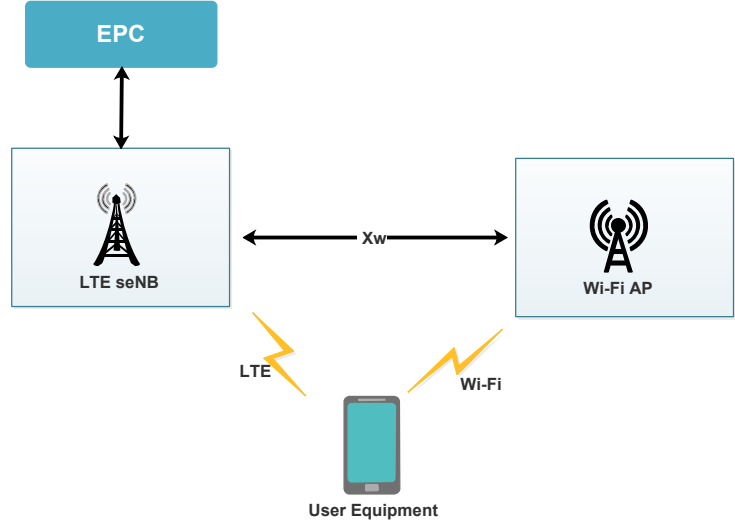


Figure 2.2: Non-colocated RLI Architecture.

architectures:

1. Wi-Fi operations are controlled directly via SeNB inside RLI node. LTE core network (*i.e.*, Evolved Packet Core (EPC)) need not manage Wi-Fi separately.
2. Radio level integration allows effective radio resource management across Wi-Fi and LTE links.
3. LTE acts as the licensed-anchor point for UEs, providing unified connection management with the network.

2.1.1 Advantages of RLI architectures

The tighter level of integration between LTE SeNB and Wi-Fi AP in RLI has several advantages compared to its predecessor interworking technologies. Some of their advantages are enumerated as follows.

Efficient Power Control: A main advantage of RLI as compared to traditional LTE Wi-Fi interworking technology is its flexibility in adopting fractional frequency reuse (FFR) scheme for mitigating inter-cell interference. Given a spatial distribution of UEs in the network region, RLI may employ FFR where LTE SeNB of an RLI node serves users in the inner region and Wi-Fi of the RLI node serves the interference-prone LTE cell-edge users.

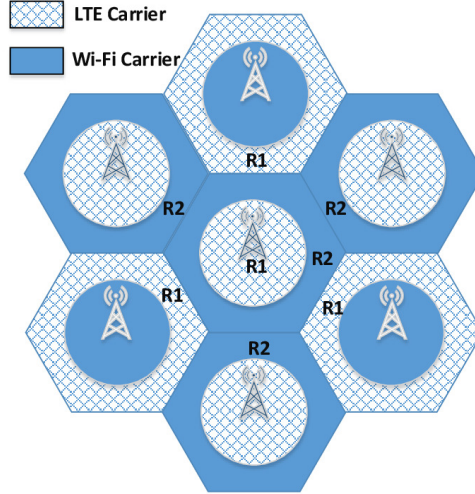


Figure 2.3: Diversification in the region of association with different RATs using RLI architectures.

In case of dense urban scenarios, RLI nodes are vital for mitigating the interference among neighbour RLI nodes by assigning non-overlapping LTE and Wi-Fi bands appropriately as shown in Fig. 2.3. The coverage regions of RLI nodes shown in Fig. 2.3 are spatially marked distinctly as regions $R1$ and $R2$. The users residing in $R1$ will be served using LTE interface of RLI node. Similarly, the users residing in region $R2$ could be served potentially using Wi-Fi interface in order to mitigate the inter-cell interference. This is possible due to unified control plane signaling between LTE SeNB and Wi-Fi AP in RLI node. If the region $R2$ suffers interference from the adjacent Wi-Fi APs, then the APs with common channel will be set dynamically to operate on orthogonal channels. The mechanism prevents two $R1$ regions to fall adjacent, because LTE which is captured in $R1$ works with reuse factor one. In simple words, LTE has limited bandwidth, whereas Wi-Fi operating in unlicensed band has many orthogonal channel to choose from.

In case of traditional LTE Wi-Fi interworking techniques, the interference mitigation could not be achieved effectively because LTE and Wi-Fi radios are uncoordinated and also placed at geographically different locations (spatially separated). Hence, traditional LTE Wi-Fi interworking techniques do not employ FFR effectively. They are limited to support offloading of data plane traffic from LTE to Wi-Fi.

Enhanced Security: Traditional LTE Wi-Fi interworking techniques (s2a/s2b) employ tunnels from LTE network to Wi-Fi network. It involves encryption of packets at IP layer

(to send through untrusted Wi-Fi) followed by link-level encryption of Wi-Fi (optionally). An RLI architecture reduces the overhead of double encryption (*i.e.*, at both IP and Layer 2 of WLAN) by using Wi-Fi key per client derived from existing SeNB key K_{eNB} . Also, every packet sent through the tunnel is added with tunnel endpoint header, which adds to inefficient use of resources over the wireless channel. Whereas RLI architectures proposed in this thesis do not require any additional headers.

Traditional LTE Wi-Fi interworking techniques offer ready-to-work solutions with existing Wi-Fi APs, but the decision for traffic offloading is taken at a coarse level of granularity *e.g.*, based on observed throughput and round trip delay on LTE and Wi-Fi networks. But RLI architectures support decision making at a very fine granularity of information *i.e.*, channel load, received SNR of Wi-Fi, and channel characteristics such as pathloss and fading. This makes RLI architectures to perform better compared to traditional LTE Wi-Fi interworking techniques.

2.2 Existing and proposed RLI architectures

Radio level integration can be realized at different layers of radio protocol stack *viz.*, IP, PDCP, RLC, and MAC. This section describes the architectures introduced by 3GPP and proposed architectures in this thesis.

2.2.1 3GPP architectures on radio level integration

3GPP has developed specifications for realizing integration at PDCP and IP layers. LTE-WLAN Aggregation (LWA) and LTE Wi-Fi interworking with IPsec tunnel (LWIP) are the terms coined for realizing integration at PDCP and IP layers, respectively. Figs. 2.4 and 2.5 show 3GPP architectures for realizing integration at PDCP in colocated and non-colocated fashion, respectively. In colocated LWA deployment, Wi-Fi AP is placed alongside LTE eNB (SeNB) in the same device. In non-colocated deployment, the LTE eNB is connected to Wi-Fi AP over X_w interface. LWA supports split and switched bearer functionalities. Switched bearer refers to switching a bearer completely from one interface to other, whereas split bearer refers to splitting a bearer, which allows some packets/flows (PDCP PDUs) belonging to an LWA bearer to be sent through LTE link and the rest through Wi-Fi link. The decision of offloading multiple bearers to Wi-Fi could be taken based on LTE and Wi-Fi

link measurements and feedback from PDCP PDUs sent via Wi-Fi. The PDCP PDUs are encapsulated in LWA Adaptation Protocol (LWAAP), and bearer identity is added to it. This bearer identity is used at the receiver to map the PDU to the corresponding bearer. The control and data planes of these architectures are discussed as follows.

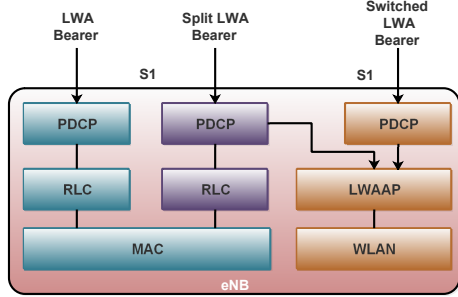


Figure 2.4: 3GPP collocated LTE Wi-Fi aggregation architecture [2].

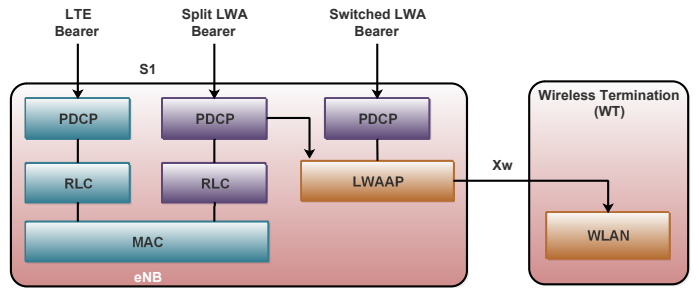


Figure 2.5: 3GPP non-collocated LTE Wi-Fi aggregation architecture [2].

LWA Control Plane

LWA activation and deactivation are controlled by LWA node. SeNB configures Wi-Fi mobility set for UE based parameters such as Wi-Fi measurements reported by UE. Wi-Fi mobility set is a group of Wi-Fi APs identified by Service Set Identifier (SSID), Homogeneous Extended Service Set Identifier (HESSID) or Basic Service Set Identifier (BSSID). Wi-Fi mobility set is UE-specific and there is only one set configured for UE at a time. All Wi-Fi APs in the mobility set are connected to the same Wireless Termination (WT) within the WLAN mobility set. When LWA is activated, SeNB configures one or more bearers as LWA bearers.

LWA X_w Control Plane [37]

X_w Application Protocol (X_w -AP) is used on the X_w control plane interface. X_w -AP supports the following procedures: (1) WT Addition Preparation, (2) SeNB or WT Initiated WT Modification, (3) WT Status Reporting, (4) WT Association Confirmation, and (5) SeNB or WT Initiated WT Release.

- WT Addition Request is used by SeNB to request preparation of resources for LWA in WT. It carries: UE id, WLAN security key, bearer information (including QoS), WLAN mobility set, *etc.*

- WT Modification Request is used by SeNB to modify mobility set, security key or bearers configured for LWA for a UE.
- WT Status Report is used by WT to report WLAN measurements per BSS. It carries BSSID, BSS load, WAN metrics, and channel utilization.
- WT Association Confirmation is used by WT to indicate that a UE successfully connected to WLAN.

LWA Wi-Fi Measurements

UE compatible with LWA operation shall support Wi-Fi measurement reporting. Measurement configurations include SSIDs, Wi-Fi band, and frequency/channel. Measurement reporting is triggered based on Received Signal Strength Indication (RSSI) threshold. Measurement report contains: SSIDs, RSSI, STA count, backhaul rate, admission capacity, channel utilization, *etc.* Wi-Fi measurement can trigger one of the following cases:

1. Event W1: A Wi-Fi AP becomes better than a threshold RSSI (T1).
2. Event W2: All Wi-Fi APs inside the Wi-Fi mobility set become worse than a threshold RSSI (T1) and a Wi-Fi AP outside the Wi-Fi mobility set becomes better than a threshold RSSI (T2).
3. Event W3: All Wi-Fi APs inside the Wi-Fi mobility set become worse than a threshold RSSI (T1).

Wi-Fi measurement framework is common to LWA and LWIP. There are separate UE capability indications for LWA, LWIP, and Wi-Fi measurements.

LWA X_w Dataplane [38]

X_w data plane uses GPRS Tunnelling Protocol for User Plane (GTP-U) on top of UDP for data transfer between SeNB to WT. Downlink stream is used for data forwarding. The uplink stream is used for feedback/flow control. Optional downlink data delivery status procedure is used by WT to indicate its buffer status and lost PDUs to SeNB. Every PDU is assigned an X_w -U sequence number.

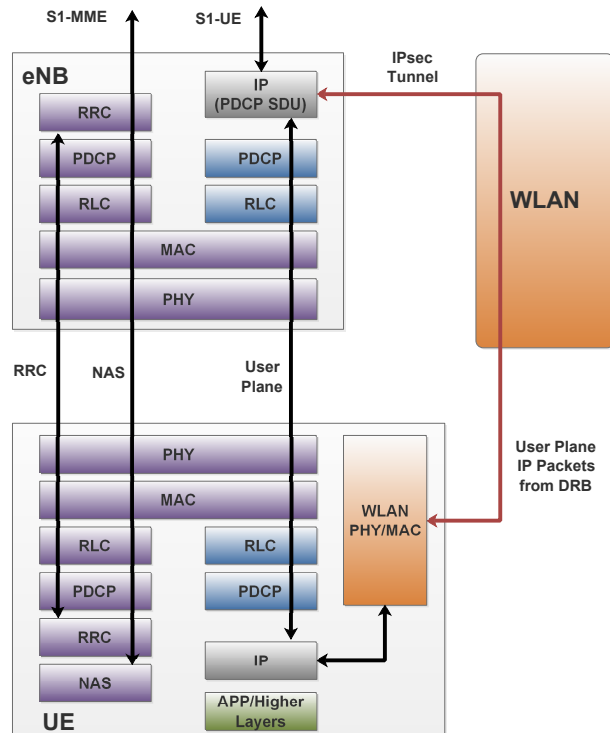


Figure 2.6: 3GPP LTE Wi-Fi Integration with IPsec tunnel (LWIP) architecture.

LWA UE Feedback

LWA supports deployment with limited WLAN infrastructure impact. If WT does not support feedback/flow control, SeNB may trigger status reporting from UE on air interface (at PDCP layer) using either: (1) PDCP status report: First Missing PDCP Sequence Number (SN), and bitmap of received PDCP SDUs or (2) LWA status report: First Missing SN (FMS), Number of Missing PDUs (NMP), and Highest Received SN on WLAN (HRW). Note that SeNB can also derive information about packets lost on LTE from RLC layer since only RLC Acknowledged Mode (AM) is allowed for LWA. If configured by SeNB, UE reports association confirmation on air interface (at RRC layer).

LWIP Data Plane

Fig. 2.6 shows the LWIP architecture introduced by 3GPP. LWIP supports both uplink and downlink data transfer over Wi-Fi link. One or more bearers can be offloaded to WLAN via IPsec. In the uplink, PDCP SDUs are encapsulated using Generic Routing Encapsulation (GRE) protocol [39]. GRE key carries bearer identifier, hence bearer differentiation is not needed in the downlink. LWIP does not support re-ordering, hence split bearer is not

recommended by 3GPP. Each DRB may be configured so that traffic for that bearer can be routed over the IPsec tunnel in either only downlink or both uplink and downlink over Wi-Fi.

LWIP Control Plane

Activation and deactivation of LWIP operation are controlled by SeNB. When LWIP is activated, the following activities take place:

- SeNB sends Wi-Fi mobility set, bearer information, and LWIP-SeGW IP address to whom.
- After WLAN association and Extensible Authentication Protocol (EAP/AKA) authentication, UE establishes IPsec connection with LWIP-SeGW using Internet Key Exchange (IKE).
- IPsec keys are derived (by SeNB and UE) based on SeNB Key (K_{eNB}).

LWIP re-uses same WLAN measurement reporting framework and WLAN mobility concept of LWA.

2.2.2 Proposed RLI architectures

We have proposed various RLI architectures which are contemporary with 3GPP architectures. The proposed integration architectures are slightly different from 3GPP architectures in which the integration across LTE and Wi-Fi links has been realized by introducing a Link Aggregation Layer (LAL). LAL is responsible for steering packets/flows/bytes across LTE and Wi-Fi links in both downlink and uplink. Our proposed integration architectures include (i) LWIP, (ii) LWA, and (iii) LWIR. Fig. 2.7 captures all the proposed integration architectures with LAL. In the following, we present each of the proposed RLI architectures in detail.

LWIP-Proposed

As shown in Fig. 2.7(a), LWIP is realized by introducing a LAL in the protocol stack of the LWIP node and LWIP-UE. LAL does not add any new header to the IP data packets received from EPC via S1-U interface. Packets going through LTE and Wi-Fi interfaces

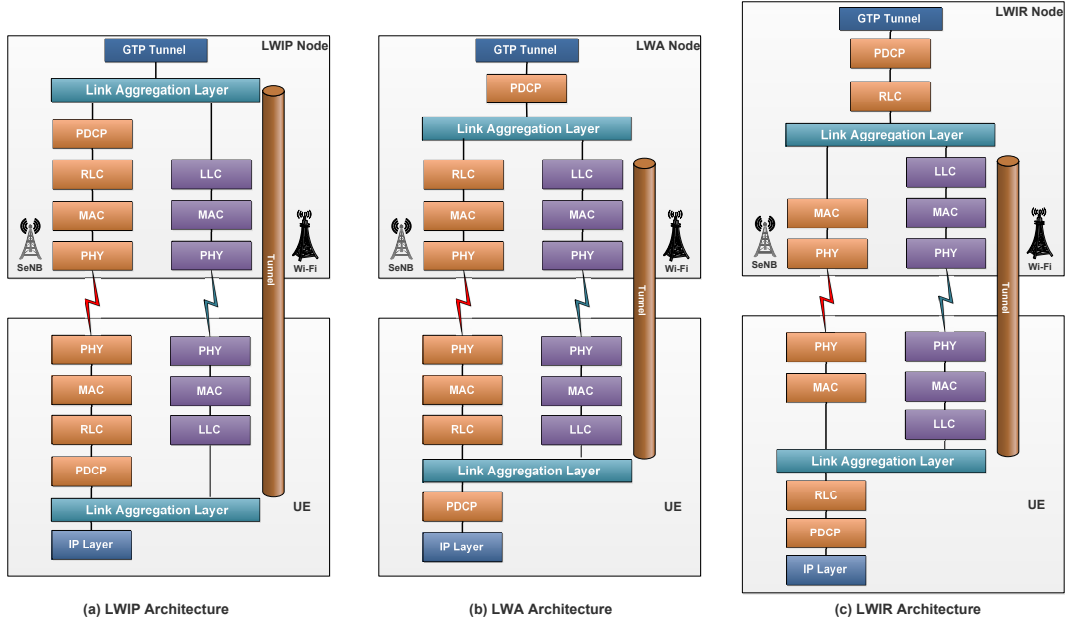


Figure 2.7: Proposed LWIP, LWA, and LWIR architectures.

follow regular packet forwarding procedures at their protocol stacks and get delivered to IP layer. LWIP is leveraged by its ease of implementation to achieve aggregation benefits. Also, LAL supports collecting various network parameters and actively participates in intelligent decision making for steering IP traffic across LTE and Wi-Fi interfaces in the downlink. LAL can also be introduced at the UE stack for uplink steering.

LWA-Proposed

LAL implemented below PDCP layer of LTE does the steering across LTE and Wi-Fi links in LWA architecture (refer Fig. 2.7(b)). The LAL is also responsible for collecting link-level information of LTE and Wi-Fi, which will be used for steering the traffic more efficiently. LWA requires modifications in protocol stacks at both UE and SeNB. PDCP layer at UE employs reordering function to minimize the out-of-order packet delivery to higher layers. Unlike LWIP, split bearers functionality is enabled in LWA due to its ability to deliver packets of a bearer/flow in-order to higher layers. In-order-delivery is achieved by employing Dual Connectivity (DC) procedure [40]. The purpose of realizing aggregation at the PDCP layer is to achieve:

- In-sequence delivery of packets to higher layers.
- Robust Header Compression (RoHC).

- Encryption of the packets sent through the Wi-Fi interface.

In-sequence delivery is required for aggregation because in case of split bearer at packet level the out-of-order packets have to be reassembled and delivered to the higher layer in-order. RoHC further enhances the aggregation capacity by compressing the IP header of packets sent through the Wi-Fi interface. Encryption for data through Wi-Fi interface is provided by legacy LTE encryption function at PDCP layer and this removes the need for additional encryption at Wi-Fi interface.

LWIR-Proposed

LWIR architecture is shown in Fig. 2.7 (c). The traffic is steered from the RLC layer of LTE SeNB protocol stack to Wi-Fi stack. In LTE radio protocol stack, based on resources allocated by LTE MAC scheduler, the RLC layer does segmentation and reassembling of PDCP payloads and creates RLC frames. These RLC frames are then forwarded to the MAC layer of LTE. In order to perform traffic steering at LWIR node, a Virtual Wi-Fi Scheduler (VWS) is introduced inside LAL. This VWS is above the Logical Link Control (LLC) layer of Wi-Fi AP device at LWIR node and it takes data at the granularity of bytes from RLC queue for sending over Wi-Fi link. VWS picks bytes from different RLC queues based on their QoS requirements and the observed CQI of all the associated users.

Steering traffic from SeNB to Wi-Fi AP is realized by establishing a layer-2 tunnel between the RLC layer of LTE protocol stack and the LLC layer of Wi-Fi protocol stack. The Virtual Wi-Fi Scheduler (VWS) retrieves data from the RLC layer of the LTE stack only when the Wi-Fi backoff is about to expire. This notification of Wi-Fi queue status and monitoring the backoff counter value are done by VWS. The VWS periodically queries the Wi-Fi driver to get these parameters and chooses one of the RLC queues from which data has to be steered through Wi-Fi in the downlink. The VWS chooses an RLC queue based on one of the following criteria:

1. Longest RLC buffer first : Bytes are taken out from the longest RLC buffer of a UE for steering through Wi-Fi.
2. Highest CQI first : Bytes are taken out from the RLC buffer of the UE which is having highest CQI among all UEs.

3. Longest RLC buffer with highest CQI : UE with longest RLC buffer is chosen. If there is a tie among UEs with the longest RLC buffer, the tie is broken by choosing the UE that is having highest CQI.
4. Longest RLC buffer with lowest CQI : UE with longest RLC buffer is chosen. If there is a tie among UEs with the longest RLC buffer, the tie is broken by choosing the UE that is having lowest CQI.

The LAL creates IP packets with destination IP corresponding to UE's IP address. The packet includes as its payload, the bytes taken from the RLC queue. The packet is tagged with RLC header corresponding to the destination RLC queue. At the UE side, when the packet is received at LLC layer, it forwards the packet to the IP layer. A listening socket on the corresponding port which is denoted as Tunnel End Point (TEP) captures the packet. The TEP deserializes the packet and reads the tagged value of RLC and forwards to the corresponding RLC queue.

LWIR architecture supports high reliability for the packets sent through LTE and Wi-Fi links. When a packet is lost in transmission over LTE or Wi-Fi link, RLC retransmission procedure is invoked to retransmit the lost packet. One of the major problems in steering traffic across multiple interfaces is the out-of-order delivery of packets, which arises due to the long waiting time of packets on one interface compared to the other. The VWS brings down the waiting time of packets in the Wi-Fi queue and thereby avoids out-of-order delivery and improves the performance of TCP flows significantly.

In summary, the LWIR system has the following advantages:

- Like in LWA and LWIP systems, LTE acts as the licensed anchor in LWIR system.
- High flexibility is achieved by employing steering at the granularity of bytes *i.e.*, a fraction of PDCP payload could be sent through LTE link and the remaining through Wi-Fi link based on their channel conditions.
- High reliability in traffic steering, which is achieved by retransmission functionality of RLC layer.
- Reduced contention delay on Wi-Fi link, which is achieved by retrieving data from RLC buffer only when the Wi-Fi queue is empty.

Table 2.1: Comparison of proposed RLI architectures

Feature	LWIP	LWA	LWIR
Operating Layer	Above LTE PDCP	LTE PDCP	LTE RLC
Compatibility with existing UEs	Works readily	Requires changes	Requires changes
Traffic Steering Granularity	Flow Level, Packet Level	Flow Level, Packet Level	Flow, Packet, Byte Level
WLAN Measurement	Yes	Yes	Yes
Feedback	No	Yes	Yes
WLAN Changes	No	Yes	Yes
Reordering	No	Yes	Yes
Retransmission	No	No	Yes

- Enhanced fairness in user throughput. The fairness is achieved by considering decision making metrics such as link quality, user requirement, and RLC queue status.

Table 2.1 compares the three RLI architectures in a nutshell. Each architecture has its applicability based on the network requirements. In the rest of this thesis, we will explore LWIP system primarily in all aspects like downlink traffic steering, uplink traffic steering, optimization to efficiently support transport layer protocol, and optimal placement. However, the solutions presented in the thesis are also suitable for other RLI architectures.

2.3 Link aggregation strategies for RLI architectures

LAL in above discussed LWIP system adapts one of the following Link Aggregation Strategies (LASs) to send the traffic across LTE and Wi-Fi links.

1. **Naive LAS or N-LAS:** In this approach, LTE and Wi-Fi links are simultaneously used for sending uplink and downlink IP data traffic. A generic solution to integrate multi-RAT involves allowing a fraction of total traffic to be sent through LTE and Wi-Fi links based on their corresponding link rates. The traffic split across LTE and Wi-Fi links can be performed at different granularity *viz.*, packet level or flow level.
 - **Flow Split N-LAS:** LWIP node and LWIP-UE steer the incoming IP flows across LTE and Wi-Fi links in such a way that a flow is routed via one of the links. For example, odd numbered flows are sent over LTE and even numbered

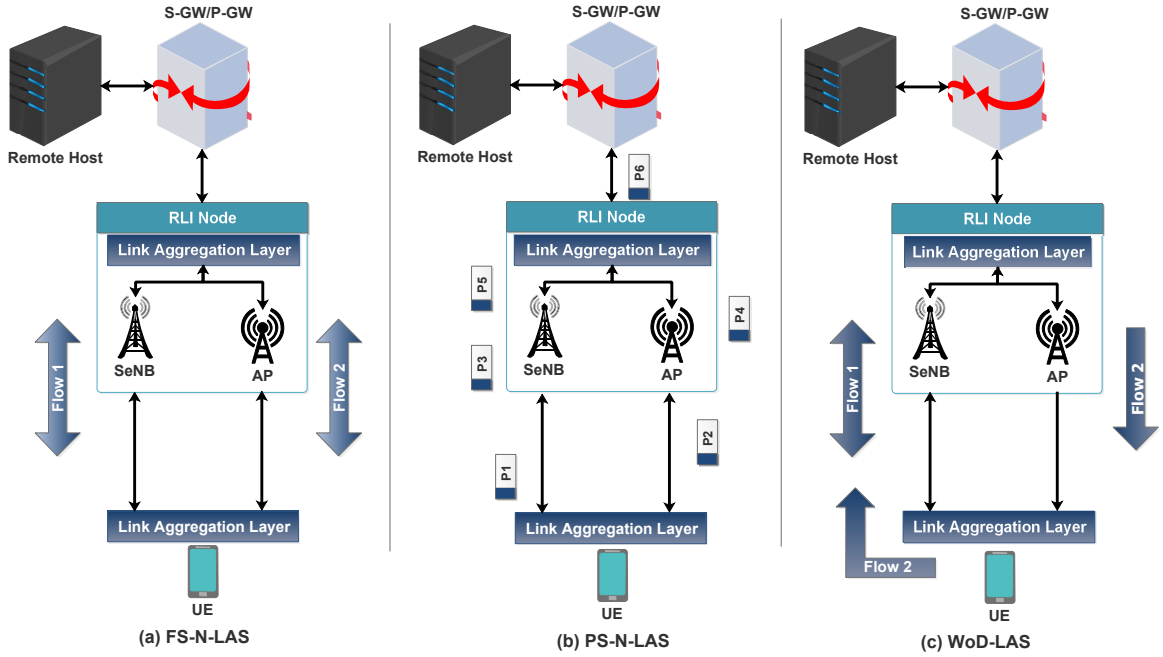


Figure 2.8: Link Aggregation Strategies for RLI architectures.

over Wi-Fi. Fig. 2.8(a) captures the flow level traffic steering at LWIP node and at UE.

- **Packet Split N-LAS**: The packets belonging to each IP flow are sent through LTE and Wi-Fi links. For example, odd numbered packets of a flow over LTE and even numbered packets over Wi-Fi. Fig. 2.8(b) captures the packet level traffic steering at LWIP node and at UE.

2. **Wi-Fi only on Downlink LAS or WoD-LAS**: In this approach, Wi-Fi is used to send downlink traffic while LTE is used for transmitting both uplink and downlink traffic as shown in Fig. 2.8(c). WoD-LAS adopts flow level steering across LTE and Wi-Fi. The key motive behind this approach is, when the number of users increases in the network, due to CSMA/CA, contention on Wi-Fi channel also increases which brings down the throughput of Wi-Fi network. WoD-LAS lowers the possibility of contentions on the Wi-Fi channel as it involves only downlink IP data transmissions. Fig. 2.8(c) captures the WoD-LAS operation at both LWIP node and UE.

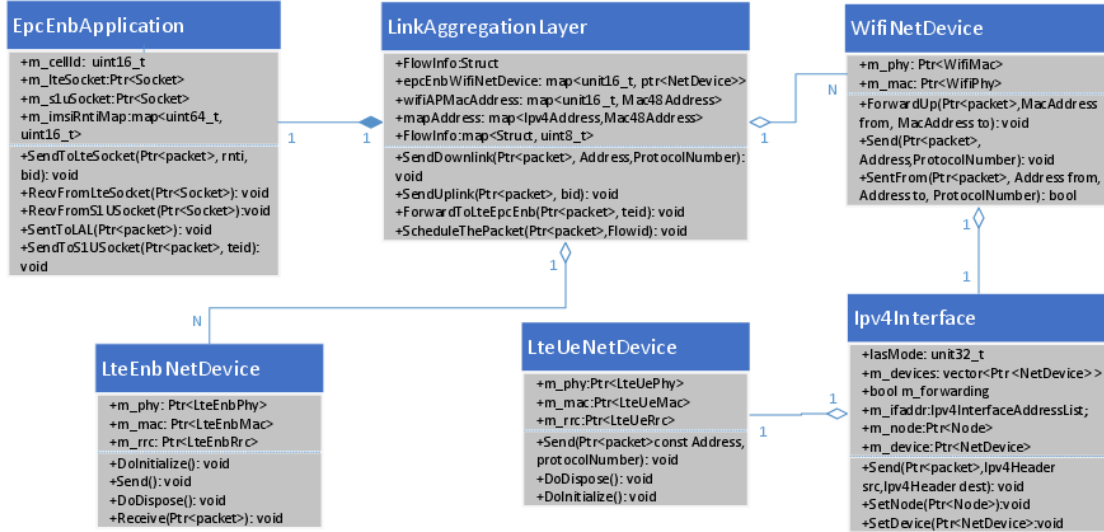


Figure 2.9: NS-3 class diagram for LWIP implementation.

2.4 Simulation setup

The experimental platform has LWIP module which has been developed in house by extending the LTE and Wi-Fi modules of NS-3 simulator. Fig. 2.9 shows the class diagram of LWIP implementation in NS-3. The epc-eNB application is the function running at LTE SeNB which decapsulates the GTP header from the LTE packet received through GTP-tunnel. It routes packets to and from the LTE SeNB protocol stack. The current implementation enables packets to be forwarded to LAL which further takes the decision of forwarding them to LTE or Wi-Fi NetDevice. LTE NetDevice and Wi-Fi NetDevice correspond to nodes installed with LTE SeNB protocol stack and Wi-Fi protocol stack, respectively. A UE corresponds to a node which implements both LTE and Wi-Fi NetDevices.

The simulation parameters are given in Table 2.2. In order to simulate the scenarios realistically, a backhaul delay of 40 ms is introduced between SeNB and remote host. The simulation test bench is used to evaluate various link aggregation schemes which are described as follows.

1. **LTE NoLAS:** Traffic between UE(s) and LWIP nodes is sent only through LTE link, *i.e.*, no aggregation of LTE and Wi-Fi.
2. **Wi-Fi NoLAS:** Traffic between UE(s) and LWIP nodes is sent only through Wi-Fi link, *i.e.*, no aggregation of LTE and Wi-Fi.

3. **Packet Split N-LAS (PS-N-LAS):** Traffic is symmetrically split in round-robin fashion across LTE and Wi-Fi links at the granularity of packets.
4. **Flow Split N-LAS (FS-N-LAS):** Traffic is symmetrically split in round-robin fashion across LTE and Wi-Fi links at the granularity of flows.
5. **WoD-LAS:** Unlike FS-N-LAS, in this strategy, Wi-Fi is used only in the downlink for steering IP flows whereas LTE is used for steering both uplink and downlink IP flows. All uplink flows of UEs through their LTE interfaces is achieved by inserting appropriate forwarding rules in UE's *iptables* [41] without any protocol stack modification.

Table 2.2: Simulation parameters for evaluation of different LASs in LWIP architecture

Parameter	Value
Number of LWIP Nodes	1 and 10
Tx power of SeNB and Wi-Fi APs	23 dBm and 17 dBm
LTE Configuration	10 MHz, 50 RBs, FDD
Wi-Fi Configuration	IEEE 802.11a, 20 MHz
Traffic Type	Mixed (voice, video, web, FTP)
Distance b/w UE & LWIP node	25 Meters
Simulation Time	100 Seconds
Error Rate Model	NIST Error Rate Model [42]
Mobility Model	Static
Wi-Fi Rate Control Algorithm	Adaptive Auto Rate Fallback
LTE MAC Scheduler	Proportional Fair Scheduler
Number of seeds	10
Wi-Fi Queue size	400 packets
RLC Queue size	10^5 bytes
Backhaul Delay	40 ms

Depending on the number of LWIP nodes, the number of UEs, and the nature of traffic, five sets of experiments have been conducted with different link aggregation strategies. First, two experiments (#1 and #2) are performed to benchmark LWIP benefits in an ideal case of one and four users with UDP traffic, respectively. The next experiments (#3 and #4) are conducted to observe the performance of LWIP in a typical home scenario with mixed traffic *i.e.*, voice, video, web, and FTP. The last experiment (#5) mimics a real-world indoor stadium scenario involving multiple LWIP nodes with mixed traffic. The

Table 2.3: Percentage distribution of user traffic

Traffic Class	Protocol	Expt #3	Expt #4	Expt #5	Inter-Packet Interval	Packet Size
Voice	UDP	20%	20%	40%	40 ms	20 bytes
FTP	TCP	20%	60%	50%	-	1 KB
Video	UDP	60%	20%	30%	20 ms	1 KB
Web	TCP	20%	40%	60%	-	1 KB

exact percentage of users in each of the traffic types in mixed traffic scenarios and the traffic parameters for all categories are shown in Table 2.3. For instance, if 20% of users have voice traffic, then bidirectional voice flows (uplink and downlink) exist for those users, similarly for other traffic classes. It is to be noted that same users have traffic belong to multiple traffic classes as shown in Table 2.3. The details of each experiment conducted are given as follows.

- **Expt #1:** This experiment involves one LWIP node with only one user to study the ideal behavior of the system. We considered default bearer with four UDP data flows (two in uplink and two in downlink) and observed network throughput w.r.t. UDP Application Data Rate (ADR) by varying the offered load as 1, 6, 12, 24 Mbps per flow.
- **Expt #2:** It involves one LWIP node with four users. We considered default bearer with four UDP data flows per user (two in uplink and two in downlink), thus, with 16 flows in total for the study. The network throughput is observed w.r.t. ADR by varying the offered load as 1, 2, 4, 8 Mbps per flow.
- **Expt #3:** To demonstrate the interworking benefits in a typical home scenario, this experiment involves one LWIP node with varying number of users: five to 30 users. It is a mixed traffic scenario having the majority of UDP flows (UDP-Heavy).
- **Expt #4:** This experiment involves one LWIP node with varying number of users: five to 30 users. Unlike the previous experiments, it is a mixed traffic scenario having a majority of TCP flows (TCP-Heavy).
- **Expt #5:** To observe the performance of LWIP in a real-world indoor stadium, this experiment involves 10 LWIP nodes with a varying number of users from 50 to 400.

LTE of LWIP nodes are operating with reuse factor one, and every Wi-Fi AP of LWIP node operates in the same channel for creating high interference scenario.

2.5 Performance results

The variations of UDP throughput w.r.t. UDP ADR of uplink and downlink flows for one UE (Exp #1) and four UEs (Exp #2) are shown in Figs. 2.10 and 2.11, respectively. UDP traffic types tend to harvest maximum capacity of the links, hence this experimental result sets a classical benchmark for aggregation advantages over individual LTE and Wi-Fi radio links.

2.5.1 Analysis of Expt #1 results

In one UE case with 4 Mbps and 24 Mbps ADR, the network is able to deliver the offered load in all the LASs as shown in Fig. 2.10. The observed throughput variation in Wi-Fi NoLAS does not vary much after 48 Mbps ADR and thereafter saturates, because, it reaches its maximum achievable rate of 24 Mbps for 802.11a with maximum PHY rate of 54 Mbps. Similarly, LTE NoLAS attains saturation after 48 Mbps. However, by leveraging the radio level integration benefits of LWIP node, PS-N-LAS and FS-N-LAS are able to deliver higher network throughputs than that of individual LTE and Wi-Fi only networks. The two variants of N-LAS are indistinguishable in performance due to its naive approach of symmetrically dividing flows and type of user traffic. WoD-LAS is no better than both FS-N-LAS and PS-N-LAS due to the presence of only one user and no contention in Wi-Fi. The next experiment encompasses a contention based scenario.

2.5.2 Analysis of Expt #2 results

The inclusion of four users in the network leads to contentions and therefore, Wi-Fi NoLAS performance is observed to be poor as compared to other LASs. Wi-Fi NoLAS yields poor throughput of 8 Mbps though it achieved 24 Mbps in previous experiment. Such phenomenon is not only due to collisions on the Wi-Fi channel but also the rate control algorithm which is sensitive to packet loss and its conservative action. The rate control algorithm used in this experiment is adaptive-auto-rate-fallback, which reduces the transmission rate on observing collisions and it could resort to the lowest transmission rate very quickly.

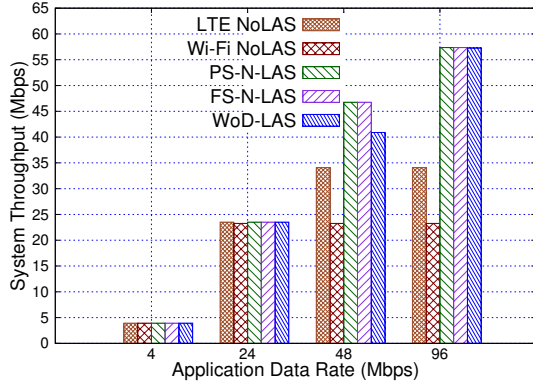


Figure 2.10: Expt #1: Variation in UDP throughput vs ADR of UDP flows; One UE case.

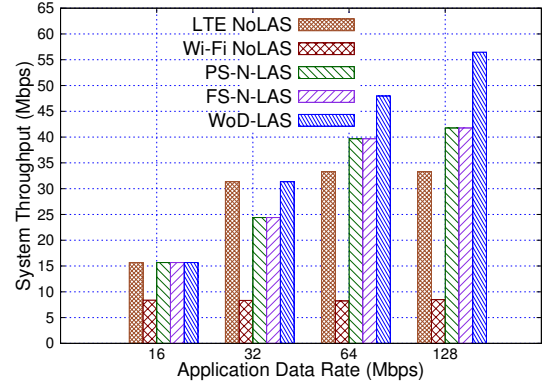


Figure 2.11: Expt #2: Variation in UDP throughput vs ADR of UDP flows; Four UEs case.

As LTE operates on the principle of scheduler based MAC, its throughput continues to rise with an increase in ADR but attains saturation after 34 Mbps (as shown in Fig. 2.11). Like the previous experiment, this experiment also shows almost equal throughputs due to the naive approach of equally dividing flows and type of user traffic across both links.

An important takeaway by comparing the results of N-LAS and WoD-LAS is that contentions of Wi-Fi degrade the performance of N-LAS and thereby resulting in lower peak value than in WoD-LAS. However, WoD-LAS does not suffer from this drawback by preventing contentions on Wi-Fi, as Wi-Fi link is used only in the downlink. One of the solutions to improve the throughput is to use constant rate manager. But in case of real-time environment, where the rate control algorithms conservatively reduce the transmission rate upon observing packet losses would be well assisted by WoD-LAS.

2.5.3 Analysis of Expts #3 and #4 results

In order to understand the behavior of LWIP system for a typical home deployment scenario, the next two experiments demonstrate performance benefits of LWIP considering UDP-heavy and TCP-heavy mixed traffic scenarios which are shown in Figs. 2.12 and 2.13, respectively. In both plots, with an increase in the number of users, the aggregation of LTE and Wi-Fi has resulted in enhanced throughputs than that in LTE NoLAS and Wi-Fi NoLAS. The Wi-Fi performance has been degraded due to high contentions on the Wi-Fi channel. Packet split mechanism could not improve proportionally due to the inherent issue of out-of-order deliveries and Dupack transmissions for TCP flows. These problems

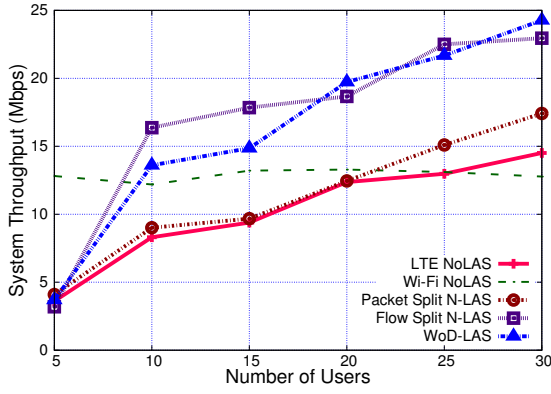


Figure 2.12: Expt #3: Home Scenario with one LWIP node; variation in system throughput vs number of UEs; Mixed Traffic, UDP-Heavy.

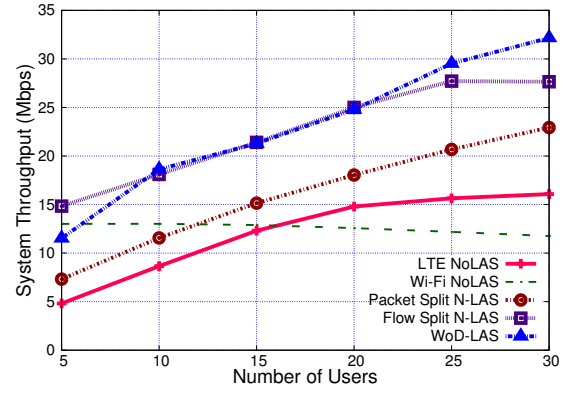


Figure 2.13: Expt #4: Home Scenario with one LWIP node; variation in system throughput vs number of UEs; Mixed Traffic, TCP-Heavy.

are avoided in FS-N-LAS, because a flow is pushed as a single unit to the destined radio interface. Comparison of WoD-LAS and FS-N-LAS shows that WoD-LAS suppresses the demerits of FS-N-LAS by restricting uplink flows only to LTE. In WoD-LAS, Wi-Fi utilizes its spectrum resources to carry user data and provides best-effort services by smartly utilizing the flow constraints in one direction. This facilitates a significant reduction in the number of collisions, thereby improving the system throughput over N-LAS schemes.

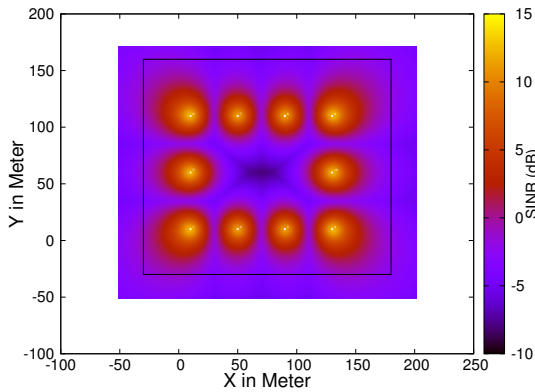


Figure 2.14: Expt #5: REM Plot for Indoor Stadium layout with 10 LWIP Nodes.

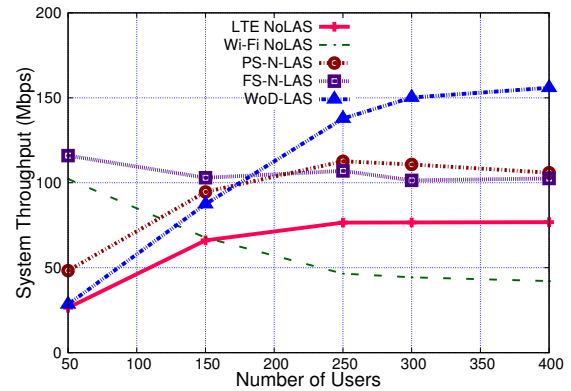


Figure 2.15: Expt #5; Indoor Stadium with 10 LWIP nodes; variation in system throughput vs number of UEs; Mixed Traffic.

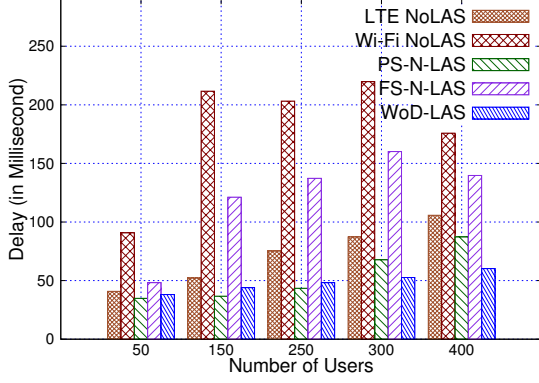


Figure 2.16: Expt #5: Delay of Voice Traffic in Indoor Stadium with 10 LWIP nodes.

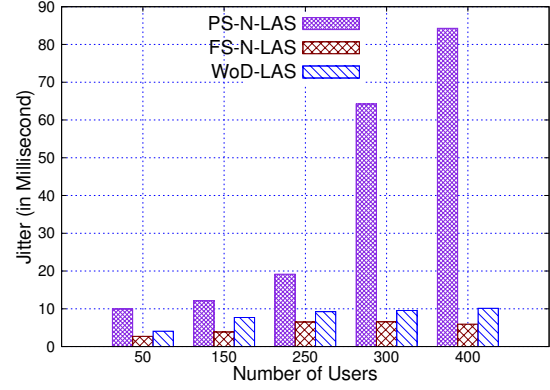


Figure 2.17: Expt #5: Jitter of Voice Traffic in Indoor Stadium with 10 LWIP nodes.

2.5.4 Analysis of Expt #5 results

Fig. 2.14 shows the LTE Radio Environment Map (REM) of an indoor stadium where 10 LWIP nodes are deployed. REM shows variation in SINR observed at each location in a given two dimensional region. The variation of system throughput with large number of UEs is shown in Fig. 2.15. Clearly, like in the previous experiments, Wi-Fi performance degradation is largely contributed by collisions. On the other hand, LTE throughput tends to produce less and nearly flat variation, because available radio resources are shared among all the active users. PS-N-LAS and FS-N-LAS do not show any notable difference as both the schemes are largely affected by reduced throughput on Wi-Fi. WoD-LAS results in highest system throughput over all other LASs under study. WoD-LAS achieves a system throughput of 155 Mbps for 400 users in Fig. 2.15 and shows nearly 50% more throughput than that of two variants of N-LAS.

As shown in Fig. 2.16, PS-N-LAS experiences less end-to-end delay when compared to other LASs. This is because of two radio interfaces having different packet service rates. FS-N-LAS incurs higher delay than PS-N-LAS as all packets of a flow are routed through one of the interfaces. With less number of users and traffic on Wi-Fi, WoD-LAS delay is higher than that of PS-N-LAS, but for a large number of users, Wi-Fi contention plays a role, thus increasing the delay of PS-N-LAS in case of 300 and 400 users as compared to WoD-LAS. Fig. 2.17 shows variation in jitter for three link aggregation strategies, where PS-N-LAS has highest jitter because Wi-Fi and LTE offer different PHY data rates for their packet transmissions. The jitter for FS-N-LAS and WoD-LAS are much less than that of

PS-N-LAS and it does not significantly impact voice traffic. Depending on network requirements, network operators could dynamically switch among various LASs for enhancing user experience and responsiveness of the system.

2.6 Challenges associated with LWIP architecture

This section describes various shortcomings of RLI architectures, especially LWIP, and potential challenges that have to be addressed. LWIP architecture has the potential to compete with other contemporary solutions [43] such as LTE-U (LTE in Unlicensed) [44] and LAA (Licensed Assisted Access) [45]. But LWIP can be successful only if we address the problem of steering across LTE and Wi-Fi effectively. This section describes various challenges and the way forward to address those challenges.

2.6.1 Does packet split (split bearer) has merits?

Packet split has a finer offloading granularity and finds its goodness in the case of UDP transmissions. It is an ideal offloading solution, where offloading decisions are instantaneous based on interface availability, delay, jitter, and losses due to fading, collision, and interference on that particular link. A finer level of offloading is beneficial only if the link information is available.

2.6.2 Is TCP a stumbling block for packet split?

Even after supporting dynamic offloading mechanism and finest offloading granularity, packet split is not able to offer better throughput because of difference in time of delivery of the packets over LTE and Wi-Fi link to the destination. TCP, being a highly reliable protocol, on observing a missing packet (which is due to arrival delay on another link - but no loss due to congestion) starts retransmission procedure by sending DUPLICATE ACKNOWLEDGEMENTS (DUPACKs). TCP sender understands these DUPACKs as actual packet loss due to congestion in the network and reduces the congestion window on receiving three consecutive DUPACKs, which is the most undesirable reaction for packet split. This problem arises because the IP layer of the receiver fails to reorder the packets which are received out-of-order. A reordering mechanism to ensure in-order delivery of packets in case of split bearer mechanism is needed for reaping in full benefits of packet split in LWIP.

2.7 Summary

RLI architectures aggregate LTE and Wi-Fi radio links better as compared to traditional interworking architectures. RLI exhibits enhanced control over the radio links and it has the ability to steer the traffic at the granularity of flows/packets/bytes. LWIP of RLI architecture adapts various link aggregation strategies which facilitate a way forward to better utilizing multiple radio links. The developed simulation workbench supports different link aggregation strategies. It can be clearly observed that WoD-LAS has improved the system throughput by 50% as compared to N-LAS in an indoor stadium environment. The following chapters discuss on effective steering across LTE and Wi-Fi in order to harvest the aggregated benefits of RLI.

Chapter 3

Downlink traffic steering in LWIP architecture

The previous chapter enumerated various challenges with RLI architectures. One of the important challenges which prevents RLI architectures from achieving aggregated link bandwidth is the co-tier interference between adjacent RLI nodes deployed. This chapter details the root cause of the problem and proposes a solution to address it.

3.1 Motivation

Challenges with small cell deployments include co-tier interference due to densification of small cells and QoS provisioning. The choice of intensifying the deployment of LTE small cells in order to improve the network capacity leads to high co-tier interference. The usage of orthogonal RATs (LTE and Wi-Fi) emerges as a prominent solution to address this problem. The users located at the high interference zone of LTE can connect to Wi-Fi, thereby reducing the effect of co-tier interference in LTE. Currently, LTE small cells and Wi-Fi APs are independently deployed, which make an LTE user who is facing high interference difficult to find a suitable Wi-Fi AP to associate with for obtaining better service. The co-located LWIP architecture that integrates stacks of LTE small cell and Wi-Fi AP in a single hardware unit has been proposed in order to address this problem, which ensures Wi-Fi link available for users even in the interference region. Co-located LWIP (C-LWIP) facilitates a unified control over LTE and Wi-Fi links. But C-LWIP deployment also has some issues. For example, consider a non co-located deployment of LWIP by an operator

for a shopping mall with ' N ' number of LTE SeNBs and ' N ' number of Wi-Fi APs that are connected to each other using Xw interface for interworking. A typical setup can cover a shopping mall of size say ' A ' sq. meters without any coverage holes *i.e.*, each location is ensured good SINR from at least one network: LTE or Wi-Fi. But it is impractical to cover the same area with ' N ' number of co-located LWIP nodes. Suppose the number of co-located LWIP nodes deployed is increased in order to solve the coverage hole problem, then this densification of LWIP nodes would lead to high co-tier interference.

The second most important challenge is to ensure QoS for LWIP users, which corresponds to allocating sufficient radio resources for their guaranteed bit rate (GBR) flows. In a typical indoor scenario, the SINR received by a user a.k.a. User Equipment (UE) is constrained by the number of walls and number of interfering LWIP nodes that exist in its vicinity. Many a time UEs with poor SINR fail to meet their GBR flow requirements. LTE MAC scheduler such as *Priority Set Scheduler* (allocates radio resources primarily to GBR bearers, after serving GBR bearers it schedules other bearers), allocates more resources to the UEs with poor SINR in order to meet their GBR requirements. Such a QoS centric allocation adversely affects the overall system throughput. This problem of efficient QoS provisioning pertains with C-LWIP nodes as well.

An important advantage of LWIP architecture is its ability in steering the flows dynamically across LTE and Wi-Fi links without requiring time-consuming core network signaling. Hence, a solution to maximize network throughput of LWIP by efficiently steering the flows dynamically across LTE and Wi-Fi links is needed. In order to address the above-mentioned challenges, in this chapter, a novel Power aware dynamic traffic Steering (PRECISE) algorithm is proposed for C-LWIP system which performs dynamic transmit power control and traffic steering in both LTE and Wi-Fi networks.

3.2 Related work

This section details the work in literature pertaining to interference management, QoS fulfillment, and flow steering. The existing solutions for interference mitigation include Inter-Cell Interference Coordination (ICIC) and eICIC [46]. These solutions employ frequency reuse and subframe muting to reduce interference in LTE networks. The offloading algorithm presented in [47] prioritizes the traffic with specific QoS requirement. The voice and video

flows are sent through the cellular network while the elastic flows are sent through Wi-Fi network. This approach ensures the QoS of GBR flows, but it does not intend to maximize the utilization of network resources. In [48], to overcome poor availability and performance of the cellular network, the authors have used two key ideas *viz.*, leverage delay tolerance and fast switching from cellular to Wi-Fi to reduce the load on the cellular network. Initially, all flows are sent through Wi-Fi. If Wi-Fi is unable to transmit packets of a flow in a small time window (delay tolerance limit), then that flow is quickly switched onto the cellular network. This solution focuses on maximizing the utilization of Wi-Fi, but it fails to maximize the overall network throughput.

Here are a few offloading solutions in the literature on traditional LTE Wi-Fi interworking. Significant work has been done for LTE Wi-Fi interworking which involves offloading decisions made at the cellular gateway of LTE network [49], [50], [47], [51], and [52]. Also, a lot of work has been carried out on modelling the downlink steering performance of cellular gateway-based solutions [53], [54], and [55]. In [56], the authors have shown that delaying the application data transmission until a user gets in Wi-Fi coverage has reduced the load on the cellular network. The authors project that offloading through Wi-Fi is the most preferable solution as it reduces the load on the cellular network, but the solution leads to inefficient utilization of Wi-Fi resources due to contention. In [36], the authors have proposed different LTE Wi-Fi interworking techniques, where flow offloading is realized by steering traffic at the transport layer, network layer, and link layer. All these works intent to perform flow offloading, and not much work has been done in tight coupling of LTE Wi-Fi networks as in the case of RLI architectures, which give LTE a finer control over Wi-Fi interface for efficient traffic steering.

Here are some works in the literature on RLI architectures. In [30], the authors proposed an α -optimal scheduler in which scheduling across multiple Radio Access Technologies (RATs) is formulated as an optimization problem. Steering the incoming traffic across different RATs *viz.*, LTE and Wi-Fi is done based on the value of α . For different values of α , the scheduler morphs its purpose as a proportional fair scheduler, maximum throughput scheduler, or maximize minimum rate scheduler. In [57], the authors proposed a “water-filling” based interpretation for resource allocation across multiple RATs. The fraction of traffic sent over a RAT is proportional to the ratio of users peak capacity on two RATs. The above mentioned schedulers enable efficient scheduling across both LTE and Wi-Fi RATs

simultaneously, but they do not aim to reduce interference in dense deployment scenarios.

To address the problems which exist with the aforementioned works in the literature, and to efficiently utilize the C-LWIP architecture for downlink traffic steering, Power-Aware Dynamic Traffic Steering (PRECISE) algorithm has been proposed in this chapter. The proposed PRECISE algorithm does efficient flow steering with intelligent power control for minimizing interference and thereby ensuring GBR QoS requirements with improved overall network throughput.

3.3 Proposed work: PRECISE

The PRECISE algorithm has been designed with the following objectives:

1. Mitigation of co-tier interference in dense deployment of LWIP system.
2. Meeting GBR requirements of the users including those experiencing poor SINR.
3. Dynamic steering of the flows across LTE and Wi-Fi links to maximize the overall system throughput.

Algorithm 1 details the components and working of the PRECISE algorithm. Table 3.1 lists the notations used in PRECISE algorithm. PRECISE has the following two phases:

1. Interference Mitigation (IM) Phase: regulates the transmit power of LTE and Wi-Fi interfaces to minimize the co-tier interference.
2. GBR Improvement (GI) Phase: targets to satisfy the GBR requirements of the users/flows.

Initially, the flow state information of all downlink flows is collected by a centralized decision making entity (*e.g.*, LWIP gateway). Note that this LWIP gateway assists only in regulating the transmit power across LWIP nodes. If requirements of GBR flows are met, then the algorithm aims to improve the system throughput by mitigating the co-tier interference by triggering IM Phase. In this phase, optimal transmit power values are computed and set for LTE and Wi-Fi interfaces in order to reduce co-tier interference across interfering C-LWIP nodes. The IM Phase is continued as long as QoS requirements of GBR flows are met. If GBR requirements of some of the flows are not met, then GBR Improvement Phase (GI Phase) is triggered in which the transmit powers of LTE and Wi-Fi interfaces

of C-LWIP nodes are adjusted in order to meet the GBR requirements. \mathcal{G}^s corresponds to percentage of GBR flows satisfied, it is given by $\mathcal{G}^s = \frac{\sum_{j \in \{GBR\}} \mathcal{F}_j}{\sum_{i \in \{GBR, NGBR\}} \mathcal{F}_i} \times 100$. Here, \mathcal{F}_i corresponds to information of the i^{th} flow in the network *i.e.*, information about i^{th} flow such as, (i) Type of flow: GBR or NGBR, (ii) Bandwidth requirement, (iii) Delay budget, (iv) Status of GBR [met or unmet], and (v) Throughput observed by that flow). Both IM and GI phases are followed by flow steering across LTE and Wi-Fi links in order to achieve their corresponding objectives. Flow steering involves ordering different flows based on their affinity to an interface. An i^{th} flow's affinity to an interface is given by its affinity index (\mathcal{AI}_i). If there exists GBR flows not meeting the GBR requirements, then a set of unmet GBR flows (Φ_G) are moved first to lightly loaded interface of the C-LWIP node. If GBR requirements are met, then a set of NGBR flows (Φ_{NG}) with high affinity are moved to the corresponding interface to maximize the throughput of the system. Φ_G is obtained by iteratively picking a set of unmet GBR flows that are currently being served in a heavily loaded link but can be accommodatable on the other link. Accommodating a flow on a new link is discussed later in Section 3.3.4.

Table 3.1: Notations used in PRECISE algorithm

Symbols	Definition
\mathcal{F}_i	Flow information of i^{th} flow
\mathcal{G}^j	Percentage of GBR flows met their QoS requirement
$\alpha_{i,j}^L$	Association of i^{th} UE with j^{th} LWIP node over LTE link
$\alpha_{i,j}^W$	Association of i^{th} UE with j^{th} LWIP node over Wi-Fi link
P^L	Transmit power of LTE link in LWIP node
P^W	Transmit power of Wi-Fi link in LWIP node
$\mathcal{L}^L, \mathcal{L}^W$	Load on LTE and Wi-Fi links
\mathcal{AI}	Flow affinity index
\mathcal{BT}	Wi-Fi channel busy time
\mathcal{IT}	Wi-Fi channel idle time
Φ_G	Set of unsatisfied GBR flows
Φ_{NG}	Set of unsatisfied NGBR flows

3.3.1 System model

Our system model (shown in Fig. 3.1) comprises of LWIP nodes, deployed in a given region of interest, which run proposed PRECISE algorithm to achieve the targeted objectives. Fig. 3.2 depicts an example of coverage pattern exhibited by the considered system during

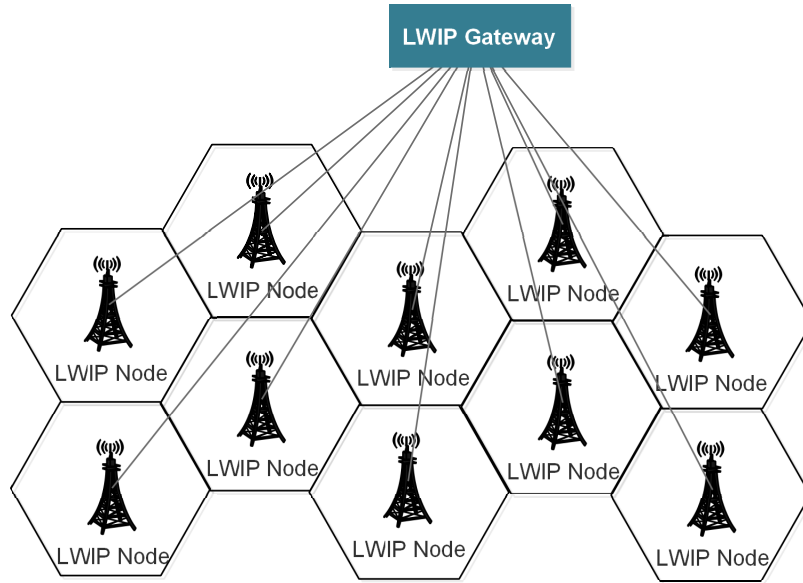


Figure 3.1: System Model.

IM and GI phases. It includes LTE operating on one licensed frequency band across all the cells and Wi-Fi using one unlicensed channel across all the cells. During IM phase, LTE and Wi-Fi coverages appear to cover the alternate cell edge regions in order to reduce co-tier interference (note that this figure is a closer approximation and it may vary based on user density and their positions in the network). In Fig. 3.2, points 'A' and 'D' denote locations of two C-LWIP nodes whereas 'B' and 'C' denote the regions of interest. When C-LWIP nodes at 'A' and 'D' transmit with the same power, then the regions 'B' and 'C' suffer from high co-tier interference. IM Phase is then triggered which reduces LTE co-tier interference in the regions 'B' and 'C' by reducing the transmit power of LTE eNodeB in C-LWIP node 'A'. Similarly, Wi-Fi interference at regions 'B' and 'C' is reduced by reducing the transmit power of Wi-Fi AP in C-LWIP node 'D'. During GI phase, the edge of coverage region is expanded or shrank based on the number of UEs with unmet GBR flows. Expansion or increase in transmit power on a link corresponds to improving bit rate for a UE with unmet GBR requirements. Reduction in coverage region corresponds to reducing interference for UEs associated with other C-LWIP nodes without degrading GBR guarantees of the current C-LWIP node. The power control function of PRECISE algorithm runs at LWIP gateway whereas the flow steering runs at the C-LWIP node so that it can take independent and fast steering of flows across LTE and Wi-Fi links. The flow steering algorithm is executed once in every N TTIs.

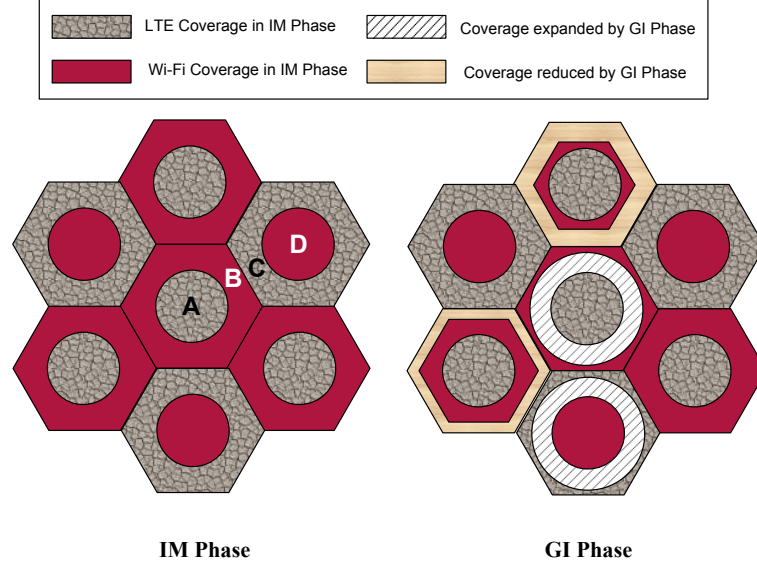


Figure 3.2: Variation in coverage regions of LTE and Wi-Fi cells observed in different phases of PRECISE algorithm.

Algorithm 1 Power aware dynamic traffic Steering (PRECISE)

Input: Set of all flows information in the system (\mathcal{F}_i), $i \in \{\text{flows } 1, \dots, k\}$, SINR of UEs associated with C-LWIP nodes

- 1: **for** Every N ms **do**
- 2: **if** $\mathcal{G}^s \geq 90\%$ **then** ▷ Trigger IM Phase
- 3: $\Theta^{IM}(P_j^L, P_j^W)$
- 4: Set Tx powers obtained through Θ^{IM} optimization
- 5: **else** ▷ Trigger GI Phase
- 6: $\Theta^{GI}(P_j^L, P_j^W)$
- 7: Set Tx powers obtained through Θ^{GI} optimization
- 8: **end if** ▷ Flow Steering

- 9: $\mathcal{AI} \leftarrow \text{TOPSIS}(\mathcal{F}^i)$
- 10: **if** $\mathcal{L}^L > \mathcal{L}^W$ **then**
- 11: **if** GBR flows unsatisfied **then**
- 12: Steer a set of unmet GBR flows (Φ_G) to Wi-Fi
- 13: **else**
- 14: Steer a set of NGBR flows (Φ_{NG}) with high affinity index to Wi-Fi
- 15: **end if**
- 16: **else**
- 17: **if** GBR flows unsatisfied **then**
- 18: Steer a set of unmet GBR flows (Φ_G) to LTE
- 19: **else**
- 20: Steer a set of NGBR flows (Φ_{NG}) with high affinity index to LTE
- 21: **end if**
- 22: **end if**
- 23: **end for**

3.3.2 IM Phase of PRECISE: Interference mitigation using orthogonal RATs

In this work, the interference mitigation sub-problem is formulated as a mixed integer non-linear programming (MINLP) problem with an objective of minimizing co-tier interference within a RAT. IM phase sets the optimal transmit powers to LTE and Wi-Fi interfaces of C-LWIP node. The SINR maximization of C-LWIP is formulated as follows:

$$\text{Maximize } \Theta^{IM} = \sum_{i=1, j=1}^{U, B} (\alpha_{i,j}^L \times SINR_i^L + \alpha_{i,j}^W \times SINR_i^W) \quad (3.1)$$

s. t.

$$\sum_{j=1}^B \alpha_{i,j}^L \leq 1 \quad \forall i \quad \text{and} \quad \sum_{j=1}^B \alpha_{i,j}^W \leq 1 \quad \forall i$$

$$\alpha_{i,j}^L = \begin{cases} 1, & \text{if } SINR_i^L \geq Th_{LTE} \\ 0, & \text{otherwise} \end{cases}$$

$$\alpha_{i,j}^W = \begin{cases} 1, & \text{if } SINR_i^W \geq Th_{Wi-Fi} \\ 0, & \text{otherwise} \end{cases}$$

$$\alpha_{i,j}^L = \begin{cases} 0 \text{ or } 1, & \text{if } \alpha_{i,j}^W = 1 \\ 0, & \text{otherwise} \end{cases}$$

$$\alpha_{i,j}^W = \begin{cases} 0 \text{ or } 1, & \text{if } \alpha_{i,j}^L = 1 \\ 0, & \text{otherwise} \end{cases}$$

$$P_{min}^L \leq P_j^L \leq P_{max}^L$$

$$P_{min}^W \leq P_j^W \leq P_{max}^W$$

Θ^{IM} is the sum over LTE and Wi-Fi SINRs of users associated with LTE and Wi-Fi links of C-LWIP nodes. Here, P_j^L and P_j^W are the transmit powers of LTE and Wi-Fi interfaces of j^{th} LWIP node, respectively. The power is a regulatory parameter which can

be varied from the lower limit (P_{min}^L) to upper limit (P_{max}^L). $\alpha_{i,j}^L$ is a binary variable which corresponds to association of i^{th} user with j^{th} C-LWIP node over LTE interface and $\alpha_{i,j}^W$ denotes association of i^{th} user with j^{th} C-LWIP node over Wi-Fi interface. B and U denote the number of C-LWIP nodes and number of users in the system, respectively. This optimization problem (Θ^{IM}) can be solved using an MINLP solver. $SINR_i^L$ corresponds to the SINR observed by i^{th} user over LTE link. $SINR_i^W$ corresponds to the SINR observed by i^{th} user over Wi-Fi link.

3.3.3 GI Phase of PRECISE: GBR improvement using dynamic power control

The objective of this sub-problem is to maximize the throughput of GBR flows. GI is formulated as an MINLP problem with an objective to improve the throughput of UEs whose GBR requirements are not met. This can be achieved by maximizing the sum of weighted SINRs of those UEs. Weights associated with each UE depends on number of unsatisfied GBR flows associated with that UE.

$$\text{Maximize } \Theta^{GI} = \sum_{i=1, j=1}^{U, B} (r_{i,j}^L \times SINR_i^L + r_{i,j}^W \times SINR_i^W) \quad (3.2)$$

s.t.

$$\begin{aligned} P_{min}^L &\leq P_j^L \leq P_{max}^L \\ P_{min}^W &\leq P_j^W \leq P_{max}^L \end{aligned}$$

$$\begin{cases} SINR_i^L - (\gamma \times \Theta(SINR_i^L)) \geq 0 & \text{if } \Theta(SINR_i^L) \geq S_M \\ SINR_i^L - \Theta(SINR_i^L) \geq 0 & \text{otherwise} \end{cases}$$

$$\begin{cases} SINR_i^W - (\gamma \times \Theta(SINR_i^W)) \geq 0 & \text{if } \Theta(SINR_i^W) \geq S_M \\ SINR_i^W - \Theta(SINR_i^W) \geq 0 & \text{otherwise} \end{cases}$$

The term $r_{i,j}^L$ corresponds to the weight given to UEs having different number of unmet

GBRs flows. $r_{i,j}^L = \frac{\vartheta_{i,j}}{\sum_i \vartheta_{i,j}}$, here $\vartheta_{i,j}$ corresponds to number of unmet GBR flows of i^{th} user associated with j^{th} C-LWIP node. $\Theta(SINR_i^L)$ and $\Theta(SINR_i^W)$ correspond to SINRs of LTE and Wi-Fi observed during the IM phase, respectively. γ denotes the tolerable fraction in reduction of SINR for the users who operate with the highest Modulation and Coding Scheme (MCS). S_M corresponds to the minimum SINR at which a UE gets to transmit with the highest MCS.

3.3.4 Flow steering across LTE and Wi-Fi links

The PRECISE algorithm selects a flow to be steered from one interface to other using multi-attribute decision making (MADM) technique called as Technique for Order Performance by Similarity to Ideal Solution (TOPSIS) [58]. TOPSIS makes use of various decision making parameters (DMPs) from UEs such as LTE SINR, Wi-Fi SINR, and available bandwidths on LTE and Wi-Fi links. Link Aggregation Layer (LAL) of C-LWIP node gathers all these DMPs. TOPSIS then chooses the best suitable flow to be moved to an appropriate link based on these DMPs.

TOPSIS: Subroutine TOPSIS shows the procedure involved in prioritizing the flows. For every flow i , DMPs are obtained from LAL of the C-LWIP node. All these DMPs are normalized and appropriate decision making weights (w) are given to them. Following processing of DMPs, Positive Ideal Solution (PIS) and Negative Ideal Solution (NIS) are computed. PIS is a set of best values among all flows for each parameter while NIS is a set of worst values among all flows for each parameter. For example, PIS will contain the largest $SINR$ value but the smallest value in packet error rate (PER). Relative Closeness (RC) is a metric which emphasizes how close a flow is to PIS or NIS. Affinity Index (\mathcal{AI}_i) of i^{th} flow towards a specified interface is obtained by ranking them based on its RC. Flow with a large difference from NIS and less difference from PIS has high affinity to be steered.

3.3.5 Obtaining decision making parameters for TOPSIS

TOPSIS uses the following DMPs for decision making: load of LTE (\mathcal{L}^L), load of Wi-Fi (\mathcal{L}^W), and GBR requirements of the flows. Loads on both LTE and Wi-Fi links are calcu-

Subroutine: TOPSIS for Ranking Flow Affinity

Input: Set of all flow parameters (\mathcal{F}_i), Link to which flow affinity has to be obtained

- 1: Vector Normalization of all flow parameters $F_{i,j}$ where $i \in \{\text{flows } 1, \dots, k\}$, $j \in \{\text{network parameters}\}$
 - 2: Apply given set of weights $w^T = \{w_1, w_2, w_3, w_4\}$
 - 3: $F_{i,j} \leftarrow F_{i,j} \times w_j$
 - 4: Find A^+ (Positive ideal solution) and A^- (Negative ideal solution)
 - 5: Find Positive ideal separation (S^+) and Negative ideal separation (S^-)
 - 6: Calculate relative closeness (RC_i) for each flow: $RC_i \leftarrow \frac{S_i^-}{S_i^+ + S_i^-}$
 - 7: $\mathcal{AI} \leftarrow \text{sort } \{RC_i\}$ in descending order
 - 8: Return the flow affinity index \mathcal{AI}_i for every flow \mathcal{F}_i
-

lated as follows:

$$\mathcal{L}^L = \frac{\sum_{i=1}^N uPRB_i}{tPRB \times N} \quad (3.3)$$

$$\mathcal{L}^W = \frac{\mathcal{BT}}{\mathcal{BT} + \mathcal{IT}} \quad (3.4)$$

Here, tPRB is the total number of physical resource blocks available in a TTI. $uPRB$ is the number of PRBs used for data transmission in a TTI. In Equation (3.3), \mathcal{L}^L is found as the ratio of the total number of uPRB to the total number of available PRBs over N TTIs (the value is set to $N=200$ which corresponds to the Decision Making Interval - DMI). Equation (3.4) is used to obtain load on Wi-Fi by estimating channel busy time over time window of N ms. \mathcal{BT} and \mathcal{IT} correspond to busy and idle times of Wi-Fi channel, respectively.

In order to find out how many flows LTE can accommodate, the cumulative throughput of all GBR flows is subtracted from the maximum achievable throughput. Available bandwidth in LTE (\mathcal{A}^L) can be obtained as follows.

$$\mathcal{A}^L = \mathcal{M}^L - \sum_{i=1}^U \mathcal{O}_i^L \quad (3.5)$$

Here, \mathcal{M}^L denotes the maximum throughput that can be achieved by LTE under the given network conditions, given by $\mathcal{M}^L = BW \times \log(1 + \Psi^L)$, where Ψ^L corresponds to average SINR of UE in LTE. \mathcal{O}_i^L corresponds to the throughput observed by i^{th} user in LTE. Similarly, to estimate how many flows Wi-Fi can accommodate, current channel utilization by all GBR and NGBR flows (*i.e.*, \mathcal{L}^W) is subtracted from the maximum channel utilization

under the given network conditions.

$$\mathcal{A}^W = (\mathcal{M}\mathcal{C}^W - \mathcal{L}^W) \times \mathcal{P}\mathcal{D} \quad (3.6)$$

Here, $\mathcal{M}\mathcal{C}^W$ denotes the maximum channel utilization (network is fully loaded), \mathcal{L}^W denotes the load on Wi-Fi and $\mathcal{P}\mathcal{D}$ denotes the average physical layer data rate of Wi-Fi, which is given by,

$$\mathcal{P}\mathcal{D} = BW \times \log(1 + \Psi^W)$$

where Ψ^W corresponds to average SINR of UE in Wi-Fi.

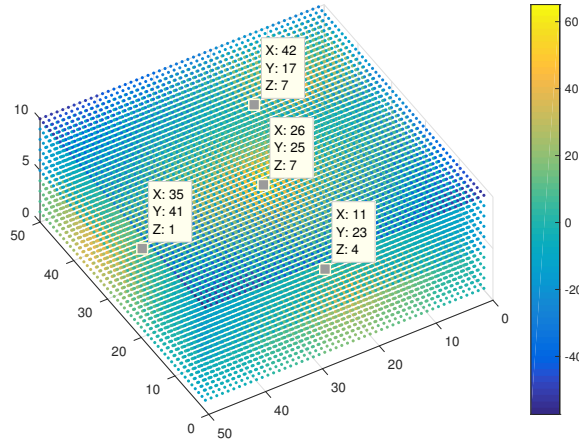


Figure 3.3: SINR distribution 3D-map of the building chosen for conducting experiment with four C-LWIP nodes. The x, y, and z values of C-LWIP nodes are also given in the map.

3.4 Simulation setup

Fig. 3.3 shows the SINR distribution presented as a heat map of the simulation scenario considered for evaluating the proposed PRECISE algorithm. The SINR reference bar presents the SINR color code in dB. A building of dimensions 50 m \times 50 m \times 10 m is considered. Four C-LWIP nodes are placed (one per room) in such a way that the mean euclidean distance between LWIP nodes is measured to be at least 20 meters. The positions of C-LWIP nodes in the building are marked in Fig. 3.3. The building has two floors and a wall per every 10 meters. Path loss model includes wall and floor losses. For creating more challeng-

ing environment, LTE is considered to operate with reuse factor one, and all Wi-Fi APs are configured to operate on the same channel. The other important simulation parameters are shown in Table 3.2. MATLAB based solver (*fmincon*) is employed in this work to solve the optimization problem. The time taken to obtain the optimal solution is in the order of ms, which makes the proposed solution to work in real-time.

Table 3.2: Simulation parameters for evaluating PRECISE algorithm

Parameter	Value
# of UEs, LWIP Nodes	100, 4
Max Tx power of LTE & Wi-Fi	23, 20 dBm
LTE path loss model	3GPP indoor path loss model [59]
Wi-Fi path loss model	ITU path loss model [60]
LTE MAC Scheduler	Priority Set Scheduler (PSS)
UE position	Random
Wi-Fi Standard	IEEE 802.11n
Wi-Fi frequency and bandwidth	2.4 GHz, 20 MHz
LTE frequency and bandwidth	2.6 GHz, 10 MHz
Simulation duration	10^4 Seconds
Number of seeds	10

3.5 Performance results

The performance of the PRECISE algorithm has been evaluated in a dense deployment scenario. The PRECISE algorithm is compared with existing Wi-Fi offload algorithms [61], [48], 3GPP Rel. 12 [62], and a state-of-the-art α -optimal scheduler [30] to observe its performance benefits. Wi-Fi offload algorithm prefers to use only Wi-Fi link whenever Wi-Fi is available and switches to LTE link on observing poor SINR in Wi-Fi. In 3GPP Rel. 12 solution, a UE gets associated with either LTE or Wi-Fi link of C-LWIP node. The UE prefers to associate with the link having higher SINR. The α -optimal scheduler associates a set of flows through LTE and Wi-Fi links based on achievable throughputs by that UE in different RATs. When $\alpha=1$, the scheduler does a proportionally fair split among the flows sent through LTE and Wi-Fi links.

3.5.1 SINR distribution in the indoor scenario

The SINR distributions of UEs are observed in two cases: (i) LWIP with fixed power (set to the maximum power) and (ii) LWIP power obtained from the PRECISE algorithm. Fig. 3.4

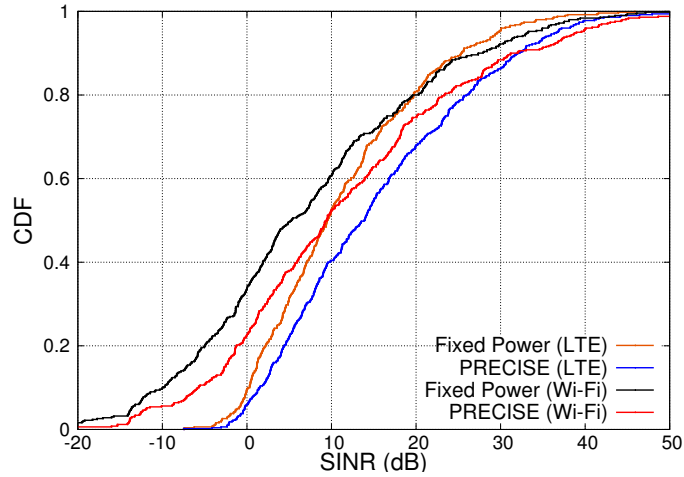


Figure 3.4: CDF of SINR of UEs.

shows CDF of SINR of UEs. It can be observed that PRECISE algorithm has improved SINR of UEs by 4 dB in both LTE and Wi-Fi links as compared to the fixed power allocation scheme. This improvement is achieved because PRECISE algorithm optimizes the transmit power of LTE and Wi-Fi links in order to reduce the co-tier interference across multiple LWIP nodes. The co-tier interference refers to interference cause by LTE link of one LWIP node to the LTE link of adjacent LWIP node. The operation of PRECISE algorithm resembles fractional frequency reuse, but the frequency split in this context is between LTE and Wi-Fi frequencies.

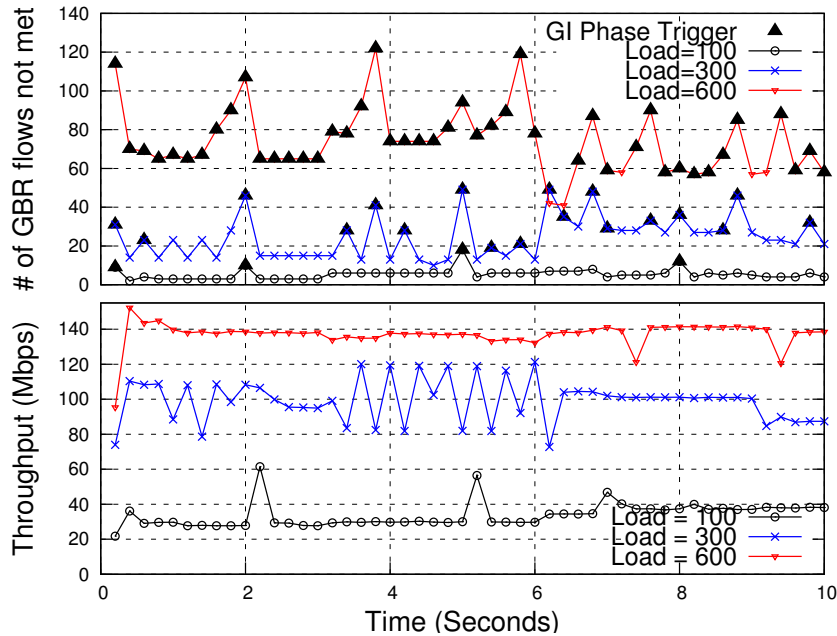


Figure 3.5: Different events triggered over time in case of $load = 100, 300,$ and 600 flows in the network.

3.5.2 Ensure GBR in the network

The PRECISE algorithm ensures data rate requirements of GBR flows and maximizes the throughput for NGBR flows thereby maximizing the entire network throughput. In this experiment, UE traffic includes GBR and NGBR flows. GBR flows comprise of conversational voice (G.711) at 87.2 Kbps GBR, Video call (HD) at 1.2 Mbps, and Streaming Video at 1.2 Mbps [63]. NGBR flows include Sync Apps and file downloads. The total number of downlink flows in the network at any instance follows Poisson distribution with mean following load in the network. Fig. 3.5 is an instantaneous capture of throughput and number of unmet GBR flows. Data points are plotted for every 200 ms which corresponds to a DMI of the PRECISE algorithm. The experiment is conducted for low, medium, and high load conditions (load= 100, 300, and 600 flows), and number of triggers observed in all the cases are examined. In case of load=100 flows, the number of GBR flows are low and they are satisfied. As the load increases, the number of unmet GBR flows increases. This triggers GI phase, which regulates the transmit power of LWIP nodes in order to reduce the number of unmet GBR flows. During GI phase, the transmit power of LTE and Wi-Fi links are obtained by solving the optimization problem shown in Equation (3.2). In case of high load (load=600 flows), GI phase is triggered more than IM phase as the unmet GBR flows are very high.

3.5.3 Different phases of PRECISE algorithm

To study different phase of the PRECISE algorithm, four different experiments have been conducted. In each experiment, the mean number of flows in LWIP network is varied from 100 to 600. The number of IM triggers and GI triggers observed for different loads are counted. Fig. 3.6 shows the number of times IM and GI phases are triggered. As the load in the network by increasing the number of flows from 100 to 600, the number of unmet GBR flows increases. In order to reduce the number of unmet GBR flows, GI phase is triggered accordingly.

3.5.4 Throughput analysis

Performance of different algorithms are compared with the PRECISE algorithm. Fig. 3.7 shows CDF of throughput of UEs observed for a fixed load (load = 600 flows) when different

algorithms are employed. In case of Wi-Fi preferred algorithm, UE throughput is low because UE associated with LWIP node strictly confines to use Wi-Fi resources even when both LTE and Wi-Fi SINRs are high. The UE prefers to use LTE only when Wi-Fi SINR is lesser than a threshold which leads to inefficient resource utilization. Rel-12 allows the UE to choose and associate the flow to the link with better SINR. Hence, the UE throughput has improved significantly compared to Wi-Fi preferred algorithm. α -optimal scheduler distributes the flows of a UE proportionally across LTE and Wi-Fi links based on the throughput of a UE on each RAT (observed over each DMI). In case of the PRECISE algorithm, not only the flow steering that has been done across LTE and Wi-Fi links, but also the efficient power regulation for improving UE throughput. The experiment is repeated by varying the load (number of flows), and throughputs achieved by different algorithms are captured in Fig. 3.8. As the load increases, the throughput of the network increases significantly in case of PRECISE compared to other algorithms because of efficient flow routing and power regulation. The PRECISE algorithm has improved the network throughput by 48% as compared to the state-of-the-art α -optimal scheduler. The PRECISE algorithm has outperformed 3GPP Rel-12 based LTE Wi-Fi interworking solution by 84%. The α -optimal thrives to maximize the throughput of all the UEs in the network, hence it indulges in steering the flows with high data requirement onto the best interface. The PRECISE algorithm also considers the type of traffic (GBR, NGBR) involved in order to maximize the GBR satisfaction at high load. Fig. 3.9 captures the fraction of unmet GBR flows in the network when different algorithms are employed. The PRECISE algorithm minimizes the unmet GBR flows compared to other algorithms because of its ability to pick

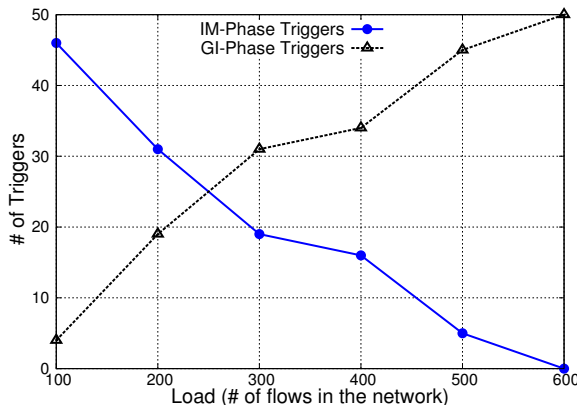


Figure 3.6: Triggers for different network loads.

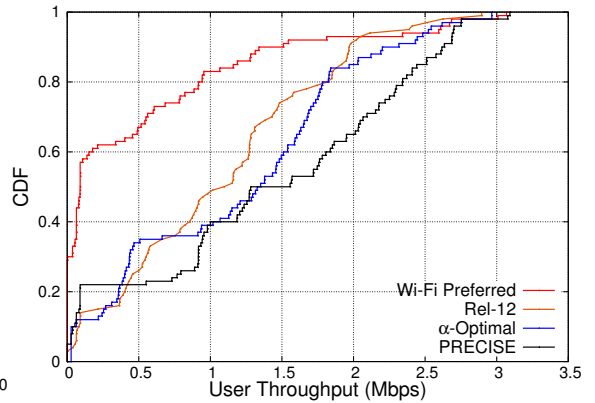


Figure 3.7: CDF of throughput of UEs.

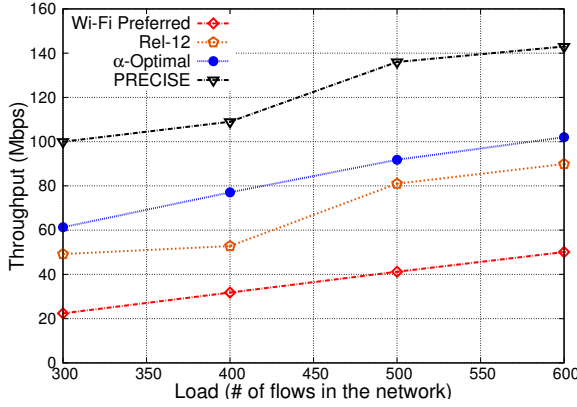


Figure 3.8: Throughput observed with different loads.

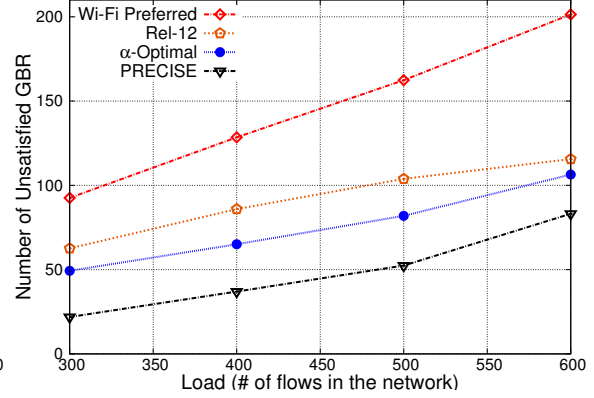


Figure 3.9: Number of unmet GBR flows.

GBR flows first and then steer to best interface in order to satisfy its requirement. The PRECISE algorithm has reduced the number of unmet GBR flows by 35% as compared to α -optimal scheduler.

3.6 Summary

The co-located LWIP system offers sophisticated control over LTE and Wi-Fi links. The proposed downlink traffic steering algorithm, PRECISE, ensures QoS and maximizes the network throughput in dense deployment scenarios. The improvement in throughput was achieved because the PRECISE algorithm employed dynamic power control in order to reduce the interference in dense deployment scenario, which also resulted in improved performance of GBR flows. PRECISE algorithm dynamically steered the flows across LTE and Wi-Fi links using MADM technique, which associated a flow through the most affine interface in order to improve the network throughput. The PRECISE algorithm has outperformed the throughput of α -optimal scheduler by 48% and 3GPP Rel-12 LTE Wi-Fi interworking by 84%. The PRECISE algorithm has reduced the number of unmet GBRs compared to other existing algorithms; notably it has reduced unmet GBR flows by 35% as compared to the α -optimal scheduler. Following this downlink traffic steering solution, solutions for uplink traffic steering in the context of LWIP architecture will be discussed in the following chapter.

Chapter 4

Uplink traffic steering in LWIP architecture

In the previous chapter, it was discussed about effectively utilizing the radio resources of LWIP nodes in downlink. It was concluded in Chapter 2 that employing Wi-Fi to carry only downlink IP traffic improves the overall performance of the LWIP system (since uplink in Wi-Fi involves contentions). However, completely preventing uplink transmissions in Wi-Fi of LWIP system could incur longer uplink queuing delay. Also, when LTE link quality becomes poor then *Wi-Fi only in downlink* fails to meet the QoS requirements. This chapter addresses the fundamental problems which prevent Wi-Fi performing efficient uplink transmissions in LWIP system by proposing various uplink traffic steering mechanisms.

4.1 Motivation

The major challenge to enable uplink transmissions through Wi-Fi in LWIP system is its contention based MAC operation. It allows a Wi-Fi node to transmit on the expiry of chosen backoff value, which could lead to collision if backoffs of two or more nodes expire at the same time. This collision probability increases with the number of contending nodes on the channel in Wi-Fi. LWIP involves tight coupling of LTE and Wi-Fi, and it enables LTE to have finer control over Wi-Fi. This property of LWIP will be exploited in this chapter in order to reduce the number of collisions in the Wi-Fi domain by regulating uplink transmissions.

Towards this, an uplink traffic steering framework in the context of LTE Wi-Fi integra-

tion is proposed in this chapter with the following objectives:

1. Obtaining the optimal fraction of uplink traffic to be steered through Wi-Fi to maximize uplink throughput.
2. Reducing number of collisions with distributed access control.
3. Achieving fair operation with other background Wi-Fi nodes operating on the channel.

4.1.1 Design requirements for Uplink traffic steering

Fig. 4.1 shows the possible optimization in saturated and unsaturated regions in Wi-Fi domain. In the unsaturated region, the activity on Wi-Fi channel is low. Hence, the UEs associated with LWIP node can offload traffic from the LTE interface to the Wi-Fi interface and thereby enhancing the utilization of the Wi-Fi channel. In the saturated region, the activity on Wi-Fi channel is high. The channel efficiency can be achieved by avoiding collisions among users contending in the uplink. Hence, the primary challenge which has to be addressed is a large number of collisions occurring in Wi-Fi domain. Reduction in collisions can be achieved by coordinating uplink transmissions on Wi-Fi channel with the help of a primary carrier like LTE. An efficient uplink traffic steering algorithm should have the following properties:

1. The uplink traffic steering algorithm should operate fairly with other users operating on Wi-Fi channel *i.e.*, native Wi-Fi users on the channel should not be affected.
2. The uplink traffic steering algorithm should facilitate at least the transmission opportunity that DCF (Distributed Co-ordination Function) would have provided.
3. The uplink traffic steering algorithm should reduce the number of collisions due to simultaneous transmissions by multiple nodes on the Wi-Fi channel as compared to DCF.
4. The decision taken by uplink traffic steering solution should be prominent and hold till subsequent control channel broadcast (Master Information Block - MIB and System Information Block - SIBs) in LTE in order to maintain consistency in traffic steering. In other words, between two consecutive LTE broadcast messages, any decision taken such as uplink flow offloading or uplink packet scheduling should not change.

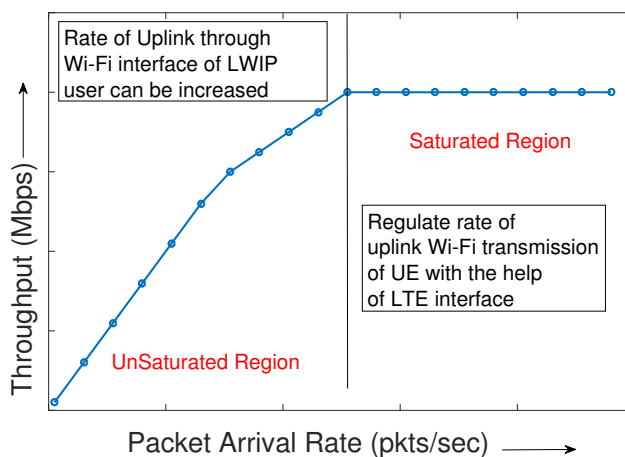


Figure 4.1: The optimization which is feasible in Wi-Fi domain.

4.2 Related work

In this section, the evolution of LTE Wi-Fi integration will be elaborated and the state-of-the-art integration architectures will be presented.

It is reported in [64] that not much work has been done on uplink traffic steering; instead some works have been done in the context of power saving. The existing uplink traffic offloading techniques aim to save the battery power of the UEs. Here are a few existing uplink traffic offloading works in the literature with the objective to improve power efficiency and enable proportional routing. In [65], the authors have proposed two uplink traffic offloading algorithms to improve the energy efficiency of the UEs and to increase the offloaded data volume under concurrent use of two access technologies using IP Flow Mobility and Seamless Offload (IFOM). In the first algorithm, UEs with high volume data are promoted and given priority in accessing Wi-Fi Access Point (AP) to offload their data. The second algorithm does a proportionally fair bandwidth allocation based on data needs of the UEs. In [66], a weighted Proportionally Fair Bandwidth (PFB) allocation algorithm for the Wi-Fi access in conjunction with a pricing-based rate allocation for the LTE uplink access is developed. In [67], the authors have proposed an energy efficient offloading algorithm which chooses the users to be offloaded at a lower computational complexity, with an objective of minimizing the energy spent by the users associated with LTE and Wi-Fi networks. To the best of our knowledge, none of the existing works have focused on improving the Wi-Fi channel utilization by using LTE for regulating uplink Wi-Fi transmissions. Even though there exist numerous solutions for steering traffic across LTE and Wi-Fi links in downlink steering, interestingly, not much work has been done in uplink traffic steering.

4.3 Proposed NCF algorithms for uplink traffic steering

In order to realize efficient uplink traffic steering in LWIP, in this chapter we propose a Network Coordination Function (NCF) which has various uplink traffic steering algorithms aggregated. Fig. 4.2 shows the enhanced LWIP architecture which supports uplink traffic steering as well. Link Aggregation Layer (LAL) is responsible for steering the traffic across LTE and Wi-Fi links which exists at both LWIP node and LWIP-UE. NCF includes novel medium access control algorithms and flow regulation algorithms employed at SeNB and UE. The list of proposed algorithms are as follows:

1. Dynamic Optimal Uplink Traffic steering Algorithm (DOUTA)
2. Fast Uplink through Direct medium access (FUND)
3. FUND with fair Channel Access (FUND++)
4. Enhanced Uplink With viRtual Polling (E-UNWRAP)

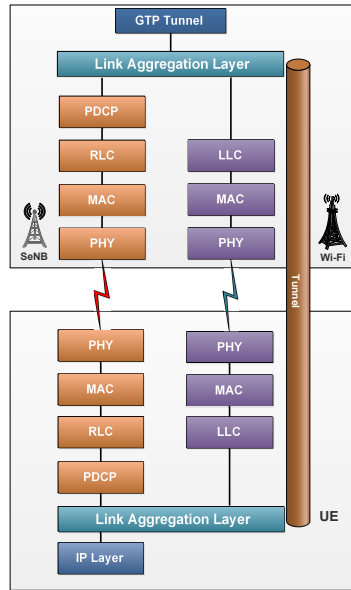


Figure 4.2: Enhanced LWIP architecture which supports both downlink and uplink traffic steering.

Fig. 4.3 shows design objectives for developing various NCF algorithms. These algorithms operate at different layers with multiple objectives, but all the algorithms have one common objective, which is to maximize the Wi-Fi channel utilization by reducing channel

time wasted due to collisions. NCF facilitates the network to make intelligent decisions rather than individual UEs deciding to steer the uplink traffic onto LTE or Wi-Fi link. The NCF algorithms work by leveraging the availability of LTE as the anchor to improve the channel utilization of Wi-Fi. Also, these algorithms do uplink traffic steering by taking inputs from both LTE and Wi-Fi links. NCF coordinates both the LTE and Wi-Fi transmissions by regulating the uplink flow rate and improving the existing medium access techniques.

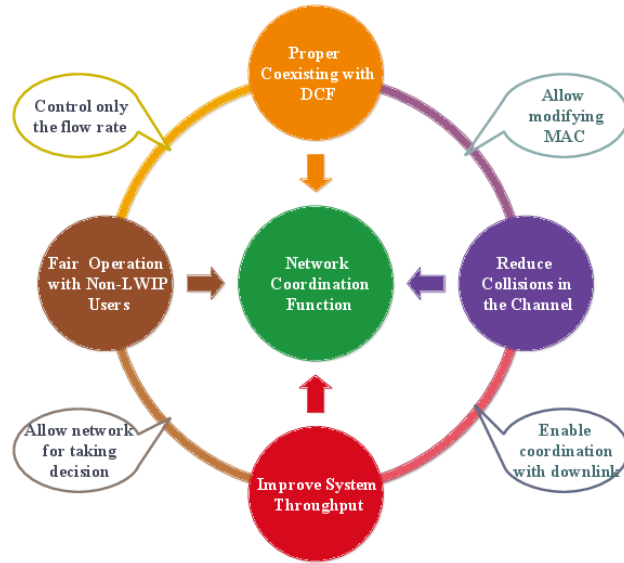


Figure 4.3: Objectives of Network Coordination Function Algorithms.

The proposed NCF, implemented at LWIP node and LWIP-UEs, maximizes the channel utilization of Wi-Fi link as compared to DCF mechanism, and ensures fairness in the channel access. NCF targets to maximize the network level throughput along with fairness by employing a centralized coordination among LWIP users, but in case of DCF, user level fairness is ensured in a long run even though it may not lead to efficient channel utilization. Fig. 4.4 shows proposed NCF algorithms and their features.

Table 4.1, in a nutshell, presents the layer of operation for different NCF algorithms and the kind of operations performed by them. A network operator can employ these algorithms: either one of them at a time or couple the algorithm operating at the IP layer with the algorithm operating at the MAC layer. Among NCF algorithms, DOUTA does not require any modification at UE side and hence it can be readily deployed with

modifications restricted only to LWIP node. If the finer level of coordination at the MAC layer is required, then FUND, FUND++, and E-UNWRAP can be employed. It is to be noted that the proposed NCF algorithms focus on improving the network throughput without changing the semantics of Wi-Fi QoS. Each of these algorithms has its own merits which are enumerated below, they are as follows:

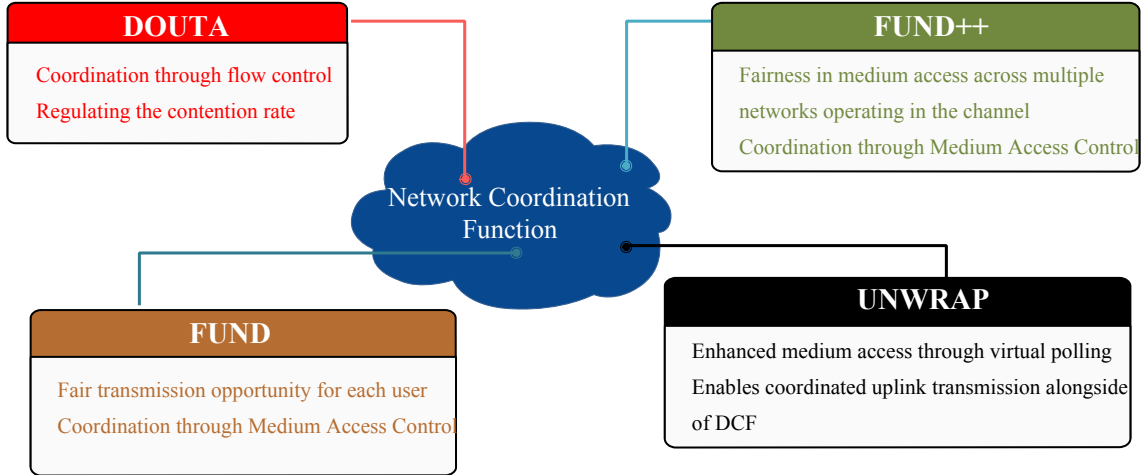


Figure 4.4: Proposed NCF Algorithms.

- FUND is preferred in situations where the time duration that is given to an LWIP user is proportional to that of legacy Wi-Fi user in accessing the Wi-Fi channel.
- FUND++ is most appropriate in situations where the transmission opportunities given to LWIP user and legacy Wi-Fi user on the channel are equal.
- DOUTA is chosen in situations where user's Wi-Fi MAC has to be kept unaltered and better throughput has to be obtained only by optimizing the flow rate.
- E-UNWRAP is recommended when LWIP users and legacy Wi-Fi users contend for the channel at the same time. Internally, the LWIP users collisions are resolved by LWIP node, so LWIP users do not physically collide and thereby preventing collisions on the Wi-Fi channel.

It is notable that NCF algorithms focus on optimizing Wi-Fi uplink transmissions considering that LTE is available to send out the outstanding packets which Wi-Fi could not

Table 4.1: Characteristics of proposed NCF algorithms

Algorithm	Operating Layer	Operation performed
DOUTA	IP Layer	Controlling the packet steering rate
FUND	MAC Layer	Facilitates fair medium access opportunity
FUND++	MAC Layer	Regulates medium access duty cycles
E-UNWRAP	MAC Layer	Coordinates through virtual polling

transmit. For all the NCF algorithms, we study only the performance of Wi-Fi uplink transmissions with an assumption that LTE performance is unaltered due to scheduled MAC employed in LTE.

4.3.1 Dynamic Optimal Uplink Traffic steering Algorithm (DOUTA)

DOUTA has been designed with the objective of controlling collisions on the Wi-Fi channel by regulating the packet steering rate onto LTE and Wi-Fi interfaces of LWIP node (downlink) and LWIP-UE (uplink). Here is a small network scenario which explains the importance of uplink steering. A Wi-Fi network of one BSS is considered. The number of Wi-Fi stations (users) in the network connected to the AP is varied and the performance is observed. The users transmit packets of size 1500 bytes with varying inter-packet interval defined by the experiment. The packet inter-packet interval for a packet transmitted is varied from 10 packets/sec to 50 packets/sec for each Wi-Fi station. Figs. 4.5, 4.6, and 4.7 show that by varying the number of users in the network (5, 10, and 20) and varying the packet arrival rate (10, 20, 30, 40, and 50 pkts/sec/station) the normalized network throughput reaches to the maximum value at a particular packet arrival rate. This value is specific for a given number of users in the network. The peak is observed at certain packet arrival rates, because at that given packet arrival rate the DCF mechanism is able to deliver more packets successfully as compared to the saturated case (where the number of collisions becomes constant). DOUTA explores this phenomenon and finds the optimal point at which the network could attain maximum throughput. Packet steering rate (PSR) onto LTE and Wi-Fi links correspond to the fraction of packets sent to LTE and Wi-Fi queues out of the total incoming packets from the higher layer.

Fig. 4.8 and 4.9 show the traffic steering structure at LWIP node and LWIP-UE, respectively. The Traffic Steering Master (TSM) runs the DOUTA algorithm and obtains the PSR onto LTE and Wi-Fi interfaces for both the LWIP node and LWIP-UEs. The Traffic

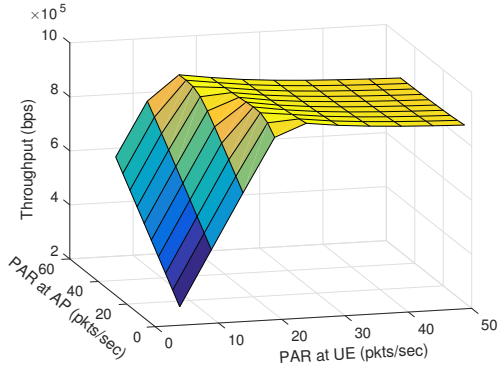


Figure 4.5: Aggregate Wi-Fi throughput observed with five UEs in the network.

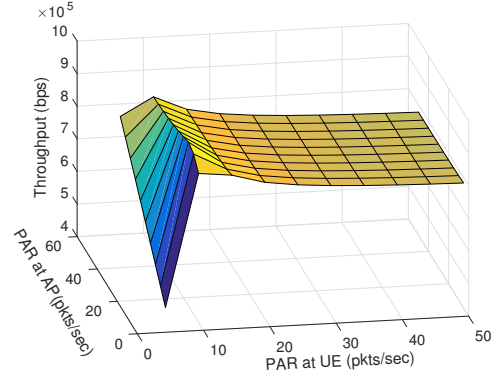


Figure 4.6: Aggregate Wi-Fi throughput observed with 10 UEs in the network.

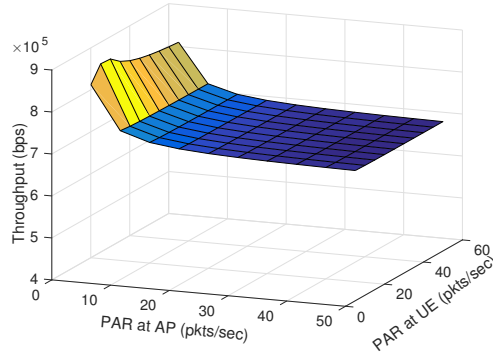


Figure 4.7: Aggregate Wi-Fi throughput observed with 20 UEs in the network.

Steering Slave (TSS) obtains the uplink PSR from TSM and regulates the LWIP-UE uplink traffic through Wi-Fi and LTE interfaces. We have considered a scenario with an LWIP node and a set of ‘ N ’ LWIP-UEs associated to it. The objective function of the optimization problem is to maximize network throughput, subjected to medium access constraints (abiding DCF rules). As users run different applications, and the volume of traffic generated by each user is non-identical, which makes the constraints of the optimization problem multi-dimensional.

Optimal uplink packet steering rate

An optimization problem is formulated for maximizing the Wi-Fi network throughput given ‘ N ’ LWIP-UEs and one LWIP node in the LWIP system. The optimal fraction of incoming packets that has to be sent through Wi-Fi interface of LWIP node and LWIP-UE can be

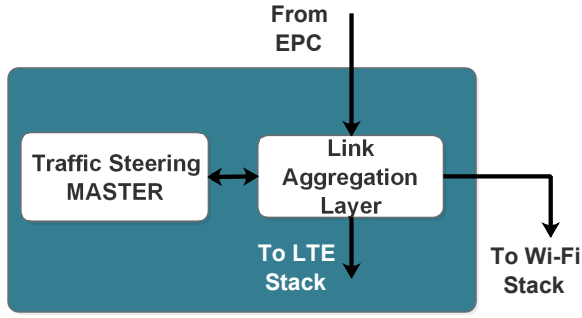


Figure 4.8: Traffic Steering at LWIP Node.

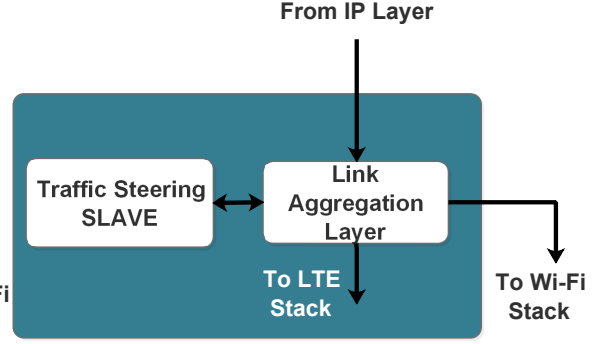


Figure 4.9: Traffic Steering at UE associated to LWIP Node.

obtained by solving the following objective function,

$$\text{Maximize } \Phi = \frac{P_t P_s (1 - P_e) E[PL]}{(1 - P_t) \sigma + P_t P_s (1 - P_e) T_s + P_t (1 - P_s) T_c + P_t P_s P_e T_e} \quad (4.1)$$

where,

$$P_t = 1 - \left[\prod_{i=1}^N (1 - \tau_i^{UE}) \right] (1 - \tau^{AP}) \quad (4.2)$$

$$\tau = \frac{2(1 - 2P_f)q}{q[(W + 1)(1 - 2P_f) + (W P_f (1 - (2P_f)^m))] + 2(1 - q)(1 - P_f)(1 - (2P_f))} \quad (4.3)$$

$$q = 1 - \exp(-\lambda \times E[S_t]) \quad (4.4)$$

$$P_s = \frac{\sum_{i=1}^N \tau_i^{UE} \left[\prod_{j=1, j \neq i}^N (1 - \tau_j^{UE}) \right] (1 - \tau^{AP}) + \tau^{AP} \prod_{i=1}^N (1 - \tau_i^{UE})}{P_t} \quad (4.5)$$

$$E[S_t] = ((1 - P_t) \sigma) + (P_t (1 - P_s) T_c) + (P_t P_s (1 - P_e) T_s) + P_t P_s P_e T_e \quad (4.6)$$

Subject to the following constraints,

$$N \geq 1; \quad (4.7)$$

$$0 \leq W \lambda_i^{UE'} \leq \lambda_i^{UE}, \quad i \in [1 \text{ to } N]; \quad (4.8)$$

$$0 \leq W \lambda^{AP'} \leq \lambda^{AP}; \quad (4.9)$$

Here, Φ is the objective function to be maximized, which is a closed form expression for the throughput of a Wi-Fi network, derived from [68] by considering the Wi-Fi channel to be ideal with non-saturated traffic. In Equation (4.1), P_e corresponds to the packet error probability and $E[PL]$ corresponds to the expected payload length. P_t corresponds to probability that at least one transmission happens in the network which is expressed by Equation (4.2) and P_s corresponds to the probability that a given transmission is successful. λ_i^{UE} represents i^{th} UE's packet generation rate (to be sent over uplink) and λ^{AP} represents the packet arrival rate to LWIP node (to be sent over downlink). ${}^W\lambda_i^{UE}$ and ${}^W\lambda^{AP}$ denote the packet steering rates (fraction of the total packets to be sent to the Wi-Fi interface queue) of LWIP-UE and LWIP node, respectively. ${}^W\lambda_i^{UE'}$ and ${}^W\lambda^{AP'}$ denote the optimal packet steering rates which can be obtained by varying ${}^W\lambda_i^{UE}$ and ${}^W\lambda^{AP}$ for which Φ is the maximum. The remaining packets of the stream are sent to LTE queue (${}^L\lambda_i^{UE}$) so that they could be delivered over LTE interface. This optimization problem can be extended by considering other background Wi-Fi devices on the channel. After inclusion of other devices, the objective function Φ remains unaltered where as P_t and P_s have minor modifications to factor in transmissions of all the other devices. τ corresponds to the transmission probability of a given node which is expressed in Equation (4.3). It also shows the relation between τ and probability of having at least one packet in the buffer q . Equation (4.4) shows the relation between λ and q . $E[S_t]$ corresponds to expected duration of a time slot. Here, σ , T_c , T_s , and T_e correspond to duration of time slot in case of idle, collision, successful transmission, and channel error, respectively. Values for σ , T_c , T_s , and T_e correspond to the duration of SIFS, DIFS, packet transmission time, and ACK transmission time, respectively. The relation between τ , P_t , and P_s is given in Equation (4.5). The throughput of the system (Equation (4.1)) increases with the increase in the success probability, which is controlled by λ and N . For a network with known user count, throughput is solely controlled by λ . Hence, altering λ value varies the network throughput. The control parameter ${}^W\lambda_i^{UE'}$ varies from zero to λ_i^{UE} ; one of the best operating solutions would be to set all ${}^W\lambda_i^{UE'}$ to zero so that ${}^W\lambda^{AP'}$ will take the value of λ^{AP} , which will reflect Wi-Fi operating only in downlink mode, and all the uplink data has to be sent through LTE. But it contradicts with our objective of enabling efficient uplink transmissions through Wi-Fi. A network operator can decide the lower bound on the fraction of uplink to be supported through Wi-Fi. Enforcing it in the lower bound of the above mentioned constraints, the optimization solution will fetch the

best packet steering rate for LTE and Wi-Fi links with minimum uplink transmission rate.

Algorithm 2 Dynamic Optimal Uplink Traffic Steering Algorithm (DOUTA).

Input:
 $\lambda_i^{UE}, \lambda^{AP} \leftarrow$ Packet arrival rates of i^{th} UE and LWIP node's AP
 $N \leftarrow$ Number of active users in the channel
 $L\lambda_i^{UE} \leftarrow$ Fraction of packets steered to LTE interface of i^{th} UE
 $W\lambda_i^{UE} \leftarrow$ Fraction of packets steered to Wi-Fi interface of i^{th} UE
Output: $W\lambda^{AP'} \leftarrow$ Optimal packet steering rate to Wi-Fi interface at AP
 $W\lambda_i^{UE'} \leftarrow$ Optimal packet steering rate to Wi-Fi interface of i^{th} UE

- 1: **for** Every T ms **do** \triangleright Trigger interval is 'T' ms \triangleright Compute the optimal offload fraction
- 2: $\Phi(W\lambda^{AP'}, \lambda^{AP}, W\lambda^{UE'}, \lambda^{UE})$
- 3: **if** $W\lambda^{AP} > W\lambda^{AP'}$ **OR** $W\lambda_i^{UE} > W\lambda^{UE'}$ $i \in [1 \text{ to } N]$ **then**
 \triangleright Current packet steering rate of LWIP-AP or LWIP-UE is higher than the obtained optimal traffic steering rate - regulate the packet steering at UE or AP
- 4: Steer a traffic fraction λ_δ to interface $I_k = \text{LTE}$
- 5: $\Omega(\lambda_\delta, I_k)$
- 6: **else if** $W\lambda^{AP} == W\lambda^{AP'}$ **and** $W\lambda^{UE} == W\lambda^{UE'}$ **then**
 \triangleright Current packet steering rate is optimal, do not let the packet steering rate to increase or decrease
- 7: $\omega(W\lambda^{AP'}, W\lambda^{UE'})$
- 8: **else**
 \triangleright Interfaces are not loaded, packet steering rate can be increased to achieve maximum throughput
- 9: Steer a traffic fraction λ_δ to interface $I_k = \text{Wi-Fi}$
- 10: $\Omega(\lambda_\delta, I_k)$
- 11: **end if**
- 12: **end for**

Algorithm 2 shows the working procedure of DOUTA. The incoming packets are steered to LTE and Wi-Fi queues in order to achieve maximum system throughput. In Algorithm 2, LWIP node obtains all the input parameters for the proposed algorithm such as uplink traffic arrival rate of each LWIP-UE (obtained from the buffer status report (BSR)) and observed throughput of each LWIP-UE (on both the LTE and Wi-Fi links) through LTE uplink control channel. The output of the DOUTA algorithm *i.e.*, allowable uplink traffic rate is conveyed to LWIP-UEs through the downlink control channel of LTE. The optimization algorithm is triggered at every T ms interval to find the optimal fraction of packets to be sent through Wi-Fi interface. We have conducted experiments and monitored the network throughput at different granularity of time intervals 'T' *viz.*, 10, 100, and 300 ms. Fig. 4.10 shows the instantaneous network throughputs reported at LWIP node. If Algorithm 2 runs at an interval of 10 or 100 ms, it can mislead decisions as fluctuations in the network

Algorithm 3 $\Omega(\lambda_\delta, I_k)$ Steering the traffic

Input: $\lambda_\delta \leftarrow$ Fraction of traffic to be steered
 $I_k \leftarrow$ Interface to which traffic has to be steered
 $\mathcal{F}_i \leftarrow$ Information of i^{th} flow
for $i=0; i < \mathcal{F}_{max}; i++$ **do**
 if $\lambda_{delta} > 0$ **then**
 $\lambda_{delta} \leftarrow \lambda_{delta} - flowsize(\mathcal{F}_i)$ \triangleright Flow size in packets per unit time
 $Interface(\mathcal{F}_i) \leftarrow I_k$
 else
 break;
 end if
end for

throughput are very high. However, the decision taken at an interval of 300 ms is stable and captures the actual network state as depicted in Fig. 4.10.

If the current packet steering rate through Wi-Fi interface is higher than the optimal packet steering rate, then the packet steering rate to Wi-Fi interface is reduced by, steering a fraction of the total packets (λ_δ) to LTE interface, which is given by Ω . The function Ω controls the fraction of traffic that has to move from LTE to Wi-Fi interface and vice-versa, whereas ω sustains the traffic offload rate when the global optimal solution is reached. Algorithm 3 details the operations of Ω .

DOUTA algorithm is scalable as it does not involve any additional signaling overhead. Also, the DOUTA algorithm of NCF can be adopted by LWIP systems without any protocol stack level modifications at the UE side, which is an added advantage. The optimization problem shown in Equation (4.1) is solved using a MATLAB-based solver (fmincon) which solves it in the order of milliseconds. In case of real deployment, for different incoming packet arrival rates and different number of UEs, the optimal allowable uplink traffic rates can be precomputed and then stored in a look-up table. Such a look-up table based solution eliminates the need for running a solver on-the-fly at LWIP node and LWIP-UEs.

4.3.2 Fast Uplink through Direct medium access (FUND)

The DOUTA algorithm, explained in the previous section, aims to improve the network throughput by regulating the traffic at the IP layer. DOUTA maximizes the network throughput by regulating the flows (load), but it may not completely eliminate collisions on the channel (which is the primary reason for poor throughput in dense deployment scenarios), which can only be done by coordinating the uplink transmissions at the MAC layer.

the fast uplink is achieved by enabling LWIP-UEs to transmit after the PCF Inter Frame Spacing (PIFS) time interval, which ensures that LWIP-UEs will occupy the channel earlier than any standalone Wi-Fi stations using DCF mechanism for channel access. LWIP-UEs transmission/scheduling order is pre-computed by LWIP node and sent through LTE control messages. The scheduling order is obtained by choosing those LWIP-UEs which have uplink data to transmit; this information is obtained from buffer status report (BSR) which is a periodic report sent to LTE SeNB by each UE through LTE uplink control channel. LWIP-UEs which have uplink data to transmit are sorted based on their buffer occupancy to obtain the scheduling order. Every LWIP-UE after receiving the scheduling order (S_o) through LTE control messages waits for its opportunity. S_o remains unmodified till next scheduling order which is given via LTE control messages. Every LWIP-UE waits for its opportunity and transmits. During FUND OFF PERIOD none of the LWIP-UE contends for the channel. If an LWIP-UE needs to transmit uplink data in the next FUND CYCLE, then it should notify the uplink requirement U_i (of i^{th} LWIP-UE) in advance. LWIP node uses U_i to do a proportional allocation in uplink transmission $\mathcal{F}(U_i, m)$. Here m corresponds to the number of LWIP-UEs with the uplink requirement. FUND algorithm finds the number of nodes actively contending on the channel (N), by observing the transmissions on the channel with unique Wi-Fi MAC addresses.

4.3.3 FUND with fair channel access (FUND++)

FUND++ is designed in order to enhance FUND operation fairly with Non-LWIP-UEs on the Wi-Fi channel. Algorithm 5 details the medium access procedure of FUND++. Similar to FUND, FUND++ has FUND++ ON PERIOD and FUND++ OFF PERIOD. Duration of FUND++ ON PERIOD and FUND++ OFF PERIOD are regulated in order to achieve fair transmission opportunity with Non-LWIP-UEs. FUND++ ON PERIOD and FUND++ OFF PERIOD are controlled based on successful packet transmission of LWIP and Non-LWIP nodes on the channel. If more collisions are observed during FUND++ OFF PERIOD (DCF), then the duration of FUND++ OFF PERIOD is extended in order to allow the Non-LWIP-UEs to get fair amount of successful transmissions with those of LWIP-UEs. Number of packets successfully transmitted by i^{th} LWIP-UE and i^{th} Non-LWIP-UE through Wi-Fi interface is denoted as S_L^i and S_{NL}^i , respectively. In this algorithm, T_{ON}^{F+} and T_{OFF}^{F+} correspond to FUND++ ON PERIOD and FUND++ OFF PERIOD,

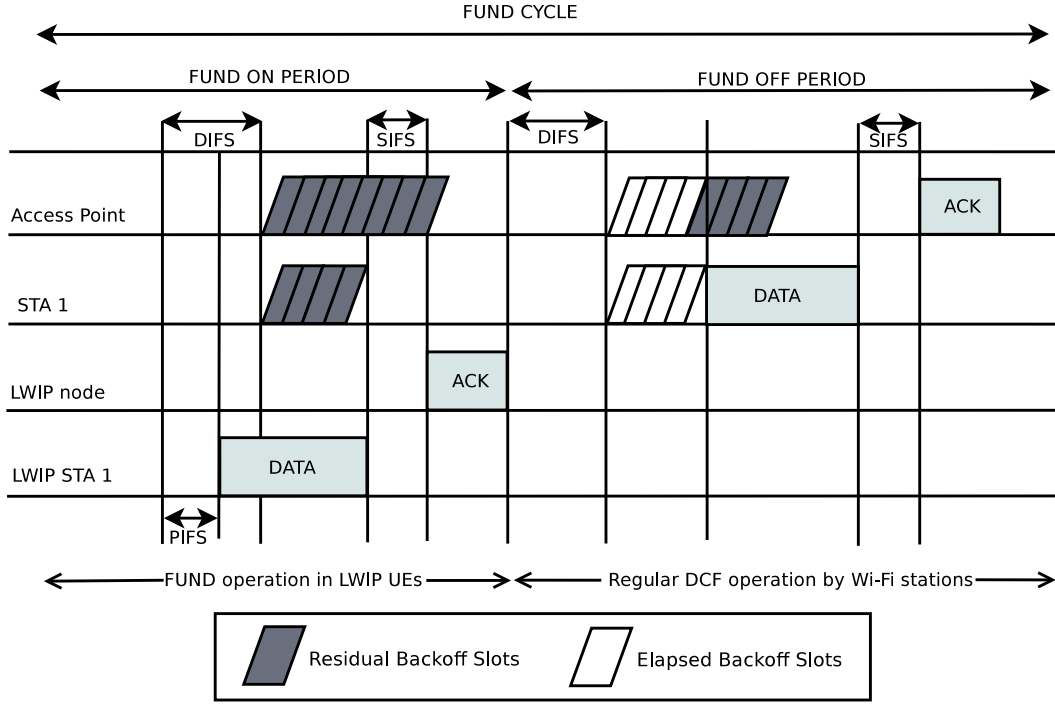


Figure 4.11: Operation of FUND algorithm.

respectively. FUND++ CYCLE (T_{CYC}^{F+}) is the sum of FUND++ ON and OFF PERIOD ($T_{CYC}^{F+} = T_{ON}^{F+} + T_{OFF}^{F+}$). The FUND++ algorithm starts with $T_{ON}^{F+} = \frac{m}{N} \times T_{CYC}^{F+}$, then based on the successful packet transmissions observed by LWIP-UEs and Non-LWIP-UEs, the value gets changed to $T_{ON}^{F+} = \frac{\sum_i S_{NL}^i}{\sum_i S_{NL}^i + \sum_i S_L^i} \times T_{CYC}^{F+}$. If more packets collide, then FUND++ OFF PERIOD extends. This ensures fairness in successful packet transmissions across LWIP-UEs and Non-LWIP-UEs.

The comparison between FUND and FUND++ is detailed as follows.

- In case of FUND, the time interval for LWIP transmissions is kept constant (only based on active users). In a FUND cycle, users are given uplink transmission opportunities based on their BSR and QoS requirements.
- In case of FUND++, the FUND++ ON and FUND++ OFF PERIODs are varied according to the fraction of successfully transmitted packets by LWIP-UEs and Non-LWIP-UEs on the channel.
- FUND++ operates in more fairer manner with other Wi-Fi nodes on the channel compared to FUND, and it also approaches the throughput achieved by FUND on the channel.

Algorithm 5 FUND++

Input: $S_L^i \leftarrow$ Number of packets successfully transmitted by i^{th} LWIP-UE
 $S_{NL}^i \leftarrow$ Number of packets successfully transmitted by i^{th} Non-LWIP-UE
 $T_{ON}^{F+}, T_{OFF}^{F+} \leftarrow$ Duration of FUND++ ON PERIOD and FUND++ OFF PERIOD
 $T_{CYC}^{F+} \leftarrow T_{ON}^{F+} + T_{OFF}^{F+}$ \triangleright A FUND++ cycle duration
 $U_i \leftarrow$ Uplink requirement of i^{th} LWIP-UE
Output: Scheduling order (S_o) for LWIP-UEs and $T_{ON}^{F+}, T_{OFF}^{F+}$
Initial Value: $T_{ON}^{F+} \leftarrow \frac{m}{N} * T_{CYC}^{F+}$ and $T_{OFF}^{F+} \leftarrow T_{CYC}^{F+} - T_{ON}^{F+}$

- 1: **for** Every FUND++ CYCLE (T_{CYC}^{F+}) **do**
- 2: **if** FUND++ ON PERIOD **then**
- 3: $S_o \leftarrow \mathcal{F}(U_i, n, L)$ \triangleright Proportional allocation based on flow requirement
- 4: Notify LWIP-UEs about S_o through LTE control message
- 5: Employ FUND medium access procedure
- 6: **else** \triangleright FUND++ OFF PERIOD
- 7: Set S_o for all the LWIP-UEs to *NULL* \triangleright LWIP-UEs do not transmit in FUND++ OFF PERIOD.
- 8: Every other node does data transmission following DCF procedure
- 9: **end if**
- 10: $T_{ON}^{F+} \leftarrow \frac{\sum_i S_{NL}^i}{\sum_i S_{NL}^i + \sum_i S_L^i} \times T_{CYC}^{F+}$
- 11: $T_{OFF}^{F+} \leftarrow \frac{\sum_i S_L^i}{\sum_i S_{NL}^i + \sum_i S_L^i} \times T_{CYC}^{F+}$
- 12: **end for**

4.3.4 Enhanced Uplink With virtual Polling (E-UNWRAP)

The problem that exists with FUND and FUND++ algorithms is that they divide the channel access for LWIP-UEs and Non-LWIP-UEs separately (FUND ON PERIOD and FUND OFF PERIOD). A Non-LWIP-UE following DCF is prevented from transmitting in uplink during FUND ON PERIOD because LWIP-UEs occupy the channel immediately after the PCF time interval. In order to relax this bifurcation of channel access time and to allow any Non-LWIP-UE to contend for the channel at any given time, we propose Enhanced Uplink With virtual Polling (E-UNWRAP) algorithm. This algorithm coordinates the medium access for LWIP-UEs and ensures no collisions among LWIP-UEs even if they follow the DCF mechanism like any other Non-LWIP-UE. The term virtual polling corresponds to LWIP node polling each LWIP-UE for uplink packet availability in its Wi-Fi queue.

PCF mode of Wi-Fi also supports similar scheduling of Wi-Fi transmissions using polling mechanism. However, polling is inefficient due to periodic query on each UE's Wi-Fi interface even when the packets are not available with UE [69]. The null frame is sent as the reply by UE to Wi-Fi AP when there is no packet to transmit in the uplink. Note that, the underutilization of resources observed in Wi-Fi domain can be resolved by leveraging

the availability of LTE interface in LWIP, where polling is carried out using LTE link. LTE control messages can be used to make a query to the LWIP-UE about its Wi-Fi queue status, which can further be used in creating a scheduling order for the uplink transmissions. Such a co-ordinated operation can ensure that no two LWIP-UEs connected to LWIP node can transmit at the same time. The actual collisions which could be happening on the Wi-Fi channel among LWIP-UEs are nullified. This way of resolving the collisions is possible only with LWIP architecture. E-UNWRAP also has an objective to regulate the virtual contention period (VCP), which is achieved by observing the collisions among other nodes on the channel, hence it operates by taking the number of observed collisions on the channel as an input.

The virtual contention period can be operated in three possible modes.

1. **Constant Cycle Operation:** In constant cycle operation, VCP has a fixed cycle duration which is unaltered. Given the fixed cycle duration, based on the effective throughput that can be achieved by an LWIP node, the uplink steering can be regulated.
2. **Varying Cycle Operation:** In varying cycle operation, VCP employs a time-varying cycle which is controlled by taking collisions observed on the channel as an input. Based on the collisions observed during the DCF period (non-VCP), the VCP is made to shrink or expand dynamically. During the non-VCP period, LWIP-UEs contend along with standalone Wi-Fi users in the network. The only difference between VCP and non-VCP period is that the contention window regulation (explained in Section 4.3.4) is made only in VCP.
3. **Full Cycle Operation:** In full cycle operation, the LWIP-UEs are made to work as if the VCP period is available all the time. LWIP node schedules each uplink transmission of the user based on the number of packets in the user's queue. Also, full cycle operation allows changing the contention window of LWIP-UE. In the following, we have detailed the working procedure of full cycle operation.

E-UNWRAP with FULL cycle operation for Virtual Polling

E-UNWRAP works with two basic approaches: (1) Scheduling Wi-Fi transmissions with an auxiliary LTE interface and (2) Regulating the Wi-Fi contention window. Scheduling

in E-UNWRAP deals with how an LWIP-UE has to be scheduled (*i.e.*, the order in which LWIP-UEs have to transmit) and the granularity of scheduling (ms or μ s). Contention window regulation unit works by regulating the growth of contention window of LWIP-UEs.

Scheduling Order: Scheduling order is generated/obtained based on packet availability in the Wi-Fi queue and QoS requirements of different users. Scheduling order can be generated using one of the following two ways.

Standard order (STD-ORD): It is a fixed scheduling of LWIP-UEs transmission order, which is a sorted list based on the availability of uplink Wi-Fi data at the LWIP-UE. The LWIP-UEs transmissions follow predefined order even if an LWIP-UE's backoff window gets expired. For instance, LWIP-UE 1 has a smaller contention window than LWIP-UE 2. However, the order for scheduling uplink transmission is LWIP-UE 2 followed by LWIP-UE 1, so LWIP-UE 1 will not transmit even after expiration of its contention window. Instead, it will wait for the LWIP-UE 2's transmission. After completion of LWIP-UE 2's transmission, LWIP-UE 1 will start its uplink transmission.

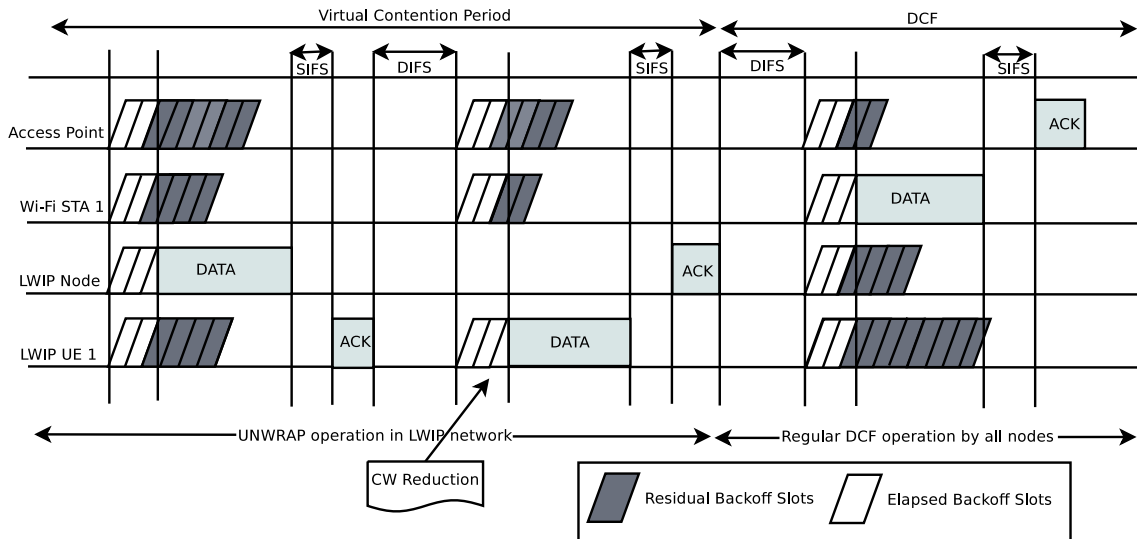


Figure 4.12: Operation of UNWRAP algorithm (Variable Operation Time).

Regulated order (REG-ORD): It follows a flexible schedule which is done dynamically based on the availability of uplink Wi-Fi data at LWIP-UEs. Uplink transmissions for all the LWIP-UEs are scheduled apriori. A universal hash function is used to ensure a proper coexistence with Non-LWIP-UEs, and to enhance interleaved transmissions among LWIP-UEs.

Contention Window Regulation: Contention window regulation procedure (CWRP) has two main purposes: (1) To support developing the REG-ORD and (2) To coexist fairly with Non-LWIP-UEs. CWRP supports REG-ORD by controlling the backoff value of LWIP-UE which in turn makes the transmission to be ordered. A universal hash function is employed to set individual LWIP-UE's backoff value. The hash function ensures that there will be no collision among the users connected to the LWIP node while maintaining the fair channel sharing with background Wi-Fi users on the same channel. A universal hash function, $h_{a,b}(x) = ((ax + b) \bmod p)$, where p is a prime number greater than or equal to the average contention window (operational contention window: CW_{opr}). The value of the average contention window is varied based on the number of collisions observed on the channel in the last observation period. Algorithm 6 shows that CW_{opr} increases when $\frac{\sum \theta_{col}^i}{T_{pkt}^s}$ is greater than the collision threshold (CT_{col}), where θ_{col}^i corresponds to the number of transmissions that got collided for i^{th} user on the channel and T_{pkt}^s counts the total number of successful packets transmitted. CW_{opr} doubles when the number of collisions observed on the channel is greater than CT_{col} . The value of CW_{opr} decreases exponentially when the number of collisions observed is lesser than CT_{col} . Hence, harmony in channel sharing is achieved with Non-LWIP-UEs operating on the channel, and at the same time collisions among LWIP-UEs are resolved internally.

4.3.5 Realization of NCF algorithms in LWIP System

This subsection describes the implementation details of proposed NCF algorithms. NCF works across (layers 2 and 3) MAC and IP layers of LWIP node. Some of the proposed NCF algorithms need LWIP-UEs to perform certain operations based on the input received from the LWIP node.

In the case of DOUTA, LWIP node instructs its associated LWIP-UEs about the allowable number of uplink packets that can be transmitted by each LWIP-UE. To obtain the number of uplink packets to be transmitted in the uplink, the optimization problem (Equation (4.1)) has to be solved. Solving the optimization problem is done at LWIP node, whereas throttling the number of uplink packet transmissions through Wi-Fi interface is done at LWIP-UE.

In case of FUND, during FUND ON PERIOD, LWIP-UEs will transmit one after the other, according to the transmission order given by LWIP node. During FUND OFF PE-

Algorithm 6 E-UNWRAP - Full Cycle operation of VCP

Input: $\theta_{col}^i \leftarrow$ Collision observed by i^{th} LWIP-UE on the channel during the observation period
 $N \leftarrow$ Number of users (LWIP and non LWIP users) in the channel
 $p \leftarrow$ First prime number greater than CW_{opr}
 $T_{pkts} \leftarrow$ Total number of transmissions in observation period
 $N^{UL} \leftarrow$ Number of LWIP-UEs having uplink data to transmit
 $CT_{col} \leftarrow$ Collision threshold
Output: $a, b \leftarrow$ Coefficients for universal hash function

- 1: **for** N^{UL} uplink users **do**
- 2: $h(a, b) \leftarrow (ak + b) \bmod p$ $\triangleright k$ is a unique user ID (can be MAC ID)
- 3: **end for** $\triangleright a$ and b ensure no collision by assigning different contention slots among N^{UL} uplink users
- 4: **if** $\frac{\sum \theta_{col}^i}{\sum T_{pkts}} \geq CT_{col}$ **then**
- 5: $CW_{opr} \leftarrow CW_{opr} \times 2$
- 6: **else**
- 7: $CW_{opr} \leftarrow CW_{opr}/2$ \triangleright Reduce the contention window and find new hash function
- 8: **end if**
- 9: **if** $CW \geq CW_{max}$ **then**
- 10: $CW \leftarrow CW_{max}$
- 11: **end if**
- 12: Broadcast a, b, p to all LWIP-UEs a prior, through control messages of LTE

RIOD, LWIP-UEs will not contend with Non-LWIP-UEs (standalone Wi-Fi UEs) for transmissions. Determining the transmission order for LWIP-UEs and notifying FUND ON and OFF PERIODs to LWIP-UEs are done by LWIP node, whereas performing uplink transmissions in the obtained transmission order is done by respective LWIP-UEs. In case of FUND++, the procedure involved is similar to that of FUND except for the duration of ON and OFF PERIODs which are regulated to achieve better fairness across LWIP-UEs and Non-LWIP-UEs.

In case of UNWRAP, LWIP-UEs set their backoff values based on a function determined by LWIP node. This backoff window function ensures no collisions among LWIP-UEs in the virtual polling period. During the DCF period, LWIP-UEs backoff window function follows the legacy DCF mechanism. LWIP node gives the function for choosing backoff to its associated LWIP-UEs.

4.3.6 Benefits of NCF algorithms

The benefits of different NCF algorithms are detailed as follows. *DOUTA*: It can be observed that DOUTA has focused on steering the traffic at LTE and Wi-Fi links of LWIP and LWIP-

UE, in order to reduce collisions in Wi-Fi domain and thereby improving the uplink sending rate through Wi-Fi. Using Wi-Fi link for serving only downlink data is not desirable since it restricts the uplink traffic strictly to go through only LTE link. Also, Wi-Fi offload is not the best solution as the underlying MAC (which uses DCF function) leads to high collisions on the Wi-Fi channel. DOUTA provides the optimal steering of packets across LTE and Wi-Fi links by considering this trade-off.

All NCF algorithms do uplink traffic steering by filling the Wi-Fi queue first; if the Wi-Fi queue of an LWIP-UE/LWIP node is full, then the remaining packets are sent through LTE link. Hence, their performances are compared with the DCF mechanism of Wi-Fi.

FUND: It does fast medium access and ensures that the fraction of time given to each user is equal.

FUND++: Regulates FUND++ ON PERIOD in order to ensure fair number of successful transmissions between LWIP-UEs and Non-LWIP-UEs.

E-UNWRAP: Coexists with regular Wi-Fi DCF mechanism in grabbing the transmission opportunity but reduces collisions among LWIP-UEs, which leads to improvement in the overall network throughput.

4.4 Simulation setup

Fig. 4.13 depicts the simulation scenario with an LWIP system and a standalone background Wi-Fi network. The scope of evaluation setup is confined to one-hop between UE and LWIP node. A set of LWIP-UEs gets associated with the LWIP node, and a set of Non-LWIP-UEs gets associated with the standalone AP. Each associated UE generates application traffic which is realized by varying the packet arrival rate. In all the experiments, the number of UEs associated with the LWIP node and the standalone Wi-Fi AP are in the ratio of 1:1. There are no hidden nodes in the network; hence RTS-CTS handshake of Wi-Fi is not enabled. Table 4.2 summarizes the simulation parameters used for evaluating the performance of various NCF algorithms proposed in this chapter. Simulation experiments are conducted using a MATLAB based system-level simulator. We have considered fairness index (FI) which is defined below as one of the evaluation metrics.

$$FI_i = \frac{\text{Number of successful packets in } i^{\text{th}} \text{ network}}{\text{Total Number of Successful packets on the channel}}, \text{ where } i \in \{LWIP, Non - LWIP\}$$

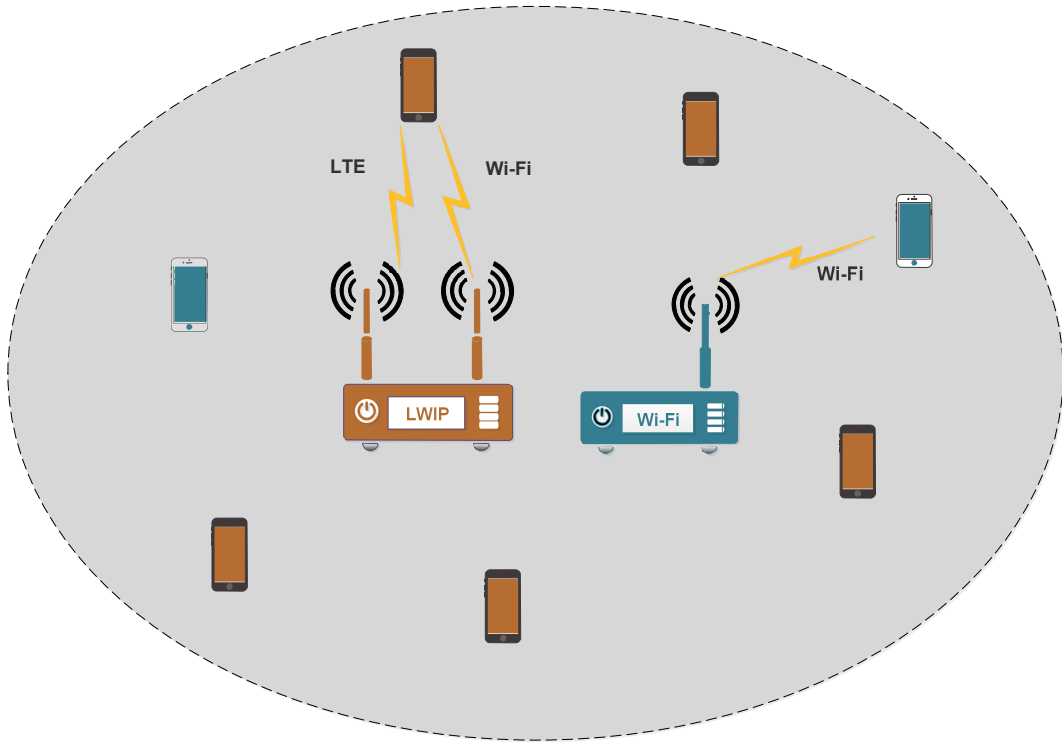


Figure 4.13: Experimental scenario for evaluation of NCF algorithms.

For simplicity, we have considered that uplink packet arrival rates of LWIP-UEs and Non-LWIP-UEs are the same. Any proposed algorithm under the given setup can be called as fair if its FI lies near 0.5. One of the most important parameters for decision making is about counting collisions on the channel. In our work LWIP node counts the number of collisions on the channel. How to count the collisions is well explained in [70]. The authors have counted collisions on the channel by differentiating the actual collisions from the weak signals. They have shown high accuracy in detecting the collisions as compared to the weak signals.

4.5 Performance results

In this section, we evaluate NCF to determine the performance of its uplink steering algorithms. Also, we monitor the effect of NCF algorithms in improving the utilization of Wi-Fi channel when LWIP system is employed. Here, we present the performance results only in Wi-Fi context, by considering that the LTE interface has a scheduled MAC, and it is available to carry out the uplink traffic which cannot be sent through Wi-Fi uplink.

Table 4.2: Simulation parameters for evaluation of NCF algorithms

Parameter	Value
Number of users	$N \Rightarrow [10 \text{ to } 30]$
The fraction of users connected to LWIP Node	$N/2$
Non-LWIP Wi-Fi users	$N/2$
Simulation Time	100 Seconds
Mobility Model	Static
Packet arrival rate per device	$[10^2 \text{ to } 10^3]$ packets per sec
Number of seeds	10
DIFS	28 μsec
PIFS	20 μsec
SIFS	10 μsec
ACK size	16 bytes
Wi-Fi PHY data rate	65 Mbps
Payload size (IP Packet)	1470 bytes
MAC of LWIP-Users	NCF
MAC of Non-LWIP-Users	DCF
MAC+PHY header size	24+16 bytes

The performance of the NCF algorithms is compared with most widely used DCF based medium access mechanism of Wi-Fi. The evaluation aims at obtaining the following three crucial metrics of analysis for all the experiments.

1. How efficiently collisions are reduced on Wi-Fi channel: Observed Collisions
2. By how much throughput of Wi-Fi network has improved because of NCF - Observed Throughput
3. How NCF works fairly with DCF in accessing the channel - Observed Fairness

4.5.1 Performance results of DOUTA algorithm

Fig. 4.14 shows variation in the Wi-Fi network throughput of both LWIP and background Wi-Fi users when DOUTA and Wi-Fi offload algorithms are employed. The load offered by each UE/STA is varied from 100 to 700 packets/sec. The variation in throughput is closely observed by increasing the number of UEs in the network from 10 to 30. In the case of Wi-Fi offload algorithm, each LWIP-UE prefers to send data through Wi-Fi interface whenever the Wi-Fi link is available (Wi-Fi Preferred Algorithm [61]) and follows DCF mechanism for medium access. DOUTA also follows the DCF procedure, but it tends to control the uplink traffic sent through Wi-Fi channel when the offered load increases. In

other words, DOUTA instructs each LWIP-UE the optimal fraction of traffic that has to be sent through Wi-Fi uplink, which is obtained by solving the optimization function discussed in Section 4.3.1 and allowing rest of the traffic to be sent through LTE interface. Such a regulated transmission in Wi-Fi uplink has reduced the contention on the network, thereby reducing the time elapsed in collisions which can be observed in Fig. 4.15. In Fig. 4.15, the X-axis captures the offered load and Y-axis represents time elapsed in collisions, over the simulation time which has been normalized to 10 seconds. It can be observed that the time elapsed in collisions varies from 2 to 3 seconds out of 10 seconds in the saturated region. Also, Wi-Fi has 7% improvement in the network throughput in case of DOUTA as compared to that of Wi-Fi offload algorithm (DCF+Wi-Fi offload). The time elapsed in collisions has also been reduced by 13%. This throughput improvement is achieved without incurring any additional signaling overhead in the core network.

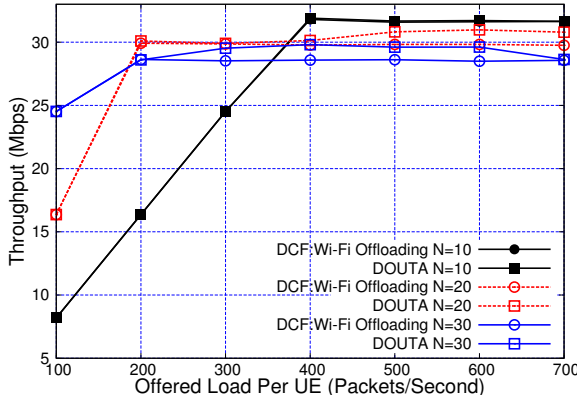


Figure 4.14: Variation in Wi-Fi throughput with offered load - DCF:Wi-Fi Offloading vs DOUTA.

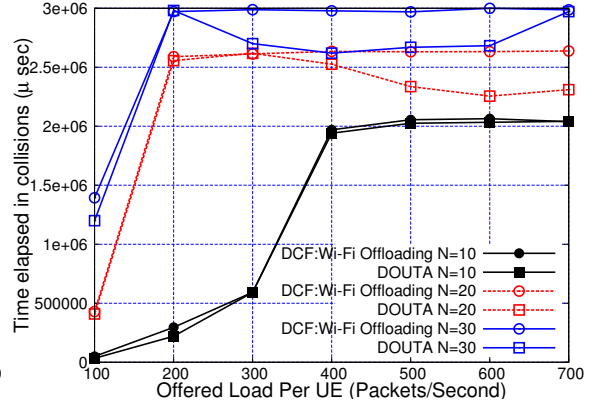


Figure 4.15: Variation in time elapsed in collisions with offered load - DCF:Wi-Fi Offloading vs DOUTA.

4.5.2 Performance results of FUND algorithm

Fig. 4.16 shows time elapsed in collisions by varying offered load for DCF and NCF:FUND mechanisms. The term NCF:FUND and FUND are used interchangeably. As the packet arrival rate (offered load) increases the number of collisions observed also increases in DCF mechanism. As the number of users vary from 10 to 30, FUND exhibits a significant performance improvement compared to DCF. FUND has reduced the number of collisions by 50% as compared to legacy DCF mechanism by coordinating the uplink transmission and by using fast channel access technique. Reduction in collisions has eventually led to

high throughput as shown in Fig. 4.17. FUND ensures collisionless transmissions among LWIP-UEs by sending the uplink schedule vector through LTE interface, which contains the transmission order for each LWIP-UE. But the greedy access to channel reduces fairness among the users on the Wi-Fi channel. Fig. 4.18 shows fairness among UEs concerning successful packet transmissions while using DCF and FUND algorithms. When LWIP-UEs and Non-LWIP-UEs employ DCF mechanism, then 0.5 is their expected FI, which is clear from the plot. Shifting FI above 0.5 conveys that the algorithm is greedy and facilitates more opportunities for LWIP-UEs as compared to Non-LWIP-UEs. This is because FUND enables the LWIP-UEs to get served immediately after the PIFS interval, whereas Non-LWIP-UEs are served after DIFS interval followed by a random backoff. Even though FUND algorithm allows a biased utilization of resources benefiting LWIP-UEs, it ensures proportional FUND ON PERIOD and FUND OFF PERIOD based on the number of LWIP-UEs and Non-LWIP-UEs present on the channel. Eventually, the fraction of time given for each user to perform uplink transmission is equal in FUND algorithm. Hence, it provides fairness at the granularity of number of users operating on the channel. FUND++ is a dynamic approach to further improve the fairness of users in terms of successful packet transmissions. Nevertheless, FUND is the most efficient of all NCF algorithms in terms of channel utilization.

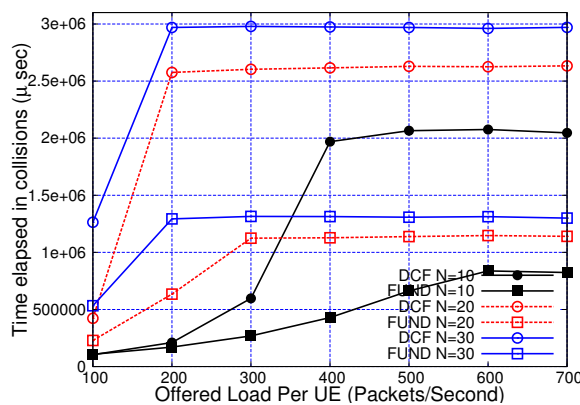


Figure 4.16: Variation in time elapsed in collisions with offered load - DCF vs NCF:FUND.

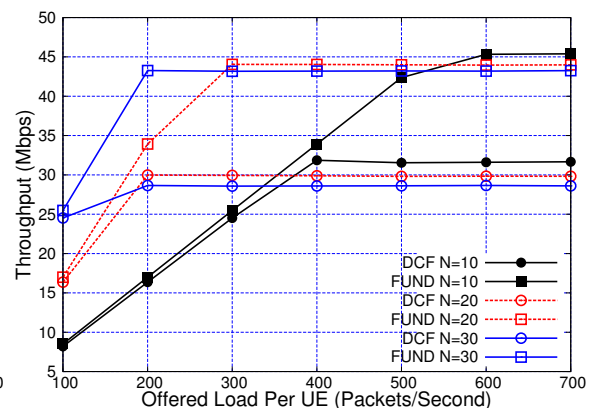


Figure 4.17: Variation in Wi-Fi throughput with offered load - DCF vs NCF:FUND.

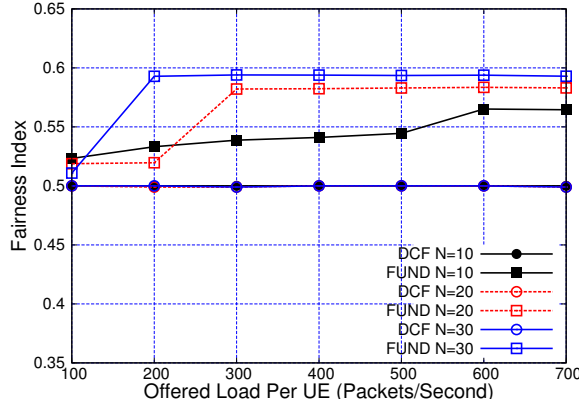


Figure 4.18: Variation in system fairness with offered load - DCF vs NCF:FUND.

4.5.3 Performance results of FUND++ algorithm

FUND++ focuses on ensuring fairness across LWIP-UEs and Non-LWIP-UEs operating on Wi-Fi channel. Fairness in such cases can be achieved by regulating the duration of FUND ON PERIOD. Fig. 4.19 shows the fairness among LWIP-UEs and Non-LWIP-UEs in case of FUND and FUND++. It can be observed that FUND++ is able to reach FI=0.5 which conveys that the system is fair. The throughput improvement of FUND++ is comparable with FUND, but FUND achieves slightly higher throughput as shown in Fig. 4.20. The time elapsed in collisions (Fig. 4.21) is high in FUND++ as compared to FUND because the FUND++ ON PERIOD is lesser as compared to FUND ON PERIOD. As the time elapsed for transmissions by Non-LWIP-UEs increases (FUND++ OFF PERIOD increases), the overall network throughput decreases. This is because, the time elapsed due to collisions increases when DCF is employed with more number of Non-LWIP-UEs. We can also observe that the FUND++ algorithm has extended the FUND++ OFF PERIOD by 8.8% as compared to FUND in order to ensure fairness to Non-LWIP-UEs on the Wi-Fi channel.

4.5.4 Performance results of E-UNWRAP algorithm

In this section, we present the evaluation of E-UNWRAP with different operation cycles *viz.*, variable and full operation.

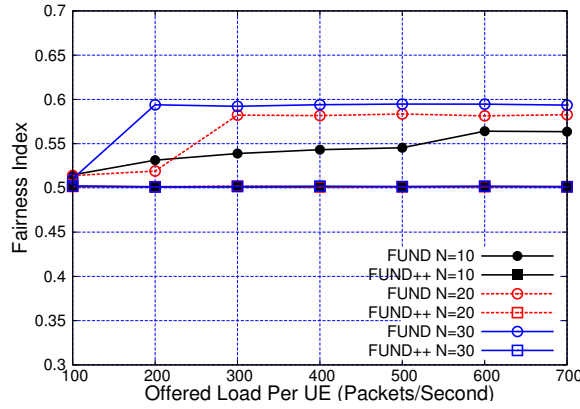


Figure 4.19: Variation in system fairness with offered load - NCF:FUND vs NCF:FUND++.

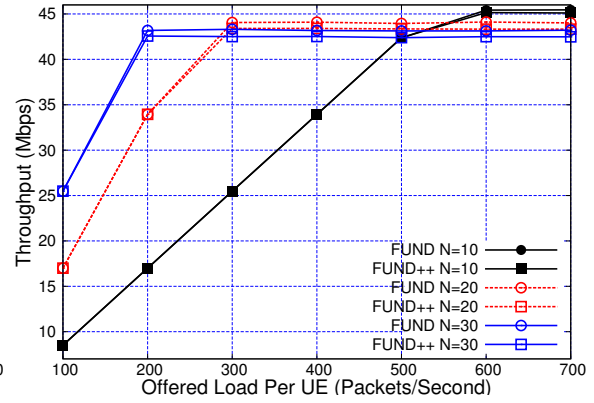


Figure 4.20: Variation in Wi-Fi throughput with offered load - NCF:FUND vs NCF:FUND++.

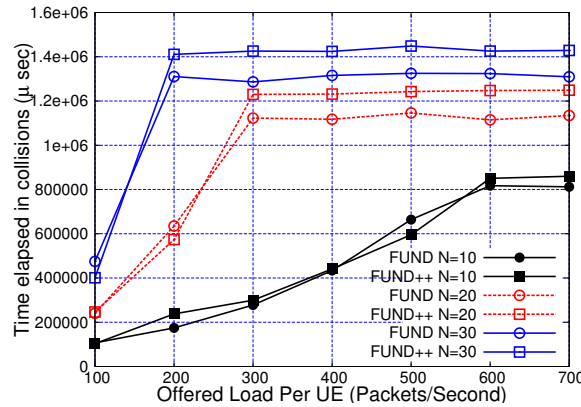


Figure 4.21: Variation in time elapsed in collisions with offered load - NCF:FUND vs NCF:FUND++.

Variable Operation

According to E-UNWRAP variable operation, during the virtual contention period, E-UNWRAP mechanism is followed as detailed in Section 4.3.4. Rest of the time it employs DCF mechanism. Scheduling packet transmissions in a predefined order has improved the overall network throughput. Fig. 4.22 shows that when large number of users are active in the network, the throughput of E-UNWRAP is better than that of DCF. This improvement is well explained by reduction in the fraction of the time elapsed in collisions. The time elapsed in collisions has reduced due to proper scheduling of Wi-Fi transmissions. Fig. 4.23 shows that fraction of LWIP transmissions has been reduced in order to improve the overall network throughput. As the number of UEs participating in the transmissions increases the effective reduction in collisions of E-UNWRAP increases as compared to DCF. Fig. 4.24

shows that LWIP-UEs have subdued their transmission opportunities in order to improve the overall network performance.

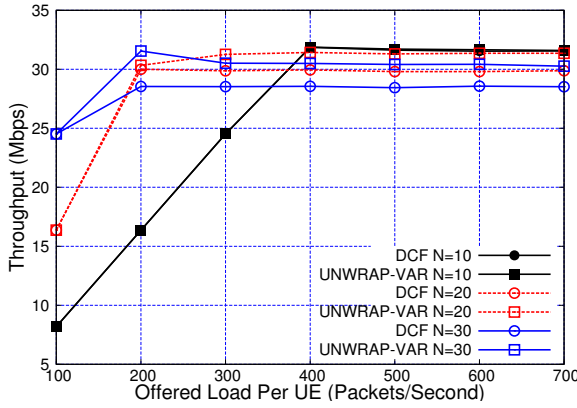


Figure 4.22: Variation in Wi-Fi throughput with offered load - DCF vs NCF:UNWRAP - Variable operation.

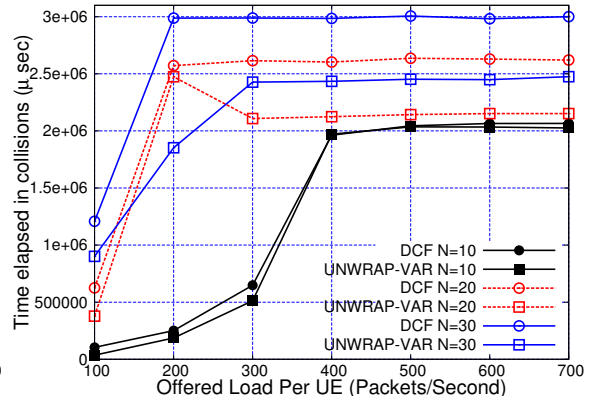


Figure 4.23: Variation in time elapsed in collisions with offered load - DCF vs NCF:UNWRAP - Variable operation.

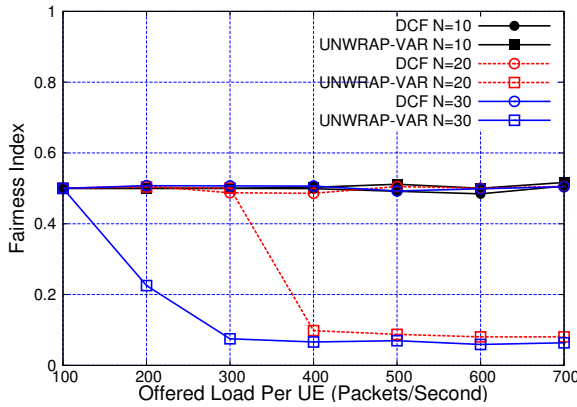


Figure 4.24: Variation in system fairness with offered load - DCF vs NCF:UNWRAP - Variable operation.

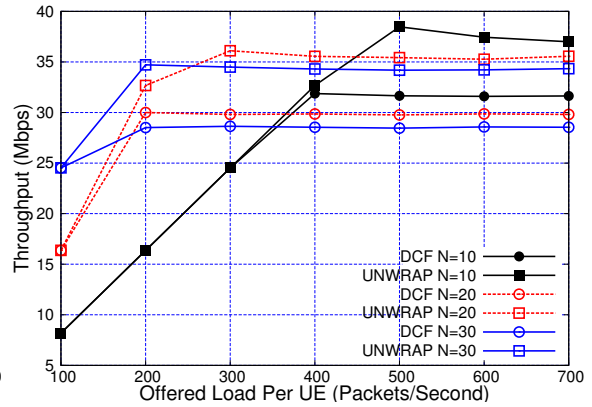


Figure 4.25: Variation in Wi-Fi Throughput with offered load - DCF vs NCF:E-UNWRAP - Full operation.

Full operation

In full operation mode, the VCP is spread over the entire duration, and contention windows of LWIP-UEs are regulated by the contention window regulation module. Fig. 4.25 shows a significant improvement (21%) in the network throughput for E-UNWRAP with full operation in comparison to DCF. This unleashes the power of LWIP in regulating the usage of Wi-Fi spectrum effectively. This phenomenon can be well explained using Fig. 4.26; it

shows the collisions among LWIP-UEs have been significantly reduced, thus resulting in the overall improvement in throughput. The number of collisions has reduced because of coordinated Wi-Fi transmission among LWIP-UEs. The coordination in Wi-Fi transmissions is achieved by sending a scheduled order through LTE link. E-UNWRAP has not grabbed more channel access opportunities as compared to DCF. It is fair and Fig. 4.27 shows that it even subdues its transmission opportunities in order to increase opportunities for legacy Wi-Fi nodes operating on the same channel.

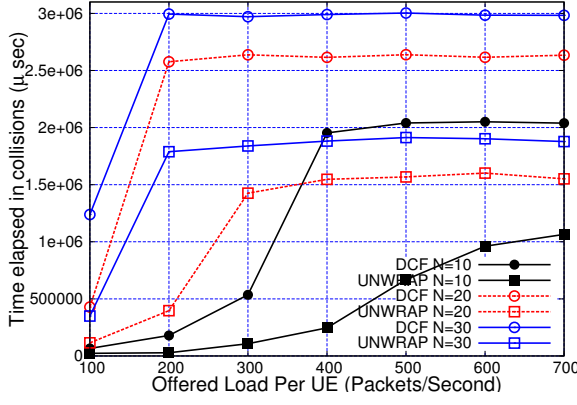


Figure 4.26: Variation in time elapsed in collisions with offered load - DCF vs NCF:E-UNWRAP - Full operation.

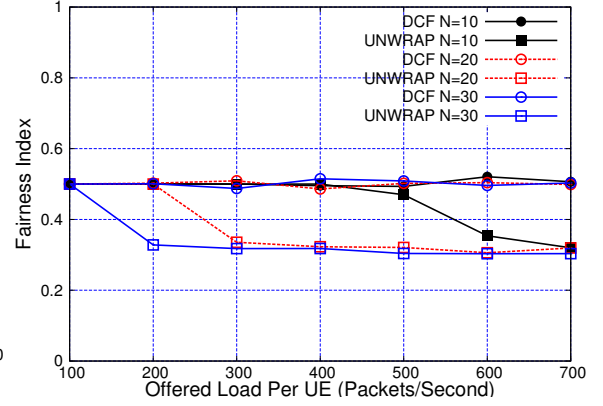


Figure 4.27: Variation in system fairness with offered load - DCF vs NCF:E-UNWRAP - Full operation.

Table 4.3: Comparison of NCF algorithms

Parameters	DOUTA	FUND	FUND++	E-UNWRAP
MAC changes	Not Required	Required	Required	Required
Fairness	Improves Non-LWIP opportunities	Improves LWIP opportunities	Operates with Fairness	Improves Non-LWIP opportunities
Throughput	Better than Wi-Fi offload by 7%	Better than DCF by 36%	Better than DCF by 23%	Better than DCF by 21%
Compatibility with UEs	Works Readily	Modifications are Required	Modifications are Required	Modifications are Required
Operation Type	Continuous	Interleaved with T_{ON}^F	Interleaved with T_{ON}^{F+}	Continuous
Time elapsed in collisions	Reduced by 13% w.r.t. to Wi-Fi offload	Reduced by 56% w.r.t. to DCF	Reduced by 52% w.r.t. to DCF	Reduced by 33% w.r.t. to DCF

4.6 Summary

In this chapter, we have presented various NCF algorithms with an objective of improving the Wi-Fi channel utilization by enabling efficient uplink transmissions in LWIP system. The developed algorithms are diverse in their objectives, layer of operation, and type of operation. We compared the proposed NCF algorithms with highly successful DCF mechanism of IEEE 802.11 standard. The existence of a primary interface (LTE) facilitates efficient coordination in uplink transmissions by LWIP-UEs and Non-LWIP-UEs on contention based Wi-Fi channel, which resulted in efficient Wi-Fi channel utilization. The developed NCF algorithms are shown to operate fairly with legacy Wi-Fi networks operating on the same Wi-Fi channel; some algorithms subdue their benefits in order to improve overall network performance.

Table 4.3 presents quantitative and qualitative comparison of various NCF algorithms with DCF of 802.11 standard. Using extensive simulation experiments, we observe that the proposed NCF algorithms have reduced collisions in Wi-Fi uplink by 13-56% and thereby improved overall network throughput by 7-36% as compared to Wi-Fi offload with DCF mechanism of Wi-Fi. A network operator can deploy the NCF algorithm, DOUTA, without requiring any modifications at UE. If a finer level of coordination at the MAC layer is required, then FUND, FUND++, and E-UNWRAP can be employed with minor modifications at UE protocol stack. The proposed algorithms could also work in case of other RLI architectures with minor modifications.

Chapter 5

Optimizing LWIP to efficiently support transport layer protocols

In Chapter 3 and 4 various traffic steering solutions are presented for LWIP architectures to effectively use the radio resources of LTE and Wi-Fi networks *i.e.*, with the perspective of optimizing link layer performance. But, this chapter introduces a technique which can be incorporated into traffic steering to improve performance of transport layer protocols such as TCP.

5.1 Motivation

Tighter interworking architectures like LWIP can harvest full benefits of link aggregation only when they do traffic steering at the packet level. Downlink packet steering in LWIP context refers to dynamically forwarding some packets of a downlink flow that arrive at LWIP node (*i.e.*, SeNB) through LTE link and the rest through Wi-Fi link. But a naive link aggregation strategy like packet split naive link aggregation strategy (PS-N-LAS) which does steering at packet level across multiple links introduces problem for TCP traffic, especially when data rates of the links are quite different. The packets steered across the links get delivered at the receiver at different times. As and when the packets are received Out-of-Order (OOO) at the TCP receiver, it leads to generation of DUPLICATE ACKNOWLEDGEMENTS (DUP-ACKs). These unnecessary DUP-ACKs adversely affect the growth of congestion window and thereby lead to poor TCP performance [71]. DUP-ACKs are predominant when links are heterogeneous *i.e.*, when one link rate is much faster/slower than the other

link. This problem is addressed to some extent in LWA architecture, where PDCP reordering procedure ensures packets are delivered in-sequence to the TCP layer at the receiver using Dual Connectivity (DC) [72] reordering procedure. But, during the reordering procedure, if the packets are buffered for longer duration, it has adverse effect on growth of TCP congestion window (for instance, congestion control algorithms such as TCP-New Reno [73], HTCP [74], STCP [75], BIC [76] and HSTCP [77] are dependent on RTT) and hence, results in poor throughput as shown later in Section 5.5. In case of LWIP, this becomes even more challenging as packet steering is done at IP layer which lacks any packet reordering mechanism. Hence, in this chapter, the problem with packet level steering of TCP flows over the LWIP architecture is addressed by proposing a novel virtual congestion control mechanism (VIRtual congeStion control wIth Boost acknowLedgEment -VISIBLE). The proposed mechanism not only improves the throughput of TCP flows by reducing number of unnecessary DUP-ACKs delivered to the TCP sender but also sends Boost ACKs in order to keep growing the congestion window and thereby reaps in the aggregate benefits of heterogeneous links. These Boost ACKs are pseudo ACKs for the actual TCP packets which are already in the downlink queue of LWIP node. VISIBLE mechanism has been implemented at LWIP node in such a way that it does not disturb the semantics of TCP.

This chapter is organized as follows, Section 5.2 presents the existing work on addressing the OOO delivery problem and spurious retransmission triggers. Section 5.3 details the proposed VISIBLE mechanism and the packet steering technique employed along with it. In Section 5.4, the simulation setup considered for evaluating the proposed algorithm and other comparative algorithms are described. Section 5.5 presents the performance results evaluated. Finally, Section 5.6 summarizes the findings and presents a concluding remarks.

5.2 Related work

This section details the existing works related to two major problems that are being addressed in this chapter: (1) Reducing triggers that lead to spurious retransmissions and (2) Reducing OOO packet delivery. Here are some existing works which capture spurious retransmission problem in multi-hop wireless ad hoc network (inline with the problem of LWIP). Reducing spurious retransmissions involves the TCP sender to precisely differentiate congestion loss from OOO packet delivery. DOOR [78] detects OOO delivered packet

by an additional ordering information in the TCP ACK to avoid redundancy. It adds one byte TCP option field known as ACK Duplication Sequence Number (ADSN) to TCP ACK header. When the receiver sends the first ACK for TCP data segment, the ADSN option is initially marked as zero. It increments ADSN number when it sends a DUP-ACK for the same sequence number. Extension of DOOR is TCP-DOOR-TS [79] which uses TCP timestamp mechanism. The sender keeps track of sending times of the packets with respect to receiving times and relatively calculates the time stamp of every packet with the previously received one for detection of OOO packet. TCP receiver sets a field known as *ooo_option_bit* and informs the same to the sender. This method needs an option field to be explicitly set for its working. Eifel algorithm [80] explains about TCP robustness against spurious re-transmissions. It has the facility of backward compatibility. It eliminates retransmission ambiguity and restores the transmission with the next unsent packet.

The forthcoming works include reordering at the receiver side. Delayed ACK [81] introduces a waiting time before the receiver generates a DUP-ACK. This delay in ACK generation provides an opportunity for the receiver to check the necessity of generating a DUP-ACK. The drawback of this method is that when an ACK is delayed in *slow start phase*, it may negatively affect the growth of TCP congestion window. Other re-ordering techniques such as Reordering Robust-TCP [82] and TCP-Packet Reordering [83] target to prevent persistent packet re-ordering from contrivedly activating congestion response by deferring packet retransmission and congestion response till the occurrence of packet loss.

Here are works specific to multi-RAT aggregation. Khadraoui *et al.* [84] studied the performance of TCP in LWA testbed and observed that LWA performs poorly even after packet reordering. Also it was found that PDCP reordering timer has negative impact on TCP growth and hence proposed a network coding technique to enhance the performance of LWA. A well known solution for aggregating multiple links/paths is Multipath TCP (MPTCP) [85]. The power of multiple sub-flows can be used to harvest the aggregated bandwidth of links in a multi-homed host. MPTCP receiver aggregates data from multiple sub-flows, reorders and then delivers it to higher layers. The problem with MPTCP is that it is not efficient in utilizing multiple links when they have heterogeneous data rates. Also, decision taken by MPTCP is based on the entire path into consideration even if the problem resides only with the last hop, which is true more often for wireless networks. Hence, in this work we propose a solution to enhance the TCP performance in LWIP architecture.

5.3 Proposed VISIBLE mechanism for downlink traffic steering

Proposed VISIBLE mechanism addresses the problems faced by downlink TCP flows in LWIP networks. It is implemented at LWIP node, and it includes two major components: (1) Packet steering and (2) Virtual congestion control. Packet steering takes care of forwarding the incoming packets of LWIP node into queues of LTE and Wi-Fi (*i.e.*, RLC queue of LTE stack and MAC queue of Wi-Fi stack) at appropriate rates. Virtual congestion control helps the TCP sender to grow its congestion window by resolving DUP-ACK problem with the help of LWIP node, thereby improving throughputs of TCP flows.

5.3.1 LWIP packet steering

The major cause for OOO packet delivery in LWIP networks is due to “speed of slowest link”. This problem arises when packets of a TCP flow are split across two interfaces and a packet that is first sent through one interface arrives later than the ones that are sent through the other interface. This limits TCP throughput to the speed of slowest link. On one hand, steering all the packets onto one link avoids OOO delivery but it is inefficient in aggregating multiple links. On the other hand, steering packets in inappropriate fraction could cause more OOO deliveries. A better packet steering technique is required to split packets of the incoming TCP flow across LTE and Wi-Fi links. Here, two packet steering techniques for LWIP networks are presented.

1. **Lowest RTT First (L-RTT):** This technique resembles MPTCP’s default scheduler which first fills the congestion window of the link with the lowest RTT and then the link with higher RTT. In LWIP context, the transmit queue of an interface with the lowest RTT is filled first before the other interface. Note that RTT here factors in delay of only the last (wireless) hop, not end-to-end path.
2. **Queue Depletion Rate (Q-Depl):** The rate of decrease in the length of each queue is used as a factor for steering the traffic across LTE and Wi-Fi links. The interface with faster depletion rate receives more packets. The queue depletion rate is comparable to available data rate of an interface.

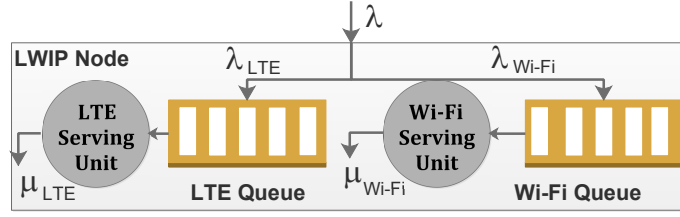


Figure 5.1: Packet steering model at LWIP node.

5.3.2 Analysis of packet steering techniques

In this section, the performance of L-RTT and Q-Depl packet steering techniques are analyzed in terms of their average queue lengths. In our analytical model, the packet arrival rate to LWIP node is assumed to follow Poisson distribution with mean arrival rate of λ . μ_{LTE} is the serving rate of LTE and μ_{Wi-Fi} is the serving rate of Wi-Fi, which are exponentially distributed. The packet steering technique steers the incoming packets across LTE and Wi-Fi queues at rates λ_{LTE} and λ_{Wi-Fi} , respectively and $\lambda = \lambda_{LTE} + \lambda_{Wi-Fi}$. Fig. 5.1 shows the packet steering model considered for the analysis.

Queue length in L-RTT packet steering

L-RTT packet steering technique aims at first to fill in the queue of the interface which has the lowest RTT. For instance, let us assume that LTE link has the lowest RTT, then in LWIP context L-RTT involves filling in LTE queue before even Wi-Fi queue gets a packet. The queue sizes of LTE and Wi-Fi interfaces are represented as N and M , respectively. Here, the total length of the system corresponds to number of packets in the queues and that in the serving unit. So, when L-RTT is employed the total length of the system can be written as $L_{L-RTT} = L_{L-RTT}^L + L_{L-RTT}^W$. Here L_{L-RTT}^L and L_{L-RTT}^W correspond to the lengths of LTE and Wi-Fi queues, respectively when L-RTT packet steering is employed. In L-RTT, packet steering rate λ_{LTE} should be sufficient for filling in the LTE queue first, which can be obtained by equating L_{L-RTT}^L to N . Using M/M/1/N/FIFO queue model [86], L_{L-RTT} can be represented as

$$\begin{aligned}
 L_{L-RTT} = & \left(\frac{\lambda_{LTE}}{\mu_{LTE} - \lambda_{LTE}} - \frac{(N+1) \times \left(\frac{\lambda_{LTE}}{\mu_{LTE}}\right)^{N+1}}{1 - \left(\frac{\lambda_{LTE}}{\mu_{LTE}}\right)^{N+1}} \right) \\
 & + \left(\frac{\lambda_{Wi-Fi}}{\mu_{Wi-Fi} - \lambda_{Wi-Fi}} - \frac{(M+1) \times \left(\frac{\lambda_{Wi-Fi}}{\mu_{Wi-Fi}}\right)^{M+1}}{1 - \left(\frac{\lambda_{Wi-Fi}}{\mu_{Wi-Fi}}\right)^{M+1}} \right)
 \end{aligned} \tag{5.1}$$

Queue length in Q-Depl packet steering

Packet steering using Q-Depl corresponds to the serving rates μ_{LTE} and μ_{WiFi} . The incoming packets are steered onto LTE and Wi-Fi links in the ratio of the interface serving rates.

$$\lambda_{LTE} = \frac{\mu_{LTE}}{\mu_{LTE} + \mu_{WiFi}} \times \lambda \quad (5.2)$$

$$\lambda_{WiFi} = \frac{\mu_{WiFi}}{\mu_{LTE} + \mu_{WiFi}} \times \lambda \quad (5.3)$$

Average queue length of L_{Q-Depl} based system is given by

$$L_{Q-depl} = \frac{2 \times \lambda}{\mu_{LTE} + \mu_{WiFi} - \lambda} - \left[\frac{(N+1) \left(\frac{\lambda}{\mu_{LTE} + \mu_{WiFi}} \right)^{(N+1)}}{1 - \left(\frac{\lambda}{\mu_{LTE} + \mu_{WiFi}} \right)^{(N+1)}} + \frac{(M+1) \left(\frac{\lambda}{\mu_{LTE} + \mu_{WiFi}} \right)^{(M+1)}}{1 - \left(\frac{\lambda}{\mu_{LTE} + \mu_{WiFi}} \right)^{(M+1)}} \right] \quad (5.4)$$

Fig. 5.2 shows CDF of the average queue length of the system when λ is varied from 0 to $(\mu_{LTE} + \mu_{WiFi})$. It can be clearly observed that if L-RTT is employed for packet steering, then a packet has to suffer a longer queuing delay compared to Q-Depl. This is because L-RTT is filling in one queue first which results in increase in its average queue length. When the queue length reaches 100, the first queue is completely filled, and packets are then steered onto the second queue, which reduces the rate of increase in the total queue length of the system. L-RTT can become comparable to Q-Depl only when serving rate of one of the links becomes zero. Hence, in a system with heterogeneous links, Q-Depl will result in better aggregation benefits than L-RTT.

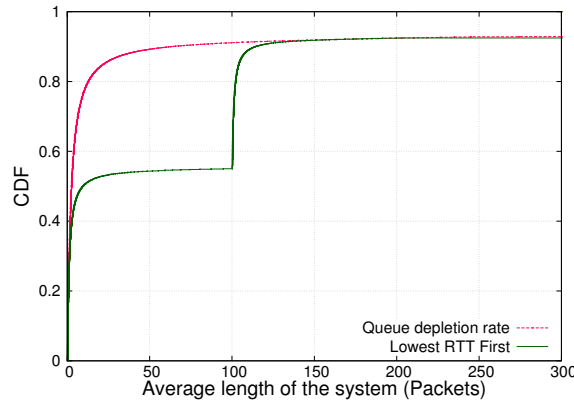


Figure 5.2: Queue length of the system for L-RTT & Q-Depl steering techniques.

5.3.3 Virtual congestion control with Boost acknowledgment: VISIBLE mechanism

VISIBLE mechanism is employed at LWIP node which allows peeking into TCP header to collect necessary information for its operation. VISIBLE mechanism employs Q-Depl for steering the traffic across LTE and Wi-Fi links, and Boost ACK mechanism to minimize DUP-ACKs which might trigger spurious retransmissions. Boost ACK is constructed by changing the ACK number field in the TCP DUP-ACK which makes the TCP sender understand that the packets are indeed delivered to the receiver successfully. Boost ACKs improve the throughput of TCP flows, which otherwise would not have happened if DUP-ACKs are dropped at LWIP node or sent without any modification to the TCP sender. VISIBLE not only reduces the delivery of DUP-ACKs to the TCP sender by boosting the DUP-ACKs but also holds the DUP-ACKs for certain duration in order to let the sender congestion window to grow. VISIBLE uses LTE interface of LWIP for both uplink and downlink TCP transmissions, but Wi-Fi interface is used only to send downlink TCP packets for which UE sends corresponding TCP ACKs through LTE interface. This ensures that there are no collisions on Wi-Fi link and thereby leads to efficient utilization of Wi-Fi link.

Illustration of VISIBLE mechanism

Fig. 5.3 shows an illustration for working of VISIBLE mechanism. For a set of TCP segments transmitted by TCP sender, LWIP node steers IP packets containing TCP segments across LTE and Wi-Fi links based on packet steering algorithm implemented. In this example, Wi-Fi is shown as bottleneck link, and so it takes longer time to deliver a packet. In due course of time, the packets sent through LTE interface reach the receiver for which the receiver generates DUP-ACKs. LWIP node on reception of a DUP-ACK applies VISIBLE mechanism. VISIBLE transforms the DUP-ACK into a Boost ACK and sends that to the TCP sender or holds the DUP-ACKs for a while in order to let the ACKs flow in-sequence. Once the packet through Wi-Fi interface gets delivered to the receiver, LWIP node sends an ACK which acknowledges all the previous successfully delivered packets. Hence, the congestion window of the TCP sender is prevented from reducing unnecessarily which helps in significantly improving throughputs of TCP flows.

In the second part of Fig. 5.3, a TCP segment with sequence number 150 is lost on LTE link. LWIP node again performs boosting and holding on reception of DUP-ACKs. As the DUP-ACKs arrival to LWIP node continues even after boost and holding phases, LWIP node concludes that the packet is actually lost and does a retransmission from its local buffer. Hence, TCP segment loss that occurred at the link level (LTE/Wi-Fi) is salvaged locally by the LWIP node.

The proposed VISIBLE is presented in Algorithm 7. Table 5.1 lists out the notations used in presenting VISIBLE mechanism. Following are the main features that VISIBLE mechanism encompasses, (1) Rate of boosting DUP-ACKs, (2) Holding DUP-ACKs, and (3) Reducing packet losses. These main features are presented below in detail.

(1) Boosting DUP-ACKs

During Boost ACK phase, a received DUP-ACK is transformed into a regular ACK by changing ACK number field of TCP header to a new ACK number. Note that this action is done only when the packet with sequence number corresponding to the new ACK number is received by LWIP node from the TCP sender before-hand. The ACK with new ACK number conveys the sender that the packet got delivered to the receiver successfully, which makes the sender to grow its congestion window. Boost ACK phase is followed by a skipped ACK (also called as ACK holding) period in order to align the boosted ACK (new ACK) to become in-sequence with actual received ACK from the receiver. The rate of boosting ACKs is a function of available buffer space in queues of LTE and Wi-Fi interfaces. Boosting of ACKs should be stopped much before the buffer space gets filled up. This ensures that the actual packets sent by the sender for the boosted ACKs will not get lost in the LWIP node due to buffer overflow phenomenon. The rate of boosting the ACKs is also reduced as the queue starts filling up. This is done in order to reduce the rate of growth of sender's congestion window so that it can sustain longer time without reduction due to packet losses induced by the full buffer.

(2) Holding DUP-ACKs

During holding DUP-ACK phase, the actual DUP-ACKs when received at LWIP node are not sent to the TCP sender instead they are dropped by LWIP node. Dropping too many DUP-ACKs leads to *timeout* [87] at the TCP sender and also increases RTT, hence rate of

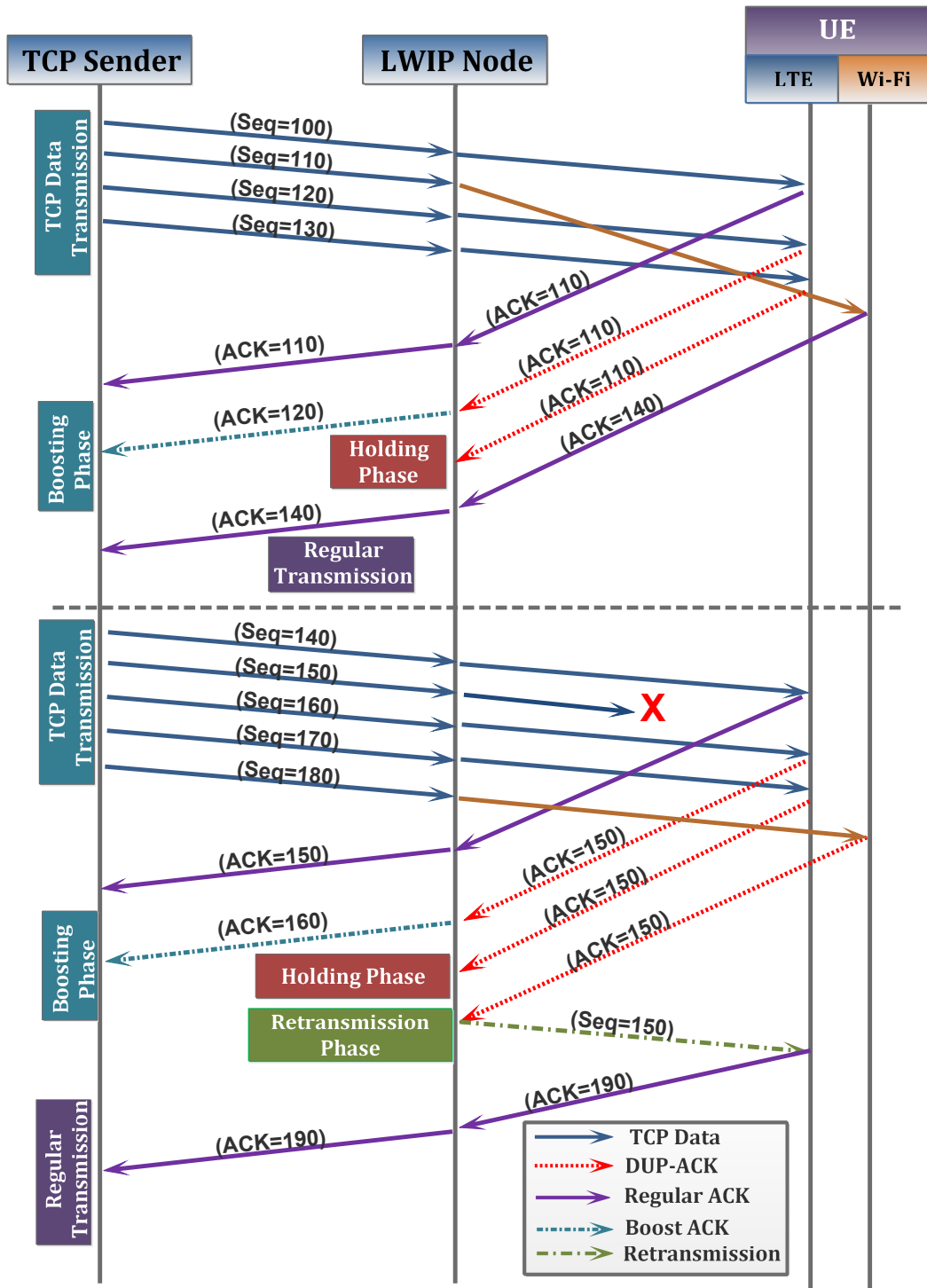


Figure 5.3: An example of virtual congestion control procedure in VISIBLE mechanism.

Algorithm 7 : VISIBLE mechanism

Input: $\mathcal{I}_i \leftarrow$ Initial sequence number of a TCP flow $\mathcal{N} \leftarrow$ Number of TCP flows in the system $\mathcal{B}_{LTE}^a, \mathcal{B}_{Wi-Fi}^a \leftarrow$ Available buffer Size in LTE and Wi-Fi queues $\mathcal{B}_{LTE}^s, \mathcal{B}_{Wi-Fi}^s \leftarrow$ Total buffer size of LTE and Wi-Fi queues**Output:** $\varphi \leftarrow$ Boost Fraction ; $\mathcal{H}_i \leftarrow$ DUP-ACK Holding Time**TCP ACK Packet Received:**

Update the TCP state information for all flows

- 1: **if** DUP-ACK of i^{th} flow $\&\& \mathcal{A}_i^r > \mathcal{I}_i \ \&\& \ \mathcal{B}_{LTE}^a > \varphi \times \mathcal{B}_{LTE}^s \ \&\& \ \mathcal{B}_{Wi-Fi}^a > \varphi \times \mathcal{B}_{Wi-Fi}^s$
 $\&\& \ \varphi + \mathcal{P}_i < \frac{1}{\mathcal{N}} \times \min(\frac{\mathcal{B}_{LTE}^a}{\mathcal{B}_{LTE}^s}, \frac{\mathcal{B}_{Wi-Fi}^a}{\mathcal{B}_{Wi-Fi}^s}) \ \&\& \ \mathcal{RT}_i == 0$ **then**

\triangleright Boost ACK Phase
- 2: $\mathcal{TH}_i \leftarrow \mathcal{CT}; \mathcal{H}_i \leftarrow 0; \mathcal{P}_i \leftarrow \mathcal{P}_i + 1$
- 3: $\mathcal{A}_i^r \leftarrow \mathcal{A}_i^r + (MSS \times \mathcal{P}_i)$
- 4: *Modify_ACK_Number*(*Packet*, \mathcal{A}_i^r); $\mathcal{A}_i^s \leftarrow \mathcal{A}_i^r$
- 5: **else if** DUP-ACK of i^{th} flow $\&\& \ \mathcal{RT}_i == 0 \ \&\& \ \mathcal{A}_i^r > \mathcal{I}_i \ \&\& \ \mathcal{P}_i < \mathcal{PH}_i^a \times$
 $\min(\frac{\mathcal{B}_{LTE}^a}{\mathcal{B}_{LTE}^s}, \frac{\mathcal{B}_{Wi-Fi}^a}{\mathcal{B}_{Wi-Fi}^s}) \ \&\& \ \mathcal{H}_i < (\frac{1}{\mathcal{N}} \times ((LTE_{LTT} + WiFi_{LTT})/2) \times \min(\frac{\mathcal{B}_{LTE}^a}{\mathcal{B}_{LTE}^s}, \frac{\mathcal{B}_{Wi-Fi}^a}{\mathcal{B}_{Wi-Fi}^s})$
 $\&\& \ \mathcal{B}_{LTE}^a > \varphi \times \mathcal{B}_{LTE}^s \ \&\& \ \mathcal{B}_{Wi-Fi}^a > \varphi \times \mathcal{B}_{Wi-Fi}^s$ **then**

\triangleright Holding ACK Phase
- 6: **if** $\mathcal{TH}_i == 0$ **then**
- 7: $\mathcal{TH}_i \leftarrow \mathcal{CT}$
- 8: **end if**
- 9: $\mathcal{H}_i \leftarrow \mathcal{H}_i + \mathcal{CT} - \mathcal{TH}_i; \mathcal{TH}_i \leftarrow \mathcal{CT}; \mathcal{P}_i \leftarrow \mathcal{P}_i + 1$
- 10: *return*

\triangleright Stops the DUP-ACKs
- 11: **else if** DUP-ACK of i^{th} flow $\&\& \ \mathcal{RT}_i < \mathcal{RT}^{max} \ \&\& \ \mathcal{B}_{LTE}^a > \varphi \times \mathcal{B}_{LTE}^s \ \&\& \ \mathcal{B}_{Wi-Fi}^a >$
 $\varphi \times \mathcal{B}_{Wi-Fi}^s$ **then**

\triangleright Retransmission Phase
- 12: $\mathcal{P}_i \leftarrow \mathcal{P}_i + 1; \mathcal{RT}_i \leftarrow \mathcal{RT}_i + 1$
- 13: *Trigger_Local_ReTx*($\mathcal{A}_i^r, \mathcal{R}_j, \mathcal{BI}_{i,j}$)
- 14: **else**

\triangleright Regular Transmission
- 15: **if** *Get_ACK_Number*(*Packet*) == \mathcal{A}_i^r **then**
- 16: $\mathcal{P}_i \leftarrow \mathcal{P}_i + 1$
- 17: **else**
- 18: **if** $\mathcal{P}_i > 0$ **then**
- 19: **if** $\mathcal{P}_i > \mathcal{PH}_i^a$ **then**
- 20: $\mathcal{PH}_i^a \leftarrow (1 - \alpha) \times \mathcal{PH}_i^a + \alpha \times \mathcal{P}_i$
- 21: **else**
- 22: $\mathcal{PH}_i^a \leftarrow (1 - \beta) \times \mathcal{PH}_i^a + \beta \times \mathcal{P}_i$
- 23: **end if**
- 24: $\mathcal{P}_i \leftarrow 0$
- 25: **end if**
- 26: $\mathcal{H}_i \leftarrow 0; \mathcal{TH}_i \leftarrow 0; \mathcal{RT}_i \leftarrow 0;$
- 27: $\mathcal{A}_i^r \leftarrow$ *Get_ACK_Number*(*Packet*)
- 28: $\mathcal{A}_i^s \leftarrow$ *Get_ACK_Number*(*Packet*)
- 29: **end if**
- 30: **end if**
- 31: *Send_to_S1U_Socket*(*Packet*)

Table 5.1: Notations used in VISIBLE mechanism

Definition	Symbol
DUP-ACK Packet Counter (i^{th} flow)	\mathcal{P}_i
Last Received Ack Number at LWIP	\mathcal{A}_i^r
Last Sent Ack Number from LWIP	\mathcal{A}_i^s
Packet Sending Time	\mathcal{T}_i
Sequence Number of Packet Sent	\mathcal{S}_i
Radio Network Temporary Identifier (j^{th} user)	\mathcal{R}_j
Bearer ID (j^{th} user)	$\mathcal{BL}_{j,i}$
Number of DUP-ACKs Held	\mathcal{PH}_i^a
DUP-ACK Holding Time	\mathcal{H}_i
Timestamp of Last Packet Held	\mathcal{TH}_i
Retransmission Counter at LWIP	\mathcal{RT}_i
Maximum number of Retransmissions from LWIP	\mathcal{RT}^{max}
Current Time	\mathcal{CT}
Available Buffer Size in LTE and Wi-Fi	$\mathcal{B}_{LTE}^a, \mathcal{B}_{Wi-Fi}^a$
Total Buffer Size of LTE and Wi-Fi	$\mathcal{B}_{LTE}^s, \mathcal{B}_{Wi-Fi}^s$
Initial sequence number	\mathcal{I}_i
Number of Flows in the System	\mathcal{N}
Boost Fraction	φ

regulating these DUP-ACKs is very crucial. The DUP-ACKs are controlled by the process of holding by taking into account various parameters such as, (a) available buffer space in queues of both LTE and Wi-Fi interfaces, (b) Link trip times of both LTE and Wi-Fi links, (c) Number of packets held currently, and (d) Holding time elapsed for DUP-ACKs. Link trip time of an interface in LWIP node corresponds to the time elapsed between sending a TCP packet to UE till getting the ACK for the same packet. The packet holding time and number of packets held are reduced by the factor of available packets in the buffer.

(3) Handling packet losses

If a TCP packet intended to the receiver gets lost on a wireless link (LTE/Wi-Fi), then the packet is retransmitted from the LWIP node instead of enforcing the actual sender to retransmit the packet. ϑ denotes the fraction of buffer size till boost and holding of ACKs can be done. An exponential moving average function is used to obtain the threshold for number of DUP-ACKs that can be held. α and β are weight fractions considered in the exponential moving average function. Steps 20-22 of VISIBLE algorithm shows the implication of α and β respectively. Typically, α is low which emphasizes that when number

of DUP-ACKs are increased, the holding threshold should be increased slowly. β takes a high value signifying that when the number of DUP-ACKs decreases the number of packets held should also be decreased rapidly, so that it reduces TCP timeouts happening because of longer holding. `Trigger_Local_ReTx` function retransmits the TCP packet locally from LWIP node with radio network temporary identifier (RNTI) (\mathcal{R}) and bearer id (\mathcal{BI}).

5.4 Simulation setup

The performance of the proposed VISIBLE mechanism is evaluated in NS-3 with experimental parameters shown in Table 5.2. The LWIP module and LWA module were developed in NS-3. Our simulation setup consists of an LWIP node and a set of associated UEs. Our proposed mechanism VISIBLE is implemented on LWIP, hence it is denoted as LWIP+VISIBLE. Fig. 5.4 shows the simulation setup. Each LWIP-UE receives two downlink TCP flows from a Remote Server (RS). Bulk-send application is used to send TCP traffic. On receiving TCP segments from RS, VISIBLE+LWIP steers them across LTE and Wi-Fi links. On reception of each TCP packet, LWIP-UE generates a TCP ACK, which is sent in uplink to RS through LWIP node. On reception of a TCP ACK, LWIP node runs Algorithm 7. In our setup, TCP New Reno [73] is chosen as the underlying congestion control mechanism. This is because unlike TCP Cubic [88], the growth of congestion window of TCP New Reno is dependant on RTTs. Hence, holding ACK packet for longer duration will adversely affect the sending rate by the TCP sender. The problem becomes more challenging if a packet is held for a longer time which could lead to TCP timeouts. In the experiments, for simplicity, it has been considered that only one LWIP-UE gets associated with the LWIP node. LWIP-UE in the system establishes a downlink TCP flow with RS.

5.5 Performance results

This section captures the performance of different phases of VISIBLE algorithms. It also shows the improvement of the proposed VISIBLE mechanism as compared to the state-of-the-art algorithms.

Table 5.2: NS-3 parameters to evaluate VISIBLE mechanism

Parameter	Value
Number of LWIP Node and UEs	1, 1
LTE SeNB bandwidth	10 MHz, FDD
LTE and Wi-Fi Tx power	20, 16 dBm
LTE antenna model	Isotropic antenna model
LTE path loss model	Friis propagation loss model [89]
LTE SeNB scheduler	Proportional fair
Wi-Fi frequency, bandwidth	2.4 GHz and 5 GHz, 20 MHz
Wi-Fi standard	IEEE 802.11 a, b, g
Wi-Fi rate control algorithm	Adaptive auto rate fallback
Application	TCP Bulk Send Application
TCP congestion control algorithm	TCP New Reno
Buffer size of LWIP Node	40 packets (per interface)
Simulation duration	100 sec
Number of seeds	10
Mobility Model	Constant position mobility model
Advertised receiver window size	65535 bytes

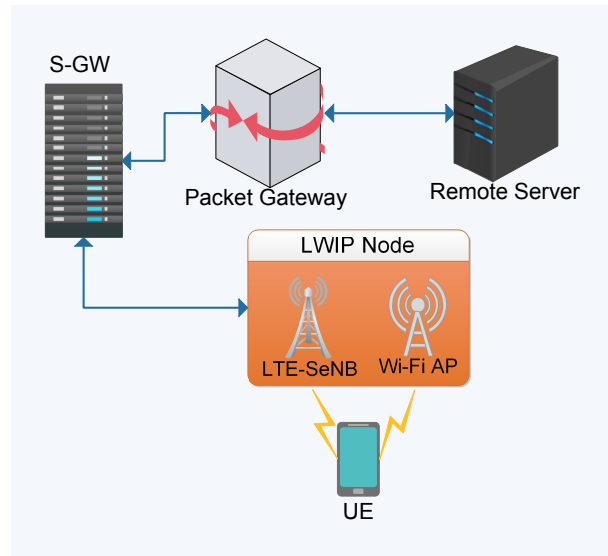


Figure 5.4: Experimental setup used for evaluation of VISIBLE mechanism.

5.5.1 Performance of different phases of VISIBLE mechanism

Various phases of VISIBLE mechanism are evaluated in this section. Fig. 5.5 shows the ACK number received at LWIP node and various operations performed on those TCP ACK packets. When LWIP node receives DUP-ACKs, then Boost ACK phase gets triggered and VISIBLE boosts the ACK numbers. Further on receiving DUP-ACKs, holding phase is

triggered. The DUP-ACKs are held by LWIP node either till the threshold time to hold these DUP-ACKs is met or till the number of DUP-ACKs threshold is met. DUP-ACKs threshold varies dynamically as regulated by the VISIBLE algorithm. Fig. 5.6 shows the duration for which the DUP-ACKs are held and threshold time to held DUP-ACKs. Fig. 5.7 shows the number of DUP-ACKs that are held and threshold for number of DUP-ACKs that can be held. The threshold in both cases (*viz.*, time to hold the DUP-ACKs and number of DUP-ACKs to be held) resembles a saw tooth pattern. Fig. 5.8 shows the queue lengths of LTE and Wi-Fi interfaces. Retransmission of packets is triggered when DUP-ACKs count exceeds threshold packets to be held or the threshold holding time. Fig. 5.7 also shows the DUP-ACKs exceeding the threshold.

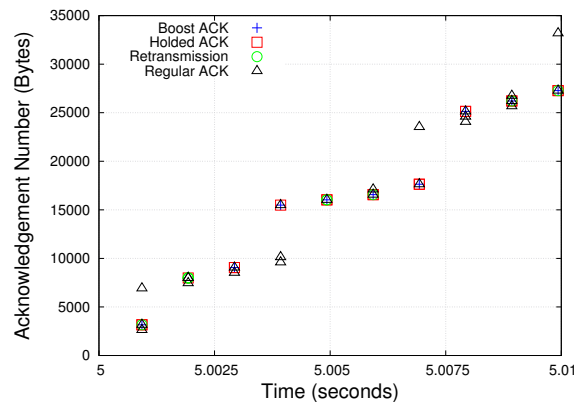


Figure 5.5: Different phases of VISIBLE in VISIBLE+LWIP system.

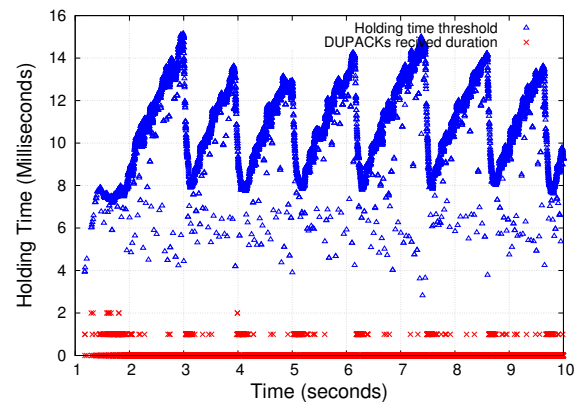


Figure 5.6: Holding time of ACK packets in VISIBLE+LWIP system.

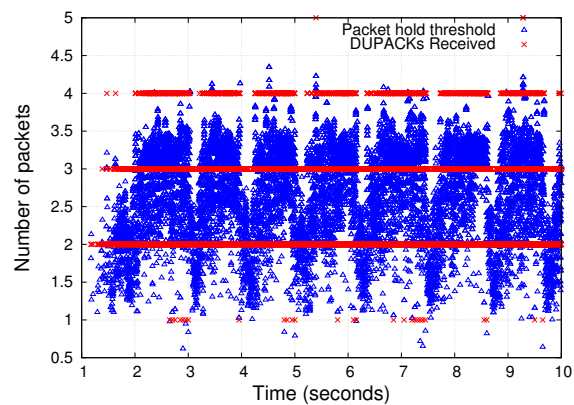


Figure 5.7: Number of DUP-ACKs held at VISIBLE+LWIP node.

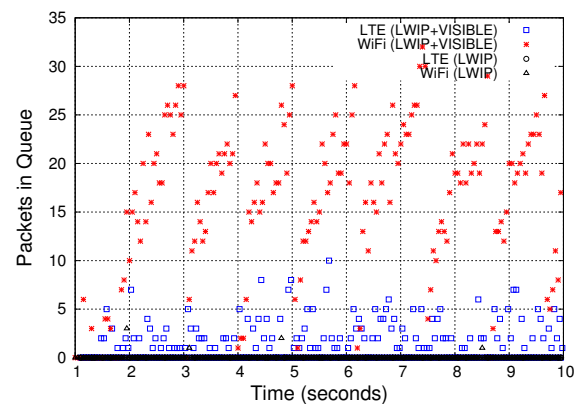


Figure 5.8: Lengths of LTE and Wi-Fi queues.

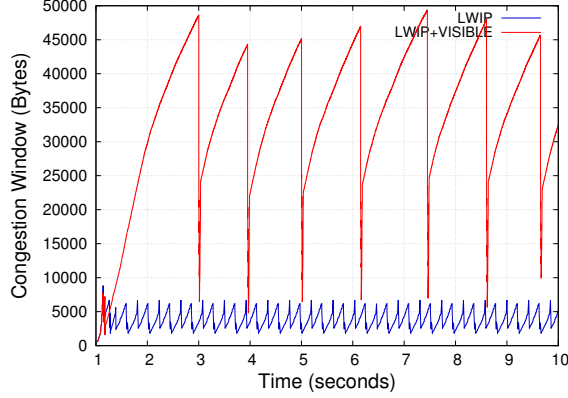


Figure 5.9: Congestion window growth of LWIP and LWIP+VISIBLE architectures.

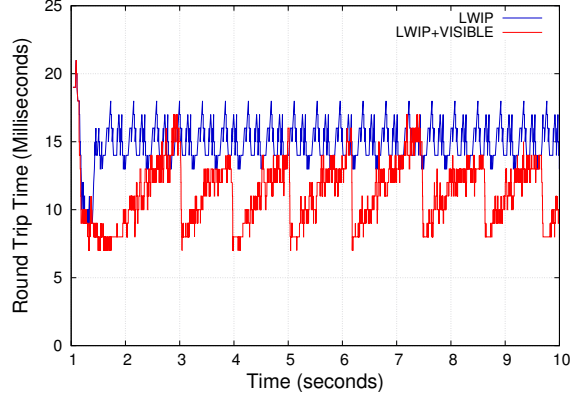


Figure 5.10: RTT of TCP flow in case of LWIP and LWIP+VISIBLE architectures.

5.5.2 Performance of LWIP vs LWIP+VISIBLE

The growth of congestion window in case of basic LWIP (*i.e.*, LWIP without employing VISIBLE mechanism at LWIP node) is heavily degraded by DUP-ACKs received which could be observed from Fig. 5.9. In LWIP+VISIBLE, the congestion window grows faster which is not only due to avoiding DUP-ACKs but also due to boosting ACKs which helps the congestion window of the sender to grow faster. Fig. 5.10 shows RTTs of both basic LWIP and LWIP+VISIBLE. The RTT for basic LWIP is constant, whereas in the case of LWIP+VISIBLE RTTs have an increase/decrease pattern *i.e.*, this pattern coincides with congestion window's growth. When the congestion window increases, RTT goes higher because of holding of TCP ACKs for longer duration by LWIP node before the fast retransmit phase of TCP gets triggered (refer Figs. 5.6 and 5.7).

5.5.3 Performance of LWIP+VISIBLE vs MPTCP

An open source NS-3 MPTCP module [90] is used in this experiment. The MPTCP simulation setup contains LTE and Wi-Fi networks (no interworking as in LWIP) connected to RS, and both RS and UE are MPTCP capable. Two downlink flows are generated between RS and UE in full mesh mode of MPTCP. The performance of LWIP+VISIBLE is compared with various congestion control algorithms of MPTCP *viz.*, Coupled, Uncoupled, and Link Increase Algorithm (LIA). Fig. 5.11 shows the throughput improvement of LWIP+VISIBLE as compared to MPTCP algorithms. LWIP+VISIBLE has improved throughput of the network by 55% as compared to MPTCP algorithms when IEEE 802.11b

is used as Wi-Fi link. This is because when LTE and Wi-Fi link rates are quite diverse, then MPTCP algorithms suffers from "the speed of the slowest link" problem, thereby MPTCP algorithms fail to achieve the aggregated throughput of both LTE and Wi-Fi networks. LWIP+VISIBLE has improved the throughput by leveraging the potential of Boost ACKs. When IEEE 802.11g is used (here LTE and Wi-Fi link rates are comparable), then MPTCP gets the aggregation benefit. LWIP+VISIBLE also achieves comparable performance with MPTCP. When IEEE 802.11a is used, then LWIP+VISIBLE improves network throughput by 12% as compared to MPTCP algorithms.

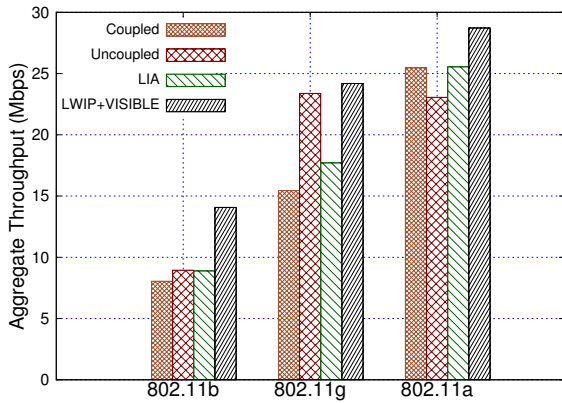


Figure 5.11: Throughputs of MPTCP and LWIP+VISIBLE.

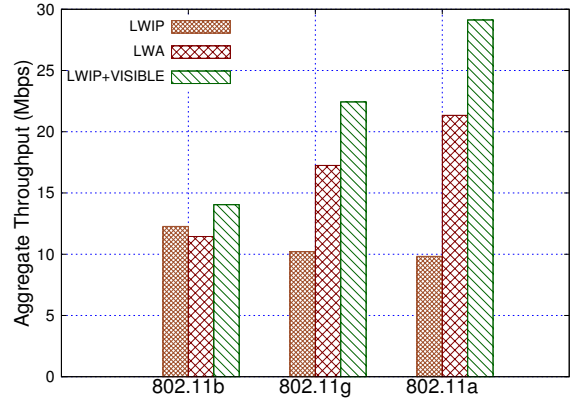


Figure 5.12: Throughputs of basic LWA, basic LWIP, and LWIP+VISIBLE.

5.5.4 Performance of different link aggregation architectures

In this experiment, four LWIP-UEs are associated with an LWIP node, and each LWIP-UE is having two downlink flows. Here, the performances of basic LWA, basic LWIP, and LWIP+VISIBLE are compared. A basic LWA system does reordering of the packets received through LTE and Wi-Fi links of LWIP-UE using PDCP sequence number. The reordering window has a threshold reordering time of 30 ms, as specified by 3GPP. Fig. 5.12 shows the throughputs achieved when different RLI architectures are used. Basic LWA has achieved 50% cumulative throughput improvement (with 802.11b, 802.11g and 802.11a) when compared to basic LWIP because of PDCP reordering procedure which it implements. But LWIP+VISIBLE has outperformed LWA by 30% due to boosting of ACKs which leads to better growth in congestion window and thereby improves the network throughput. VISIBLE mechanism (VISIBLE+LWIP) has almost doubled the throughput of basic LWIP. But

VISIBLE mechanism can be employed only when the TCP packet header is unencrypted.

5.6 Summary

In this chapter, VISIBLE mechanism was proposed for improving TCP performance in LWIP networks. The most crucial challenge was to let the congestion window of the sender to grow, which was achieved by sending Boost ACKs to TCP sender in a controlled fashion from LWIP node. The proposed VISIBLE mechanism has successfully aggregated multiple links even if they are offering quite different rates. LWIP node incorporated packet steering technique based on queue depletion rate and Boost ACKs. The proposed VISIBLE mechanism outperformed MPTCP based LTE-Wi-Fi integration by 37% and LWA architecture by 30%. The proposed mechanism can be employed in the context of 5G multi-connectivity, where different RATs can be employed to deliver the same flow.

Chapter 6

Efficient placement of LWIP nodes

In this chapter, we address issues in deployment of colocated and non-colocated LWIP nodes by mobile operators. The problem of placing LWIP nodes in dense environments is studied with the following objectives: (i) Minimize the number of LWIP nodes required to serve users in a given building with a certain threshold Signal-to-Interference-plus-Noise Ratio (SINR), (ii) Maximize SINR inside the building by placing LWIP nodes at optimal locations, and (iii) Minimize the energy spent at LWIP nodes and users without degrading SINR of users.

The above mentioned objective functions are formulated as Mixed Integer Non-Linear Programming (MINLP) problems. This chapter is organized as follows, at first the works closely related to placement of small cells in indoor environments are discussed. And the problem which is unaddressed in the literature under heterogeneous networks is elaborated. The system model considered to address the problem in LWIP context is presented, and the objective functions are presented in detail. Finally, the proposed models are evaluated and their performance is compared with other existing models.

6.1 Related work

In this section, we discuss the literature pertaining to the optimal placement of small cells in dense mobile environments. In [91] and [92], optimal placement of a single small cell inside a building is done by considering interference from Macro BS. This placement is not scalable for enterprise scenarios with multiple floors. In [93], the authors have considered enterprise scenarios and studied how to minimize number of LTE small cells required for placement

to ensure a certain threshold SINR to all regions inside a building with multiple floors. A limitation of this work is that the authors have considered the placement problem by only concerning homogeneous radio access technologies (RATs) *i.e.*, Macro BS and small cells of LTE. In [94], the authors have proposed a joint femto placement and power optimization model with an objective to minimize uplink power spent by UEs inside a building. In this context, the authors have not considered many real-world challenges such as multiple walls present inside the building and cross-tier interference from Macro BS. In [71], the authors have detailed various challenges pertaining to tighter coupling of LTE and Wi-Fi links at physical and network layers. The authors have pointed that, at the physical layer, heterogeneous reuse of spectrum (*i.e.*, users in interference region of LTE could be served by Wi-Fi and vice-versa) would be an effective solution in case of dense deployment scenarios, but the authors have not explored this property of the system. In this chapter, we focus on both colocated and non-colocated LWIP deployment in dense enterprise environments by considering factors like distance between small cells and UEs, cross-tier interference from Macro BS (in case of LTE), co-tier interference from other LWIP nodes deployed, and path loss due to obstacles such as walls across rooms inside the building.

6.2 System model

In this section, we describe the system model considered for our study.

6.2.1 Building model

Fig. 6.1 shows the building model considered in our study. Dimensions of the building considered are $48 \text{ m} \times 48 \text{ m} \times 3 \text{ m}$, where $L \times W \times H$ correspond to length, width, and height of the building, respectively. The building has 16 rooms, each of dimensions $12 \text{ m} \times 12 \text{ m} \times 3 \text{ m}$. Walls separate the rooms, and each room encloses nine sub-regions. A sub-region is of length $4 \text{ m} \times 4 \text{ m} \times 3 \text{ m}$, and the building is having only one floor. Thus, the building is divided into 144 sub-regions (I_1, I_2, \dots, I_{144}). A Macro BS is placed at a distance of 1.4 km from the building. As the size of a sub-region is much smaller when compared to the size of the building, we can safely assume that within every sub-region, SINR is constant.

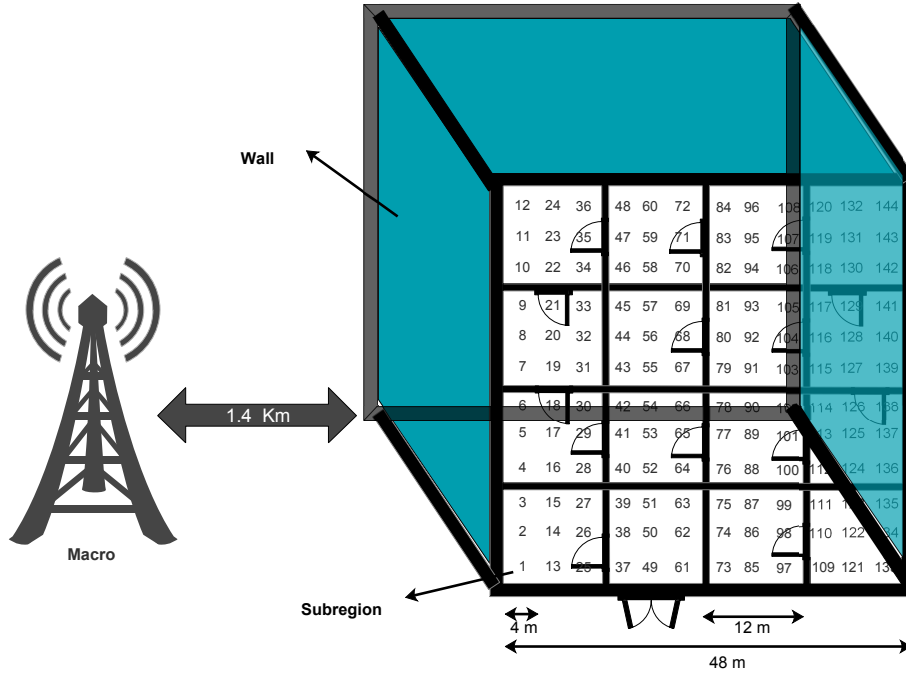


Figure 6.1: Building model considered.

6.2.2 Path Loss model for LTE network

We have used 3GPP Indoor Path Loss Model (Urban Deployment) [59] for LTE (PLM_{LTE}).

It is given by

$$PLM_{LTE} = 37 + 30 \log_{10}(d) + 18.3k^{\frac{k+2}{k+1}-0.46} + n\sigma - 1 \quad (6.1)$$

Where d is the distance of a sub-region from an LTE small cell in meters, k represents the number of floors between a sub-region and cell, and σ represents penetration loss in dB.

6.2.3 Path Loss model for Wi-Fi network

We have used International Telecommunication Union (ITU) indoor path loss model [60] for Wi-Fi. It estimates the path loss inside a room or a closed area inside a building delimited by walls of any form. This model is most suitable for the frequency range between 900 MHz and 5.2 GHz. The ITU model for Wi-Fi PLM_{Wi-Fi} is given by

$$PLM_{Wi-Fi} = 20 \log_{10}(f) + N \log_{10}(d) + (P_f \times n) - 28 \quad (6.2)$$

Where d is the distance of a sub-region from Wi-Fi AP in meters, f represents the frequency of transmission in MHz, N accounts for the distance power loss coefficient, n is the number

of walls, and P_f denotes the penetration loss in dB.

The notations which are used in the optimization problem for placement of LWIP nodes inside a building are detailed in Table 6.1.

Table 6.1: Notations used in optimization models for placement of LWIP nodes

Symbol	Definition
R_i	Set of all sub-regions inside the building
α_b^l	1 if a LTE small cell is placed at sub-region b , 0 otherwise
α_b^w	1 if Wi-Fi AP is placed at sub-region b , 0 otherwise
α_c	1 if a interfering LTE small cell or Wi-Fi AP is placed at sub-region c , 0 otherwise
$\beta_{s,b}^l$	1 if sub-region s is connected to LTE small cell at b , 0 otherwise
$\beta_{s,b}^w$	1 if sub-region s is connected to Wi-Fi AP at b , 0 otherwise
$\delta_{s,b}^l$	LTE channel gain between s and b sub-regions
$\delta_{s,b}^w$	Wi-Fi channel gain between s and b sub-regions
γ_b^l	LTE SINR observed at sub-region b
γ_b^w	Wi-Fi SINR observed at sub-region b
P_b^l	LTE transmit power of LWIP node or UE located at sub-region b
P_b^w	Wi-Fi transmit power of LWIP node or UE located at sub-region b
P_{max}^m	Maximum transmit power of Macro Base Station
P_{max}^l	Maximum transmit power of LTE small cell
P_{max}^w	Maximum transmit power of Wi-Fi AP
λ_l	LTE SINR threshold
λ_w	Wi-Fi SINR threshold
N_o	System Noise
M	Macro Base Station

6.3 Optimization models for placement of LWIP nodes

In this section, we formulate different optimization problems for colocated (C) and non-colocated (NC) LWIP deployments with the following three objectives:

- Minimal number of LWIP nodes required to ensure good coverage in the building.
- Optimal placement of LWIP nodes to maximize SINR inside the building.
- Optimal placement and power control of LWIP nodes to minimize the energy spent at LWIP nodes and UEs.

6.3.1 Models for determining minimal number of LWIP nodes required for deployment of LWIP system

The minimum number of LWIP nodes required to serve users inside the building in the case of C-LWIP and NC-LWIP are formulated as optimization problems Min-C-LWIP and Min-NC-LWIP, respectively. In the following, these two problems are described.

(A) Min-NC-LWIP model

The objective here is to find the minimum number of LTE and Wi-Fi nodes that can effectively cover the entire building in a non-colocated scenario by ensuring a certain threshold SINR. Here, we have considered minimum LTE SINR threshold as λ_l dB and minimum Wi-Fi SINR threshold as λ_w dB. The objective function is given as follows:

$$\text{Minimize } \sum_b (\alpha_b^l + \alpha_b^w) \quad (6.3)$$

subject to,

$$\sum_b \beta_{s,b}^l \leq 1 \text{ and } \sum_b \beta_{s,b}^w \leq 1 \quad \forall s \in R_i \quad (6.4)$$

$$\beta_{s,b}^l \leq \alpha_b^l \text{ and } \beta_{s,b}^w \leq \alpha_b^w \quad \forall s, b \in R_i \quad (6.5)$$

$$\sum_{s,b} (\beta_{s,b}^l + \beta_{s,b}^w) \geq 1 \quad (6.6)$$

$$\sum_b \alpha_b^l \geq 1 \text{ and } \sum_b \alpha_b^w \geq 1 \quad (6.7)$$

Equation (6.3) minimizes the sum over number of LTE small cells and Wi-Fi APs to be deployed in order to ensure a certain threshold SINR in every sub-region of the building. Equation (6.5) and Equation (6.6) constrain an LWIP-UE in a sub-region to be connected to utmost one LTE small cell and one Wi-Fi AP. Equation (6.7) ensures that a sub-region has at least one LTE or Wi-Fi connectivity. It does not restrict an LWIP-UE inside a sub-region from connecting to both RATs. Equation (6.7) ensures that at least one LTE small cell and one Wi-Fi AP must exist in the non-colocated LWIP placement inside the building.

$$\frac{Inf \times (1 - \beta_{s,b}^l) + (\delta_{s,b}^l \cdot P_{max}^l \cdot \alpha_b^l)}{N_o + \sum_{c \in R_i \setminus b} \delta_{s,c}^l \cdot P_{max}^l \cdot \alpha_c + \sum_{e \in M} \delta_{s,e}^l \cdot P_{max}^m} \geq \lambda_l \quad \forall s, b \in R_i \quad (6.8)$$

$$\frac{Inf \times (1 - \beta_{s,b}^w) + (\delta_{s,b}^w \cdot P_{max}^w \cdot \alpha_b^w)}{N_o + \sum_{c \in R_i \setminus b} \delta_{s,c}^w \cdot P_{max}^w \cdot \alpha_c} \geq \lambda_w \quad \forall s, b \in R_i \quad (6.9)$$

For LWIP-UE at sub-region s to be connected to an LTE small cell or a Wi-Fi AP located at sub-region b , the sub-region has to receive a certain minimum SINR from that LTE small cell or Wi-Fi AP. Equation (6.8) captures this constraint on LTE SINR threshold (λ_l) and Equation (6.9) on Wi-Fi SINR threshold (λ_w). In the case of LTE, Macro BS interference is also considered. Inf in Equation (6.8) is an infinitely large value which is introduced because solver ignores the case where the values are very high and thus the computation time is reduced. Inf signifies that, if a sub-region s is not associated with LTE small cell or Wi-Fi AP at sub-region b , then the SINR becomes infinite. Hence the solver ignores such cases during its execution.

(B) Min-C-LWIP Model

The minimum number of C-LWIP nodes that can effectively cover the building with a certain minimum SINR threshold at every sub-region is given by:

$$Minimize \sum_b (\alpha_b^l + \alpha_b^w) \quad (6.10)$$

The objective function given in Equation (6.10) for C-LWIP deployment is same as that given in Equation (6.3) for NC-LWIP deployment along with the constraints given in Equation (6.5) to Equation (6.9). The only additional constraint that the colocated deployment requires over non-colocated deployment is given in Equation (6.11). It states that the location of the LTE small cell and Wi-Fi AP must be in the same sub-region, as the colocated deployment involves placing them together in the same integrated box.

$$\alpha_b^l - \alpha_b^w = 0 \quad \forall b \in R_i \quad (6.11)$$

6.3.2 Model for optimal placement of LWIP nodes

Min-C-LWIP and Min-NC-LWIP models, presented in the previous section, give out number of LTE small cells and Wi-Fi APs that have to be deployed inside a given building by mobile operators. Given the number of LTE small cells and Wi-Fi APs, placing them at the optimal locations will maximize the overall SINR of the building while ensuring a certain minimum SINR for all sub-regions inside the building. The objective function to maximize SINR is given in Equation (6.12).

$$\text{Maximize } \sum_b (\gamma_b^l + \gamma_b^w) \quad (6.12)$$

subject to,

$$\frac{\text{Inf} \times (1 - \beta_{s,b}^l) + (\delta_{s,b}^l \cdot P_{max}^l \cdot \alpha_b^l)}{N_o + \sum_{c \in R_i \setminus b} \delta_{s,c}^l \cdot P_{max}^l \cdot \alpha_c + \sum_{e \in M} \delta_{s,e}^l \cdot P_{max}^m} \geq \lambda_l \quad \forall s, b \in R_i \quad (6.13)$$

$$\frac{\text{Inf} \times (1 - \beta_{s,b}^w) + (\delta_{s,b}^w \cdot P_{max}^w \cdot \alpha_b^w)}{N_o + \sum_{c \in R_i \setminus b} \delta_{s,c}^w \cdot P_{max}^w \cdot \alpha_c} \geq \lambda_w \quad \forall s, b \in R_i \quad (6.14)$$

$$\sum_b \alpha_b^l = N^L \quad \text{and} \quad \sum_b \alpha_b^w = N^W \quad (6.15)$$

$$\sum_b \beta_{s,b}^l \leq 1 \quad \text{and} \quad \sum_b \beta_{s,b}^w \leq 1 \quad \forall s \in R_i \quad (6.16)$$

$$\beta_{s,b}^l \leq \alpha_b^l \quad \text{and} \quad \beta_{s,b}^w \leq \alpha_b^w \quad \forall s, b \in R_i \quad (6.17)$$

Here terms γ_b^l and γ_b^w denote LTE SINR and Wi-Fi SINR observed at sub-region b , respectively. The variables N^L and N^W denote the number of LTE small cells and Wi-Fi APs obtained by solving optimization model given in Equation (6.3) and Equation (6.10). Note that $N^L = N^W$ in case of C-LWIP deployment.

6.3.3 Models to obtain optimal power setting for operation of LWIP nodes and LWIP-UEs

Power control in LWIP architecture reaps the highest improvement in LWIP performance in dense deployment scenario [95]. The placement of LWIP nodes plays a vital role in optimizing the energy spent at LWIP nodes and LWIP-UEs. In this section, we have formulated optimization problems to minimize the energy spent at LWIP nodes and LWIP-UEs by first placing the LWIP nodes at optimal locations (obtained by solving Equation (6.12)) and then by setting transmit power levels at LWIP nodes and LWIP-UEs to optimal values.

(A) Model to optimize transmit power of LWIP nodes to save energy

Min-Power-LWIP-node Model: This model saves energy spent by LWIP nodes. Energy spent at LWIP nodes can be reduced by reducing transmit power levels of LWIP nodes while still ensuring a certain SINR threshold to every sub-region inside the building. Equation (6.18) shows the objective function to minimize the energy spent at LWIP nodes.

$$\text{Minimize } \sum_{b \in R_i} (\alpha_b^l \times P_b^l) + (\alpha_b^w \times P_b^w) \quad (6.18)$$

subject to,

$$\frac{\text{Inf} \times (1 - \beta_{s,b}^l) + (\delta_{s,b}^l \cdot P_b^l \cdot \alpha_b^l)}{N_o + \sum_{c \in R_i \setminus b} \delta_{s,c}^l \cdot P_b^l \cdot \alpha_c + \sum_{e \in M} \delta_{s,e}^l \cdot P_{max}^m} \geq \lambda_l \quad \forall s, b \in R_i \quad (6.19)$$

$$\frac{\text{Inf} \times (1 - \beta_{s,b}^w) + (\delta_{s,b}^w \cdot P_b^w \cdot \alpha_b^w)}{N_o + \sum_{c \in R_i \setminus b} \delta_{s,c}^w \cdot P_b^w \cdot \alpha_c} \geq \lambda_w \quad \forall s, b \in R_i \quad (6.20)$$

$$P_{min}^l \leq P_b^l \leq P_{max}^l \quad \forall b \in R_i \quad (6.21)$$

$$P_{min}^w \leq P_b^w \leq P_{max}^w \quad \forall b \in R_i \quad (6.22)$$

$$\beta_{s,b}^l \leq \alpha_b^l \quad \text{and} \quad \beta_{s,b}^w \leq \alpha_b^w \quad \forall s, b \in R_i \quad (6.23)$$

$$\sum_b \alpha_b^l = N^L \quad \text{and} \quad \sum_b \alpha_b^w = N^W \quad (6.24)$$

Constraints shown in Equations (6.19)-(6.24) ensure that SINR received above the SINR threshold in all the sub-regions, with transmit power values bounded within the limits, and

associativity condition ensuring that a LWIP-UE associates with utmost one LWIP node. Finally, the sum of LTE nodes deployed and sum of Wi-Fi nodes deployed must be N^L and N^W , respectively.

(B) Model to optimize transmit power of LWIP-UEs to save energy

Min-Power-LWIP-UE Model: This model is to save the energy spent by LWIP-UEs. The energy spent at LWIP-UE can be reduced by first placing the LWIP nodes at optimal positions. We formulate an optimization problem to find the optimal locations for LWIP nodes which minimizes the energy spent at LWIP-UEs as follows. Equation (6.18) presented in last subsection varies the transmit power of LWIP node in order to save energy at LWIP node, whereas in Equation (6.25), the energy spent by LWIP-UE is reduced by varying the transmit power and the position of LWIP node. The implicit vision is, closer the LWIP nodes to LWIP-UEs it prevents UEs from transmitting with higher transmit power, thereby saving energy spent by LWIP-UEs.

$$\text{Minimize } \sum_{b \in R_i} (\beta_{s,b}^l \times P_b^l) + (\beta_{s,b}^w \times P_b^w) \quad (6.25)$$

subject to,

$$\frac{\text{Inf} \times (1 - \beta_{s,b}^l) + (\delta_{s,b}^l \cdot P_b^l \cdot \alpha_b^l)}{N_o} \geq \lambda_l \quad \forall s, b \in R_i \quad (6.26)$$

$$\frac{\text{Inf} \times (1 - \beta_{s,b}^w) + (\delta_{s,b}^w \cdot P_b^w \cdot \alpha_b^w)}{N_o} \geq \lambda_w \quad \forall s, b \in R_i \quad (6.27)$$

$$P_{min}^l \leq P_b^l \leq P_{max}^l \quad \forall b \in R_i \quad (6.28)$$

$$P_{min}^w \leq P_b^w \leq P_{max}^w \quad \forall b \in R_i \quad (6.29)$$

$$\beta_{s,b}^l \leq \alpha_b^l \quad \text{and} \quad \beta_{s,b}^w \leq \alpha_b^w \quad \forall s, b \in R_i \quad (6.30)$$

$$\sum_b \alpha_b^l = N^L \quad \text{and} \quad \sum_b \alpha_b^w = N^W \quad (6.31)$$

The objective function shown in Equation (6.25) minimizes the overall energy spent by LWIP-UEs. We have assumed that the number of LWIP-UEs in all sub-regions is the same. Equations (6.26)–(6.31) show the constraints on minimum SINR threshold to be met in

every sub-region, transmit power bounds, and guaranteeing association of every sub-region with exactly one LWIP node. Solving the optimization problem gives out the optimal locations to place LWIP nodes and optimal power levels for transmission by LWIP-UEs.

6.4 Performance results

Various optimization models proposed in the previous sections for colocated and non-colocated deployment of LWIP nodes are evaluated in this section. The results of proposed optimal placement of LWIP nodes are compared with the placement of LWIP nodes at Minimum Interference Region (MIR). MIR is another way of placing LWIP nodes, since our system model considers cross-tier interference from a Macro BS. In MIR, each LTE small cell is placed in the building at a sub-region with minimum interference from the Macro BS, and each Wi-Fi AP is placed at a sub-region with maximum SINR from Macro BS. Thereby potential sub-regions which receive high interference from Macro BS are served using Wi-Fi and the regions with lesser Macro BS interference are served using LTE small cells. Fig. 6.1 is the building model considered for evaluating the performance of proposed optimization models. Also for evaluation purpose, the values for LTE SINR threshold λ_l and Wi-Fi SINR threshold λ_w are set to -2 dB and 0 dB, respectively. The performance of proposed and MIR are compared in terms of number of LWIP nodes required for deployment under each mechanism, perceived SINR in each sub-region, and energy consumption at LWIP-UEs and LWIP node. The evaluation is done using MATLAB based solver.

6.4.1 Result of Min-NC-LWIP and Min-C-LWIP models

The optimal number of LWIP nodes required to cover the given building dimensions of 48 m \times 48 m \times 3 m in non-colocated deployment scenario is found to be one LTE small cell and one Wi-Fi AP. Fig. 6.2 shows respective positions of one LTE small cell and one Wi-Fi AP using $\langle x, y, z \rangle$, where x and y tell the position of LTE SeNB/Wi-Fi AP with respect to sub-region indices and z gives out SINR in the corresponding sub-region. Fig. 6.2 shows SINR (in dB) distribution when the LTE small cell and Wi-Fi AP are placed based on MIR placement. This set up ensures threshold SINR (-2 dB for LTE and 0 dB for Wi-Fi) to every sub-region either through LTE, Wi-Fi or both.

In case of colocated deployment, the optimal number of C-LWIP nodes to be placed is

found to be two. Fig. 6.3 captures SINR distribution when the colocated nodes are placed as per MIR placement inside the building.

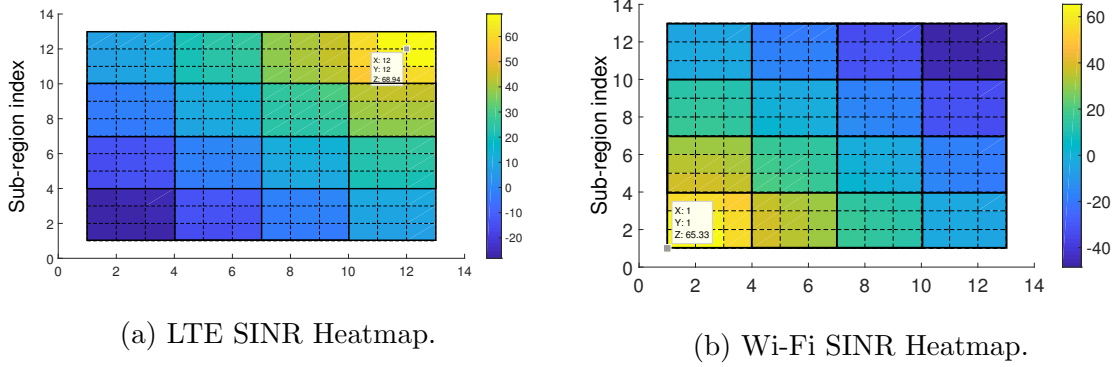


Figure 6.2: Non-colocated LWIP deployment with MIR placement.

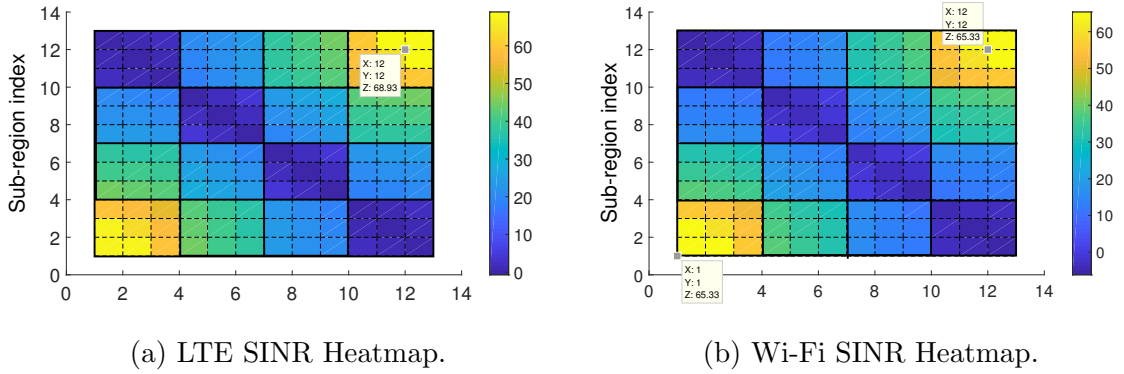
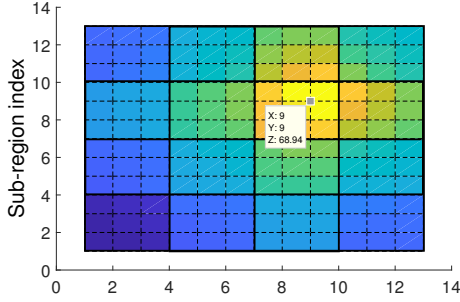


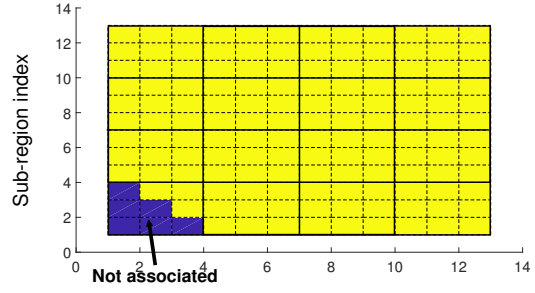
Figure 6.3: Colocated LWIP deployment with MIR placement.

6.4.2 Result of optimal LWIP placement model

When LWIP nodes are placed as per MIR placement, it does not ensure maximized SINR. Solving Equation (6.12) gives the optimal positions for LTE small cells and Wi-Fi APs in case of colocated and non-colocated deployments. Figs. 6.4 and 6.5 capture SINR distribution of LTE and Wi-Fi networks across all sub-regions inside the building when LTE small cell and Wi-Fi AP are placed at optimal positions in case of non-colocated deployment. It can be noted from the figures that in case of optimal placement, LTE and Wi-Fi could not serve all the sub-regions individually. But when combined they could serve the entire building. In case of colocated LWIP deployment, on solving the optimization problem (Model 6.3.1), we have obtained that two LWIP nodes are sufficient to serve all the

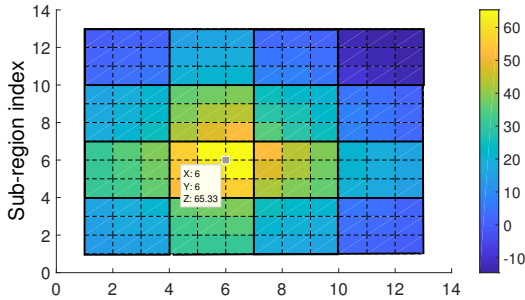


(a) LTE SINR Heatmap.

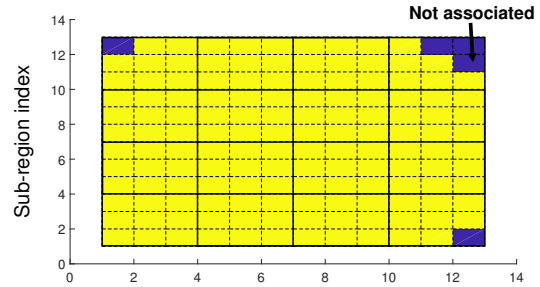


(b) LTE sub-region associativity.

Figure 6.4: LTE SINR heatmap and subregion association in case of non-colocated LWIP deployment with optimal placement model.



(a) Wi-Fi SINR Heatmap.



(b) Wi-Fi sub-region associativity.

Figure 6.5: Wi-Fi SINR heatmap and subregion association in case of non-colocated LWIP deployment with optimal placement model.

sub-regions in the building. Figs. 6.6 and 6.7 capture LTE and Wi-Fi SINR distributions inside the building, respectively. They also capture which sub-regions are associated with LTE small cells and Wi-Fi APs. It is clear from the figures that LTE small cells in colocated LWIP deployment could serve all the sub-regions but Wi-Fi APs fail to serve some of sub-regions.

We have compared SINR distributions in case of optimal placement (Model 6.3.2 - Optimal Placement - OPP) and MIR placement of the LWIP nodes. Fig. 6.8 shows the SINR comparison between non-colocated LWIP optimal placement and MIR placement. Fig. 6.9 shows the SINR comparison between colocated LWIP optimal placement and MIR placement. OPP of C-LWIP has improved average SINR by 8 dB when compared to MIR placement. This is because MIR placement focuses on minimizing the co-tier interference (either with Macro BS or with other small cells), but it fails to maximize SINR for every sub-region. From Figs. 6.4 and 6.5, it is clear that optimal locations for maximizing SINR

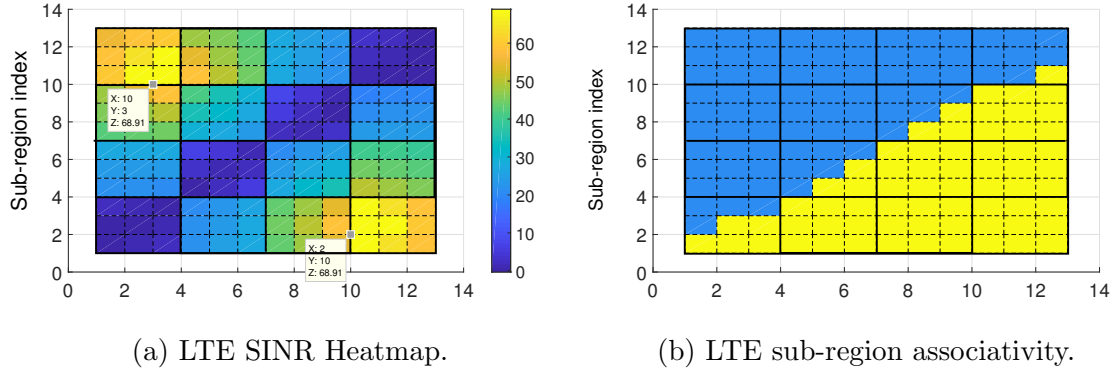


Figure 6.6: LTE SINR heatmap and subregion association in case of colocated LWIP deployment with optimal placement model.

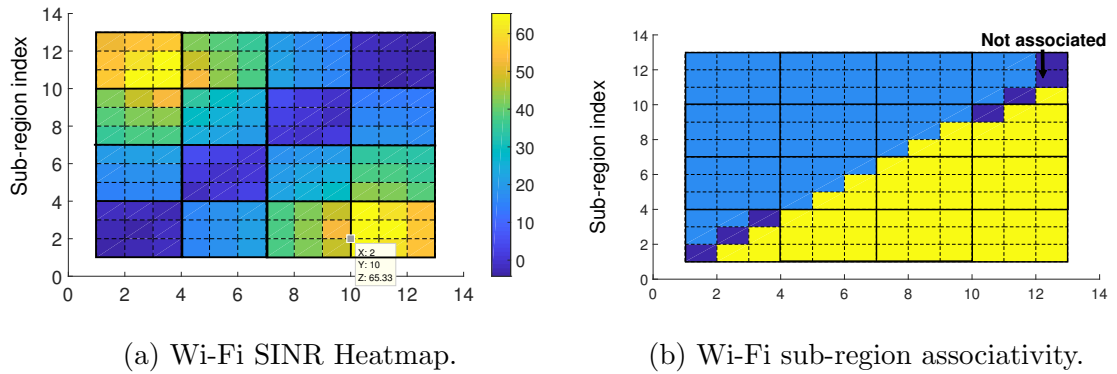


Figure 6.7: Wi-Fi SINR heatmap and subregion association in case of colocated LWIP deployment with optimal placement model.

lie towards the center of the building but MIR placement is confined towards the corners. Figs. 6.10 and 6.11 show the number of sub-regions associated only with LTE, only with Wi-Fi and with both LTE and Wi-Fi in case of colocated and non-colocated deployments. It can be observed that the number of sub-regions associated with both LTE and Wi-Fi in case of OPP has improved by 43% on average when compared to MIR placement.

6.4.3 Result for energy saving at LWIP nodes and LWIP-UEs

To minimize the energy spent at LWIP nodes and UEs, the LWIP nodes have to be placed in optimal locations by optimizing the transmit power levels of LWIP nodes in order to ensure a certain threshold SINR in all the sub-regions inside the building. The optimization problem described in Section 6.3.3 with the above objectives is evaluated here. The optimization problem thrives to obtain the optimal locations for placement of LWIP nodes and minimal

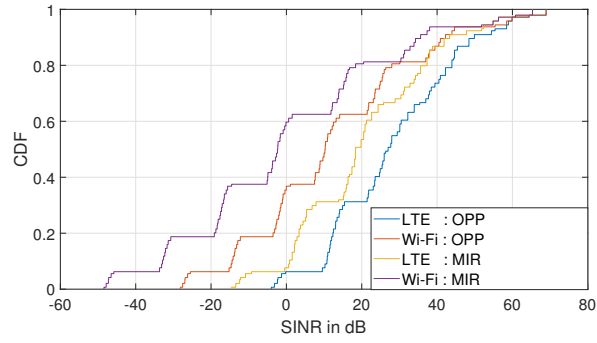


Figure 6.8: SINR CDF observed in all the sub-regions for a non-colocated deployment with optimal placement model.

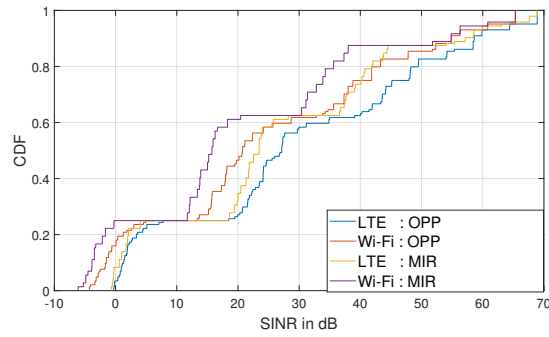


Figure 6.9: SINR CDF observed in all the sub-regions for a colocated deployment with optimal placement model.

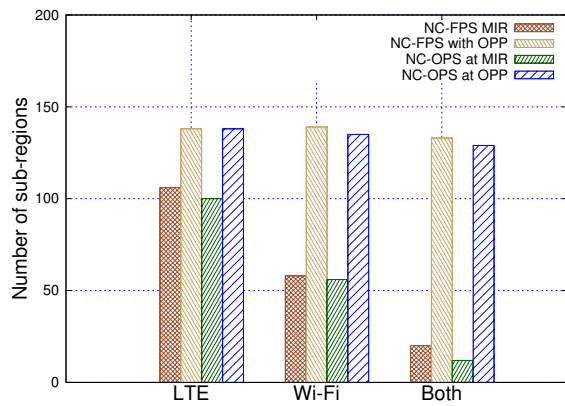


Figure 6.10: Sub-regions associativity : non-colocated placement.

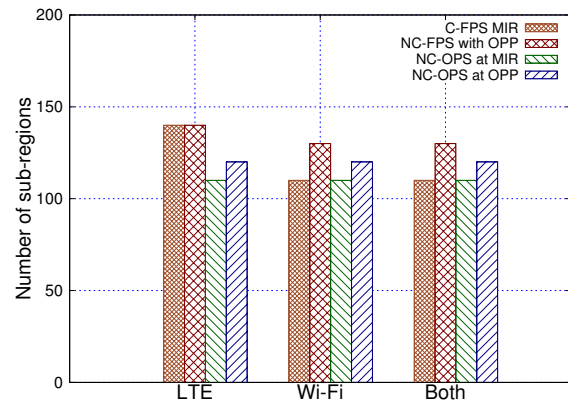


Figure 6.11: Sub-regions associativity : colocated placement.

transmit power levels that can cover all the sub-regions inside the building.

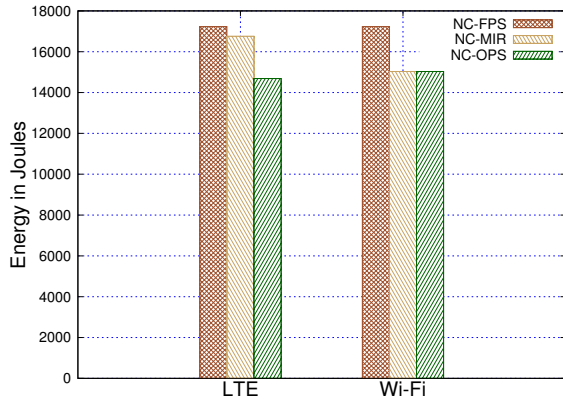


Figure 6.12: Energy consumed at LWIP node : non-colocated deployment.

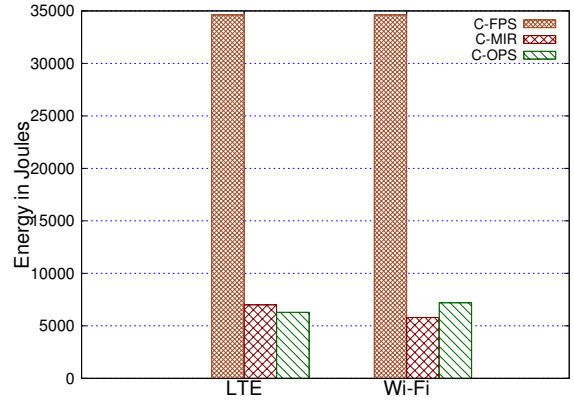


Figure 6.13: Energy consumed at LWIP node : colocated deployment.

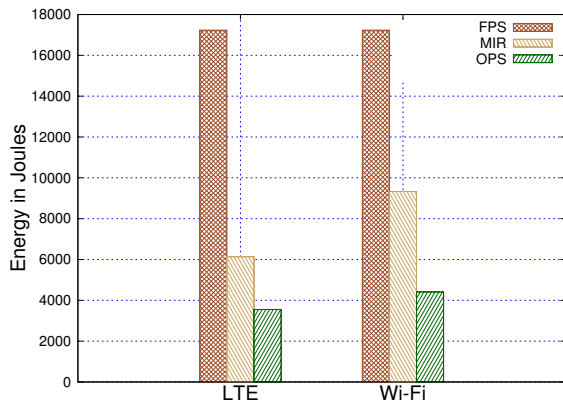


Figure 6.14: Average energy spent by a UE : non-colocated deployment.

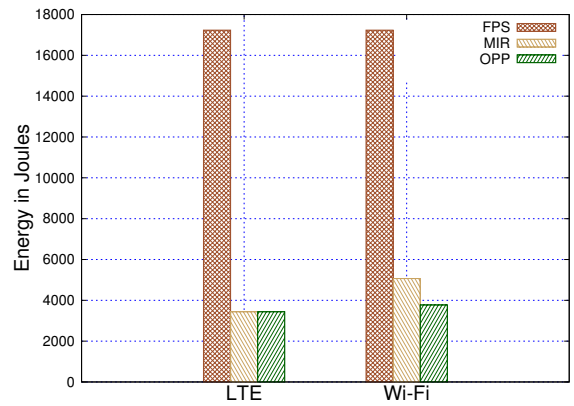


Figure 6.15: Average energy spent by a UE : colocated deployment.

Energy saving at LWIP nodes

The energy consumed by LWIP nodes has a significant reduction when the transmit power levels are optimized. The energy values when the LWIP nodes operates with their peak transmit power level (Full Power Scheme -FPS) and deployed with MIR, is compared with LWIP nodes operating with optimal transmit power scheme (OPS) placed at optimal positions. Figs. 6.12 and 6.13 capture the energy spent in Joules in case of non-colocated and colocated LWIP deployments. OPS at LWIP nodes has reduced the energy consumption by 15% and 72% as compared to FPS operation of LWIP node in non-colocated and colocated deployments, respectively. More energy savings are achieved because the number of LTE and Wi-Fi nodes deployed is high in colocated compared to non-colocated deployment. In the case of colocated deployment the optimal reuse of the spectrum is employed

as presented in Section 2.1.1 of Chapter 2. The optimal reuse of the spectrum involves regulation of transmit power in LTE and Wi-Fi links of LWIP nodes. In a given LWIP node, LWIP-UEs in the inner coverage region are served using LTE, and those UEs which lie in the outer coverage region are served using Wi-Fi. This pattern happens alternatively in adjacent colocated LWIP nodes (where the outer coverage region is served by LTE, while Wi-Fi serves the inner coverage region). This alternate pattern avoids the outer coverage regions of two adjacent colocated LWIP nodes served using the same RAT *viz.*, LTE or Wi-Fi, thereby using the available spectrum efficiently.

Energy savings at LWIP-UE

The energy spent by LWIP-UEs can be reduced by placing the LWIP nodes at the sub-regions obtained by solving the Model 6.3.3. Figs. 6.14 and 6.15 capture the average energy spent by an LWIP-UE for different deployment cum power control scenarios. In case of non-colocated deployment, OPS with OPP has reduced the energy spent at LWIP-UE by 47% as compared to placement at MIR with optimal power. In case of colocated deployment, the energy spent at LWIP-UE has reduced by 25% compared to operating LWIP nodes at MIR with optimal power. In both the figures, full power is given for reference which shows the energy spent by an LWIP-UE if it operate at the full transmit power.

6.5 Summary

The placement of LWIP nodes has a significant impact on SINR observed and rates achievable in different sub-regions of buildings. We have addressed the placement problem with three major objectives, which include (i) Minimizing the number of LWIP nodes to be placed, (ii) Maximizing the SINR for all sub-regions, and (iii) Minimizing the energy spent by LWIP-UEs and LWIP nodes. Solutions obtained for these optimization problems have improved the performance of the LWIP system significantly. The OPP have achieved 8 dB improvement in SINR and 43% improvement in number of sub-regions connected to both LTE and Wi-Fi as compared to MIR placement. Also, the OPS with OPP lead to 10% energy saving at LWIP node and 36% energy saving at LWIP-UE side compared to MIR placement. Either NS-3 or MATLAB based simulations were carried out to evaluate the performance of RLI architectures in all previous chapters. It is of high interest

to study the performance of these architectures and traffic steering solutions proposed in real-time. The next chapter will describe the testbed implementation of RLI architectures using open-source tools.

Chapter 7

Prototyping of RLI architectures

This chapter details prototype implementation of different RLI architectures. Also, the performance of these architectures has been studied in various realistic network scenarios.

7.1 Introduction to prototyping of RLI architectures

In Chapter 2, the following RLI architectures and their layer of interworking were studied.

1. LTE Wi-Fi Integration with IPsec tunnel (LWIP)
2. LTE Wi-Fi Aggregation (LWA)
3. LTE Wi-Fi Integration at RLC layer (LWIR)

Fig. 7.1 shows the difference in the layer of integration of LTE and Wi-Fi radio protocol stacks for LWA, LWIP, and LWIR architectures. RLI architectures target to steer incoming traffic across LTE and Wi-Fi links. Steering at IP is flexible and easily adaptable. Steering at PDCP and RLC require modifications at the radio protocol stacks of LTE and Wi-Fi, but they ensure in-sequence and reliable delivery, respectively. In subsequent sections, prototype implementation of each architecture is described in detail.

7.2 LWIP prototyping

This section provides an overview of LWIP architecture and its prototype implementation. LWIP enables a tighter level integration between LTE and Wi-Fi radio protocol stacks at IP layer to perform traffic steering at the granularity of bearer level, flow level, and packet

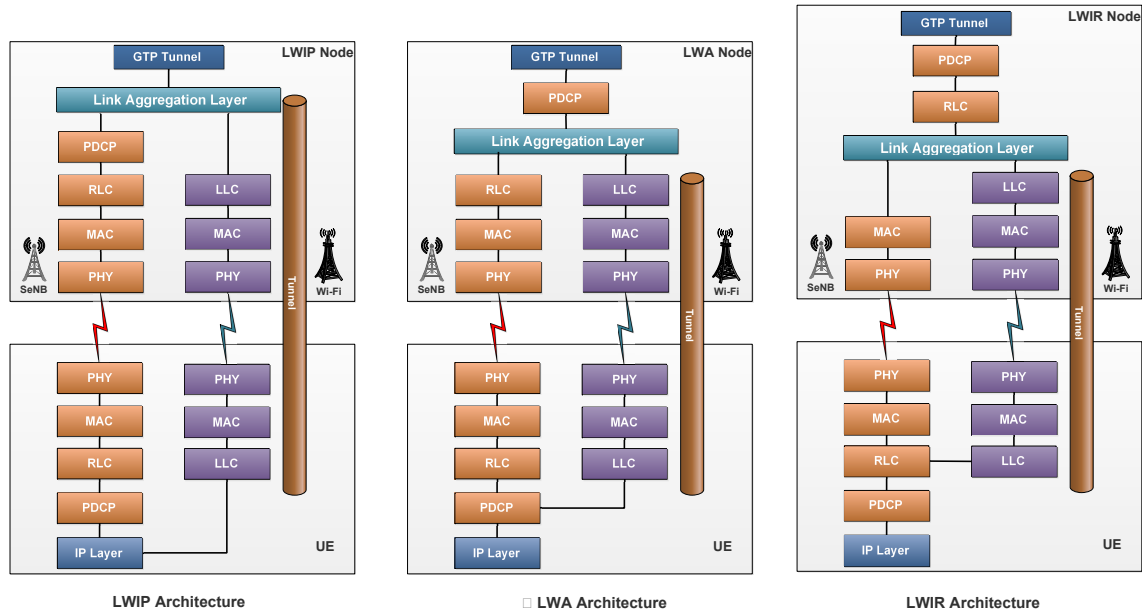


Figure 7.1: RLI architectures and their layer of integration.

level. LWIP is realized by introducing a Link Aggregation Layer (LAL) in the protocol stack of the LWIP node. The traffic steering is done above the PDCP layer of LTE and the LLC layer of Wi-Fi in their respective protocol stacks. Based on the traffic steering mechanism, the LAL decides which packets/flows/bearers to be transmitted over LTE and Wi-Fi and sends them over the corresponding radio interface. The LAL does not add any new header to the IP data packets received from EPC via S1-U interface. Packets going through LTE and Wi-Fi interfaces follow regular packet forwarding procedures at their protocol stacks and get delivered directly to IP layer.

LWIP is leveraged by its ease of implementation to achieve the aggregation benefits. Also, LAL supports collecting various network parameters and actively participates in intelligent decision making for steering IP traffic across LTE and Wi-Fi interfaces in the downlink. It is notable that LWIP architecture does not require any modification to the protocol of UE. In our implementation, LWIP supports downlink traffic steering across LTE and Wi-Fi.

LWIP testbed is setup using OpenAirInterface (OAI) platform as LTE network and a Cisco access point as Wi-Fi AP. The following subsections present more details on LTE testbed and LWIP testbed.

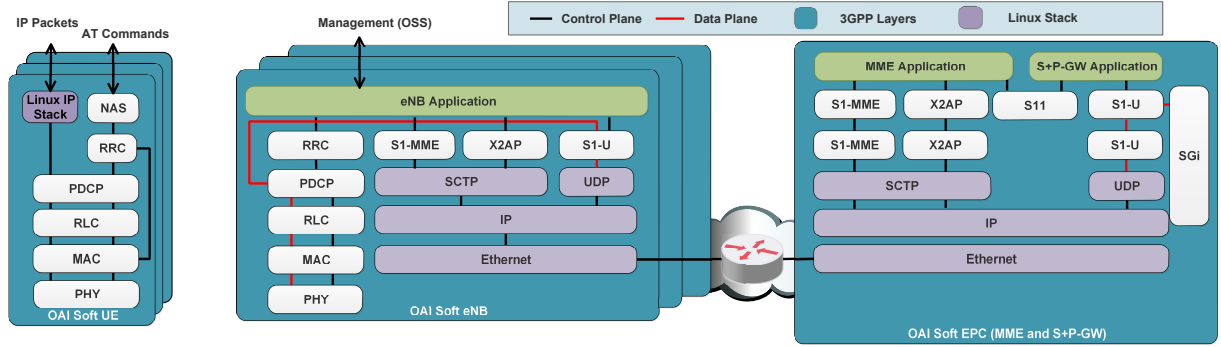


Figure 7.2: OpenAirInterface LTE software stack [3].

7.2.1 LTE testbed using OAI platform

OpenAirInterface [3] is a complete implementation of 4G-LTE (Rel-10). It includes OpenAirInterface User Equipment (OAI-UE), OpenAirInterface eNodeB (OAI-eNB), and OpenAirInterface Core Network (OAI-CN). OAI-eNB works with many commercial UEs such as Nexus 5, Samsung Galaxy S5, iPhone 5s, *etc.*

OAI-eNB implements MAC, RLC, PDCP, and RRC layers according to the LTE standard. It also supports eMBMS services (MCH, MCCH, MTCH). OAI-CN has EPC components which comply with 3GPP releases up to Rel-10. It includes Serving Gateway (S-GW), Packet Data Network Gateway (P-GW), Mobility Management Entity (MME), Home Subscriber Server (HSS), and Non-Access Stratum (NAS).

ExpressMIMO2 (ExMIMO2) board, which is PCI express based, is used as RF frontend in the testbed setup. ExMIMO2 boards belong to the class of Software Defined Radio (SDR) that can work up to 80 MHz of carrier aggregation [96]. Fig. 7.2 shows the software stack of LTE in OAI.

7.2.2 Realization of LWIP testbed using OAI platform

Fig. 7.3 illustrates the protocol implementation structure of LWIP prototype. The LWIP implementation follows the architecture proposed in [97], which includes a minor modification to 3GPP LWIP architecture. The main difference between 3GPP LWIP architecture and implemented architecture is that there is no IPsec tunnel to deliver the packets to destined UE in our implementation. This is because the security aspect of LWIP system is not a primary focus in our work. However, the security procedures of our proposed architecture are detailed in Chapter 2. The UE obtains an IP address for each interface *viz.*, LTE and

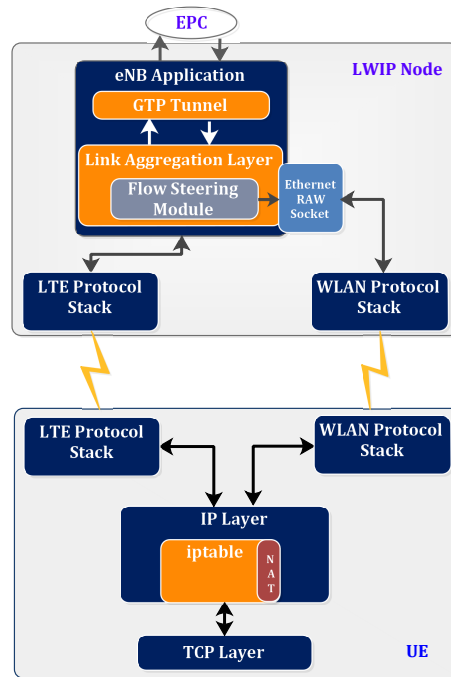


Figure 7.3: Protocol implementation structure of LWIP prototype system.

Wi-Fi. The information about the interface availability and IP addresses of interfaces are made available at LWIP node. When a packet arrives at LWIP node through LTE network, it is forwarded to UE through LTE protocol stack without any changes. If the packet has to be sent through Wi-Fi interface, then the actual destination IP address of each incoming packet is changed from LTE UE IP address to Wi-Fi UE IP address by LWIP node. At UE, the destination IP address of packet received from Wi-Fi interface is changed back to LTE UE IP address.

Our LWIP testbed setup is shown in Fig. 7.4. The following issues and challenges are addressed for realizing a fully functional LWIP testbed system.

- **A socket connection should be established with LTE interface of LWIP-UE:** In Android Operating System (OS), when Wi-Fi radio is enabled, it gets the highest priority over all available radio interfaces for data communication. This priority issue has to be solved because the connection is LTE anchored in LWIP system. With a stringent motive of making the existing UE to work, an Android application is developed in-house which changes the priority for a set of flows to use LTE interface even when Wi-Fi interface is available for communication. During socket creation, the Android application binds new flow to LTE interface using socket bind function.

- **The Wi-Fi interface details of UE have to be informed to LTE SeNB:** The SeNB of LWIP node should be aware of the destination interface information for enabling traffic steering. In our LWIP testbed, the information of LWIP-UE's Wi-Fi IP address is made known to LWIP node. This information can be communicated using control channel of LTE.
- **Some packets from LTE core network have to be steered to Wi-Fi network:** This action mangles the packet headers to achieve successful routing between LTE and Wi-Fi networks. This also involves recomputing the header checksum of appropriate layers in order to avoid the packet drop at the destination. In our LWIP testbed, the actual packet destination IP address is changed by LWIP node in order to deliver the packet over the Wi-Fi link. When the destination IP gets changed, the higher layer checksum has to be recomputed for the mangled packet. For instance, to compute the transport layer checksum, the pseudo header and transport header information are required. Pseudo header includes (Destination IP, Source IP, TCP segment length, Protocol type, and Reserved bit). Thus change in the destination IP requires the checksum of TCP to be recomputed, without which the packet is dropped due to incorrect checksum.
- **An unmodified connection between LTE-SeNB and UE through Wi-Fi interface has to be maintained:** Packets received at the destination (UE) should get delivered to the socket to which it is bounded to. If a packet is not transformed, the packet gets lost. In our LWIP testbed, each packet upon reaching the LWIP-UE with Wi-Fi UE IP address is changed back to LTE UE IP address with the help of *iptables* rule, thereby managing the connection alive even through Wi-Fi interface. Thus, the state of a flow is unalterably maintained by inserting flow rule in *iptables* of LWIP-UE. Here is a sample *iptables* rule which is inserted. The rule is inserted at the prerouting chain of Network Address Translation (NAT) table. It changes the current destination IP address (Wi-Fi IP address of UE) of the packet to new destination IP address (LTE IP address of UE).

```
iptables -t nat -A PREROUTING -d current_ip -j DNAT
--to-destination new_ip
```

This *iptables* rule make the packet look as if it is unaltered to the destination socket. Hence, it enables the aggregation of LTE and Wi-Fi links.

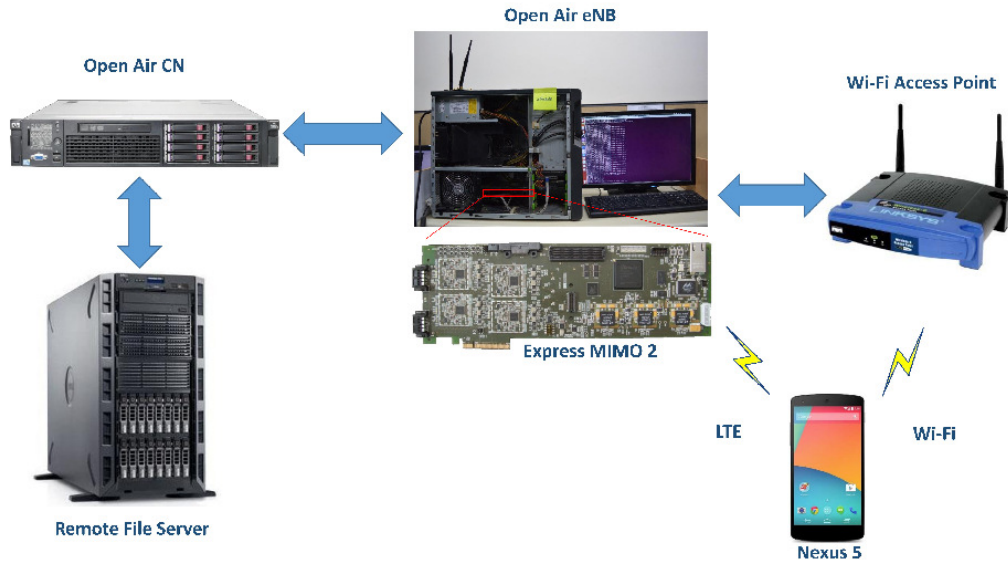


Figure 7.4: LWIP testbed setup.

LWIP testbed configurations are shown in Tables 7.1 and 7.2. In our testbed, the LWIP-UE (Google Nexus 5 phone), is downloading a file from the remote server using LWIP. Both interfaces are enabled through an Android application. We have enhanced the functionality of open-source Android application, HIPRIKeeper [98] which can enable both LTE and Wi-Fi interfaces of LWIP-UE at the same time to support LWIP operation. Incoming traffic is steered across LTE and Wi-Fi proportionally based on the physical layer data rates of the individual links, which was later enhanced to support dynamic traffic steering.

Table 7.1: Parameters to evaluate real-time performance of LWIP testbed

Parameter	Value
LTE SeNB Bandwidth	5 MHz
LTE operation band	Band 7
Number of Resource Blocks	25
Tx Power of Wi-Fi AP	20 dBm
Tx Power of LTE SeNB	15 dBm
LTE Scheduler	Round Robin
Traffic Steering	Proportional to link rates
Wi-Fi Frequency, Bandwidth	2.4 GHz, 20 MHz
Wi-Fi Standard	IEEE 802.11b and 802.11g

7.2.3 LWIP testbed: UDP results

The performance of LWIP system is studied using following experiments:

1. iPerf [99] UDP test over LTE network *i.e.*, LTE-NoLAS
2. iPerf UDP test over Wi-Fi network *i.e.*, Wi-Fi-NoLAS
3. iPerf UDP test over LWIP system

Table 7.2: Hardware parameters of LWIP testbed

Parameter	Value
OAI LTE eNB Hardware Configuration	ExMIMO2, Intel Xeon 8 core, 12GB DDR, Gigabit Ethernet 1 Gb/s
OAI LTE eNB Software Configuration	Ubuntu 14.04, Low Latency Kernel 3.19
OAI EPC Hardware Configuration	Intel Xeon Server 24 core, 64GB DDR, Gigabit Ethernet 10 Gb/s
OAI EPC host OS Configuration	Ubuntu 14.04, Kernel 3.19 generic
Remote Server Hardware Configuration	Intel Xeon 8 core, 32GB DDR, Gigabit Ethernet 1 Gb/s
Remote Server OS Configuration	Ubuntu 14.04, Kernel 3.2 Apache 2 Web server, TCP - High Speed
User Equipment (LWIP-UE)	Nexus 5 - hammerhead, Android 4.4.4 (KitKat)
Wi-Fi Access Point	Cisco AP (WRT54GH)

UDP iPerf test is conducted from a remote server in the LAN to the LWIP-UE. In this experiment, LWIP setup is created using IEEE 802.11b and 802.11g in different tests. The experiment also includes evaluating the UDP performance over legacy LTE without any link aggregation (LTE-NoLAS), legacy Wi-Fi (Wi-Fi - NoLAS), and LWIP with link aggregation (proportional steering based on link rates). Here are a set of commands which give an idea of testcase taken.

```
# For LTE test
iperf -u -c server_ip -t 100 -b 100M -B LTE_IP_address -i 1
#For Wi-Fi test
iperf -u -c server_ip -t 100 -b 100M -B Wi-Fi_IP_address -i 1
#For LWIP test
#Enable both radios and LWIP operation
iperf -u -c server_ip -t 100 -b 100M -B LTE_IP_address -i 1
```

In the above commands, “ $-t 100$ ” specifies that the experiment duration is 100 seconds. “ $-B LTE_IP_address$ ” allows binding the iperf operation to the specified *LTE_IP_address*. “ $-b 100M$ ” specifies that amount of data pumped through a link is 100 MB.

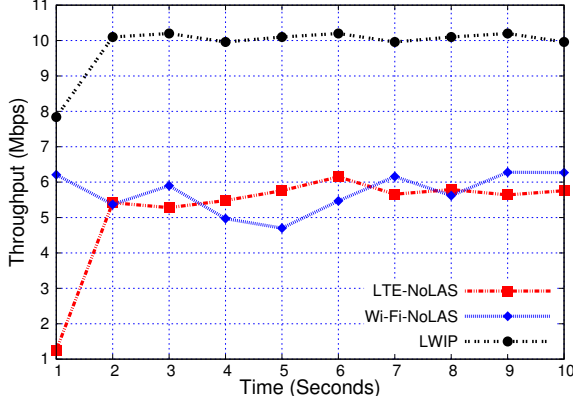


Figure 7.5: Instantaneous throughput in iPerf UDP test (in downlink \rightarrow 802.11b).

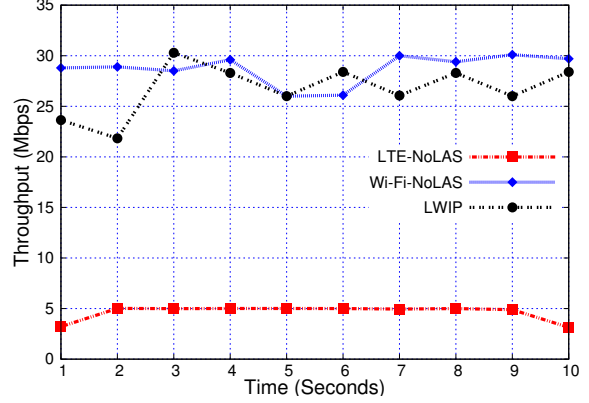


Figure 7.6: Instantaneous throughput in iPerf UDP test (in downlink \rightarrow 802.11g).

In case of LWIP system, the LWIP node steers a set of incoming UDP packets (LAS-packet split) through LTE and Wi-Fi based on the ratio of their link rates. Figs. 7.5 and 7.6 show instantaneous throughputs observed during the iPerf test in case of LTE-NoLAS, Wi-Fi-NoLAS, and LWIP configurations. In Fig. 7.5, when Wi-Fi AP is configured to operate on IEEE 802.11b, the LWIP performance is nearly equal to the sum of combined throughputs of LTE and Wi-Fi links, since the MAC throughputs of LTE and IEEE 802.11b are comparable. Whereas, in case of IEEE 802.11g configuration at Wi-Fi AP, LWIP achieves throughput that is close to the throughput of Wi-Fi-NoLAS. This phenomenon is because the downlink traffic is split across LTE and Wi-Fi links at LWIP node in a fixed ratio (1:5) corresponding to LTE and Wi-Fi physical link rates. However, the available link capacities vary dynamically due to variations on the channel. Hence, the throughput observed in LWIP is not equal to the sum of throughputs observed in LTE-NoLAS and Wi-Fi-NoLAS configurations. This puts forth the need for an efficient traffic steering mechanism to yield better benefits. Fig. 7.7 shows CDF of observed jitter during the experiment with Wi-Fi configuration as 802.11g. LWIP jitter is higher than that of Wi-Fi-NoLAS, but it is lesser than that of LTE-NoLAS. In summary, integration at radio level improves the throughput when link rates are comparable and demands efficient steering when link rates

are heterogeneous.

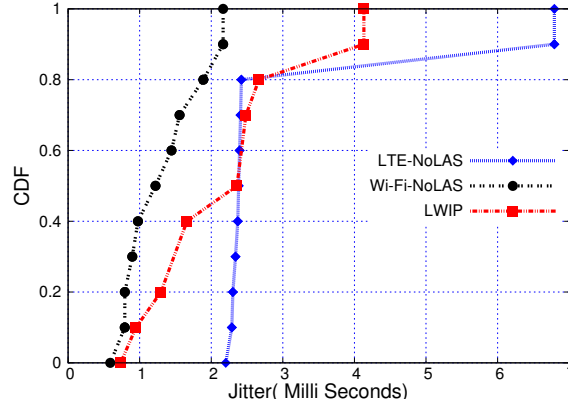


Figure 7.7: CDF of jitter for iPerf test (in downlink → 802.11g).

7.2.4 LWIP testbed: TCP results

To observe the performance of TCP under different Link Aggregation Strategies (LASs), a set of experiments have been conducted. To better investigate the LASs, scenarios are created for different loads *viz.*, low and high load. Wi-Fi AP uses IEEE 802.11g standard for following experiments. An Android application is developed in-house which downloads two files simultaneously from a remote server and measures their throughputs. Apart from LTE-NoLAS and Wi-Fi-NoLAS, the UE performance is evaluated using the following LASs:

- **PS-N-LAS:** Packet split enables set of packets of incoming traffic to be sent through LTE and other packets through Wi-Fi.
- **FS-N-LAS:** Flow split enables one flow to be downloaded through LTE and other through Wi-Fi.
- **WoD-LAS:** Wi-Fi-only-in-Downlink enables both the flows to use Wi-Fi for downlink, and the corresponding TCP ACKs are sent through LTE in the uplink.

We have not included the performance evaluation of PS-N-LAS in this section. This is because PS-N-LAS exhibits poor performance in LWIP due to "speed of the slowest link" problem as discussed earlier in Chapter 2.

TCP Experiment 1 - Lightly Loaded Scenario: The setup consists of a UE and an LWIP node with background transmissions on Wi-Fi channel (observed channel load is 8%). Now, UE downloads two files from the remote server using different LASs. Files of different

sizes are downloaded *viz.*, 16 and 32 MB. Fig. 7.8 shows the throughput observed in case of different file downloads. It can be observed that FS-LAS has achieved higher throughput since it effectively aggregates LTE and Wi-Fi links. Fig. 7.9 shows that all the LASs employed utilize Wi-Fi link at its maximum link rate and therefore achieve throughput of 25 Mbps (approx.) for IEEE 802.11g mode of operation. Time to download a file using different LASs is shown in Fig. 7.10. Even though the throughput of FS-LAS and WoD-LAS are comparable, the time to download a file through FS-LAS incurs longer time than WoD-LAS because file download through LTE interface incurs longer download time.

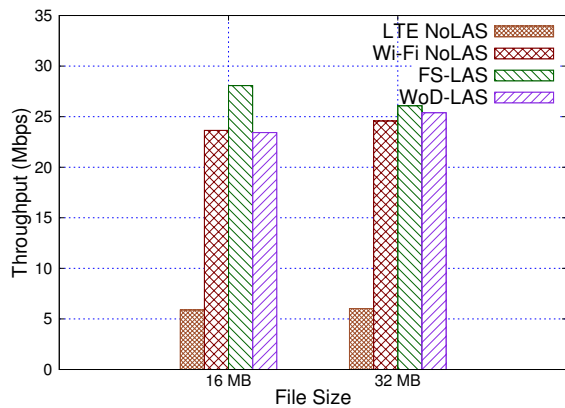


Figure 7.8: Overall throughput observed for 16 MB and 32 MB file sizes in low contention scenario.

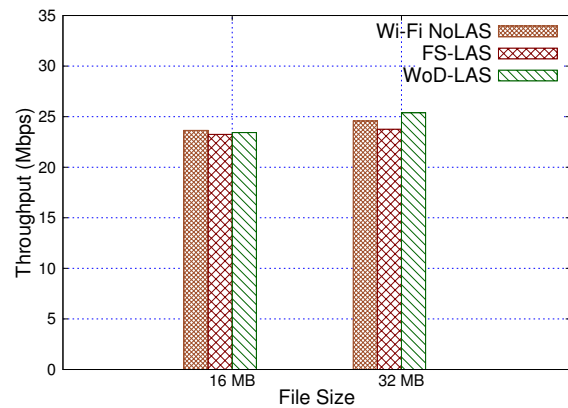


Figure 7.9: Throughput of Wi-Fi observed for 16 MB and 32 MB file sizes in low contention scenario.

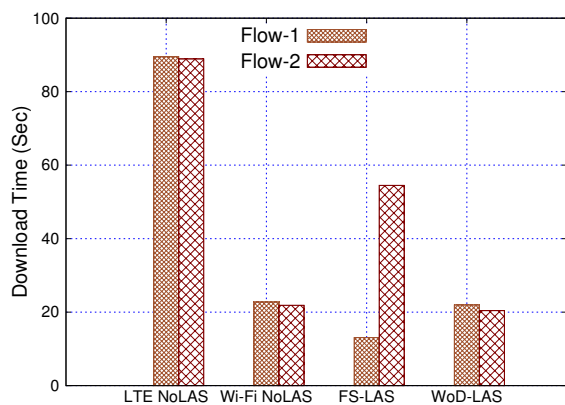


Figure 7.10: Time to download a 32 MB file using different LASs in low contention scenario.

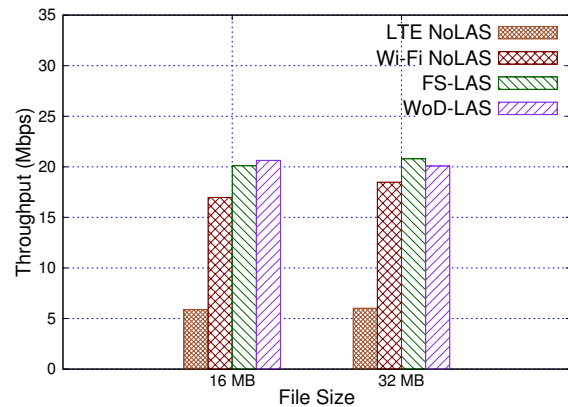


Figure 7.11: Overall throughput observed for 16 MB and 32 MB file sizes using different LASs in high contention scenario.

TCP Experiment 2 - Heavily Loaded Scenario: In this setup, for creating a heavily loaded condition, five laptops are used while each of them streaming video traffic at a bit rate of 900 Kbps using UDP to a background Wi-Fi AP operating on the same Wi-Fi channel of Wi-Fi AP of LWIP node. The streaming introduces load in addition to existing 8% background Wi-Fi channel load. Now, the LWIP system performance is analyzed using different LASs. Fig. 7.11 shows that with high load, throughput of FS-LAS and WoD-LAS has reduced by 28% compared to scenario with lower load. The contentions on the channel has brought down the throughput of UE. Fig. 7.12 shows that the performance of WoD-LAS has improved compared to FS-LAS. In case of FS-LAS, the TCP ACK packets which are generated for the flow through Wi-Fi have to be sent through Wi-Fi link only. Since Wi-Fi contentions are high, it brings down the throughput of that flow. This problem is solved when WoD-LAS is employed, as the uplink of LTE does not have contention unlike uplink of Wi-Fi; hence it achieves a higher throughput. Fig. 7.13 shows the time to download two files using different LASs, which are 30% high as compared to low loaded scenario.

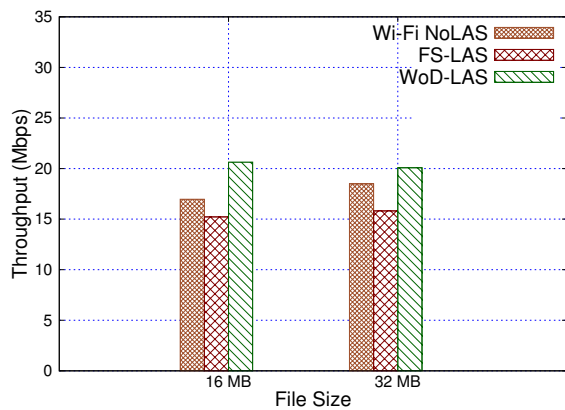


Figure 7.12: Throughput of Wi-Fi observed for 16 MB and 32 MB file sizes with high contention.

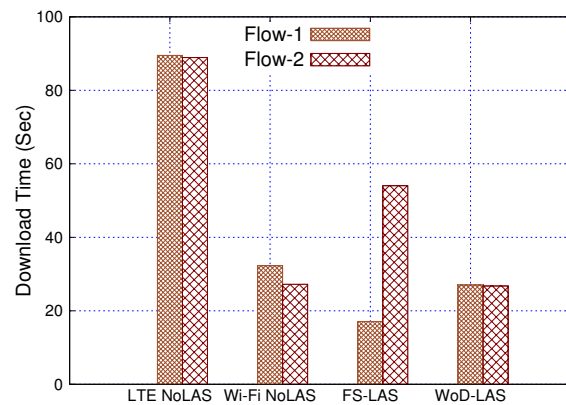


Figure 7.13: Time to download a 32 MB file with high contention for different LASs.

7.3 LWA prototyping

This section describes the design and implementation details, and evaluation of LWA prototype using OAI.

7.3.1 Traffic steering in LWA testbed

A dynamic packet steering solution is introduced in this section. It minimizes the number of packets delivered out-of-order by aggregating the two link rates effectively. It is different from the solutions discussed in the previous chapters. Chapter 3 detailed the traffic steering solution combined with an approach for power control. Whereas the dynamic steering solution discussed below does not involve power control solution instead it considers the link statistics such as link delay, instantaneous packet loss on a link, *etc.* to take steering decisions.

Dynamic packet steering solution that runs at LAL takes inputs such as link round trip time (LRTT) of LTE and Wi-Fi link, and the packet loss rates of LTE and Wi-Fi links. LRTT of each link is obtained by sending probe packets on corresponding links. Probing packets which are originated at PDCP layer of LWA node (ICMP packets are used) are sent over LTE and Wi-Fi links. The LWA UE on receiving the probe packets sends the probe responses back to LWA node. The size of probe packets are in order of few bytes (approx. 30 bytes), which are generated at an interval of 3 *ms* to get the link information more accurately. A smoothed LRTT (SLRTT) estimator is used to calculate the steering ratio. SLRTT of a link l is given by,

$$SLRTT_l = (1 - \alpha) \times LRTT_l + \alpha \times SLRTT_l ; l \in \{Wi - Fi, LTE\} \quad (7.1)$$

where α is the smoothing factor. The value of α is determined by probe packet interval P_i , where $\alpha = 1/P_i$. The probe response for the probe packet received through Wi-Fi interface of LWA-UE is rerouted through LTE interface in uplink to reduce contentions on Wi-Fi channel.

The steering window can be of fixed size or variable. Steering window size is the sum of packets sent through LTE and Wi-Fi links in one cycle. For instance, if $x : y$ is the steering ratio across LTE and Wi-Fi, $x + y$ corresponds to steering window size and time elapsed to send $x + y$ packets is referred to as a cycle. A fixed steering window does not change the sum of x and y , whereas the steering window with variable size allows variations in it. This work employs variable steering window at LWA node as adapts quite well to channel variations on both links.

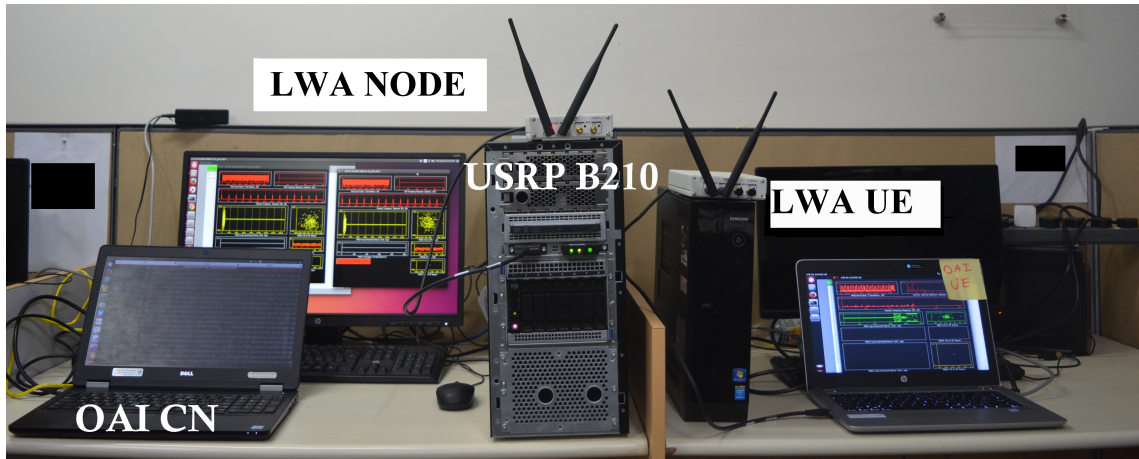


Figure 7.14: LWA testbed setup.

7.3.2 Realization of LWA testbed using OAI platform

This section describes the testbed setup for LWA. Fig. 7.14 shows LWA prototype and its components. LWA testbed setup consists of LWA-eNB, LWA-UE, and EPC. The testbed can be set up without using S1-interface *i.e.*, the testbed can also be set up without EPC. LWA-eNB and LWA-UE are Linux machines which run Ubuntu 14.04 with low-latency kernel. The implementations of LWA-eNB and LWA-UE are built on top of OpenAirInterface (OAI) platform [3], which offers Software Defined Radio (SDR) based software implementation of LTE written in C. Ettus USRP B210 boards were used as RF transceivers. In LWA setup, the LTE-eNB is connected to off-the-shelf 802.11g Wi-Fi AP through Ethernet cable. 802.11g is preferred in these experiments in order to have comparable link rates across LTE and Wi-Fi. The LWA-UE is associated with the same Wi-Fi AP. The LTE is configured to operate on band 7, where the downlink and uplink frequencies are 2.68 GHz and 2.56 GHz, respectively. LTE operates with 5 MHz bandwidth which corresponds to 25 Physical Resource Blocks (PRB). PDCP reordering time at the LWA-UE is set to $2 \times \text{Max}(\text{LRTT of Wi-Fi, LRTT of LTE})$.

7.4 Performance comparison of LWA and LWIP prototypes

This section compares the performance of LWA and LWIP prototypes developed. LWA and LWIP employ dynamic traffic steering algorithms which involve continuous monitoring of the link qualities using feedback mechanism explained in Section 7.3.1. Files of large and medium sizes are downloaded from a file server using different architectures. Fig. 7.15

shows the variation in download time when packet level steering was employed to perform file download operation in LWA and LWIP architectures. LWA effectively aggregates the link capacities of LTE and Wi-Fi links compared to LWIP, because LWIP suffers from out-of-order packet delivery problem at the receiver due to varying link rates of different interfaces. Downloading a file using LWIP many a times leads to failure. Though LWA is better than LWIP but is inefficient in aggregating link capacities in certain use cases such as mobility [84]. The results obtained in our experiment are in line with our NS-3 simulation results discussed in Section 5.5.3. Even with an efficient traffic steering algorithm LWIP fails to aggregate link capacities. In the forthcoming sections, we therefore make use of LWA prototype for experimentation.

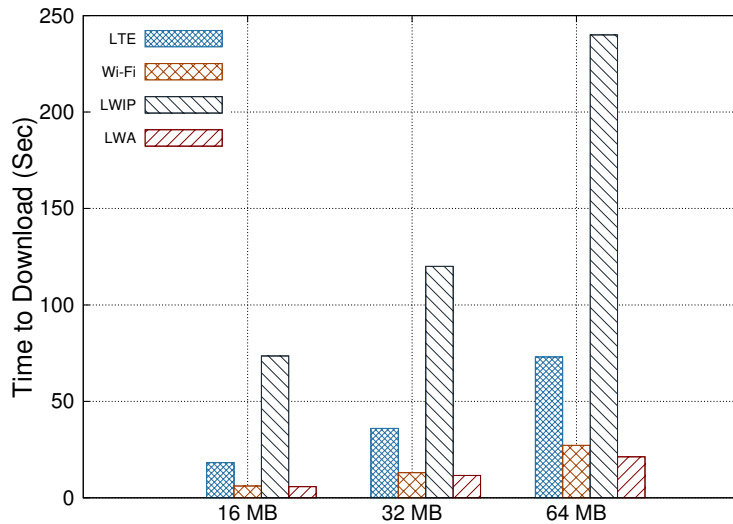


Figure 7.15: Download time observed with different RLI prototypes.

7.5 Coupling LWA architecture with MPTCP

This section describes the integrated MPTCP and LWA solution in order to efficiently aggregate LTE and Wi-Fi links under challenging link and network conditions.

7.5.1 Multipath TCP

Multipath TCP is a transport layer solution which enables simultaneous use of multiple interfaces *e.g.*, Wi-Fi and LTE. MPTCP uses multiple paths to deliver the segments corresponding to one end-to-end connection. MPTCP implements congestion control algorithms

which are developed obeying the following principles: (a) MPTCP should not get more throughput than single path TCP in case of shared bottleneck, (b) The performance of all MPTCP subflows together should be at least that of regular TCP on any of the paths used by an MPTCP connection, and (c) MPTCP should prefer efficient paths to deliver the larger fraction of the traffic. The packets sent through different paths are reordered at the receiver.

In spite of its significant benefits, MPTCP miserably fails in many cases. MPTCP offers higher throughput and robustness compared to single path TCP, but when the path characteristics such as RTT and loss rates become diverse, then the performance is affected significantly. This makes MPTCP inefficient in reacting to the path diversities [100]. Also, MPTCP congestion control algorithms are very conservative in the growth of their congestion window obeying to the first design principle [101], even when no bottleneck link exists. MPTCP suffers from larger reordering buffer at the receiver. These challenges prevent MPTCP from acting as a standalone solution for aggregating multiple links.

7.5.2 MPTCP over LWA

Fig. 7.16 shows the integration architecture of MPTCP over LWA (MLWA). In this setup, both LTE network and Wi-Fi are connected to public Internet. Initially, MPTCP establishes two subflows across LTE and Wi-Fi links on observing the presence of multiple interfaces, revealed by the option *MP – CAPABLE*. A subflow through LTE interface is subjected to LWA operation, whereas the subflow through Wi-Fi remains undisturbed.

In this work, LWA employs Wi-Fi link to be used only in the downlink to minimize contentions on Wi-Fi channel. LTE link is used in both uplink and downlink *i.e.*, for the downlink TCP data packets of LWA and all TCP ACKs on LTE uplink.

7.6 Performance results of MPTCP over LWA

This section describes the setup considered for experimenting with different aggregation architectures *viz.*, LWA, MPTCP, and MLWA. Fig. 7.17(a) shows MPTCP setup, Fig. 7.17(b) shows LWA setup, and Fig. 7.17(c) shows MLWA setup and its components. A file server is setup by launching Apache web service on a Linux machine to evaluate the performance. To emulate an Internet like scenario, backhaul delay of 80 ms [102] has been introduced

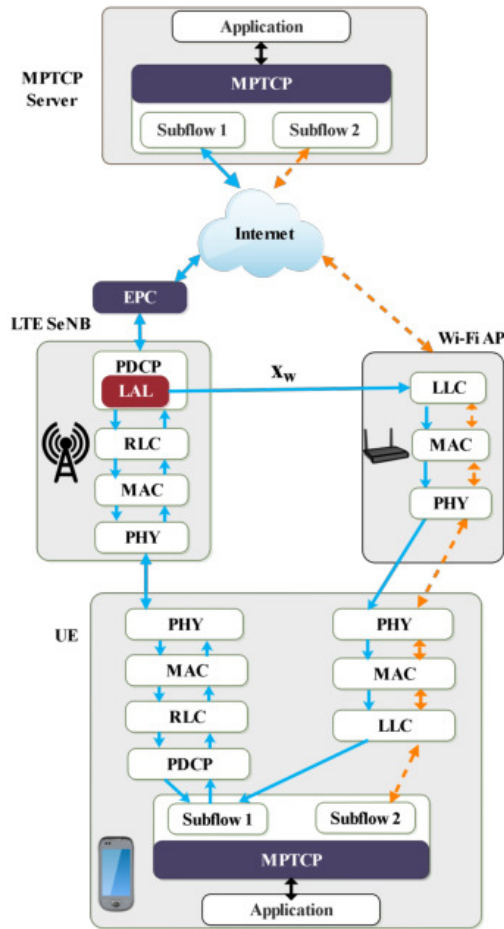


Figure 7.16: Architecture of MPTCP over LWA (MLWA).

at the Ethernet interface of the file server with the help of *netem* network emulator [103]. The performance of aggregation architectures is evaluated by conducting file download operations of various file sizes *viz.*, 16, 32, and 64 MB. Table 7.1 captures various parameters used in these experiments. The aggregation architectures are evaluated under the following three challenging scenarios:

1. Network congestion in the backhaul.
2. Contention on the Wi-Fi channel.
3. Mixed: network congestion in the backhaul and contention on Wi-Fi channel.

The experiments are conducted by varying packet loss rates (which mimics network congestion), file sizes, and channel contentions under different scenarios. Each experiment

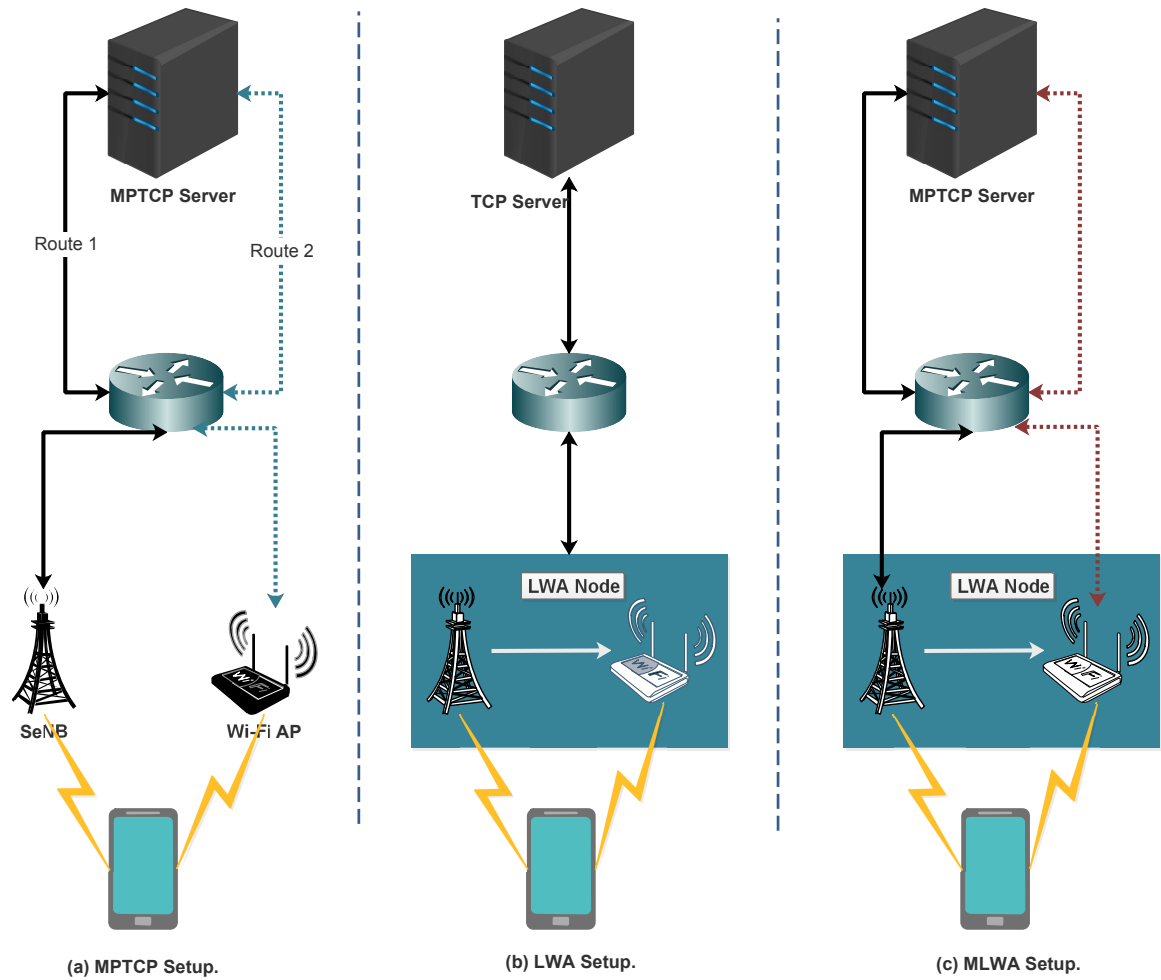


Figure 7.17: Experimental setup for evaluation of MPTCP, LWA and MLWA.

is repeated for multiple trials. In total, 972 experiments have been conducted to make concrete conclusions.

7.6.1 Network congestion scenario

Network congestion is emulated by introducing packet loss at the Ethernet interface of the file server using *netem* tool. Experiments are conducted by varying the packet loss rates *viz.*, no loss, 0.01%, 0.1%, and 1% ($0, 10^{-4}, 10^{-3}, 10^{-2}$), to observe the reaction of different aggregation architectures to network congestion.

Throughput vs. Packet loss rate results:

Figs. 7.18-7.20 show variations in observed throughputs by varying packet loss rates for different file sizes for LWA, MPTCP and MLWA systems. As the network congestion

increases, MPTCP efficiently handles the network level packet losses compared to LWA and MLWA. Hence, it achieved the highest throughput. LWA could not achieve comparable throughput because there exists only one congestion window (single TCP) for the end-to-end connection, whereas MPTCP manages a separate congestion window for each subflow. On observing packet losses, the congestion window is reduced significantly in the case of LWA. MLWA cannot perform as good as MPTCP because the fraction of packets which are lost over the Wi-Fi subflow gets retransmitted faster, whereas the packets sent over LWA subflow of MLWA take longer time to get retransmitted. The longer RTT over LWA is because of reordering delay at the LWA receiver. In summary, when congestion in the network is low, the aggregation architectures exhibit different phenomenon, however as the congestion in the network increases, they achieve similar performance.

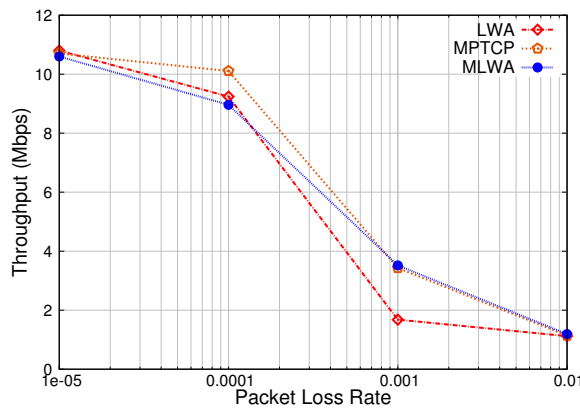


Figure 7.18: Throughput observed while downloading a file of 16 MB by varying congestion losses in the network.

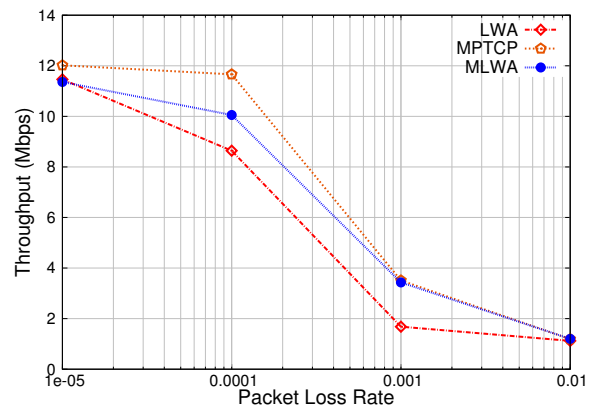


Figure 7.19: Throughput observed while downloading a file of 32 MB by varying congestion losses in the network.

Congestion window results:

Figs. 7.21-7.23 show variations in congestion window growth for LWA, MPTCP, and MLWA systems for downloading a 64 MB file with packet loss rate of 10^{-4} . On observing packet losses, the growth of LWA congestion window is hindered significantly. Following are some of the interesting observations from the plots: (1) Congestion window for LWA grows faster due to dynamic traffic steering solution employed, whereas MPTCP grows conservatively, (2) LWA can deliver its maximum benefits for the small file downloads (*e.g.*, web browsing and real-time services), and (3) The ratio of the total number of packets sent through LTE

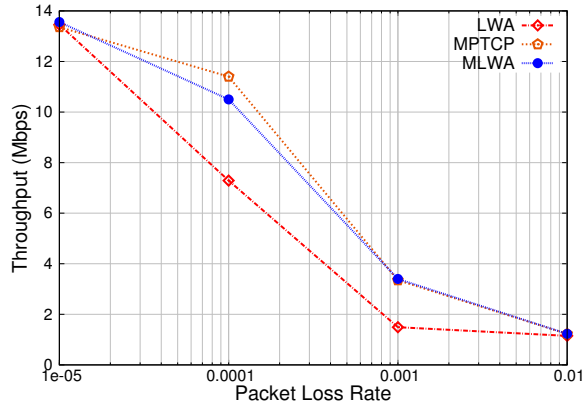


Figure 7.20: Throughput observed while downloading a file of 64 MB by varying congestion losses in the network.

and Wi-Fi is in the order of 1 : 4 and 1 : 27 in case of LWA and MPTCP, respectively. Though MPTCP achieves higher throughput it is inefficient in aggregating multiple links, MLWA reaches the throughput of MPTCP when loss rates are low, but falls behind MPTCP when the packet losses are high.

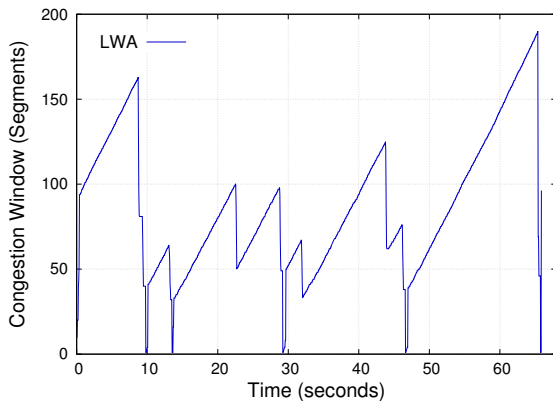


Figure 7.21: Congestion window observed for LWA operation while downloading a file of 64 MB with 10^{-4} loss rate.

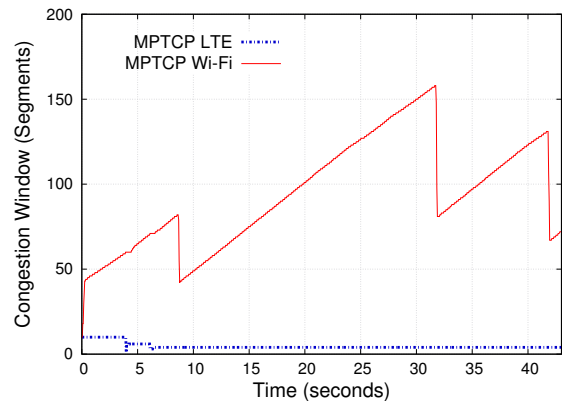


Figure 7.22: Congestion window observed for MPTCP operation while downloading a file of 64 MB with 10^{-4} loss rate.

7.6.2 Channel contention scenario

A controlled contention environment has been setup to evaluate the performance of LWA, MPTCP, and MLWA systems with different levels of contention. The contention on the

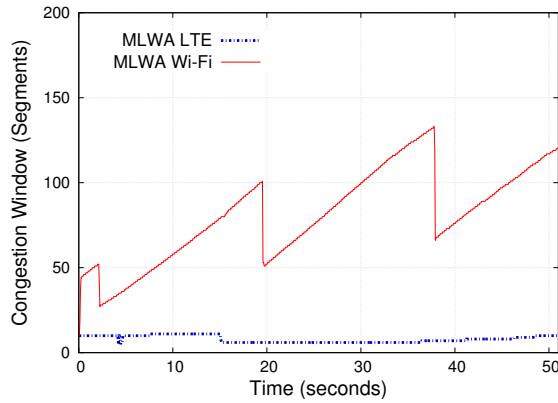


Figure 7.23: Congestion window observed for MLWA operation while downloading a file of 64 MB with 10^{-4} loss rate.

Wi-Fi network is introduced by connecting 2 to 4 laptops to the same Wi-Fi AP. Each of those laptops is continuously sending UDP packets at 1.5 Mbps in uplink using iPerf tool. The contention on the network introduced by two laptops and four laptops are termed as low and moderate contention scenarios, respectively.

Download time vs. channel contention:

Time to download files of sizes 16, 32, and 64 MB under low and moderate contentions scenarios are shown in Fig. 7.24 and Fig. 7.25, respectively. MPTCP performs well when the contention on the network is low, but it performs poorly compared to LWA when there is moderate contention on the network. This is because the uplink TCP ACK packets in MPTCP which are sent through Wi-Fi interface suffer contention, while they do not suffer any contention in case of LWA. Since LWA employs both LTE and Wi-Fi links to send TCP data packets in downlink, but in uplink it uses only LTE link and hence it does not suffer from any contention. Hence, LWA achieves higher throughput. MLWA achieves the best performance in low contention scenario and comparable performance with that of LWA in moderate contention scenario.

Channel busy time:

Channel busy times in low and moderate contention scenarios are captured in Fig. 7.26 and Fig. 7.27, respectively. The reason for the poor performance of MPTCP is due to contentions which can be observed in Fig. 7.26. LWA reduces channel contentions in the

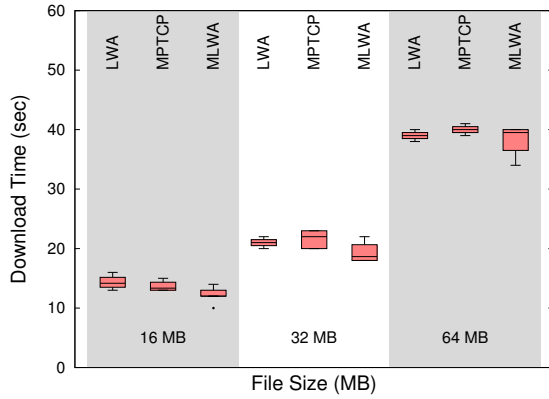


Figure 7.24: Download time in case of LWA, MPTCP, and MLWA by varying file sizes under low Wi-Fi channel contention scenario.

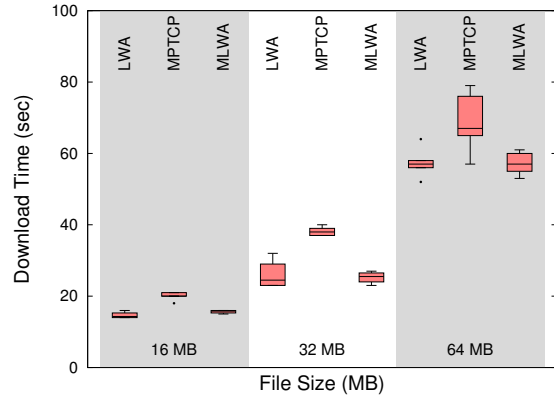


Figure 7.25: Download time in case of LWA, MPTCP, and MLWA by varying file sizes under moderate Wi-Fi channel contention scenario.

network by allowing the LWA-UE to send uplink packets through LTE and thereby it facilitates improved transmission opportunities to other Wi-Fi stations in the network. MLWA achieves high throughputs in both moderate and low contention scenarios because it employs the merit of MPTCP in low contention scenario (which employs different congestion regulation mechanism per subflow), and it employs LWA feature (no uplink contention) in case of moderate or high contention scenario.

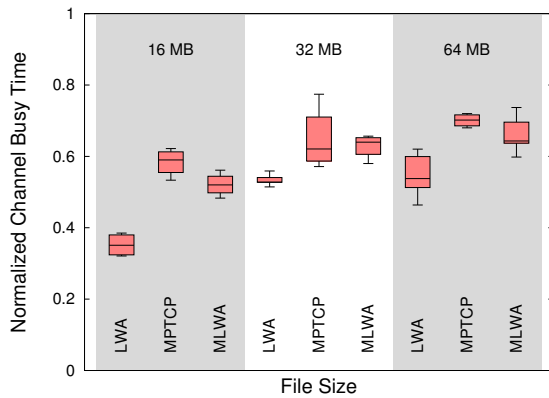


Figure 7.26: Channel busy time observed in Wi-Fi channel when a 32 MB file was downloaded under low Wi-Fi channel contention scenario.

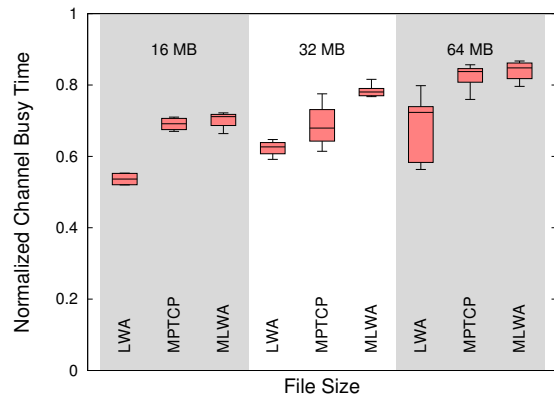


Figure 7.27: Channel busy time observed in Wi-Fi channel when a 32 MB file was downloaded under moderate Wi-Fi channel contention scenario.

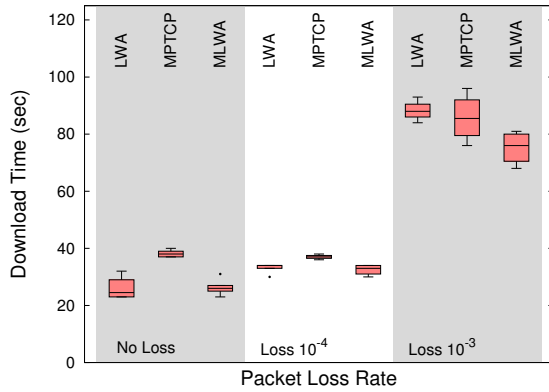


Figure 7.28: Download time for a 32 MB file with network congestion and moderate channel contention scenario.

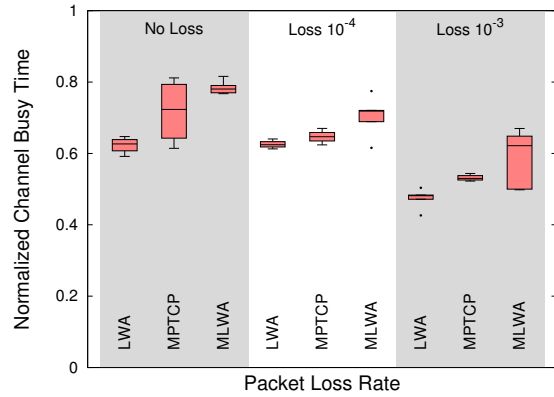


Figure 7.29: Download time for a 32 MB file with network congestion and moderate channel contention scenario.

7.6.3 Mixed: Network congestion and channel contention scenario

The more challenging scenario is considered to evaluate the full potential of LWA, MPTCP, and MLWA architectures. The experiment is conducted with moderate channel contention for a file download of size 32 MB with different packet loss rates of 0, 10^{-4} , and 10^{-3} . The motive behind this experiment is to check the robustness and agility of LWA, MPTCP, and MLWA to aggregate multiple links in case of different congestion losses and tolerate channel contention. From Fig. 7.28, it can be observed that LWA outperforms MPTCP in moderate contention scenario when the network congestion is low. As packet loss increases LWA performance degrades, and it performs poorly compared to MPTCP even though it does not suffer from channel contention. MLWA performs equivalently to LWA when there is no loss with moderate contention, and it outperforms MPTCP and LWA when the packet loss rate is high due to moderate contention. This is because, in contention scenario, LTE subflow of MLWA which is split over LTE and Wi-Fi link does not create contention for Wi-Fi subflow of MLWA which sends all the TCP ACKs over Wi-Fi. Thereby a cooperative operation between LTE subflow and Wi-Fi subflow of MLWA has improved the performance, which is captured in Fig. 7.29. When the congestion loss rate is increased to 10^{-3} , LWA and MPTCP exhibit similar performance in terms of file download time, but LWA still preserves the lowest channel contention as shown in Fig. 7.29.

Figs. 7.30, 7.31, and 7.32 show the congestion window growth of LWA, MPTCP, and MLWA systems when the packet loss rate is high and channel contentions are moderate. "MPTCP LTE" and "MPTCP Wi-Fi" in Fig. 7.31 correspond to congestion window sizes of

MPTCP subflows through LTE and Wi-Fi networks, respectively. It can be observed that a significant amount of traffic is sent through MLWA LTE subflow as compared to MPTCP LTE subflow. This is the key enabler for the improved performance of MLWA architecture.

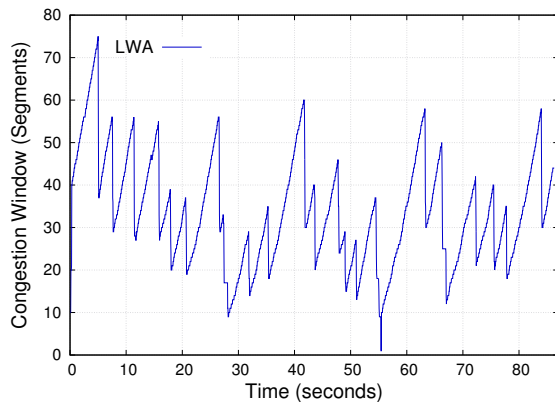


Figure 7.30: Congestion window for LWA operation while a 32 MB file downloaded with 10^{-3} loss rate under moderate channel contention.

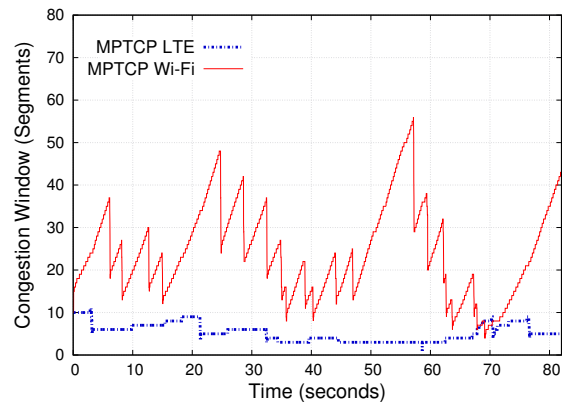


Figure 7.31: Congestion window for MPTCP operation while a 32 MB file is downloaded with 10^{-3} loss rate under moderate channel contention.

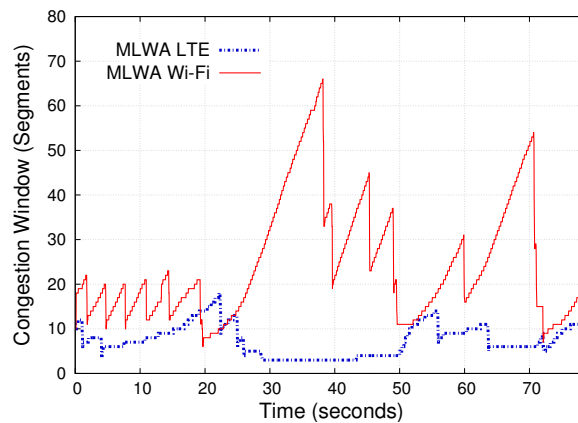


Figure 7.32: Congestion window for MLWA operation while a 32 MB file is downloaded with 10^{-3} loss rate under moderate channel contention.

7.7 Summary

Prototypes for different RLI architectures are detailed in this chapter. Also, the implementation details for LWIP and LWA architectures were provided. In case of LWIP, it does not require any modifications to the protocol stack of the UE and SeNB. The developed LWIP

prototype was evaluated using different link aggregation strategies. The experiment results conclude that WoD-LAS has improved sum of flow throughputs by 28% as compared to FS-LAS when the contention on Wi-Fi channel is high. Thus, enabling WoD-LAS will be the most preferred link aggregation solution.

In case of LWA, the changes to the radio protocol stack are done both at the LWA node and LWA-UE. Also, the integrated performance of LWA with MPTCP is studied under challenging environments. From the conducted experiments, the following inferences were drawn, (i) In case of network congestion, MPTCP is an ideal solution which can adequately handle the network level losses, (ii) LWA fails to aggregate link capacities when there is a congestion in the network, (iii) LWA is well suitable when the download files are of smaller size (less than 1 MB like Web traffic), (iv) When the channel contentions are moderate or high, LWA not only improves the performance of its users, but also improves overall performance of all users on the Wi-Fi channel, and (v) MLWA is robust and exhibits significant performance when the congestion losses are high and channel contentions are high. The experiments revealed that the transport layer solution and radio level interworking solutions are complementing each other and co-operation between these two solutions in any scenario is better than at least one of their performances.

Chapter 8

Conclusions and Future work

8.1 Conclusions

Radio Level Integration architectures are developed to address the challenges which prevailed in traditional LTE Wi-Fi interworking architectures. In this thesis, various radio level integration architectures were studied, and the fundamental challenges which prevent them from achieving integrated benefits are addressed. The main contributions of this thesis are:

1. Proposed radio level integration architectures with an objective to enhance the level of interworking (in terms of steering the traffic, balancing the load, and regulating the transmit power) between LTE and Wi-Fi networks.
2. Proposed a solution to address co-tier interference across LTE small cells in dense deployment scenarios of RLI systems.
3. Proposed a dynamic traffic steering solution which efficiently handles the time-varying channel conditions on LTE and Wi-Fi links.
4. The problem of out-of-order packet delivery which arises for packet level steering in LWIP architecture was addressed by proposing an efficient algorithm.
5. Efficient placement of the devices and effective radio resource management are studied for indoor deployments of RLI systems.
6. Designed and developed prototypes of radio level integration architectures using open source tools. The developed prototypes were profiled. The problems of link level

contention and network level congestion were studied, and solutions were developed and evaluated using these prototypes.

In Chapter 2 of the thesis, novel link aggregation strategies were proposed to address various challenges in realizing full benefits of RLI architectures. Primarily, traffic steering solutions were proposed in Chapters 3 and 4 to enable efficient uplink and downlink steering, respectively. In Chapter 3, a downlink traffic steering solution was proposed targeting to reduce the co-tier interference across the deployed LWIP nodes and to maximize QoS of the network. The proposed downlink traffic steering algorithm, PRECISE has outperformed the state-of-the-art α -optimal scheduler by 48% and 3GPP Rel-12 LTE Wi-Fi interworking by 84% on system throughput. We have observed from our experiments that, Wi-Fi when employed to carry only downlink traffic uses the Wi-Fi channel more efficiently. Hence, any downlink traffic steering solution employing Wi-Fi-only-in-downlink achieved significant improvement in system throughput and reduced number of collisions on Wi-Fi channel.

Restricting Wi-Fi to operate only-in-downlink by preventing any sort of uplink through Wi-Fi does not utilize the radio resources efficiently. Also the high demand for LTE uplink radio resources introduces longer waiting time. Hence, to overcome the problem of channel contention on Wi-Fi and to utilize the uplink radio resources more effectively, uplink traffic steering solution, Network Coordination Function (NCF) was proposed in Chapter 4 of this thesis. The proposed steering solution NCF works by coordinating Wi-Fi uplink transmissions using LTE as the anchor. The proposed solution operates fairly and improves the throughput of LWIP node by 21% as compared to LWIP system operating with default DCF mechanism.

Chapter 5 addressed another important challenge, the out-of-order packet delivery at the receiver due to packet level steering employed at LWIP node. The packets of a flow are steered across LTE and Wi-Fi links by downlink traffic steering mechanism employed; due to difference in the link rates of LTE and Wi-Fi the packets might arrive out-of-order at the receiver. Such out-of-order reception negatively affects the growth of TCP congestion window. In order to address this challenge, VISIBLE algorithm was proposed which minimizes the out-of-order packet delivery by employing a virtual boosting and virtual reordering mechanism. The proposed solution (VISIBLE) has out performed LWA and MPTCP by 30% and 37%, respectively in terms of system throughput.

In Chapter 6, the placement problem of RLI nodes was investigated with the objectives of minimizing the number of LWIP nodes to be placed, to maximize the SINR of all the sub-regions in a given building, and to reduce the energy consumed at LWIP node and LWIP-UE. It is observed that placing the RLI nodes optimally has significant performance improvement as compared to placing them with MIR placement.

Finally, in Chapter 7 of the thesis, prototypes of RLI architectures (LWA and LWIP) were built and their performance were compared with existing multi-RAT aggregation solutions. The traffic steering solution was primarily targeted to address the link layer problems. But, it is also equally important to co-operate with higher layer solutions in order improve the end-to-end network performance. Hence, co-operation between LWA and MPTCP is investigated. It was observed that the proposed co-operative solution out performed standalone LWA and MPTCP solutions when there existed network losses and high contentions on the Wi-Fi channel.

8.2 Future work

Radio level integration can be explored to address the problem of poor video delivery and optimizations can be done to enhance the quality of video delivery by understanding the semantics of video transmission and coupling appropriately with diverse properties of multiple radio access technologies.

The insights drawn from this thesis can be employed in designing and supporting 5G multi-connectivity in various contexts such as deployment, efficient steering, and efficient utilization of resources in the unlicensed band.

5G is being designed to cater to the requirements of different verticals. 5G New Radio (NR) is versatile and targets to provide numerous services which span from Mobile Broadband, Machine to Machine communication, massive Internet of Things, and Tactile Internet. The key enabling technologies of 5G include Cloud-Radio Access Network (C-RAN) and multi-RAT connectivity. As a notable point in 5G Multi-RAT design, to aggregate multiple links effectively where the link rates are diverse, the radio level interworking solution is mandatory.

The solutions proposed in this thesis to address the problems related to multi-RAT integration can be adopted to address similar problems in the context of Multi-connectivity

in 5G where LTE, Wi-Fi and 5G NR need to be integrated.

The developed solution can be used to address the problem with mmWave communication which suffers from very high fluctuations in the data rates. When mmWave transmitter and receiver are in line-of-sight (LOS) high data rate is observed. When the transmitter and receiver are not in line-of-sight (NLOS) then their data rates dwindle drastically. The existing reliable transport layer protocols are not designed to support these high fluctuations. The solution proposed in this thesis in the context of enhancement to transport layer protocols using LWIP can be reused by introducing more insights on the high fluctuation of data rates.

5G also targets to achieve bounded waiting time with very high reliability, Ultra Reliable Low-Latency Communication (URLLC) is the term coined for this requirement. Only a ubiquitous network with the high available resource can satisfy these low latency requirements. But in reality, none of the deployed networks are ubiquitous and resource-rich. A feasible solution to this target is to pool resources from multiple networks to achieve high reliability. Connected cars, autonomous driving, remote health care, industrial automation, and all mission-critical services seek URLLC. The solution proposed in this thesis can be extended to meet the targets of URLLC by optimizing proposed traffic steering algorithms.

The developed prototypes can be further extended to support cloud-based multi-RAT aggregation. Also, in case of radio aggregation cloud units, the developed prototypes can be modified to realize RAN split at different layers of LTE and Wi-Fi protocol stacks. The RAN split can be dynamically adjusted based on the objectives and capabilities of the radio aggregation unit.

List of Publications

Published Research Papers

1. **Thomas Valerrian Pasca S**, Sumanta Patro, Bheemarjuna Reddy Tamma, and Antony Franklin A, “Network Coordination Function for Uplink Traffic Steering in Tightly Coupled LTE Wi-Fi Networks,” Elsevier Computer Networks, vol. 127, pp. 296-316, November 2017.
2. **Thomas Valerrian Pasca S**, Nabhasmita Sen, Venkatarami Reddy, Bheemarjuna Reddy Tamma, and Antony Franklin A, “A Framework for Integrating MPTCP over LWA - A Testbed Evaluation,” in Proc. of Wireless Network Testbeds, Experimental evaluation & CHaracterization (WiNTECH) - ACM MobiCom Workshop, November 2018, New Delhi, India.
3. **Thomas Valerrian Pasca S**, Bheemarjuna Reddy Tamma, and Antony Franklin A, “VISIBLE: Virtual Congestion Control with Boost ACKs for Packet Level Steering in LWIP Networks,” in Proc. of IEEE GLOBECOM, December 2017, Singapore.
4. **Thomas Valerrian Pasca S**, Himank Gupta, Bheemarjuna Reddy Tamma, and Antony Franklin A, “PRECISE: Power Aware Dynamic Traffic Steering in Tightly Coupled LTE Wi-Fi Networks,” in Proc. of IEEE PIMRC, October 2017, Montreal, Canada.
5. **Thomas Valerrian Pasca S**, Sumanta Patro, Bheemarjuna Reddy Tamma, and Antony Franklin A, “A Real-Time Performance Evaluation of Tightly Coupled LTE Wi-Fi Radio Access Networks,” in Proc. of IEEE ANTS, December 2017, Bhubaneswar, India. (**Won Best Paper Award - 2nd position**)
6. **Thomas Valerrian Pasca S**, Adharsh Srivats Rangarajan, Bheemarjuna Reddy Tamma, and Antony Franklin A, “Optimal Placement of Colocated and Non-Colocated LWA Nodes in Dense Deployments,” in Proc. of IEEE ANTS, December 2017, Bhubaneswar, India.
7. **Thomas Valerrian Pasca S**, Amogh PC, Debashisha Mishra, Nagamani Dheeravath, Anil kumar Rangiseti, Bheemarjuna Reddy Tamma, and Antony Franklin A,

“Architectural Challenges and Solutions for Collocated LWIP - A Network Layer Perspective,” in Proc. of NCC, March 2017, Chennai, India.

Research Demos

1. **Thomas Valerrian Pasca S**, Himank Gupta, Sumanta Patro, Bheemarjuna Reddy Tamma, and Antony Franklin A, “LTE-Wi-Fi Radio Level Integration at RLC Layer: A Demo of LWIR,” in Proc. of COMSNETS, January 2018, Bangalore, India. (**Won Best Academic Demo Award**)
2. **Thomas Valerrian Pasca S**, Sumanta Patro, Bheemarjuna Reddy Tamma, and Antony Franklin A, “Tightly Coupled LTE Wi-Fi Radio Access Networks: A Demo of LWIP,” in Proc. of COMSNETS, January 2017, Bangalore, India.

Patents

1. **Thomas Valerrian Pasca S**, Bheemarjuna Reddy Tamma, and Antony Franklin A, “Traffic steering in aggregated LTE-Wi-Fi Networks,” Indian Patent, Application No: 4705/CHE/2015, Patent Pending.
2. Antony Franklin A, Bheemarjuna Reddy Tamma, Prashant Sharma, and **Thomas Valerrian Pasca S**, “Method and System for LTE WLAN Integration at RLC Layer (LWIR) with Integrated LTE Wi-Fi Scheduler,” Indian Patent, Application No: 201641025740, Patent Pending.
3. Antony Franklin A, Bheemarjuna Reddy Tamma, Prashant Sharma, **Thomas Valerrian Pasca S**, “Method for Scheduling Data by Network Node Aggregated With LTE and Wi-Fi Protocol Stacks,” US Patent, Application No: 20180035445, Patent Pending.

Research Papers (Under review)

1. **Thomas Valerrian Pasca S**, Himank Gupta, Bheemarjuna Reddy Tamma, and Antony Franklin A, “Energy Aware Traffic Steering Solution for Aggregated LTE Wi-Fi Networks,” submitted to Elsevier Computer Communications, January 2019.
2. **Thomas Valerrian Pasca S**, Sumanta Patro, Bheemarjuna Reddy Tamma, and Antony Franklin A, “DIDA: A Packet Level Steering Solution for LWIP Networks,” submitted to IEEE ICC, 2019.

Research Papers (In preparation)

1. **Thomas Valerrian Pasca S**, Bheemarjuna Reddy Tamma, and Antony Franklin A, “Is Packet Level Steering Feasible in Tightly Coupled LTE Wi-Fi Interworking Architecture? - A Realtime Solution” to be submitted to IEEE Transactions on Mobile Computing.
2. **Thomas Valerrian Pasca S**, Venkatarami Reddy, and Nabhasmita Sen, Bheemarjuna Reddy Tamma, and Antony Franklin A, “Radio Level Aggregation of LTE and Wi-Fi for Edge Cloud - A Testbed Approach” to be submitted to IEEE Communication Magazine.

Publications (Other supporting work)

1. **Thomas Valerrian Pasca S**, Akilesh B, Arjun V Anand, and Bheemarjuna Reddy Tamma, “A NS-3 Module for LTE UE Energy Consumption,” in Proc. of IEEE ANTS, November 2016, Bangalore, India.
2. **Thomas Valerrian Pasca S**, Siva sairam prasad Kodali, and Kotaro Kataoka, “AMPS: Application Aware Multipath Flow Routing Using Machine Learning in SDN,” in Proc. of NCC, March 2017, Chennai, India.
3. Prasanth Sharma, Ajay Brahmakshatriya, **Thomas Valerrian Pasca S**, Bheemarjuna Reddy Tamma, and Antony Franklin A, “LWIR: LTE-WLAN Integration at RLC Layer with Virtual WLAN Scheduler for Efficient Aggregation,” in Proc. of IEEE GLOBECOM, December 2016, Washington DC, USA.
4. Sreekanth Dama, **Thomas Valerrian Pasca S**, Vanlin Sathya, and Kiran Kumar Kuchi, “A Feasible Cellular Internet of Things: Enabling Edge Computing and the IoT in Dense Futuristic Cellular Networks,” IEEE Consumer Electronics Magazine, vol. 6, no. 1, pp. 66-72, January 2017.
5. Anil Kumar Rangiseti, **Thomas Valerrian Pasca S**, and Bheemarjuna Reddy Tamma, “QoS Aware load balance in software defined LTE networks,” Elsevier Computer Communications, vol. 97, pp. 52-71, January 2017.
6. Sumanta Patro, **Thomas Valerrian Pasca S**, Bheemarjuna Reddy Tamma, and Antony Franklin A, “INCARNATE: An Interference Aware Spatial Scheme for Tightly Coupled LTE-Wi-Fi Networks,” in Proc. of COMSNETS, January 2018, Bangalore, India.
7. Sumanta Patro, **Thomas Valerrian Pasca S**, Bheemarjuna Reddy Tamma, and Antony Franklin A, “mINCARNATE: An Interference and Mobility Aware Spatial Scheme for Tightly Coupled LTE-Wi-Fi Networks,” in Proc. of Lecture Notes in Computer Science (LNCS) - Communication Systems and Networks, pp. 126-149, January 2019.

Patents (Other supporting works)

1. Sreekanth Dama, **Thomas Valerrian Pasca S**, Abhinav Kumar, Bheemarjuna Reddy Tamma, and Kiran kumar Kuchi, “Method for accessing a channel in wireless communication network”, US Patent No: 20160242175, **Patent Granted**.
2. Sreekanth Dama, **Thomas Valerrian Pasca S**, Sathya Vanlin, Kiran Kumar Kuchi, and Bheemarjuna Reddy Tamma, “A Novel RACH Mechanism for Dense Cellular-IoT Deployments”, Provisional Filing: 06.11.2015, Patent Pending.

Bibliography

- [1] I. T. Union, “IMT Vision Framework and overall objectives of the future development of IMT for 2020 and beyond.” [Online]. Available: <https://www.itu.int/>
- [2] 3GPP, “Evolved Universal Terrestrial Radio Access (E-UTRA) and Evolved Universal Terrestrial Radio Access Network (E-UTRAN); Overall description,” Tech. Rep. 36.300, 2016.
- [3] N. Nikaein, M. Mahesh K, M. Saravana, D. Alex, K. Raymond, and B. Christian, “OpenAirInterface: A flexible platform for 5G research,” *ACM SIGCOMM Computer Communication Review (CCR)*, vol. 44, no. 5, pp. 33–38, 2014.
- [4] Cisco, “Global Mobile Data Traffic Forecast Update, 2016 - 2021.” [Online]. Available: <http://www.cisco.com/c/en/us/solutions/collateral/service-provider/visual-networking-index-vni/mobile-white-paper-c11-520862.html>
- [5] T. E. Klein and P. Richard, “ICT energy challenges, impact and solutions,” in *Proc. of International ICIN Conference-Innovations in Clouds, Internet and Networks*. IFIP, 2016.
- [6] Y. Chen, S. Zhang, S. Xu, and G. Y. Li, “Fundamental trade-offs on green wireless networks,” *IEEE Communications Magazine*, vol. 49, no. 6, pp. 30–37, 2011.
- [7] 3GPP, “Study on enhancement of Ultra-Reliable Low-Latency Communication (URLLC) support in the 5G Core network (5GC),” Tech. Rep. 23.725, 2018.
- [8] “Third Generation Partnership Project.” [Online]. Available: <http://www.3gpp.org/>
- [9] 3GPP, “Network architecture,” Tech. Rep. 23.002, 2018.
- [10] —, “Policy and charging control architecture,” Tech. Rep. 23.203, 2018.

- [11] —, “Evolved Universal Terrestrial Radio Access (E-UTRA); Radio Resource Control (RRC);” Tech. Rep. 36.331, 2017.
- [12] C. S. Bontu and E. Illidge, “Drx mechanism for power saving in lte,” *IEEE Communications Magazine*, vol. 47, no. 6, pp. 48–55, June 2009.
- [13] 3GPP, “Evolved Universal Terrestrial Radio Access (E-UTRA); Packet Data Convergence Protocol (PDCP) specification,” Tech. Rep. 36.323, 2018.
- [14] —, “Evolved Universal Terrestrial Radio Access (E-UTRA); Radio Link Control (RLC) protocol specification,” Tech. Rep. 36.322, 2018.
- [15] —, “Evolved Universal Terrestrial Radio Access (E-UTRA); Medium Access Control (MAC) protocol specification,” Tech. Rep. 36.321, 2018.
- [16] —, “Evolved Universal Terrestrial Radio Access (E-UTRA); LTE physical layer; General description,” Tech. Rep. 36.201, 2018.
- [17] —, “Technical Specification Group Radio Access Network; Evolved Universal Terrestrial Radio Access (E-UTRA); Base Station (BS) radio transmission and reception,” Tech. Rep. 36.104, 2018.
- [18] —, “Evolved Universal Terrestrial Radio Access (E-UTRA); Physical channels and modulation,” Tech. Rep. 36.211, 2018.
- [19] I. S. Association, “Wireless Local Area Network (WLAN).” [Online]. Available: https://standards.ieee.org/standard/802_11ac-2013.html
- [20] “IEEE Standard for Wireless LAN Medium Access Control (MAC) and Physical Layer (PHY) specifications,” *IEEE Std 802.11-1997*, pp. 1–445, Nov 1997.
- [21] M. Benveniste, “Hybrid coordination function (HCF) access through tiered contention and overlapped wireless cell mitigation,” Nov. 14 2006, US Patent 7,136,361.
- [22] Tektronics, “Wi-Fi: Overview of the 802.11 Physical Layer and Transmitter Measurements.” [Online]. Available: www.cnrood.com/en/media/solutions/Wi-Fi_Overview_of_the_802.11_Physical_Layer.pdf

- [23] C. Samsung, “Samsung Download Booster.” [Online]. Available: www.samsung.com/au/galaxys5-mobile/features.html
- [24] A. Ford, C. Raiciu, M. Handley, and O. Bonaventure, “TCP Extensions for Multipath Operation with Multiple Addresses,” Tech. Rep. RFC 6824, 2013.
- [25] H. Soliman, “Mobile ipv6 support for dual stack hosts and routers,” Tech. Rep. 5555, 2009. [Online]. Available: <https://www.rfc-editor.org/rfc/rfc5555>
- [26] 3GPP, “Proxy Mobile IPv6 (PMIPv6) based Mobility and Tunnelling protocols,” Tech. Rep. 29.275, 2015.
- [27] —, “Access Network Discovery and Selection Function (ANDSF),” Tech. Rep. 24.312, 2015.
- [28] —, “IP flow mobility and seamless Wireless Local Area Network (WLAN) offload,” Tech. Rep. 23.261, 2015.
- [29] K. Lee, J. Lee, Y. Yi, I. Rhee, and S. Chong, “Mobile data offloading: How much can WiFi deliver?” *IEEE/ACM Transactions on Networking (ToN)*, vol. 21, no. 2, pp. 536–550, 2013.
- [30] S. Singh, S. p. Yeh, N. Himayat, and S. Talwar, “Optimal traffic aggregation in multi-RAT heterogeneous wireless networks,” in *Proc. of International Conference on Communications Workshops (ICC)*. IEEE, May 2016, pp. 626–631.
- [31] 3GPP, “Evolved Universal Terrestrial Radio Access (E-UTRA); LTE-WLAN Radio Level Integration Using Ipv6 Tunnel (LWIP) encapsulation; Protocol specification,” Tech. Rep. 29.060, 1999.
- [32] —, “Study on S2a Mobility based on GPRS Tunnelling Protocol (GTP) and Wireless Local Area Network (WLAN) access to the Enhanced Packet Core (EPC) network (SaMOG),” Tech. Rep. 23.852, 2013.
- [33] —, “Network-Based IP Flow Mobility (NBIFOM),” Tech. Rep. 23.161, 2015.
- [34] —, “Evolved Universal Terrestrial Radio Access (E-UTRA); LTE-WLAN Aggregation Adaptation Protocol (LWAAP) specification,” Tech. Rep. 36.360, 2016.

- [35] —, “General Packet Radio Service (GPRS); GPRS Tunnelling Protocol (GTP),” Tech. Rep. 36.361, 2016.
- [36] J. Ling, S. Kanugovi, S. Vasudevan, and A. Pramod, “Enhanced capacity and coverage by Wi-Fi LTE integration,” *IEEE Communications Magazine*, vol. 53, no. 3, pp. 165–171, March 2015.
- [37] 3GPP, “Evolved Universal Terrestrial Radio Access Network (E-UTRAN) and Wireless Local Area Network (WLAN); Xw application protocol (XwAP),” Tech. Rep. 36.463, 2015.
- [38] —, “Evolved Universal Terrestrial Radio Access Network (E-UTRAN) and Wireless Local Area Network (WLAN); Xw interface user plane protocol,” Tech. Rep. 36.465, 2016.
- [39] S. Hanks, T. Li, D. Farinacci, and P. Traina, “Generic Routing Encapsulation (GRE),” Tech. Rep. RFC 1701, 1994.
- [40] 3GPP, “Study on Small Cell enhancements for E-UTRA and E-UTRAN; Higher layer aspects,” Tech. Rep. 36.842, 2013.
- [41] “iptables.” [Online]. Available: <https://linux.die.net/man/8/iptables>
- [42] “Nist Error Model.” [Online]. Available: https://www.nsnam.org/doxygen/nist-error-rate-model.8cc_source.html
- [43] B. Chen, J. Chen, Y. Gao, and J. Zhang, “Coexistence of LTE-LAA and Wi-Fi on 5 GHz With Corresponding Deployment Scenarios: A Survey,” *IEEE Communications Surveys Tutorials*, vol. 19, no. 1, pp. 7–32, Firstquarter 2017.
- [44] “LTE over unlicensed.” [Online]. Available: http://www.3gpp.org/news-events/3gpp-news/1603-lte_in_unlicensed
- [45] “License Assisted Access.” [Online]. Available: ftp://ftp.3gpp.org/tsg_ran/WG1_RL1/TSGR1_79/Docs/R1-145483.zip
- [46] S. Deb *et al.*, “Algorithms for eICIC in LTE HetNets,” *IEEE/ACM Transactions on Networking (ToN)*, vol. 22, no. 1, pp. 137–150, 2014.

- [47] J.-H. Lee, J. Bonnin, and X. Lagrange, “Host-based distributed mobility management: Example of traffic offloading,” in *Proc. of Consumer Communications and Networking Conference (CCNC)*. IEEE, 2013, pp. 637–640.
- [48] K. Lee, J. Lee, Y. Yi, I. Rhee, and S. Chong, “Mobile Data Offloading: How Much Can Wi-Fi Deliver?” *IEEE/ACM Transactions on Networking (ToN)*, vol. 21, no. 2, pp. 536–550, April 2013.
- [49] S. Ranjan, N. Akhtar, M. Mehta, and A. Karandikar, “User-based integrated offloading approach for 3GPP LTE-WLAN network,” in *Proc. of National Conference on Communications (NCC)*. IEEE, 2014, pp. 1–6.
- [50] M. Gerasimenko, N. Himayat, S.-p. Yeh, S. Talwar, S. Andreev, and Y. Koucheryavy, “Characterizing performance of load-aware network selection in multi-radio (WiFi/LTE) heterogeneous networks,” in *Proc. of Global Communications Conference Workshops (GC Wkshps)*. IEEE, 2013, pp. 397–402.
- [51] S.-p. Yeh, A. Y. Panah, N. Himayat, and S. Talwar, “QoS Aware Scheduling and Cross-Radio Coordination in Multi-Radio Heterogeneous Networks,” in *Proc. of Vehicular Technology Conference (VTC)*. IEEE, 2013, pp. 1–6.
- [52] Sou and Sok-Ian, “Mobile data offloading with policy and charging control in 3GPP core network,” *IEEE Transactions on Vehicular Technology*, vol. 62, no. 7, pp. 3481–3486, 2013.
- [53] N. Sapountzis, T. Spyropoulos, N. Nikaen, and U. Salim, “An Analytical Framework for Optimal Downlink-Uplink User Association in HetNets with Traffic Differentiation,” in *Proc. of Global Communications Conference (GLOBECOM)*. IEEE, Dec 2015, pp. 1–7.
- [54] P. Sermpezis and T. Spyropoulos, “Modelling and Analysis of Communication Traffic Heterogeneity in Opportunistic Networks,” *IEEE Transactions on Mobile Computing (TMC)*, vol. 14, no. 11, pp. 2316–2331, 2015.
- [55] F. Mehmeti and T. Spyropoulos, “Is it worth to be patient? Analysis and optimization of delayed mobile data offloading,” in *Proc. of INFOCOM*. IEEE, April 2014, pp. 2364–2372.

- [56] A. Balasubramanian, R. Mahajan, and A. Venkataramani, “Augmenting Mobile 3G Using WiFi,” in *Proc. of International Conference on Mobile Systems, Applications, and Services (MobiSys)*. ACM, 2010, pp. 209–222.
- [57] S. Singh, M. Geraseminko, S. ping Yeh, N. Himayat, and S. Talwar, “Proportional Fair Traffic Splitting and Aggregation in Heterogeneous Wireless Networks,” *IEEE Communications Letters*, vol. 20, no. 5, pp. 1010–1013, May 2016.
- [58] Y.-J. Lai, T.-Y. Liu, and C.-L. Hwang, “Topsis for MODM,” *European Journal of Operational Research*, vol. 76, no. 3, pp. 486–500, 1994.
- [59] 3GPP, “Evolved Universal Terrestrial Radio Access (E-UTRA); Radio Frequency (RF) requirements for LTE Pico Node B,” Tech. Rep. 36.931, 2018.
- [60] T. Chrysikos, G. Georgopoulos, and S. Kotsopoulos, “Site-specific validation of ITU indoor path loss model at 2.4 GHz,” in *Proc. of International Symposium on a World of Wireless, Mobile and Multimedia Networks Workshops (WoWMoM)*. IEEE, June 2009, pp. 1–6.
- [61] G. Americas, “Whitepaper on LTE Aggregation and Unlicensed spectrum.” [Online]. Available: http://www.5gamericas.org/files/1214/4648/2397/4G_Americas_LTE_Aggregation_Unlicensed_Spectrum_White_Paper_-_November_2015.pdf
- [62] 3GPP, “LTE/WLAN Radio Interworking,” Tech. Rep. 37.834, 2013.
- [63] Skype, “How much bandwidth does Skype need?” [Online]. Available: <https://support.skype.com/en/faq/FA1417/how-much-bandwidth-does-skype-need>
- [64] Y. He, M. Chen, B. Ge, and M. Guizani, “On wifi offloading in heterogeneous networks: Various incentives and trade-off strategies,” *IEEE Communications Surveys Tutorials*, vol. 18, no. 4, pp. 2345–2385, Fourthquarter 2016.
- [65] V. Miliotis, L. Alonso, and C. Verikoukis, “Offloading with IFOM: The uplink case,” in *Proc. of Global Communications Conference (GLOBECOM)*. IEEE, Dec 2014, pp. 2661–2666.

- [66] —, “Energy efficient proportionally fair uplink offloading for IP Flow Mobility,” in *Proc. of International Workshop on Computer Aided Modeling and Design of Communication Links and Networks (CAMAD)*. IEEE, Dec 2014, pp. 6–10.
- [67] U. Sethakaset, Y. K. Chia, and S. Sun, “Energy Efficient WiFi Offloading for Cellular Uplink Transmissions,” in *Proc. of Vehicular Technology Conference (VTC)*. IEEE, May 2014, pp. 1–5.
- [68] F. Daneshgaran, M. Laddomada, F. Mesiti, and M. Mondin, “Unsaturated throughput analysis of IEEE 802.11 in presence of non ideal transmission channel and capture effects,” *IEEE Transactions on Wireless Communications (TWC)*, vol. 7, no. 4, pp. 1276–1286, 2008.
- [69] S. Rasheed, K. Masnoon, N. Thanthry, and R. Pendse, “PCF vs DCF: a performance comparison,” in *Proc. of the Southeastern Symposium on System Theory*. IEEE, 2004, pp. 215–219.
- [70] S. Rayanchu, A. Mishra, D. Agrawal, S. Saha, and S. Banerjee, “Diagnosing Wireless Packet Losses in 802.11: Separating Collision from Weak Signal,” in *Proc. of INFOCOM*. IEEE, April 2008, pp. 735–743.
- [71] S. Thomas Valerrian Pasca, P. C. Amogh, M. Debashisha, D. Nagamani, R. Anil Kumar, T. Bheemarjuna Reddy, and A. Antony Franklin, “Architectural Challenges and Solutions for Collocated LWIP: Network Layer Perspective,” in *Proc. of National Conference on Communication (NCC)*. IEEE, March 2017, pp. 1–6.
- [72] 3GPP, “Study on Small Cell enhancements for E-UTRA.” [Online]. Available: http://www.3gpp.org/ftp/Specs/archive/36_series/36.842/36842-c00.zip
- [73] T. Henderson, Boeing, S. Floyd, A. Gurtov, and Y. Nishida, “The NewReno Modification to TCP’s Fast Recovery Algorithm,” Tech. Rep. RFC 6582, 2012.
- [74] D. Leith and R. Shorten, “H-TCP: TCP for high-speed and long-distance networks,” in *Proc. of PFLDnet*, 2004.
- [75] T. Kelly, “Scalable TCP: Improving Performance in Highspeed Wide Area Networks,” *ACM SIGCOMM CCR*, vol. 33, no. 2, pp. 83–91, 2003.

- [76] L. Xu, K. Harfoush, and I. Rhee, “Binary Increase Congestion Control (BIC) for Fast Long-Distance Networks,” in *Proc. of INFOCOM*, vol. 4. IEEE, 2004, pp. 2514–2524.
- [77] S. Floyd, “Highspeed tcp for large congestion windows,” Tech. Rep., 2003.
- [78] F. Wang and Y. Zhang, “Improving TCP performance over mobile ad-hoc networks with out-of-order detection and response,” in *Proc. of Mobile Ad Hoc Networking and Computing (MobiHoc)*. ACM, 2002, pp. 217–225.
- [79] H. Mulugeta and K. Raimond, “Performance improvement of TCP using TCP-DOOR-TS algorithm in mobile ad hoc networks,” in *Proc. of International Conference on Communication Technology*. IEEE, 2011, pp. 642–646.
- [80] R. Ludwig and R. H. Katz, “The Eifel algorithm: making TCP robust against spurious retransmissions,” *SIGCOMM Computer Communication Review (CCR)*, vol. 30, no. 1, pp. 30–36, 2000.
- [81] V. Paxson, “End-to-end Internet packet dynamics,” *IEEE/ACM Transactions on Networking (ToN)*, vol. 7, no. 3, pp. 277–292, 1999.
- [82] M. Zhang, B. Karp, S. Floyd, and L. Peterson, “RR-TCP: a reordering-robust TCP with DSACK,” in *Proc. of International Conference on Network Protocols (ICNP)*. IEEE, 2003, pp. 95–106.
- [83] S. Bohacek, J. P. Hespanha, J. Lee, C. Lim, and K. Obraczka, “A new TCP for persistent packet reordering,” *IEEE/ACM Transactions on Networking (ToN)*, vol. 14, no. 2, April 2006.
- [84] Y. Khadraoui, X. Lagrange, and A. Gravey, “TCP Performance for Practical Implementation of Very Tight Coupling between LTE and WiFi,” in *Proc. of Vehicular Technology Conference (VTC)*. IEEE, Sept 2016, pp. 1–6.
- [85] C. Paasch and O. Bonaventure, “Multipath tcp,” *Communications of the ACM*, vol. 57, no. 4, pp. 51–57, 2014.
- [86] L. Kleinrock, *Queueing systems, volume 2: Computer applications*. wiley New York, 1976, vol. 66.

- [87] V. Paxson and M. Allman, “Computing TCP’s Retransmission Timer,” Tech. Rep. RFC 6298, 2000.
- [88] S. Ha, I. Rhee, and L. Xu, “Cubic: a new tcp-friendly high-speed tcp variant,” *ACM SIGOPS operating systems review*, vol. 42, no. 5, pp. 64–74, 2008.
- [89] H. T. Friis, “A Note on a Simple Transmission Formula,” *Proceedings of the IRE*, vol. 34, no. 5, pp. 254–256, May 1946.
- [90] M. Kheirkhah, I. Wakeman, and G. Parisi, “Multipath-TCP in ns-3,” *CoRR*, 2015. [Online]. Available: <http://arxiv.org/abs/1510.07721>
- [91] W. Guo and S. Wang, “Interference-aware self-deploying femto-cell,” *IEEE Wireless Communications Letters*, vol. 1, no. 6, pp. 609–612, 2012.
- [92] W. Guo, S. Wang, X. Chu, J. Zhang, J. Chen, and H. Song, “Automated small-cell deployment for heterogeneous cellular networks,” *IEEE Communications Magazine*, vol. 51, no. 5, pp. 46–53, 2013.
- [93] S. Vanlin, R. Arun, and T. Bheemarjuna Reddy, “On placement and dynamic power control of femtocells in lte hetnets,” in *Proc. of Global Communications Conference (GLOBECOM)*. IEEE, 2014, pp. 4394–4399.
- [94] J. Liu, Q. Chen, and H. D. Sherali, “Algorithm design for femtocell base station placement in commercial building environments,” in *Proc. of INFOCOM*. IEEE, 2012, pp. 2951–2955.
- [95] S. Thomas Valerrian Pasca, G. Himank, T. Bheemarjuna Reddy, and A. Antony Franklin, “PRECISE: Power Aware Dynamic Traffic Steering in Tightly Coupled LTE Wi-Fi Networks,” in *Proc. of International Symposium on Personal, Indoor, and Mobile Radio Communications (PIMRC)*. IEEE, 2017, pp. 1–7.
- [96] N. Nikaein, R. Knopp, F. Kaltenberger, L. Gauthier, C. Bonnet, D. Nussbaum, and R. Ghaddab, “Demo: OpenAirInterface: an open LTE network in a PC,” in *Proc. of International Conference on Mobile Computing and Networking (MobiCom)*. ACM, 2014, pp. 305–308.

- [97] T. Bheemarjuna Reddy, A. Antony Franklin, and S. Thomas Valerrian Pasca, “Traffic steering strategies for LWA.” [Online]. Available: www.tdsi.org/standards/swip/30/
- [98] M. Baerts, “HIPRIKeeper.” [Online]. Available: <https://github.com/MPTCP-smartphone-thesis/MultipathControl>
- [99] D. Jon, S. Elliott, B. A. Mah, J. Poskanzer, K. Prabhu, M. Ashley, A. Brown, A. Jaible, S. Sahani, B. Simpson, and B. Tierney, “iPerf3.” [Online]. Available: <https://iperf.fr/>
- [100] S. K. Saha, A. Kannan, G. Lee, N. Ravichandran, P. K. Medhe, N. Merchant, and D. Koutsonikolas, “Multipath TCP in Smartphones: Impact on Performance, Energy, and CPU Utilization,” in *Proc. of Mobility Management and Wireless Access*. ACM, 2017, pp. 23–31.
- [101] S. Ferlin, O. Alay, T. Dreibholz, D. A. Hayes, and M. Welzl, “Revisiting congestion control for multipath TCP with shared bottleneck detection,” in *Proc. of INFOCOM*. IEEE, 2016, pp. 1–9.
- [102] Y.-C. Chen, Y.-s. Lim, R. J. Gibbens, E. M. Nahum, R. Khalili, and D. Towsley, “A Measurement-based Study of MultiPath TCP Performance over Wireless Networks,” in *Proc. of Internet Measurement Conference (IMC)*. ACM, 2013, pp. 455–468.
- [103] L. network developers, “Network emulation.” [Online]. Available: <https://wiki.linuxfoundation.org/networking/netem>

DOCTORAL COMMITTEE

**Chairperson and
Research Advisor** Dr. Bheemarjuna Reddy Tamma
Associate Professor
Department of Computer Science and Engineering
Indian Institute of Technology Hyderabad

Members: Dr. Kotaro Kataoka
Associate Professor
Department of Computer Science and Engineering
Indian Institute of Technology Hyderabad

Dr. Sathya Peri
Associate Professor
Department of Computer Science and Engineering
Indian Institute of Technology Hyderabad

Dr. Kiran Kumar Kuchi
Professor
Department of Electrical and Engineering
Indian Institute of Technology Hyderabad

Dr. P. Rajalakshmi
Associate Professor
Department of Electrical Engineering
Indian Institute of Technology Hyderabad